



The University of
Nottingham

CORDYCEPIN AND THE
ENTOMOPATHOGENIC FUNGUS
CORDYCEPS MILITARIS

PETER WELLHAM

M.A. (Oxon.) M.Res. (Imp. Lond.)

Thesis submitted for the degree of Doctor of Philosophy

September 2021



DECLARATION

I declare that, except where acknowledged in the text, this thesis is my own work. My research was undertaken at the Schools of Pharmacy and Life Sciences, Faculty of Sciences, University of Nottingham.

Supervisor: Dr. Cornelia de Moor

Co-supervisors: Dr. Dong-Hyun Kim (Metabolomics), Dr. Matthias Brock (Mycology)

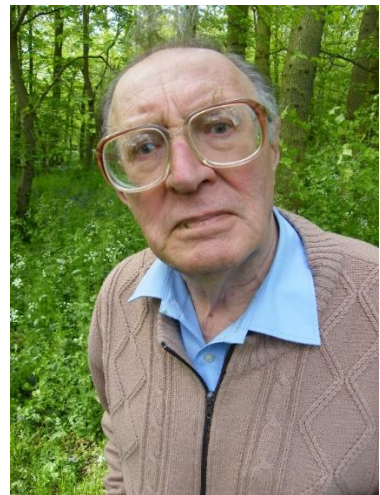
Work was carried out at:

- Gene Regulation and RNA Biology Laboratory, Molecular Therapeutics and Formulation Division, School of Pharmacy
- Centre for Analytical Bioscience, Advanced Materials and Healthcare Technologies Division, School of Pharmacy
- Fungal Genetics and Biology Group, School of Life Sciences

Funded by the Biotechnology and Biological Sciences Research Council (BBSRC) Doctoral Training Partnership (DTP)

Dedicated to Uncle Bill (1925-2011)

An early fungal mentor



ACKNOWLEDGEMENTS

First and foremost, I thank Dr. Cornelia de Moor. Lia has been a very patient and supportive supervisor throughout the project, sharing her passion for biology with me. I also particularly appreciate the freedom she gave me to design many of my experiments and decide which direction in which to take the research – whilst also keeping me in line when that was needed. She was very generous with the opportunities available to me and took a keen interest in my career aspirations and personal development.

I also thank Dr. Dong-Hyun Kim for his supervision over my work with metabolomics and the operation LC-MS systems – a set of skills I have greatly valued; and Dr. Matthias Brock for his supervision and valued advice on the fungal work. Additionally Dr. Dave Chandler at the University of Warwick helped tremendously with advice for the caterpillar experiments, as did Dr. Victoria Woolley. Dr. Salah Abdelrazig and Dr. Cath Ortori were great teachers of the operation of metabolomics instruments. I would also like to thank my good friends and PhD student peers Paul Brett and Abdul Hafeez.

I greatly enjoyed my industrial placement and otherwise working with Dr. Andrej Gregori – I thank him for him for giving me a perspective on biotechnology, and also sharing lots of good times together in Slovenia.

Thank you Prof. Paul Dyer for his encouragement and helping me get my place on the University of Nottingham DTP! And thank you to Prof. Alan Gange of RHUL for kindly giving me some crucial fungal experience and welcoming me to volunteer in his lab when I was an undergraduate.

My interest and passion for fungi came at an early age from mushroom collecting trips with my eccentric Great Uncle Bill and Auntie Pam. My parents always supported this interest. I thank them very much for nurturing and encouraging my aspirations of studying and working with biology. Finally I thank my fiancée Charlotte for supporting me and putting up with my experiments and specimens I take into our home.

ABSTRACT

Cordyceps militaris is a widespread entomopathogenic fungus found in Europe, Asia, and North America, with a large number of insect hosts, predominantly lepidopteran larvae (caterpillars). This species is well known for its production of the nucleoside analogue cordycepin (3'-deoxyadenosine). Co-produced with its protector molecule pentostatin, cordycepin is a polyadenylation inhibitor, via its active modified form as cordycepin triphosphate. Pentostatin protects cordycepin from degradation to 3'-deoxyinosine by inhibition of the enzyme adenosine deaminase. It has been shown to have anti-inflammatory effects and hence has been the subject of much pharmacological research. Until recently, very little was known about the role of cordycepin in the ecology of the fungus, or why its production is favoured by natural selection. There are also gaps in the understanding of the process of infection of the host by the fungus, which is directly followed by sexual development and the formation of stromata bearing sexual fruiting bodies and spores (ascospores). Understanding these areas could have implications for biological control of insect pests. Indeed, the related species *Beauveria bassiana* and *Metarhizium anisopliae* have been used as bioinsecticides, precluding the use of harmful chemical insecticides.

Culture degeneration is a phenomenon defined previously as a reduction in the production of cordycepin by *C. militaris*. Experiments comparing a degenerated strain of an isolate of *C. militaris* with its parental control strain were performed, involving the use of gene expression analysis and metabolomics. Reduced cordycepin production in the degenerated strain was shown to be accompanied by declines in sexual development-related gene expression, and reduced production of other metabolites involved in the citrate cycle and purine metabolism. This suggested a link between cordycepin production, primary metabolism, and sexual development. We hypothesised that the production of cordycepin by *C. militaris* aids the infection of the insect by suppression of the host immune system, and that pentostatin, by providing molecular protection, enhances this effect. In a caterpillar infection assay system involving the injection of spores into the model species *Galleria mellonella* (greater wax moth)

caterpillars, the lower cordycepin-producing degenerated strain was shown to produce a significantly-decreased pathogenic response, marked by reduced fungal growth in the host. When spores of the degenerated strain were supplemented by cordycepin and pentostatin, fungal emergence rates and levels significantly increased, restoring the infection performance of the degenerated strain to that of the parental control. Assays of insect gene expression were also performed, and cordycepin was demonstrated to suppress the upregulation of immune response genes in both *Drosophila melanogaster* Schneider 2 cells and *G. mellonella* haemolymph cells. Pentostatin enhanced the effects of low cordycepin concentrations in both models. These findings support the hypothesis that cordycepin has an important role in aiding insect infection by the fungus via immune suppression, and that the effect of cordycepin on host cell responses is maintained by pentostatin.

Biosynthesis genes (*Cns* genes) for cordycepin and pentostatin are located in the same gene cluster. We hypothesised that cordycepin-pentostatin co-production was a rare trait, and its evolution had been resultant partly due to horizontal gene transfer between different species. This was due to the lack of cordycepin in other *Cordyceps* species, and genetic evidence of its production only found previously in two other, distantly-related species. Bioinformatics work involving tBLASTn searches through the sequenced genomes of over two and a half thousand fungal species uncovered evidence of homologous *Cns* gene clusters in five new species. This together with consideration of protein structures suggests that the development of cordycepin-pentostatin co-production has occurred by convergent evolution involving duplication and subfunctionalisation of genes involved in the purine synthesis pathway, and/or through horizontal gene transfer.

CONTENTS

Declaration.....	iii
Acknowledgements.....	vi
Abstract.....	vii
Contents.....	ix
List of Abbreviations.....	xii
Chapter 1: Introduction	1
1.1 <i>Cordyceps militaris</i> , the Entomopathogen.....	2
1.1.1 <i>Cordyceps sensu lato</i>	2
1.2 <i>Cordyceps militaris</i> , the Ascomycete Fungus.....	7
1.2.1 The Ascomycetes – Form and Diversity.....	7
1.2.2 Sexual Biology of the Ascomycetes and <i>C. militaris</i>	15
1.2.3 Genomics and Transcriptomics of <i>C. militaris</i>	20
1.3 Cordycepin and Related Metabolites.....	21
1.3.1 Cordycepin and Pentostatin – Background and Research.....	21
1.3.2 <i>C. militaris</i> Strains and Cordycepin Production.....	31
1.3.3 Analytical Methods for Detection of Cordycepin and Other Metabolites.....	42
1.4 Studying Insect Hosts of <i>Cordyceps</i>	48
1.4.1 Diversity of <i>C. militaris</i> Insect Hosts.....	48
1.4.2 Use and Adaptation of Insect Models for Infection: <i>Galleria mellonella</i>	49
1.4.3 Exploring the Effects of Cordycepin on Insect Models.....	51
1.5 Project Aims and Outcomes.....	56
Chapter 2: Material and Methods	58
2.1 Material and Methods Overview.....	58
2.2 Molecular Biological Methods.....	60
2.2.1 DNA Extraction.....	60
2.2.2 RNA Extraction.....	61
2.2.3 Polymerase Chain Reaction (PCR) and Gel Electrophoresis.....	62
2.2.4 Reverse Transcription and Quantitative PCR (RT-qPCR).....	63
2.2.5 Design and Validation of Primers.....	65
2.3 Liquid Chromatography-Coupled Mass Spectrometry (LC-MS).....	66
2.3.1 Preparation of Samples.....	67
2.3.2 Liquid Chromatography.....	68

2.3.3 Mass Spectrometry.....	69
2.3.4 Settings and Steps in Performing an LC-MS Run – ZIC-pHILIC and Exactive MS.....	71
2.3.5 Analysis of LC-MS Data.....	73
2.4 Fungal Culture and Microbiological Methods.....	76
2.4.1 Establishment of Fungal Cultures.....	76
2.4.2 Subculturing on Agar.....	77
2.4.3 Single Spore Isolate Cultures.....	78
2.4.4 Liquid Broth Cultures.....	79
2.4.5 Measuring Fungal Growth.....	79
2.4.6 Preparing Inoculum and Extracts for Host Assays.....	79
2.4.7. Fungal Species Verification and Strain Characterisation.....	79
2.5 Animal Cell Culture.....	80
2.5.1 <i>Drosophila melanogaster</i> Schneider 2 Cells.....	80
2.5.2 Cell Culture Gene Expression Assays.....	81
2.6 Caterpillar Experiments.....	81
2.6.1 Caterpillar Rearing and Conditions.....	81
2.6.2 Caterpillar Assays.....	81
<u>Chapter 3: Culture Degeneration in <i>Cordyceps militaris</i></u>	87
3.1 Comparison of Parental Control and Degenerated Strains.....	87
3.1.1 Growth of Cultures.....	87
3.1.2 Cordycepin and Pentostatin Production in Cultures.....	90
3.1.3 Metabolomics of Cultures.....	95
3.1.4 Gene Expression in Cultures.....	106
3.2 Discussion.....	109
<u>Chapter 4: Methods for Use of <i>Cordyceps militaris</i> Host Models</u>	111
4.1 <i>Cordyceps militaris</i> Host Model Methods.....	111
4.1.1 Injection of Concentrations of Cordycepin into Caterpillars.....	112
4.1.2 Alternative Methods for Using <i>Galleria mellonella</i>	119
4.2 Discussion.....	133
<u>Chapter 5: Cordycepin and Degeneration in the Context of the Insect Host</u>	135
5.1 Cordycepin and Degeneration – Effects on the Host.....	135
5.1.1 Pure Cordycepin/ Pentostatin and Insect Host Immunity.....	135
5.1.2 Degeneration and the Insect Host.....	143

5.2 Discussion.....	161
<u>Chapter 6: Factors Affecting Degeneration of <i>Cordyceps militaris</i> and Regeneration</u>	
<u>Attempts</u>	163
6.1 Serial Subculturing.....	163
6.2 Exposure to the Host.....	169
6.2.1 Cultures on Silk Pupa Powder Agar.....	169
6.2.2 Cultures Extracted from Spore-Injected Hosts.....	180
6.3 Discussion.....	186
<u>Chapter 7: Diversity of <i>Cordyceps militaris</i> and Cordycepin Production</u>	188
7.1 Variation between <i>Cordyceps militaris</i> Isolates.....	188
7.1.1 Growth of <i>Cordyceps militaris</i> Strains.....	189
7.1.2 Genetics Screens of <i>Cordyceps militaris</i> Isolates.....	189
7.1.3 Cordycepin and Pentostatin Production and Metabolomics.....	192
7.1.4 Infection of <i>Galleria mellonella</i>	193
7.2 Discussion.....	198
<u>Chapter 8: Evolution of Cordycepin-Pentostatin Co-Production</u>	199
8.1 Searching for Evidence of Cordycepin Production in Other Fungi.....	199
8.1.1 Searches for Homologues of <i>Cordyceps militaris</i> Cns1-4 Using BLASTp.....	200
8.1.2 Cns1-4 Protein Structures and Functions.....	202
8.1.3 Searching Fungal Genomes for Cns1-3 Homologues Using tBLASTn.....	207
8.2 <i>Cordyceps militaris</i> in Plants.....	214
8.3 Discussion.....	215
<u>Chapter 9: Discussion and Conclusions</u>	219
9.1 Understanding Degeneration in <i>Cordyceps militaris</i>	219
9.2 Roles of Cordycepin and Pentostatin in <i>Cordyceps militaris</i>	220
9.3 The <i>Cordyceps-Galleria</i> Model System.....	221
9.4 Evolution of Cordycepin and Pentostatin Biosynthesis.....	222
9.5 Further Work and Concluding Remarks.....	223
References.....	225
Appendices.....	248

LIST OF ABBREVIATIONS

2'-keto-dA – 2'-ketodeoxyadenosine

2'-C-3'-dA – 2'-carbonyl-3'-
deoxyadenosine

3'-AMP – 3'-Adenosine monophosphate

3'dI – 3'-deoxyinosine

ABC – ATP-binding cassette domain

Act – *Actin*

ADA – *Adenosine deaminase*

AMPK – Adenosine monophosphate
kinase

Ara-A – Vidarabine

Ara-C – Cytarabine

Ara-I – Arabinofuranosylhypoxanthine

Ara-T – Spongothymidine

Ara-U – Spongouridine

ARSEF – *Agricultural Research Service
collection of Entomopathogenic Fungus*
(USA) strains

ATP – Adenosine triphosphate

Att – *Attacin (Attacin A)*

AUC – Area under the curve

BCRC – *Bioscience Collection and
Research Center (Taiwan) strains*

BLAST – Basic Local Alignment Search
Tool

BLASTn – Nucleotide BLAST

BLASTp – Protein BLAST

Cal – *Calmodulin*

CBS – *Centraalbureau voor
Schimmelcultures (Netherlands) strains*

CDD – Conserved Domain Database

Cdl. – Curdlan

CFU – Colony forming units

CGMCC – *China General Microbiological
Culture Collection strains*

CM01 – *Cordyceps militaris* strain 01
(Wang lab, China)

CM16 – *C. militaris* strain 16
(MycoMedica, Slovenia)

CM2 – *C. militaris* strain 2 (MycoMedica,
Slovenia)

Cns – *Cordycepin synthesis cluster genes*

Cpn. – Cordycepin

ddH₂O – Deionised distilled water

DMEM – Dulbecco's modified Eagle's
media

DMSO – Dimethyl sulfoxide

DS – Degenerated strain

DTT – Dithiothreitol

EEPF – Endophytic entomopathogenic
fungus

EI – Electron ionisation

ESI – Electrospray ionisation

FBS – Foetal bovine serum

Gale – *Gallerimycin*

Gali – *Galiomycin*

GaPDh – *Glyceraldehyde phosphate dehydrogenase*

GC-MS – Gas chromatography-coupled mass spectrometry

GO – Gene Ontogeny

HILIC – Hydrophilic interaction liquid chromatography

HPLC – High performance liquid chromatography

IL-1-β – Interleukin-1-beta

IMPI – *Insect metalloproteinase inhibitor*

ITS – Internal transcribed spacers

KCTC – *Korean Collection for Type Cultures* strains

KEGG – Kyoto Encyclopedia of Genes and Genomes

LaeA – *Loss of aflR expression A*

LC-MS – Liquid chromatography-coupled mass spectrometry

LOD – Limit of detection

LPS – Lipopolysaccharide

Lyso – *Lysozyme*

m4C – N6-methylcytosine

m6dA – N6-methyldeoxyadenosine

MAP/MAPK – Mitogen-activated protein/kinase

MAT – *Mating-type gene*

Met – *Methyltransferase*

MS/MS – Tandem mass spectrometry

Msh4 – *MutS protein homolog 4*

NADP/NADPH – Nicotinamide adenine dinucleotide phosphate/ reduced form

NBRC – *National Bioresource Research Center* (Taiwan) strains

NCBI – National Center for Biotechnology Information website

NF-κB – Nuclear factor kappa B

NK – Nucleotide kinase

NMR – Nuclear magnetic resonance

nr – non-redundant protein database

NTP – Nucleotide triphosphate

OPLS-DA – Orthogonal partial least squares-discriminant analysis

OR – Oxidoreductase

ORF – Open reading frame

PBS – Phosphate-buffered saline

PCA – Principle component analysis

PCR – Polymerase chain reaction

PCS – Parental control strain

PDA – Potato dextrose agar

PDB – Potato dextrose broth

PDR – Pleiotropic drug resistance domain

Pfam – Protein family search tool

Ptn. – Pentostatin

QC – Quality control

QqQ – Triple quadrupole

Q-TOF – Quadrupole time of flight

RAPD – Random amplified polymorphic DNA

Rec14 – *Meiotic recombination protein 14*

Rec8l – *Meiotic recombination protein 8-like gene*

RIN – RNA integrity number

RP49 – *Ribosomal protein 49*

RT-qPCR – Reverse transcription quantitative PCR

S1/S14 – Subculture number 1/14

S7e – *Eukaryotic (40S) ribosomal protein S7*

SAICAR – Phosphoribosyl-aminoimidazole-succinocarboxamide

SIMCA – Soft Independent Modelling of Class Analogy software

SL2/S2 – Schneider-like 2/ Schneider 2 cells

Spo11 – *Saccharomyces pombe 11* meiosis recombination gene

SPPA – Silk pupa powder agar

SR1/2/3 – Rajitar strains (Slovakia)

SteA – Gene encoding transcription factor associated with velvet proteins

tBLASTn – protein to translated nucleotide BLAST

TBRC – *Thailand Bioresource Research Center* strains

TIC – Total ion count

TNF – *Tumour necrosis factor*

UHPLC – Ultra high performance liquid chromatography

UKMS – *UK Mushroom Supplies* strains

VeA/B/C – *Velvet protein A/B/C*

VosA – *Variability of spores A*

wgs – whole genome shotgun database

ZIC-pHILIC – Zwitterionic stationary phase polymeric HILIC column

CHAPTER 1: INTRODUCTION

Fungal pathogens of insects (entomopathogens) are a highly-diverse, global guild of organisms. They play key roles in the ecology of both insects and plants and are of great economic importance particularly in crop production [Vega *et al.* 2009]. Their study has led to contributions of new ways to target insect pests of crop plants through biological control [Mascarin & Jaronski 2016; Maina *et al.* 2018]; and increased understanding of the complex ecologies of agricultural and wild settings [Vega 2018]. *Cordyceps militaris* is one such fungal species. It has been the subject of a great deal of pharmacological-based research in recent years, owing to its production of the nucleoside cordycepin. However, *C. militaris* has otherwise been scarcely studied with respect particularly to its life cycle, and relationship to its wide range of insect larval hosts [Shrestha *et al.* 2016]. A truly cosmopolitan species, with multiple strains available for research, *C. militaris* is known to have a wide range of predominantly lepidopteran insect hosts. Commonly known as the caterpillar fungus, it is part of a large and ecologically diverse phylogenetic group, the *Cordyceps sensu lato*, containing some 400+ species. *C. militaris* is the most researched of these, and yet little is known about its infection process, or the effects of its most celebrated metabolite, cordycepin, on its insect host. Cordycepin, or 3'-deoxyadenosine, is a modified nucleoside which acts as a polyadenylation inhibitor in mammalian cells, via its active product, cordycepin triphosphate [Utami 2015], and can also repress translation [Desrosiers *et al.* 1976]. Advancements in metabolomics and genetic techniques provide an opportunity to study the small molecule metabolism and genetic properties which underpin the biology of this insect pathogenic fungus.

1.1 CORDYCEPS MILITARIS, THE ENTOMOPATHOGEN

Commonly known as the orange caterpillar club fungus, *Cordyceps militaris* (Clavicipitaceae, Hypocreales, Sordariomycetes, Pezizomycotina, Ascomycota) [figure 1.1] is a cosmopolitan entomopathogen, with a broad range of insect hosts globally [Kryukov *et al.* 2011; Shrestha *et al.* 2012]. Hosts are predominantly lepidopteran larvae (butterfly and moth caterpillars) [Shrestha *et al.* 2012].



Figure 1.1: *Cordyceps militaris* stromata, photographed *in situ* with the insect host [Anton Soklič, reproduced with permission]

1.1.1 *Cordyceps sensu lato*

Cordyceps militaris has many closely-related species, which are widely distributed [Webster & Weber 2007]. With a focus of diversity in north-eastern Asia, there are between 400 and 500 species of *Cordyceps* (*sensu lato*) globally [Kobayashi 1982; Liu *et al.* 2002], including 29

in North America and 18 in Europe [Humber 2000], the majority of which are necrotrophic entomopathogens [Webster & Weber 2007]. This term – *Cordyceps sensu lato* – is used in the literature to describe members of the modern genus *Cordyceps* as well as closely-related former members of the genus, such as those of *Ophiocordyceps*, *Elaphocordyceps*, *Tolypocladium*, *Beauveria* and others [Shrestha *et al.* 2016]. Insect pathogenicity in the *Cordyceps* species has evolved multiple times [Shrestha *et al.* 2016]. *Beauveria bassiana* and *Metarhizium anisopliae* have been subject to intensive research due to their potential for biological control as entomopathogens, and both have also been described as having endophytic stages in their life cycles, and hence are described as examples of endophytic entomopathogenic fungi (EEPFs) [reviewed by Vega *et al.* 2008, 2009; Posada & Vega 2005; Vidal & Jaber 2015].

Host Infection and Life Cycle

A typical *Cordyceps*-infected host body is transformed into a sclerotium (tightly-packed hyphal mass), from which the fruiting body, a stroma (pl. stromata) bearing elongate perithecia grows. Each perithecium bears asci which in turn contain 4 or 8 ascospores [Hywel-Jones 2002]. Anamorphic genera (exhibiting asexual behaviour) – *Beauveria*, *Metarhizium*, *Tolypocladium*, *Hirsutella*, and others – exhibit conidial forms [Hodge 2003], and this wide range of *Cordyceps* anamorphs were discovered to be allied with *Cordyceps* in some cases by genomic comparison [Liu *et al.* 2002], and in others by establishing anamorph cultures from ascospores from insect cadavers, or conversely by infecting insect larvae by conidia [Webster & Weber 2007].

The stromata of *C. militaris* are orange and club shaped and protrude above the ground in autumn from subterranean host larvae [Webster & Weber 2007; Winterstein 2001]. Chitin-degrading enzymes aid conidial entry across the host cuticle upon contact with larvae. Following this, hyphae colonise the haemocoel and grow by budding until they have fully occupied the body [Kim *et al.* 2002; Yu *et al.* 2001]. Sclerotial formation does not take place until 5 days after infection, and stromatal development not until around 50 days [Webster &

Weber 2007]. However, the stromata of *C. militaris* can also be cultured on rice grain and other media types [Basith & Madelin 1968].

Elaphomyces spp. and Ophiocordyceps sinensis

Two interesting and relatively-well studied (with comparison to the wider *Cordyceps sensu lato*) taxa are the *Elaphomyces* species and *Ophiocordyceps sinensis*. Hosts of the genus *Cordyceps, sensu lato*, include lepidopteran and coleopteran species (reviewed by Shrestha *et al.* 2016). The majority of these infect arthropod hosts. Some species, such as *Elaphocordyceps ophioglossoides* and *Elaphocordyceps capitata* parasitise the subterranean false truffle species *Elaphomyces granulatus* [figure 1.2]. Four such species of *Elaphocordyceps* were found to be closely related to two cicada nymph-parasitising species, in a phylogenetic study [Nikoh & Fukatsu 2000]. An explanation for this could lie with the similarity of the habitats of the *Elaphomyces* ascocarps, which are tree-associated ectomycorrhizal fungi, and the nymphs, which live underground and feed on xylem sap exuded from tree roots. The "truffle-cicada" clade illustrates a good example of interkingdom host jumping, which is rife among the Cordycipitaceae/Clavicipitales taxa in which *Cordyceps* and related genera are nestled [Vega *et al.* 2009; Webster & Weber 2007].

Ophiocordyceps sinensis [figure 1.3], which grows at high altitude (3600-5000m) in China, Nepal, and Tibet, on hepialid moth larvae [Jiang & Yao 2002], highly prized as a Chinese medicine [Pegler *et al.* 1994], is more strongly associated with traditional remedies. However, *Cordyceps militaris* is recognised as the oldest-used medicinal *Cordyceps* species [Das *et al.* 2010]. A key advantage of focussing studies on cordycepin production around *Cordyceps militaris* is the ease at which it can be cultivated compared to *Ophiocordyceps sinensis* [Shrestha *et al.* 2012]. Another reason lies with the ecology of the species. *Cordyceps militaris* has a cosmopolitan distribution, occurring in much of Europe, and with over 30 species of lepidopterans and hymenopterans reported as hosts [Kryukov *et al.* 2011; Shrestha *et al.* 2012]. Research on the insect infection process of *C. militaris* is still rudimentary, despite the potential for this species to become a useful insect pathogen for use in pest control.



Figure 1.2: *Elaphocordyceps capitata* (left) and *Elaphocordyceps ophioglossoides* (right), photographed with the fungal host *Elaphomyces granulatus* [Anton Soklič, & Andrej Gregori, reproduced with permission]



Figure 1.3: *Ophiocordyceps sinensis*, photographed *in situ* with the insect host [Cornelia de Moor, reproduced with permission].

Clavicipitaceous Fungi

Cordyceps sensu lato species were once classified as a single family, the Clavicipitaceae, within the order Hypocreales [Sung *et al.* 2007; Kirk *et al.* 2008]. This group, also now described as the clavicipitaceous fungi, contains species with a great diversity of hosts, and has since been divided into several different and new families [Sung *et al.* 2007]. These include Ophiocordycipitaceae (containing *Ophiocordyceps*, *Elaphocordyceps*, and others),

the amended family Clavicipitaceae (containing grass symbiont genera such as *Claviceps* and *Epichloë*, as well as *Metarhizium*), and Cordicipitaceae (containing *Cordyceps* and *Beauveria*) [Sung *et al.* 2007]. Some of these related species, most notably *Beauveria bassiana* [reviewed by Mascarin & Jaronski 2016] have been used as entomopathogens for pest control of herbivorous insects, on an industrial scale. In the case of *B. bassiana*, conidial preparations and liquid cultures have been used to infect a diverse range of insect hosts [Mascarin & Jaronski 2016]. Definitions relating to these groups of fungi can be confusing due to contradictory use – and are explained in table 1.1. *Beauveria bassiana* itself has been described under rare circumstances to produce a teleomorph, *Cordyceps bassiana*, and indeed *Metarhizium* and *Beauveria* have been referred to as anamorphs of the *Cordyceps* genus [Webster & Weber 2007]. The anamorphic, conidial form of *C. militaris* has been named *Paecilomyces militaris*, but for convenience and to avoid confusion, over the course of this study, both teleomorph and anamorph states will be referred to under the name *Cordyceps militaris*.

Table 1.1: Definitions relating to *Cordyceps* and related species, used in the literature

Term	Definition
<i>Cordyceps sensu lato</i>	A general term describing all of the <i>Cordyceps</i> and <i>Cordyceps</i> -like related species which parasitise arthropods
<i>Cordyceps sp.</i>	The modern genus, or true <i>Cordyceps</i> , including only arthropod-parasitising stromatal species – but not <i>Ophiocordyceps</i>
Clavicipitaceae (old family)	A defunct family which used to contain all of the <i>Cordyceps sensu lato</i> species
Clavicipitaceous fungi	A general term for the members of the old Clavicipitaceae family, often used interchangeably with <i>Cordyceps sensu lato</i>
Clavicipitaceae (new family)	The current family which includes several grass symbiont genera, and does not include <i>Cordyceps</i>
Hypocrealean fungi	Fungi of the order Hypocreales, which contains the Clavicipitaceae

1.2 *CORDYCEPS MILITARIS*, THE ASCOMYCETE FUNGUS

1.2.1 The Ascomycetes – Form and Diversity

The fungal kingdom comprises an estimated 1.5 million species, with over 148,000 listed on Species Fungorum [Hawksworth 2001; Kirk 2020]. The largest phylum is the Ascomycota, commonly referred to as the ascomycetes, which includes over 64,000 species [Kirk *et al.* 2008; Moore *et al.* 2011]. This is a morphologically and ecologically diverse group of predominantly filamentous fungi, characterised by their production of sexual ascospores within specialised sac-like cells – asci (singular ascus) [Moore *et al.* 2011].

The ascomycete phylum is divided into several major classes each comprising fungal species with great morphological and nutritional diversity, such that mycologists were puzzled as to their evolutionary relationships until the age of molecular phylogenetics. The majority of these fall within the Pezizomycotina – the group containing most of the filamentous ascomycetes. Lichenised fungi, saprotrophs, mycorrhizae, endophytes, and pathogens of plants, other fungi and animals including humans are known nutritional modes of ascomycete species. Some of these, within their major classes, and with reference to morphological features, are listed in table 1.2 [Moore *et al.* 2011; Cannon & Kirk 2007; Webster & Weber 2007].

Regarding morphology, ascomycetes may be single celled (yeasts), moulds, or bear sexual fruiting bodies (ascocarps), or combinations of these (heteromorphic species) [Webster & Weber 2007]. Many species possess both asexual (anamorphic) and sexual (teleomorphic) stages in their life cycles.

Traditionally, the ascomycetes were divided into groups dependent on the form of their asci and fruiting bodies. Asci can be unitunicate or bitunicate (single or double walled). Further subtypes of unitunicate asci are based upon ascospore release – prototunicate asci release spores by wall degradation; operculate by the lifting of a lid structure, the operculum; and

inoperculate by the widening or a small pore or splitting of the ascus apex [Webster & Weber 2007].

Fruiting body types include the apothecium – a cup-shaped ascocarp; the perithecium – flask shaped with an ostiole or narrow opening for spore release; and the closed ascocarp types – the cleistothecium and gymnothecium, the latter being more loosely bound by hyphae. Finally, ascostromata are fruiting bodies in which asci are formed within locules – pre-developed spaces. These can be described sometimes as gymnothecia or pseudothecia – being similar in structure to cleistothecia and perithecia respectively but by contrast having bitunicate asci, and no organised hymenium (spore bearing surface) [Webster & Weber 2007]. Apothecial ascomycetes are traditionally known as discomycetes, and perithecial ones as pyrenomycetes.

In the case of *Cordyceps*, perithecia are formed on club-like stromata (singular stroma). Technically speaking, what is often termed the “fruiting body” is in fact this perithecial stroma, which bears the perithecia fruiting bodies [figure 1.4].

However, these features are only presented in half of the life cycle for many ascomycete species – the sexual phase (teleomorph). The asexual phase involves production of conidia (asexual spores), borne on specialised cells (conidiophores) by conidiogenesis. These are diverse in structure and dispersal process, but can broadly be divided into micro- and macroconidia – being undifferentiated or differentiated from the vegetative mycelium respectively [Webster & Weber 2007]. Conidia can sometimes be found in clumps (conidiomas), and conidiophores can form on stromata, even sometimes alongside sexual structures such as perithecia. The latter is the case in the example of *Xylaria hypoxylon* (candle snuff fungus) [figure 1.4].

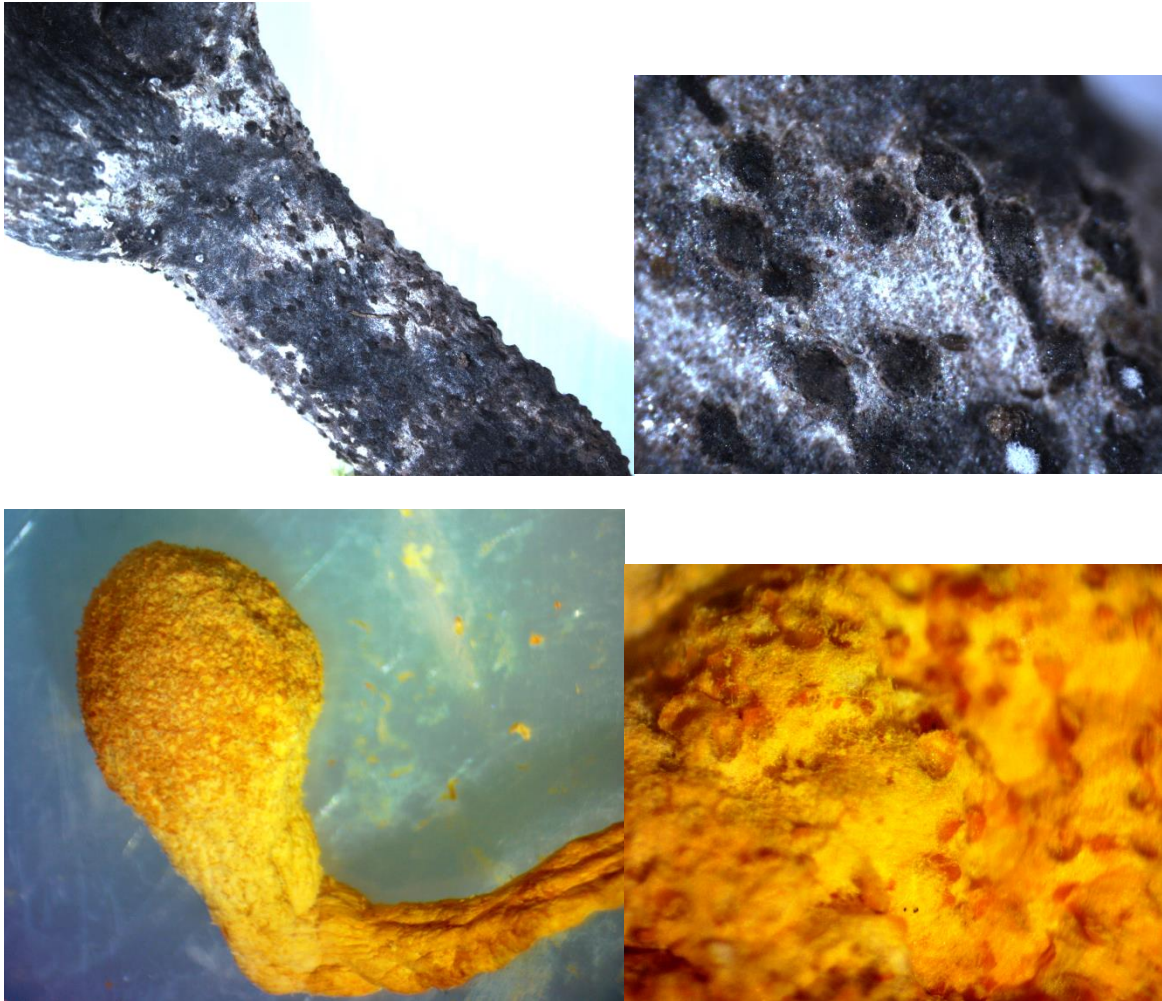


Figure 1.4: Stromata of *Xylaria hypoxylon* and *Cordyceps militaris* (top and bottom respectively). Both stromata bear perithecial fruiting bodies (magnified on the right); however the stroma of *X. hypoxylon* (top) is also covered with white conidia – making it a holomorphic structure – that being one which produced both sexual and asexual spores. Both species are members of the class Sordariomycetes. [Produced by the author.]

Table 1.2: Major classes of the ascomycetes within the Pezizomycotina, and their notable properties. [Moore *et al.* 2011; Cannon & Kirk 2007; Webster & Weber 2007]

Class (and traditional groups included)	Ecology	Notable genera	Ascus type(s)	Fruiting body type(s)
Pezizomycetes (operculate discomycetes)	Saprotrophs; ectomycorrhizae	<i>Peziza</i> , <i>Ascobolus</i> , <i>Aleuria</i> , <i>Morchella</i> , <i>Helvella</i> , <i>Tuber</i>	Operculate	Apothecia
Sordariomycetes (pyrenomycetes)	Saprotrophs; plant, animal, and fungal pathogens; endophytes	<i>Sordaria</i> , <i>Neurospora</i> , <i>Chaetomium</i> , <i>Lasiochaeria</i> , <i>Diaporthe</i> , <i>Ophiostoma</i> , <i>Magnaporthe</i> , Hypocreales [see later], <i>Xylaria</i> , <i>Daldinea</i>	Inoperculate and prototunicate	Perithecia and cleistothecia
Leotiomycetes (inoperculate discomycetes)	Saprotrophs; ericoid mycorrhizae; plant pathogens	<i>Cyttaria</i> , <i>Erysiphe</i> , <i>Blumeria</i> , <i>Chlorociboria</i> , <i>Bisporella</i> , <i>Bulgaria</i> , <i>Cudoniella</i> , <i>Leotia</i> , <i>Sclerotinia</i> , <i>Botrytis</i> , <i>Hymenoscyphus</i>	Inoperculate, prototunicate, and bitunicate	Apothecia and cleistothecia
Eurotiomycetes (loculoascomycetes)	Saprotrophs; lichenised fungi; animal and plant pathogens	<i>Verrucaria</i> , <i>Penicillium</i> , <i>Aspergillus</i> , <i>Elaphomyces</i> , <i>Onygena</i> , <i>Paracoccidioides</i>	Prototunicate and bitunicate	Perithecia, cleistothecia, and ascostromata
Dothideomycetes (loculoascomycetes)	Saprotrophs; endophytes; lichenised fungi; ectomycorrhizae; plant and animal pathogens	<i>Capnodium</i> , <i>Leptosphaeria</i> , <i>Alternaria</i> , <i>Pleospora</i> , <i>Epicoccum</i> , <i>Mycosphaerella</i> , <i>Cladosporium</i> , <i>Pseudogymnoascus</i>	Bitunicate	Ascostromata
Lecanoromycetes (lichens)	Lichenised fungi	<i>Lecanora</i> , <i>Peltigera</i> , <i>Xanthoria</i> , <i>Caloplaca</i>	Inoperculate, prototunicate, and bitunicate	Apothecia and perithecia
Laboulbeniomycetes	Arthropod parasites	<i>Laboulbenia</i> , <i>Hesperomyces</i>	Prototunicate	Perithecia
Orbiliomycetes	Carnivorous	<i>Orbilbia</i>	Inoperculate	Apothecia

As presented in table 1.2, there is great diversity in ascomycete ecology even within phylogenetic groups. Ascomycete life cycles can consist of both sexual and asexual phases – and this can be of great importance with respect to ecological differences between the teleomorph and anamorph forms of a species. A typical life cycle is shown in figure 1.5.

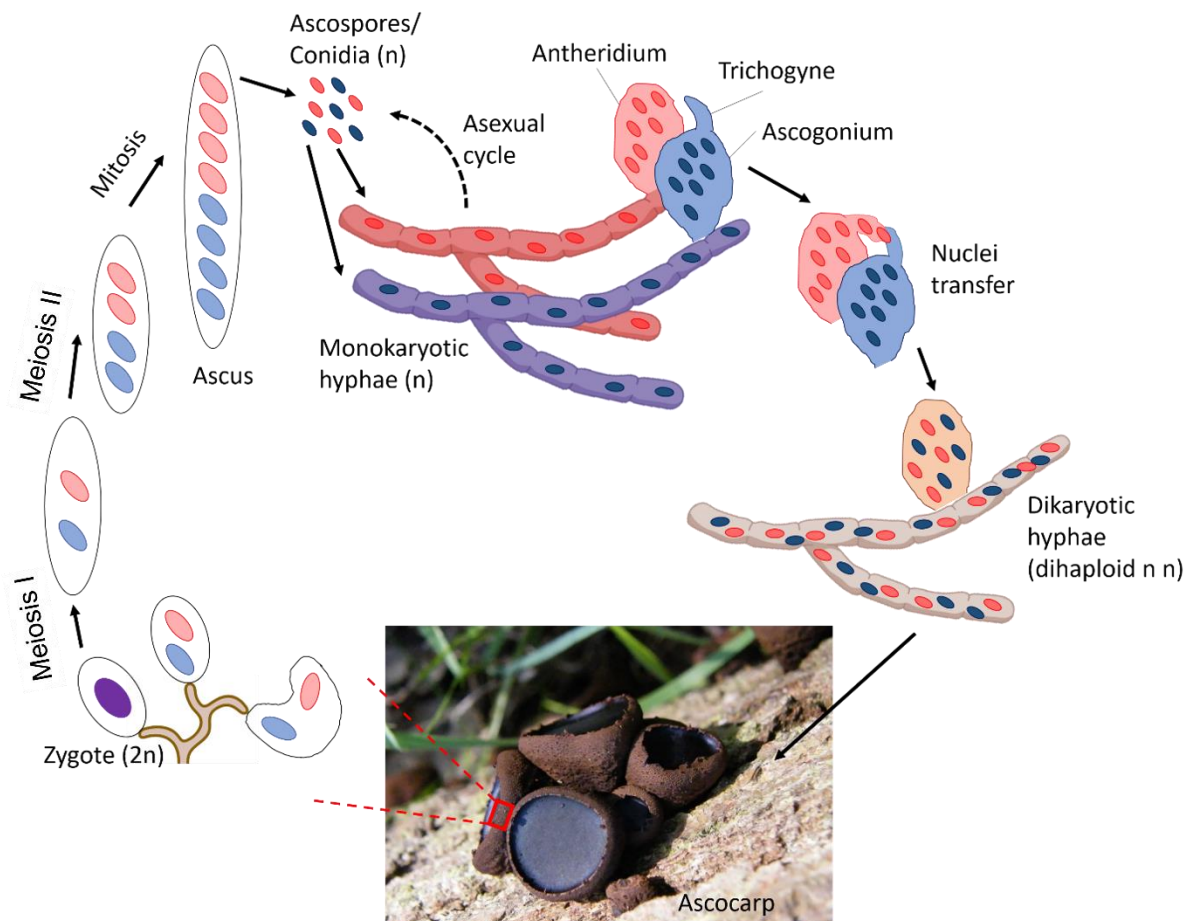


Figure 1.5: The typical life cycle of an ascomycete [produced by author]. The species pictured is *Bulgaria inquinans*, an inoperculate discomycete commonly found in the UK. The fruiting body (ascocarp) is in this case an apothecium, which is partially consistent of dikaryotic hyphae, in which cells contain the haploid nuclei from parents of different mating types (dihaploid). Nuclear fusion (karyogamy) occurs resulting in the formation of a zygote, which subsequently undergoes meiosis and mitosis twice to form haploid ascospores. These sexual spores are released from the ascus, and can germinate to form a haploid monokaryotic mycelium. When two haploid mycelia, of different mating types, meet, nuclei can be transferred from one into the other, to form a dikaryotic mycelium.

Modern Ascomycete Classification

No longer based upon morphology, modern classification of the ascomycetes and other fungi has been constructed using molecular phylogenetics, since the first use of ribosomal DNA (rDNA) loci around thirty years ago [White *et al.* 1990]. More recently, studies have used sequences from multiple loci – including small and large subunit rDNA, 5.8S rRNA (ribosomal RNA), and relatively-conserved gene loci such as *Actin* and *Calmodulin* [e.g. James *et al.* 2006]. A classification of the fungi at a phylum-based level is laid out in a seminal paper [Hibbett *et al.* 2007]. Closely-related fungal strains, usually within a species, can be compared using other genetic techniques, such as RFLP (restriction fragment length polymorphism – which involves digestion of a total DNA extract sample) and RAPD (random amplified polymorphic DNA – which involves the unspecific binding of short DNA primers to multiple loci resulting in the amplification of multiple sites). RAPD is hence a type of PCR-based technique. Another PCR-based technique, used often to identify species or genus from a fungal DNA sample, is ITS amplification and sequencing. ITS (internal transcribed spaces) sequences separate 18S, 5.8S, and 26S/28S regions of rRNA regions [White *et al.* 1990; shown in figure 1.6].

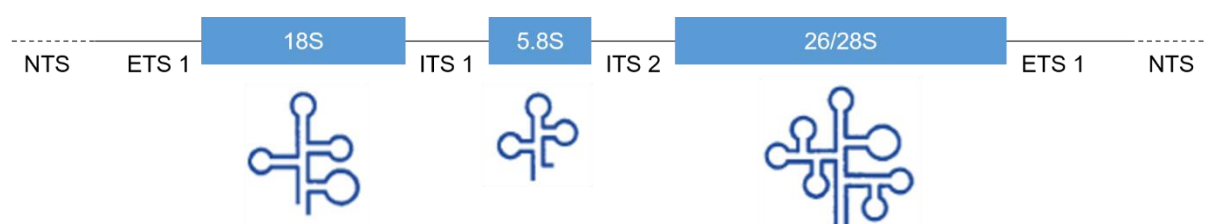


Figure 1.6: Arrangement of ribosomal DNA (above), showing non-, external- and internal transcribed spacers (N/E/ITS), and the sizes of RNA fragments from the regions separated by ITS sequences. Below are the formations of RNA, after the transcription, splicing and folding of RNA from the respective rDNA regions. [Adapted from Webster & Weber 2007].

Anamorphs and Teleomorphs

There are many examples of ascomycete fungal species with starkly different anamorphic and teleomorphic phases – some of these are presented in table 1.3. Understanding the processes behind sexual development in ascomycetes is therefore of great importance, for example because differences in morphology and biochemistry of closely related anamorphic and teleomorphic species or forms of the same species may greatly affect their abilities to infect hosts.

In some cases, manipulating such properties can result in the finding of so-called “cryptic species” – teleomorphic phases of fungal species which were previously thought to have been exclusively asexual, and can also enable new crosses of fungal strains important in biotechnology, to enable strain improvement, which has been reviewed [Ashton & Dyer 2016]. There may also be applications in aiding the fight against ascomycete plant pathogens, and utilisation or improvement of insect pathogenic fungi for use in pest control from crops.

Table 1.3: Examples of related teleomorphic and anamorphic genera in various ascomycete taxa [adapted from Webster & Weber 2007; Kirk 2020]

Fungal taxon	Teleomorphic genera	Teleomorph description	Anamorphic genera	Anamorph description	Dimorphic species example
Trichocomaceae "aspergilli"	<i>Petromyces</i> , <i>Eurotium</i> , <i>Emericella</i>	Cryptic cleistothecial forms	<i>Aspergillus</i> , <i>Penicillium</i>	Moulds – saprotrophs and human pathogens	<i>Aspergillus</i> / <i>Emericella</i> <i>nidulans</i>
Onygenaceae	<i>Onygena</i> , <i>Amauroascus</i> , <i>Ajellomyces</i>	Cage-like gymnothecia. Saprotrophs and animal pathogens growing on bones and feathers	<i>Paracoccidioides</i> , <i>Blastomyces</i>	Saprotrophs and human pathogens	<i>Ajellomyces</i> / <i>Blastomyces</i> <i>dermatidis</i>
Elaphomycetaceae	<i>Elaphomyces</i> , <i>Monascus</i>	Cleistothecial hypogeous false truffles; moulds	<i>Basipetospora</i>	Moulds	
Nectriaceae	<i>Nectria</i> , <i>Giberella</i>	Perithecial saprotrophs; plant pathogens	<i>Fusarium</i> , <i>Verticillium</i> , <i>Cylindrocarpon</i>	Plant pathogens	<i>Nectria radiculicola</i> / <i>Cylindrocarpon</i> <i>destructans</i>
Hypocreaceae	<i>Hypocrea</i>	Perithecial stromata. Saprotrophs and plant pathogens	<i>Trichoderma</i>	Endophytes and plant pathogens	
Cordycipitaceae	<i>Cordyceps</i>	Perithecial stromata. Insect and fungal pathogens	<i>Beauveria</i> , <i>Metarhizium</i> , <i>Isaria</i> , <i>Lecanicillium</i>	Insect pathogens and endophytes	<i>Beauveria</i> / <i>Cordyceps</i> <i>bassiana</i>
Pleosporales	<i>Leptosphaeria</i> , <i>Phaeosphaeria</i>	Pseudothecial saprotrophs and plant pathogens	<i>Stagonospora</i> , <i>Phoma</i>	Saprotrophs and plant pathogens	<i>Leptosphaeria</i> / <i>Phoma acuta</i>
Mycosphaerellaceae	<i>Mycosphaerella</i>	Pseudothecial plant pathogens	<i>Zymoseptoria</i> , <i>Cladosporium</i> , <i>Cercospora</i>	Plant pathogens	<i>Mycosphaerella</i> <i>graminicola</i> / <i>Zymoseptoria tritici</i>
Sclerotiniaceae	<i>Sclerotinia</i> , <i>Botryotinia</i>	Apothecial plant pathogens and saprotrophs	<i>Botrytis</i>	Endophytes and plant pathogens	<i>Botrytis</i> <i>cinerea</i> / <i>Botryotinia</i> <i>fuckeliana</i>

1.2.2 Sexual Biology of the Ascomycetes and *C. militaris*

Given the importance of understanding fungal sexuality and the developmental differences between anamorph and teleomorph stages of fungal life cycles, this has been a particular focus of research in mycology in recent years. Much of this research has been carried out with regard to the aspergilli group of fungi – specifically the genus *Aspergillus*. Some of the species in this genus are of great economic importance – for example *A. niger* is used for the industrial production of citric acid, and *A. fumigatus* is a pathogen infecting the respiratory system in immune-compromised humans [Karaffa & Kubicek 2003; Zureik *et al.* 2002]. Meanwhile, *A. nidulans* (teleomorph *Emericella nidulans*) is a model species for studying sexual development [Bayram & Braus 2012].

Mating Types in the Pezizomycotina

Within the sexual cycle (teleomorph phase) of ascomycetes within the Pezizomycotina, the ability of two individuals to mate depends on mating-type identities. These are determined by mating-type loci (called *MAT* loci), typically which consist of two types – *MAT1-1* and *MAT1-2* or positive (+) and negative (-) as they are labelled in some cases. These are not different alleles, but rather referred to as idiomorphs, due to large sequence variations [Metzenberg & Glass 1990]. Protein domains encoded by these sequences are the α 1 domain (*MAT1-1-1* gene on the *MAT1-1* locus) and the MATA_HMG domain (high mobility group – *MAT1-2-1* on the *MAT1-2* locus) [Debuchy *et al.* 2010]. Uses of sexual reproduction in ascomycete fungi are reviewed [Ashton & Dyer 2016]. A useful example is strain improvement by the sexual crossing of useful closely-related parent strains, to enhance productivity in fungal biotechnological processes such as citric acid production.

The Velvet Family of Proteins

Key in sexual development of fungi are the velvet genes, encoding the velvet family of proteins, which are highly conserved in the ascomycetes. The velvet family of proteins were first discovered in the *Aspergillus* species. They play key roles in regulating sexual

development and secondary metabolism in response to abiotic stimuli such as light (reviewed by Bayram & Braus 2012). Often acting in protein complexes, VeA, VelB, VelC (velvet proteins A, B, C) VosA (variability of spores A), are subject to control by non-velvet protein master regulator LaeA (loss of *afIR* expression A) [Bayram *et al.* 2010]. They, as well as LaeA, which is a methyltransferase, are conserved across the ascomycetes and also known in some basidiomycetes [Bayram & Braus 2012]. These protein interactions among different velvet proteins and with LaeA, as well as with transcription factors such as SteA, help mediate responses from signal transduction pathways, such as the MAP kinase pathway [Bayram & Braus 2012].

The members of the velvet family of proteins share a roughly 150 amino acid-length velvet domain, which is proposed to be involved in protein-protein interactions – forming velvet protein heterodimers, for example VelB-VosA and VelA-Vel-B [Bayram *et al.* 2010]. The origin of the velvet proteins is believed to be an ancient one; the velvet domain being conserved in distantly related fungi to the ascomycetes such as chytrids [Bayram & Braus 2012]. Table 1.4 presents some currently known functions of velvet protein dimers in *Aspergillus nidulans*.

Table 1.4: Currently-known functions of various velvet protein dimers in the model species *Aspergillus nidulans* [adapted from Bayram & Braus 2012].

Heterodimer	Downstream function	External stimulus; notes
VosA-VelB	Supports spore viability; represses asexual development	Inhibited by light; blocked by LaeA
VelB-VelB	Unknown	
VelB-VelA	Formation of fruiting body; secondary metabolism coordination – through interaction with LaeA	Inhibited by light; imported into the nucleus by KapA α -importin

Other Genes Involved in Sexual Development

The velvet genes are not the only examples of genes known to be involved in sexual development which have come to attention from studies on cryptic sexuality in the aspergilli. The activities velvet proteins represent an early set of steps leading on from the receipt for

environmental stimuli, in the complex system of sexual development. Proposed to be downstream of the velvet proteins are products encoded by the *MAT* loci, and sexual pheromones, their precursors and their receptors [Dyer & O’Gorman 2011]. Proteins engaging in signal transduction – for example MAP kinases, G protein-coupled receptors, and transcription factors also are involved in sexual development, as activators and repressors. At the later stages of sexual development, factors required for ascospore maturation and production have also been described [Dyer & O’Gorman 2011]. A summary of the sexual development genes relevant to the experiments in the study is provided in table 1.5.

Table 1.5: Genes involved in sexual development, including those assessed in the experiments later [adapted from Dyer & O’Gorman 2011].

Gene	Encoded Protein	Role in Sexual Development	Reference
<i>LaeA</i>	Methyl transferase	Response to light/dark stimuli	Bayram <i>et al.</i> 2010
<i>VeA</i>	Velvet complex protein	Response to light/dark stimuli	Kim <i>et al.</i> 2002
<i>VosA</i>	Velvet complex protein	Response to light/dark stimuli; trehalose production	Ni & Yu 2007
<i>MAT 1</i>	Mating type (alpha)	Mating processes, signal transduction	Paoletti <i>et al.</i> 2007
<i>MAT 2</i>	Mating type (a/HMG)	Mating processes, signal transduction	Paoletti <i>et al.</i> 2007
<i>PreA</i>	Transmembrane G protein-coupled receptor	Receptor for alpha-type pheromone	Dyer <i>et al.</i> 2003; Seo <i>et al.</i> 2004
<i>PreB</i>	Transmembrane G protein-coupled receptor	Receptor for a-type pheromone	Dyer <i>et al.</i> 2003; Seo <i>et al.</i> 2004
<i>Ste7</i>	MAP kinase kinase	Signal transduction, downstream of pheromone receptors	Paoletti <i>et al.</i> 2007
<i>SteA</i>	Transcription factor with zinc finger and homeodomain	Signal transduction, downstream of pheromone receptors	Vallim <i>et al.</i> 2000

Sexual Toolkit Genes

More highly conserved still, present in the many of eukaryotes, are the sexual “toolkit” genes – those involved in the process of meiosis [Schurko & Logsdon 2008]. These are largely involved in cellular processes needed for meiosis, and have been targeted with PCR primers

to find evidence for sexuality in species previously thought only to reproduce asexually. Examples of these are described in table 1.6.

Table 1.6: Sexual toolkit genes [adapted from Schurko & Logsdon 2008].

Gene	Encoded Protein	Role in Sexual Reproduction	Reference
<i>Msh4</i>	Mismatch repair mutS (bacteria) homolog	Holliday junction arrangement, as a heterodimer with Msh5	Kolas <i>et al.</i> 2004
<i>Spo11</i>	Topoisomerase VI subunit (archaeobacterial) homolog	Creates double strand breaks required for recombination	Bergerat <i>et al.</i> 1997; Keeney <i>et al.</i> 1997
<i>Rec8</i>	Paralog of Rad21 – part of cohesin	Part of cohesin protein complex before meiotic anaphase	Haering <i>et al.</i> 2003

Homo/Heterothallism of C. militaris

C. militaris has been indicated as both homothallic (able to self-mate, possessing both required mating-type (*MAT*) loci) and heterothallic (possessing only one mating-type locus) in different studies, with experiments involving different strains reaching contradicting conclusions. For example, Shrestha and colleagues confirmed the production of viable stromata when single spores of different mating types were inoculated at opposite sides of an agar plate, with strains unable to produce stromata bearing perithecia with one mating type present, whilst Zheng and colleagues showed the same effect by injection of caterpillars with suspensions of mixtures of conidia from each mating type – only sterile, perithecia-lacking stromata were formed when conidia of only one mating type were injected [Shrestha *et al.* 2004; Zheng *et al.* 2011]. In contrast, Wen *et al.* claimed that at least some strains are homothallic, by producing fruiting bodies from single conidial isolates, and also by screening strains for mating-type (*MAT*) loci in a genomic method using previously-described [Yokoyama *et al.* 2004] degenerate primers [Wen *et al.* 2004; 2017]. Several other studies have demonstrated the heterothallism of *C. militaris* [shown in table 1.9], and the evidence more strongly supports this case.

Across the ascomycetes, heterothallic and homothallic species are described, with mode switching and variability within lineages – and the *Cordyceps sensu lato* are no exception [Zheng *et al.* 2013]. The haploid nuclei of a heterothallic species contain either only the *MAT 1-1* gene or genes (encoding a protein with a high mobility group DNA-binding domain) or the *MAT 1-2* gene (encoding a protein with an alpha box motif), whilst haploid nuclei of homothallic species contain both. *MAT 1-1-1* and *MAT 1-1-2* (variations of the *MAT 1-1*) gene, and *MAT 1-2-1* (*MAT 1-2*) genes have been described in *C. militaris*, with a mixture of orthologs in related species [Zheng *et al.* 2013, see figure 1.7]. It has been proposed that single-spore *C. militaris* cultures able to form viable stromata are themselves already dikaryotic, containing haploid nuclei of opposite mating types, rather than being monokaryotic homothallic strains [Wen *et al.* 2012] (this could explain the findings for example by Wen *et al.* 2017); and that strains showing degeneration (characterised by an inability to produce fruiting bodies) have lost one of the pair of haploids possessing one of the mating-type loci needed. However, strains with both mating types have been also found to be unable to produce viable stromata. The issue of degeneration is a complex one which will be discussed further later. There is also a possibility that the global *C. militaris* is a complex of similar species, and that homo- and heterothallism varies within this group.

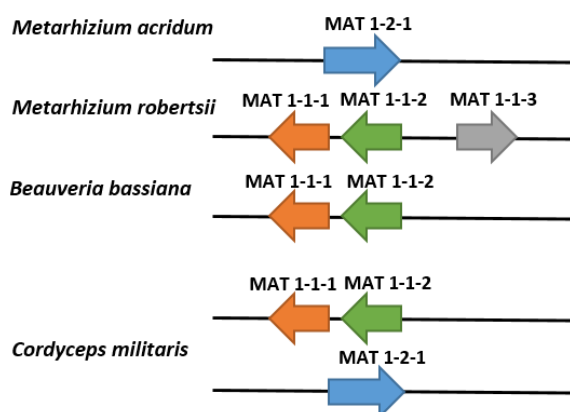


Figure 1.7: *MAT* gene orthologs described in relatives of *C. militaris* (*Metarhizium* and *Beauveria*) within the *Cordyceps sensu lato* [adapted from Zheng *et al.* 2013]. These authors are describing *C. militaris* as a heterothallic species.

1.2.3 Genomics and Transcriptomics of *C. militaris*

Zheng and colleagues sequenced the genome of *C. militaris* and found it to be 32.2 Mb in size [Zheng *et al.* 2011]; and in a study using three strains of *C. militaris*, Chen and colleagues sequenced the 32.57 Mb genome [Chen *et al.* 2019]. This is smaller than those of relatives *Metarhizium anisopliae* (39.0 Mb) and *Metarhizium acridum* (38.1 Mb). 9,684 protein-encoding genes have been predicted in the genome, and 102 pseudogenes [Zheng *et al.* 2011]. Wang and colleagues showed through karyotype analysis that there are seven chromosomes, of sizes between 2.0 and 5.7 Mb [Wang *et al.* 2010]. Many genes were found from this dataset based on sequence similarities, including some velvet proteins and transcription factors involved in regulating sexual development.

Zheng and colleagues used *Agrobacterium*-mediated transformation of *C. militaris* to investigate several genes for their involvement in stomata formation. By finding T-DNA insertion sites in loss-of-function mutants, they identified the involvement of serine/threonine phosphatase in *in vivo* stomata formation, and ubiquitin-like activating enzyme, cytochrome oxidase subunit I, and ATP-dependent helicase in *in vitro* formation [Zheng *et al.* 2015].

Investigating transcriptomes of *Cordyceps militaris* at different stages in development can also lead to better understanding of the host infection process. Transcriptomes of *C. militaris* mycelium and stroma were obtained by high-throughput illumina sequencing, revealing the upregulation of 2,113 genes in the mycelium and 599 in the stroma [Yin *et al.* 2012]. GO (Gene Ontology) and KEGG (Kyoto Encyclopedia of Genes and Genomes) analyses were used to ascertain differences in expression between stages of development, and between fungal cultures on different media types.

Chen and colleagues investigated the transcriptomes of three strains of *C. militaris* using single-molecule real-time (SMRT) sequencing technology and by building a C-DNA library. The authors also assessed the methylome of *C. militaris*, using molecular weight determination of nucleotides by LC-MS, with an ion trap time of flight (IT-TOF) mass analyser.

From molecular weight types the authors deduced not only the occurrence of methylated adenosine and cytosine in the genome, but also mG and mT [Chen *et al.* 2019]. The major DNA methylation motifs found were: GA and GGAG for deoxyadenosine methylation (m6dA methylation) and GC and CG/GC for cytosine methylation (m4C methylation) [see figure 1.8]. Methylation could be an influential force in the plasticity of this species in its life cycle, underlying epigenetic changes in gene expression.

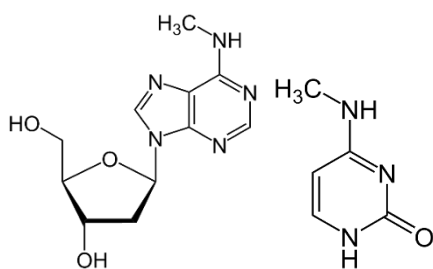


Figure 1.8: Methylation modifications underlying epigenetic changes in *C. militaris* [Chen *et al.* 2019]. Left: N6-methyldeoxyadenosine (m6dA); right: N4-methylcytosine (m4C).

1.3 CORDYCEPIN AND RELATED METABOLITES

1.3.1 Cordycepin and Pentostatin – Background and Research

Cordycepin

Cordyceps militaris is well known for the production of cordycepin, or 3'-deoxyadenosine, a secondary metabolite and nucleoside analogue [Cunningham *et al.* 1950]. Traditionally used in Chinese herbal medicine [Shrestha *et al.* 2012], *Cordyceps* and species from related genera including the widely-used *Ophiocordyceps sinensis* have been in more recent times subject to a great deal of pharmacological scientific research mainly focusing on cordycepin, with a great increase in the rate of papers published over the last decade [figure 1.10]. Although

traditionally consumed in fruiting bodies, in research cordycepin was originally extracted by the filtration of a *Cordyceps militaris* culture grown from conidia [Cunningham *et al.* 1950].

Cordycepin is a polyadenylation inhibitor [Kondrashov *et al.* 2012], acting to decrease the lengths of mRNA poly(A) tails. It has been shown to have immune-modulating effects on both mammalian [Kondrashov *et al.* 2012] and insect cells [Kim *et al.* 2006; Woolley *et al.* 2020]. Evidence for anti-inflammatory properties have been demonstrated [e.g. Ashraf *et al.* 2019], as well as effects on signal transduction pathways [e.g. Hawley *et al.* 2020]. Less explored are the potential agricultural applications of cordycepin as an insect biocontrol agent, given evidence for its influence on insect immune systems [Woolley *et al.* 2020]. Cordycepin is converted to cordycepin triphosphate [figure 1.9] after entry into the cell, this being the molecule which performs its functional activity [Desrosiers *et al.* 1976].

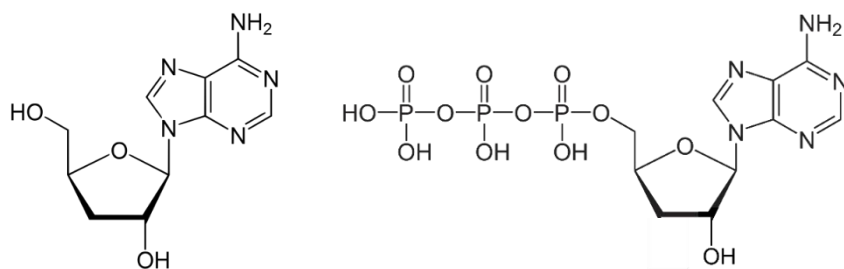


Figure 1.9: Structures of cordycepin (left) and cordycepin triphosphate (right) [Cunningham *et al.* 1950; Karlson 1984]

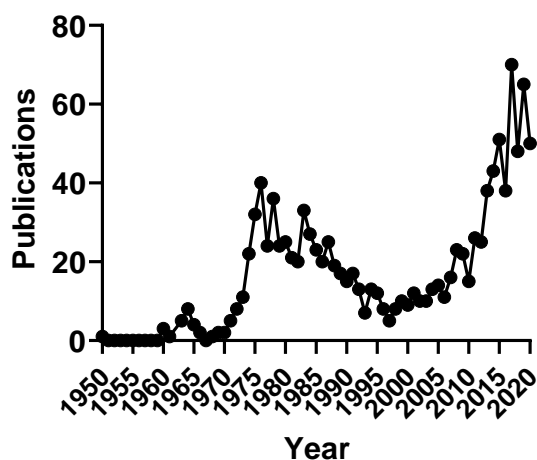


Figure 1.10: Numbers of publications about cordycepin per year between 1950 and 2018 [taken from Radhi *et al.* 2021]

Effects of Cordycepin in Vertebrate Models

Evidence for anti-inflammatory activity of cordycepin in vertebrate models is compelling, with no fewer than 36 papers describing cordycepin causing reductions in inflammatory products [Radhi *et al.* 2021]. These products include cytokines (e.g. TGF β , TNF and IL1 β), prostaglandin synthases, genes involved in tissue remodelling, cell migration, and metalloproteinases. In multiple studies [e.g. Choi *et al.* 2014; Cui *et al.* 2018], cordycepin has been reported to reduce translocation of the transcription factor NF κ β to the nucleus [Radhi *et al.* 2021]. Triggered by inflammatory signalling cascades, this translocation is key for the activation of genes involved in inflammation [Mitchell & Camody 2018]. Anti-inflammatory properties are of medicinal importance due to the undesired role of inflammation in chronic pain [Ji *et al.* 2016] – manifesting in conditions such as arthritis – as well as neurodegeneration [Heppner & Becher 2015], cancer metastases [Piotrowski *et al.* 2020], and age-related diseases [Wyss-Coray 2016].

There is a large amount of evidence for effects of cordycepin on signal transduction pathways – particularly the PI3K/AKT (phosphatidylinositol 3-kinase/ protein kinase B), mTOR (mammalian target of rapamycin), AMPK (5'-adenosine monophosphate kinase), and MAPK (mitogen-activated protein kinase) pathways, typically in cell culture models – immune cells, neuronal cells, and cancer cell lines [Radhi *et al.* 2021]. AKT and mTOR are downstream effectors of PI3K, and together their intertwined pathways regulate processes including growth, angiogenesis, cell migration and differentiation – with roles in cancer and neurodegenerative diseases [Chamcheu *et al.* 2019; Gong *et al.* 2018]. For example, cordycepin has been shown to inhibit phosphorylation of AKT at the important site of serine residue 473 by mTORC – preventing the maximised activation of this family of kinases [e.g. Pan *et al.* 2015]. Multiple studies also show that cordycepin increases phosphorylation of the threonine 172 site of AMPK [e.g. Bi *et al.* 2018], a modification which greatly stimulates its activity and thus has effectors on the regulation of cellular energy homeostasis.

Cordycepin and Pentostatin Biosynthesis

In *C. militaris*, cordycepin is produced along with stabilising molecule pentostatin with the genes encoding enzymes for the biosynthesis of both metabolites (names *Cns1*, *Cns2*, and *Cns3* for cordycepin; *Cns3* for pentostatin) present on the same gene cluster, along with the pentostatin exporter-encoding gene *Cns4* [Xia *et al.* 2017, see figure 1.11]. Analogues of these genes for cordycepin and pentostatin synthesis have also been found in *Cordyceps kyushuensis* – named *Ck1-4* [Zhao *et al.* 2019], as well as more distantly related fungi *Acremonium chrysogenum* and *Aspergillus nidulans* [Xia *et al.* 2017]. Pentostatin prevents the deamination of cordycepin by suppressing the activity of adenosine deaminase (ADA) which converts cordycepin (3'-deoxyadenosine) into 3'-deoxyinosine, an inactive molecule, in the same way which it does adenosine in purine metabolism; it has been proposed that *C. militaris* itself uses this as a detoxification process for its own metabolite. This repression is lifted when levels of cordycepin which are toxic to the fungus are reached [Xia *et al.* 2017]. Pentostatin, or 2'-deoxycoformycin, originally discovered in and isolated from *Streptomyces antibioticus* [Hanvey *et al.* 1984], is also an adenosine analogue [Xia *et al.* 2017].

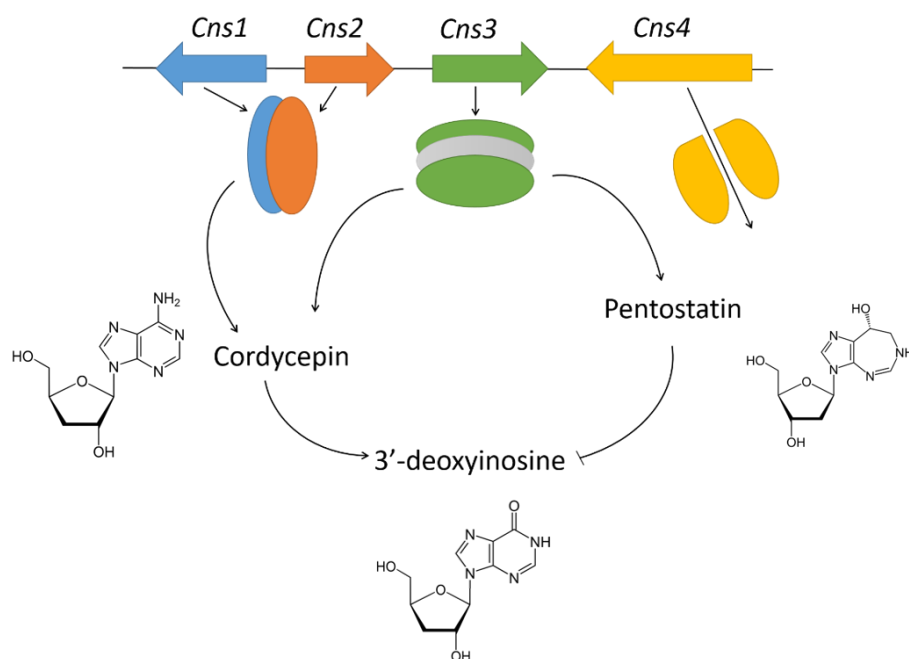


Figure 1.11: Simplified diagram of the *Cns* gene cluster, responsible for cordycepin and pentostatin synthesis [adapted from Xia *et al.* 2017]

Given that the precursor to cordycepin [Lennon & Suhadolnik 1976; Suhadolnik *et al.* 1964] and also to pentostatin [Hanvey *et al.* 1984] is adenosine, Xia *et al.* proposed a biosynthetic pathway for both metabolites starting with the formation of 3'-AMP (adenosine-3'-monophosphate) by the phosphorylation of 3'-OH on adenosine by Cns3 kinase activity [Xia *et al.* 2017]. Following this, Cns2 catalyses the dephosphorylation of 3'-AMP to 2'-C-3'-dA (2'-carbonyl-3'-deoxyadenosine), before conversion to cordycepin by oxidoreduction by Cns1 [Xia *et al.* 2017]. The Cns3 has been described as a bifunctional protein – possessing two domains of interest. Besides the nucleotide kinase domain (near to the N terminus), there is a HisG domain (C terminus) [Xia *et al.* 2017]. The presence of the latter domain on Cns3 suggests a role in the synthesis of pentostatin, by a pathway similar to that of the initial steps in the biosynthesis of L-histidine [Hanvey *et al.* 1988; Xia *et al.* 2017]. The hypotheses put forward by Xia *et al.* were corroborated by Chen and colleagues, in a study where cordycepin production by *C. militaris* was enhanced by the addition of L-alanine to cultures. Using both RNA-seq and RT-qPCR, the authors demonstrated the upregulation of the genes *Cns1*, *2*, and *3*, as well as the proposed pentostatin exporter-encoding *Cns4* [Chen *et al.* 2020]. Yin *et al.* had previously proposed a similar pathway for cordycepin synthesis and the genes for enzymes involved in the synthesis were upregulated in the mycelium. These included genes coding for adenosine kinase, adenosine deaminase, AMP deaminase, ribonucleotide reductase, purine nucleosidase, pyruvate kinase, 5'-nucleotidase, and adenylosuccinate lyase; whereas only adenylosuccinate lyase and purine nucleoside phosphorylase were upregulated in the stroma [Yin *et al.* 2012]. Data obtained from qPCR showed similarities to the transcriptome data but there were some discrepancies with expression profiles in mycelia and stromata, and expression of genes relevant to cordycepin biosynthesis varied between different strains [Yin *et al.* 2012].

Evolution of Cordycepin Synthesis in Cordyceps

The findings by Xia *et al.* have implications for the understanding of the evolution of cordycepin production in fungi, with applications for the use of fungi related to *C. militaris*, as we discussed

in a recent editorial paper [Wellham *et al.* 2019]. The failure of the authors to detect the production of cordycepin in closely related species – including *Ophiocordyceps sinensis*, *Metarhizium robertsii*, *M. rileyi*, *Isaria fumosorosea*, *Beauveria bassiana* and other *Cordyceps sensu lato* species – is consistent with the lack of cordycepin biosynthesis genes in these other fungi [Wellham *et al.* 2019]. In *O. sinensis*, cordycepin biosynthesis has been proposed to be the result of another fungus in turn colonising it – *Paecilomyces hepiali* – which has had its genome sequenced and is a member of the order Eurotiales (Eurotiomycetes) [Yu *et al.* 2016]. This could be the reason for the contradiction with previous studies [Huang *et al.* 2003; Wellham *et al.* 2019]. The presence of cordycepin production in *Aspergillus nidulans* (Eurotiales, Eurotiomycetes), a phylogenetically-distant species and *Acremonium chrysogenum* lends to the hypothesis that the pentostatin-cordycepin biosynthesis system has been passed between different species by horizontal gene transfer [Wellham *et al.* 2019]. However, the production and function of cordycepin in these species has not been studied in detail.

In a study by Vongsangnak *et al.*, consisting of 894 metabolites and 1,267 metabolic reactions, a genome-scale metabolic network was assembled for *Cordyceps militaris*, considering processes in the extracellular space, cytoplasm, cell membrane, mitochondria, and peroxisome [Vongsangnak *et al.* 2017]. A notably but predictably-high presence of polysaccharide, lipid and protein-degrading enzymes were detected [Vongsangnak *et al.* 2017], adaptations to invading insect cuticles [Zheng *et al.* 2013]. The authors proposed a lack of the ribonucleotide reductase inhibitor-encoding gene as a factor contributing to the high production of cordycepin by *Cordyceps militaris*. A phylogenetic gene tree for eight notable enzymes in the cordycepin synthesis pathway showed that the sequences were phylogenetically distinct in *Cordyceps militaris* compared to closely-related species *Beauveria bassiana*, *Cordyceps brongniartii*, and others [Vongsangnak *et al.* 2017]. This suggests that the gene sequences for these species share a common ancestor whilst those for *Cordyceps militaris* form a separate lineage, in contrast to the established overall species phylogeny

[Vongsangnak *et al.* 2017]. Perhaps horizontal gene transfer event(s) could reason this phenomenon.

We proposed that the evolution of the “protector-protégé” system of pentostatin and cordycepin production is a result of the entomopathogenic activities of *Cordyceps*, and the evolutionary pressures associated. The function of cordycepin in ecology could be as a repressor of the insect immune system [Wellham *et al.* 2019]. Cordycepin has been described as the proximate cause of death in the insect host [Kim *et al.* 2002]. These properties could be relevant for the development of novel biological control methods for insect pests of crops [Wellham *et al.* 2019].

Vidarabine and Other Nucleoside Analogues

The cordycepin-pentostatin protector-protégé co-production system in *C. militaris* and others is not the only known example of safeguarding of a nucleoside analogue by pentostatin. Arabinofuranosyladenine (Ara-A), also known as vidarabine [see figure 1.12], is produced by the bacterium *Streptomyces antibioticus* and also by the soft coral *Eunicella (Gorgonia) cavolini* [Farmer & Suhadolnik 1972; Cimino *et al.* 1984]; but was previously synthesised artificially with arabinofuranosylcytosine (Ara-C) following the discovery of arabinofuranosylthymine/ spongothymidine (Ara-T) and arabinofuranosyluracil/ spongouridine (Ara-U) in the demosponge *Tectitethya (Cryptotethya) crypta* [Mayer *et al.* 2010]. Vidarabine is used as an antiviral agent particularly against herpes viruses as well as a leukaemia drug [Farmer & Suhadolnik 1972; Mayer *et al.* 2010]. Like cordycepin, vidarabine requires phosphorylation for functionality, and is active as vidarabine phosphate [Mayer *et al.* 2010]. Pentostatin is also produced by *S. antibioticus* – the species in which the metabolite was discovered [Kodama *et al.* 1979]. As well as being an adenosine deaminase (ADA) inhibitor and thus a safeguarding molecule for vidarabine (and cordycepin elsewhere), pentostatin has been used as a cancer drug against several forms of leukaemia [Showalter *et al.* 1992]. Wu *et al.* showed that *S. antibioticus* produces these two metabolites in a protector protégé strategy similar to *C. militaris* and others by having genes essential to their synthesis, in two independent metabolic

pathways, present in a single biosynthetic gene cluster. The authors confirmed this by using a mutant with the gene cluster deleted compared to wild type *S. antibioticus* and an LC-MS assay of vidarabine and pentostatin [Wu *et al.* 2017]. Like the cordycepin-pentostatin cluster in *C. militaris*, the vidarabine-pentostatin cluster in *S. antibioticus* contains oxidoreductase(s), an ATP phosphoribosyltransferase, a phosphohydrolase, and a SAICAR synthetase [Wu *et al.* 2017]. Hence the authors also support the hypothesis of the similarity of pentostatin biosynthesis to the early steps of L-histidine [Xia *et al.* 2017; Wu *et al.* 2017]. Wu *et al.* proposed a vidarabine synthesis pathway involving the oxidation of adenosine to 2'-ketodeoxyadenosine (2'-keto dA) and subsequently the reduction to vidarabine, both performed by (an) oxidoreductase(s). The authors also found the presence of arabinofuranosylhypoxanthine (Ara-I) in *S. antibioticus*, which they propose to be formed by deamination of vidarabine by host ADA [Wu *et al.* 2017].

In addition to the cordycepin-pentostatin and vidarabine-pentostatin production systems, other examples of nucleoside analogue-antibiotic pairs have been discovered [Wu *et al.* 2017] – such as coformycin and formycin in bacteria *Nocardia interforma* and *Streptomyces kaniharaensis* [Nakamura *et al.* 1974] and 2'-Cl pentostatin and 2'-amino-2'-deoxyadenosine in the bacterium *Actinomadura* [Suhadolnik *et al.* 1989] [see figure 1.12].

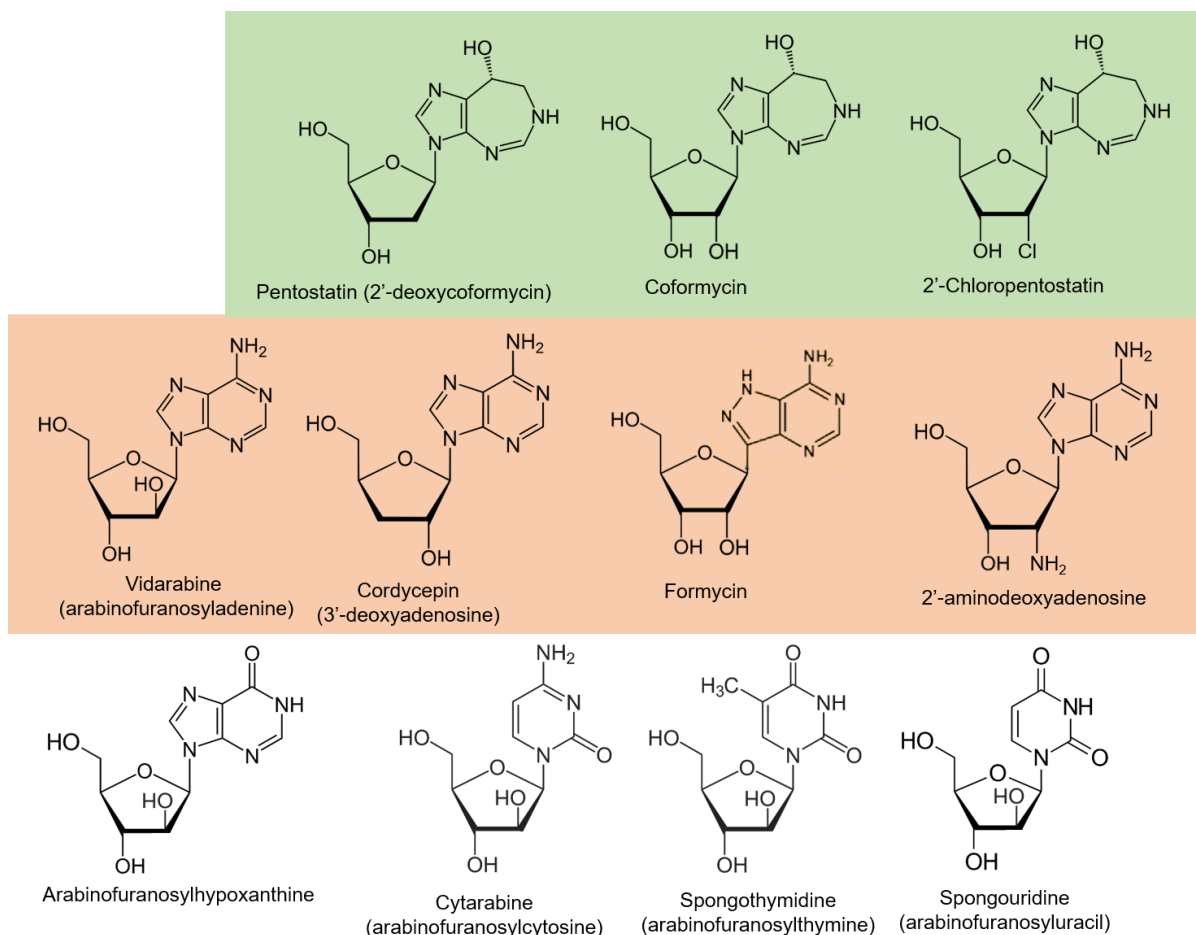


Figure 1.12: Nucleoside analogues and accompanying antibiotic metabolites as described in the text. Several are examples of “protector-protégé” systems found in living organisms – these are highlighted in green and red for protector and protégé respectively. Below and not highlighted are other arabinose-based nucleoside analogues.

Natural Products as a Source of Medicines

Some of the nucleoside analogues described above are used as medicines or have possible potential for so doing; all originate from studies on natural products. Products from natural resources represent a vast reservoir of future drugs, and newly-discovered therapeutic compounds. Many of these are classed as secondary metabolites, being distinct from the conserved fundamental biomolecules described as primary metabolites – involved in highly conserved metabolic processes within cells [Mushtaq *et al.* 2018]. Natural sources of medicines have been used in ethnic communities for centuries, and modern science has

allowed pharmacologists and molecular biologists to elucidate an evidence-based understanding of their biological and potential medicinal effects. This process is the basis of the study of ethnopharmacology.

Hence it is worth investigating the biochemistry of fungal species. In the case of cordycepin, and associated metabolite pentostatin, studies have focussed not only on *O. sinensis*, the traditionally more commonly-used remedy, but also *C. militaris* and other *Cordyceps* species. Cordycepin is widely sold as a range of herbal medicinal products mainly in the form of fungal extracts [see figure 1.13]; there have as yet been no human clinical trials or safety tests initiated for the development of purified cordycepin into an approved drug.



Figure 1.13: Various *Cordyceps*-based commercial herbal medicinal products. [Author.]

1.3.2 *C. militaris* Strains and Cordycepin Production

Strains in Culture Collections

C. militaris strains are available for research purposes from a range of culture collections including CBS/Westerdijk collection (Netherlands), KCTC (Korea), BCRC (Taiwan), and TBRC (Thailand). A list is provided in table 1.7.

Table 1.7: *Cordyceps militaris* strains available from culture collections. Abbreviations: CBS – Centraalbureau voor Schimmelcultures (Netherlands); KCTC – Korean Collection for Type Cultures (South Korea); BCRC – Bioscience Collection and Research Center (Taiwan); CGMCC – China General Microbiological Culture Collection (China); NBRC – National Bioscience Resource Center (Taiwan); TBRC – Thailand Bioscience Resource Center (Thailand). Strains in bold are featured in this study.

Geographic Origin	Culture Collection/Strain Name
UK	<i>CBS 108.70 / BCRC 33735</i>
Germany	<i>CBS 109.70 / BCRC 33736</i>
Germany	<i>CBS 110.70 / BCRC 33737</i>
Germany	<i>CBS 116546 CBS 116547</i>
USA	<i>CBS 123843</i>
Netherlands	<i>CBS 128.25 / KCTC 16931 / BCRC 33738</i>
Luxembourg	<i>CBS 133218</i>
Unknown	<i>CBS 178.59 / KCTC 6862 / BCRC 33739</i>
Denmark	<i>CBS 181.64 / BCRC 33740</i>
Japan	<i>KCTC 6064 KCTC 6472</i>
Canada	<i>KCTC 16932</i>
China	<i>CGMCC 5.0855 CGMCC 5.0856 CGMCC 5.0699</i>
Unknown	<i>DSM 1153 / NBRC 5298</i>
Austria	<i>DSM 23612</i>
Canada	<i>IHEM 5792</i>
France	<i>BRFM 1581</i>
Canada	<i>BCRC 32219</i>
China	<i>BCRC 34380</i>
Taiwan	<i>BCRC 34266</i>
Japan	<i>BCRC 34194 / NBRC 9787 / TBRC 1502</i>
Unknown	<i>CICC 14015 CICC 14014 CICC 14013</i>
Japan	<i>NBRC 103753 NBRC 103752 NBRC 103729 NBRC 100741 NBRC 30377 NBRC 103754 NBRC 103755 NBRC 103756 NBRC 103757 NBRC 103758 NBRC 103759 NBRC 103760 NBRC 103763 NBRC 103767 NBRC 103768 NBRC 103772 NBRC 111637</i>

Taiwan	<i>BCRC FU30404</i>	<i>BCRC FU30403</i>	<i>BCRC FU30401</i>	<i>BCRC FU30312</i>
	<i>BCRC FU30311</i>	<i>BCRC FU30310</i>	<i>BCRC FU30309</i>	<i>BCRC FU30308</i>
	<i>BCRC FU30951</i>	<i>BCRC FU30950</i>	<i>BCRC FU30821</i>	<i>BCRC FU30820</i>
	<i>BCRC FU30406</i>	<i>BCRC FU30405</i>		
China	CM2 (MycoMedica)			
Slovenia	CM16 (MycoMedica)			
China	SR1 (Rajtar)		SR2 (Rajtar)	
	SR3 (Rajtar)			
UK	UKMS			
USA	ARSEF 11703			
Japan	TBRC 5106	TBRC 5457	TBRC 5105	TBRC 6838
China	TBRC 6801	TBRC 6930	TBRC 6931	TBRC 6802
	TBRC 6804			

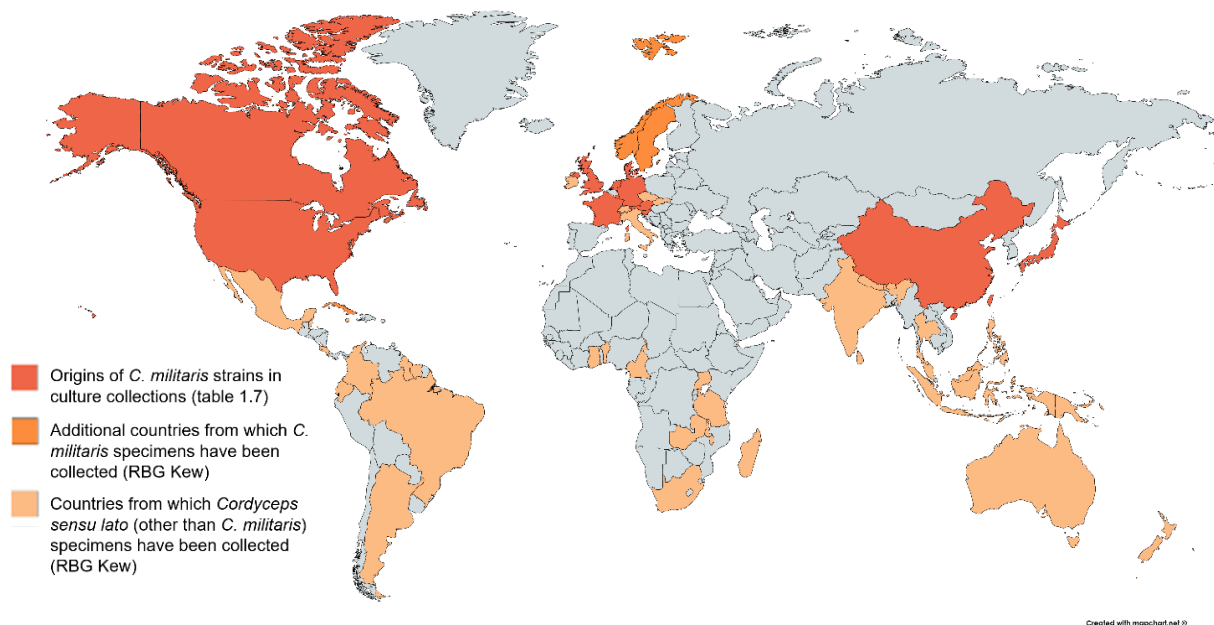


Figure 1.14: Distribution (by country) of culture collection *C. militaris* strain origins (listed in table 1.7), and *Cordyceps (sensu lato)* species from the fungarium collection at the Royal Botanic Gardens, Kew

Cordycepin Production and Extraction

Both the growth of *C. militaris* in artificial environments and maximisation of the production of cordycepin from the fungus have been investigated in various studies. Culturing techniques and media types for growing *Cordyceps militaris* in the laboratory setting are discussed by Das *et al.* [Das *et al.* 2010b]. Cereal grains and silkworm larvae have been predominantly used in the past for culture of the *Cordyceps militaris* mycelium for commercial use, to successfully produce the stroma [Holliday *et al.* 2004]. Surface growth and submersion (where fungal biomass is grown in aerobic conditions in liquid media) are two methods of fermentation and cultivation of mycelium. HPLC (high performance liquid chromatography) coupled with mass spectrometry and other methods such as UV detection have been proposed for the detection of cordycepin [Chang *et al.* 2005]. This will be discussed later.

A variety of methods for extracting cordycepin have been demonstrated, most of which however are unsuitable for an industrial scale (reviewed by Tuli *et al.* 2017) [Tuli *et al.* 2017]. Examples include evaporation and cold precipitation followed by Dowex-I-chloride column filtering [Kredich & Guarino 1960]; hydrothermal reflux [Wang *et al.* 2004]; butanol, hexane, and ethyl acetate solvent extractions from dried stroma [Kim *et al.* 2006; Rao *et al.* 2010]; ion-exchange resin/silica gel chromatography [Jiansheng 2008]; water, ethanol, and ultrasonic extraction methods [Zhang *et al.* 2012]; and microwave-assisted extraction [Chen *et al.* 2012; Tuli *et al.* 2017].

Recently there has been interest in methods for the maximisation of cordycepin production by cultures of *C. militaris* in published literature. Earlier examples of this include reaching peak production quantity of 2.5g/L of cordycepin by adding 1g/L adenine and 16 g/L glycine to liquid medium (potato dextrose agar) [Masuda *et al.* 2007]; and optimisation of media conditions 6.84 g/L cordycepin production, under conditions of glucose (86.2 g/L) and yeast extract (93.8 g/L) media, in a *C. militaris* mutant generated via ion beam irradiation [Das *et al.* 2010a]. Optimum conditions of growth for maximal cordycepin production, with regards to ammonium

content of media and feeding frequency, were assessed in another study [Mao *et al.* 2005].

Table 1.8 lists published effects on cordycepin production from cultures.

Strains of *C. militaris* with increased cordycepin production have repeatedly been identified – for example new cultivars [Zhang *et al.* 2010]; and mutant strain developed by methods such as ultraviolet radiation [Che *et al.* 2004]. Producing sexual crosses in the laboratory could be used further to form even higher cordycepin-producing strains [Shrestha *et al.* 2012].

Table 1.8: Published tested factors effecting cordycepin production by *Cordyceps militaris* cultures (various strains).

Factor	Study	Strain	Notes
Adenosine addition	Masuda <i>et al.</i> 2007	NBRC 9787	
Amino acid addition	Wen <i>et al.</i> 2016	CM016 (Beijing Jixiaoyuan Ltd., China)	Amino acids A, C, D, E, F, G, H, I, K, L, M, N, P, Q, R, V, W, Y; cystine, and L-hydroxyproline
Amino acid concentration change	Wen <i>et al.</i> 2016	CM016 (Beijing Jixiaoyuan Ltd., China)	G, K, and H concentration changes (0, 0.5, 1, 2, 4, 6, 8, 10g/L)
Carbon : nitrogen ratio change	Mao <i>et al.</i> 2005	Unnamed (Huazhong Agricultural University)	Various ratios
Carbon source change	Mao <i>et al.</i> 2005	Unnamed (Huazhong Agricultural University)	Lactose, sucrose, glucose, fructose, galactose, maltose, and xylose
Crossing of strains	Kang <i>et al.</i> 2017	KSP8 (new strain)	Found from crosses of various KACC, SPNU, EFCC and MPNU strains
Crossing of strains	Lee <i>et al.</i> 2017	KASP 1-8 (new strains)	
Culture type change	Sari <i>et al.</i> 2016	NBRC 10352	Submerged and surface broths
Culture type change	Shih <i>et al.</i> 2007	CCRC 32219	Shake, static, and shake + static broths
Cytosine addition and concentration change	Wen <i>et al.</i> 2016	CM016 (Beijing Jixiaoyuan Ltd., China)	0, 0.5, 1, 2, 4, 6, 8, and 10g/L
Degeneration of strain	Chen <i>et al.</i> 2017	PM53	Degenerated strain was revived by back crosses
Dissolved oxygen level change	Mao & Zhong 2008	Unnamed	
Glucose concentration change	Das <i>et al.</i> 2010	GL81-3 (NBRC 9787 mutant)	86.2g/L optimum

Glucose concentration change	Mao <i>et al.</i> 2005	Unnamed (Huazhong Agricultural University)	25, 40, 55, and 70g/L
Glucose concentration change	Zhang <i>et al.</i> 2013	Unnamed	30.16g/L optimum
H ⁺ -ATPase inhibitor addition	Mao & Zhong 2006	Unnamed (Huazhong Agricultural University)	Diethylstilbestrol and sodium orthovanadate (50μM)
Illumination time and treatment changes	Chiang <i>et al.</i> 2017	101 (Hsing-Tai Biotech. Ltd., Taiwan)	Time change (0, 4, 8, 12, 16h/day), and various blue, green, and red light ratios
Incubation time change	Adnan <i>et al.</i> 2017	ATCC 34164	Maximum reached at 21 days
Inoculum size change	Tuli <i>et al.</i> 2014	3936 (IMTECH, Chandigarh, India)	8% optimum
Iron salt addition	Fan <i>et al.</i> 2012	Unnamed (Huazhong Agricultural University)	FeCl ₃ , ferric citrate, FeSO ₄ , and Fe ₂ (SO ₄) ₃
KH ₂ PO ₄ concentration change	Zhang <i>et al.</i> 2013	Unnamed	2.04g/L optimum
Media change	Adnan <i>et al.</i> 2017	ATCC 34164	Oat, rice, and wheat media
Media change	Kang <i>et al.</i> 2017	KSP8	PDA, rice, and silk worm
Media change	Lee <i>et al.</i> 2017	SPNU 1000-3,5, KACC 44459, and KASP 1-8	PDB, brown rice, and silk worm pupae
Metal salt addition	Hung <i>et al.</i> 2015	BCRC 32219	NaCl, KCl, CaCO ₃ , Mg(NO ₃) ₂ , (NH ₄) ₂ Fe(SO ₄) ₂ , and “deep ocean water”
Metal sulphate addition	Fan <i>et al.</i> 2012	Unnamed (Huazhong Agricultural University)	ZnSO ₄ , CuSO ₄ , CaSO ₄ , and MnSO ₄
MgSO ₄ concentration change	Zhang <i>et al.</i> 2013	Unnamed	1.46g/L optimum
Mutant by ion beam irradiation	Das <i>et al.</i> 2008	NBRC 9787 mutant (new strain)	
Mutant by proton beam irradiation	Masuda <i>et al.</i> 2007	G81-3 (NBRC 9787 mutant – new strain)	
Mutant by UV irradiation	Lee <i>et al.</i> 2019	KYL05 mutant (new strain)	
Nitrogen source change	Mao & Zhong 2006	Unnamed (Huazhong Agricultural University)	YE, peptone, CEH, and CAH, and peptone addition to YE
Nitrogen source change	Mao & Zhong 2006	Unnamed (Huazhong Agricultural University)	Amino acids A, C, D, E, F, G, H, I, K, L, M, N, P, Q, R, S, T, V, W, Y, and peptone, and ammonium sulphate
Nitrogen source change	Shih <i>et al.</i> 2007	CCRC 32219	PE, YE, and CSP. YE concentration change (10 – 30g/L)
Nucleoside addition	Wen <i>et al.</i> 2016	CM016 (Beijing Jixiaoyuan Ltd., China)	Adenine, guanine, guanosine, inosine, uridine, thymine, cytosine, hypoxanthine,

			adenosine, thymine, and deoxyuridine
Nucleoside concentration change	Wen <i>et al.</i> 2016	CM016 (Beijing Jixiaoyuan Ltd., China)	Adenine, cytosine, and thymidine concentration changes (0, 0.5, 1, 2, 4, 6, 8, and 10g/L)
Oil addition	Tang <i>et al.</i> 2018	CICC 14014	Soybean, corn, olive, peanut, rapeseed, palm, sunflower, and cottonseed oils
pH change	Adnan <i>et al.</i> 2017	ATCC 34164	pH 5.5 optimum
pH change	Lee <i>et al.</i> 2019	KYL05 mutant	pH 6 optimum
pH change	Shih <i>et al.</i> 2007	CCRC 32219	pH 7 and pH 4
pH change	Tuli <i>et al.</i> 2014	3936 (IMTECH, Chandrigarh, India)	pH 5.5 optimum
Shaking speed change	Lee <i>et al.</i> 2019	KYL05 mutant	150RPM optimum
Temperature change	Adnan <i>et al.</i> 2017	ATCC 34164	25°C optimum
Temperature change	Hung <i>et al.</i> 2009	BCC 1974, 1975, 2790, 2814, 2815, 2816, 2817, 2818, 2819, 2824, 2826, 2838, and NBRC 5298, 9787, 100741	15, 20, 25, and 30°C
Temperature change	Lee <i>et al.</i> 2019	KYL05 mutant	25°C optimum
Temperature change	Tuli <i>et al.</i> 2014	3936 (IMTECH, Chandrigarh, India)	25°C optimum
Thymidine addition and concentration change	Wen <i>et al.</i> 2016	CM016 (Beijing Jixiaoyuan Ltd., China)	0, 0.5, 1, 2, 4, 6, 8, and 10g/L
YE concentration change	Das <i>et al.</i> 2010	GL81-3 (NBRC 9787 mutant)	93.8g/L optimum
YE concentration change	Zhang <i>et al.</i> 2013	Unnamed	10g/L optimum

A forest plot featuring effect size data from a meta-analytical approach to reviewing these studies is present in the supplementary material [supplementary figure S1].

Very few studies have investigated genetic factors affecting cordycepin production – through transgenic techniques. Xia *et al.* used this approach to demonstrate evidence for the genetic basis of the proposed cordycepin synthesis cluster [Xia *et al.* 2017]. More recently, Wang *et al.* created a knock-out mutant of the strain CM01, for the gene *CmSnf1*, encoding an AMPK

(adenosine monophosphate kinase) homologue [Wang *et al.* 2020]. This $\Delta CmSnf1$ mutant had significantly higher cordycepin production than the wild type and the complementation control mutant as well as corresponding upregulation of the *Cns* genes. *CmSnf1* may play a role as an effector in conditions, as indicated by the influence on the expression of oxidative stress-related genes, but may also have other effects downstream in secondary metabolism [Wang *et al.* 2020]. It also appeared to accompany downregulation of protease- and chitinase-encoding genes, as well as a reduced growth rate. The authors proposed the former to be a major factor explaining the inability of the mutant strain to colonise an insect host – which was not the case when it was cultured on rice media [Wang *et al.* 2020].

The Problem of Culture Degeneration

The issue of culture degeneration is relevant both to cordycepin production, and ability to produce stromata.

Culture degeneration is a significant problem affecting cordycepin output by *Cordyceps militaris* cultures kept for a long periods of time under laboratory conditions. [Sun *et al.* 2017; Yin *et al.* 2017]. This is characterised by fruiting body (stroma) formation deficiencies or absence, sporulation reduction, and reduced production of secondary metabolites including cordycepin [Yin *et al.* 2017]. Culture degeneration is also observed widely across other ascomycetes, and is an important issue in biotechnology, being associated with deterioration of sexual development and secondary metabolism.

Despite its importance, the degeneration process and associated features have not been thoroughly studied. Yin *et al.* conducted a transcriptional study in order to ascertain some of the possible changes in gene expression causing this effect. The authors looked at the transcriptomes of six generations of potato dextrose agar (PDA) sub-cultured *C. militaris* RNA-sequencing to find differentially-expressed genes, and validating 51 of these with qPCR. Downregulated genes included mating-type genes, and genes involved in the putative cordycepin synthesis pathway; whilst notable downregulated genes included those involved

in chromatin structure such as methyltransferases, and DNA repair protein-encoding genes [Yin *et al.* 2017]. However this study only involved one biological replicate, and considered only one strain of *Cordyceps militaris*. Sun *et al.* looked at several different *C. militaris* strains with varying levels of degeneration. They found that degenerated strains had lower carotenoid content, reduced extracellular polysaccharide but increased intracellular polysaccharide, and slightly decreased cellulase and amylase activity [Sun *et al.* 2017].

The yet limited research on the degeneration of *C. militaris* cultures has been reviewed [Lou *et al.* 2019]. As the authors explain, much of the research on external factors affecting degeneration focus on storage and growth conditions of cultures. As found by Sun and colleagues, storage at 4°C resulted in a stabilising effect on cultures, halting degeneration for at least a period of a year. Both exposure to metal ions and oxidative stress have been shown to affect fruiting body formation ability of strains [He *et al.* 2009; Xiong *et al.* 2013]. The issue of mating types and homo- or heterothallism in *C. militaris* is of importance to understanding degeneration. Studies have shown that sexual crosses of strains has stimulated increased production of cordycepin [Kang *et al.* 2017; Lee *et al.* 2017]. Additionally, Chen *et al.* found that successive subculturing of a strain led to an imbalance of mating types, which was restored by crossing single-spore isolates of opposite mating types from the strain. This not only resulted in a renewed ability of the fungus to produce viable stromata, but an increase in cordycepin and adenosine production [Chen *et al.* 2017].

Hence there is limited but intriguing evidence for the link between cordycepin production and sexual development in *C. militaris*. Given that the sexual life cycle of this species is based around parasitism of the insect host, this begs the question of the possible role of cordycepin in the host infection process by the fungus – i.e. the real ecological function of this modified nucleoside, and reason(s) for its evolutionary selection. Studies on the formation of stromata, the principle morphological feature of *C. militaris* sexual development, and factors affecting this are summarised in table 1.9.

Lou and colleagues reviewed the causes of degeneration in *C. militaris*, concluding that factors of media used, culture storage, subculturing and oxidative stress can be involved, but that genetic changes notably underlie degeneration [Lou *et al.* 2019].

Table 1.9: Studies examining methods for and factors affecting stromata formation in *C. militaris* cultures. SDAY: Sabouraud dextrose yeast extract agar, SDB: broth; SSB: Sabouraud sucrose broth, PDA: potato dextrose agar, PDB: broth

Pre-culture	Culture method	Factor(s) affecting stromata	<i>C. militaris</i> strain	Reference
SDAY, subcultured to SSB, 25°C	Injection of hyphal suspension into moth and beetle larvae (<i>Mamestra brassicae</i> , <i>Spodoptera litura</i> , <i>Bombyx mori</i> , <i>Tenebrio molitor</i>), 100 µL in <i>B. mori</i> and 5 µL in the others	Temperature: 25°C more stromata than 20°C, none at 15°C - <i>M. brassicae</i> Light: 50-100 lux better for stromata formation than higher intensities, none over 1000 lux - <i>S. litura</i> Host larval stage: stromata formation faster in 1 day-old than 2 or 5 day-old injected larvae - <i>S. litura</i>	F1176-21; Japan, wild	Sato & Shimazu 2002
PDA, subcultured to PDB- static, 25°C	Injection of hyphal suspension into <i>Bombyx mori</i> –silk moth larvae, 100 µL	Host larval body part injected: made no significant difference, head/thorax/abdomen Hyphal suspension inoculum concentration: 2x10 ⁵ CFU significantly higher infection rate than 2x10 ⁴	Cmb233, cross between mated strains Cmb186 and Cmb209; from culture collection - Rural Development Administration, South Korea	Hong <i>et al.</i> 2010
PDA; SDB- shaken 25°C	Injection of <i>Bombyx mori</i> pupae; inoculation of rice media, 50 days	Knock out mutant $\Delta CmSnf1$ was unable to colonise host and produce stromata unlike the wild type and complementation control mutant. However, $\Delta CmSnf1$ mutant was able to produce stromata on rice media, like its counterparts.	CM01 (see Zheng <i>et al.</i> 2011), wild type and <i>CmSnf1</i> knock out and complementation mutants. <i>CmSnf1</i> encodes AMPK	Wang <i>et al.</i> 2020
SDAY, subcultured to SSB- shaken, 25°C	Brown rice silkworm media, 60 days in the light, 20°C	Mating types: presence of different mating types in crossing strains required from stromata formation	Entomopathogenic Fungal Culture Collection strains, South Korea, wild	Shrestha <i>et al.</i> 2005
PDA, subcultured to PDB- shaken, 23°C	Rice media, 2 days in the dark, 45 days 6/15 L/D, 23°C	Ditto	Not specified	Zhang & Liang 2013

PDA and liquid broth	Injection of conidial suspension into moth larvae (<i>Antheraea pernyi</i> – Chinese Tussah silk moth), 50µL, 5x10 ⁶ conidia/mL, 60 days in 12/12 L/D, 22°C	Ditto – only sterile stromata (without perithecia) formed when only a single mating type present	CM01 – genome sequenced strain (CGMCC3.14242)	Zheng <i>et al.</i> 2011
PDA, subcultured to minimal broth media-shaken, 26°C	Rice media, 10 days in the dark, 20°C, 50 days 14/10 L/D, high humidity, 25°C	Ditto, using single-spore isolates from one strain, but some reported homothallism observed	CGMCC2459; China, wild	Wen <i>et al.</i> 2012
SDAY, subcultured to SSB- shaken, 25°C	Brown rice silkworm media, 60 days in the light, 20°C	Subculturing caused decreases in stromata production - from first to second subculture	Entomopathogenic Fungal Culture Collection strains, South Korea, wild	Shrestha <i>et al.</i> 2004
PDA, subcultured to minimal broth media-shaken, 23°C	Rice media, 12 days in the dark, 20°C, 12 days 23/16°C day/night temp., high humidity	Fine tuning of carbon and nitrogen sources by supplementing rice media increased stromata production	Ditto	Wen <i>et al.</i> 2014

1.3.3 Analytical Methods for Detection of Cordycepin and Other Metabolites

Studies focussing on the metabolites of *C. militaris* have used analytical chemical techniques such as liquid chromatography (LC), UV detection, and mass spectrometry (MS). In particular, coupled LC-MS methods have been adapted for detection of small molecules, including nucleosides and their homologues, such as cordycepin and pentostatin. Further background to these methods is discussed in chapter 2.

Untargeted Metabolomics Studies of Cordyceps

Untargeted metabolomics has been used to compare different samples of *Cordyceps militaris* and related species – for example temporally, assessing the process of stromata senescence [Oh *et al.* 2019], between wild and laboratory-cultured samples [He *et al.* 2019], and between samples of different species [Chen *et al.* 2018], and to verify the species identity of an extract sample [Zhang *et al.* 2015]. Multivariate statistical methods such as principle component analysis (PCA) can be used to compare metabolomic outputs of samples.

Following metabolic pathway analysis from GC-MS (gas chromatography-coupled mass spectrometry) data, Oh *et al.* found that cordycepin production was enhanced in senesced stromata of *C. militaris*, and that this was simultaneous with stimulation of the glutamine and glutamic acid pathway [Oh *et al.* 2019]. The authors used electron ionisation and identified compounds using retention time and accurate mass.

He *et al.* used an LC-MS (electrospray ionisation) method to compare wild and laboratory-cultured mycelial samples, as well as sclerotium (insect host hyphal) and stromata with vegetative culture samples, of the related species *Cordyceps (Isaria) cicadae* – a pathogen of cicada nymphs. PCA plots showed the metabolomic differences between sclerotial and stromata samples to be greater than those between wild and laboratory-cultured samples, based on metabolites identified using retention time and accurate mass. The authors found higher levels of non-ribosomal peptides including beauvericins, and sphingolipids in the sclerotial samples, proposing that the immune response of the insect host stimulated their

production [He *et al.* 2019]. However, they did not analyse an insect control sample for comparison, and hence were unable to deduct potential cicada metabolites from the data.

An LC-MS (electrospray ionisation)-based method was also used by Chen and colleagues to compare three samples – brown rice-grown and tussah moth caterpillar-grown *C. militaris* and wild collected *Ophiocordyceps sinensis* [Chen *et al.* 2018]. An enhanced method, with LC-MS/MS (tandem mass spectrometry with electrospray ionisation), was used by Zhang and colleagues to discriminate between genuine and counterfeit *O. sinensis* samples by multivariate analysis (PCA) [Zhang *et al.* 2015]. Tandem mass spectrometry, providing the highest level of identification by fragmentation, is presently considered the standard for untargeted metabolomics studies.

Targeted Metabolomics with Cordycepin and Related Small Molecules

There have been several published studies on small molecule-targeted mass spectrometry analysis of *Ophiocordyceps sinensis* and *C. militaris* samples, which have exclusively involved the use of dried often mycelial or unspecified extracts. Some of these are presented in table 1.10, and metabolites of interest in figure 1.15 – being nucleobases, nucleosides, and derivatives and analogues including cordycepin. As shown in the table, in recent years the published standard procedures in LC-MS analysis have improved, with an emphasis of metabolite identification confidence by fragmentation – achieved by using either triple quadrupole (QqQ) or quadrupole and time of flight (Q-TOF) mass analysers. Limits of detection (LOD) have also improved.

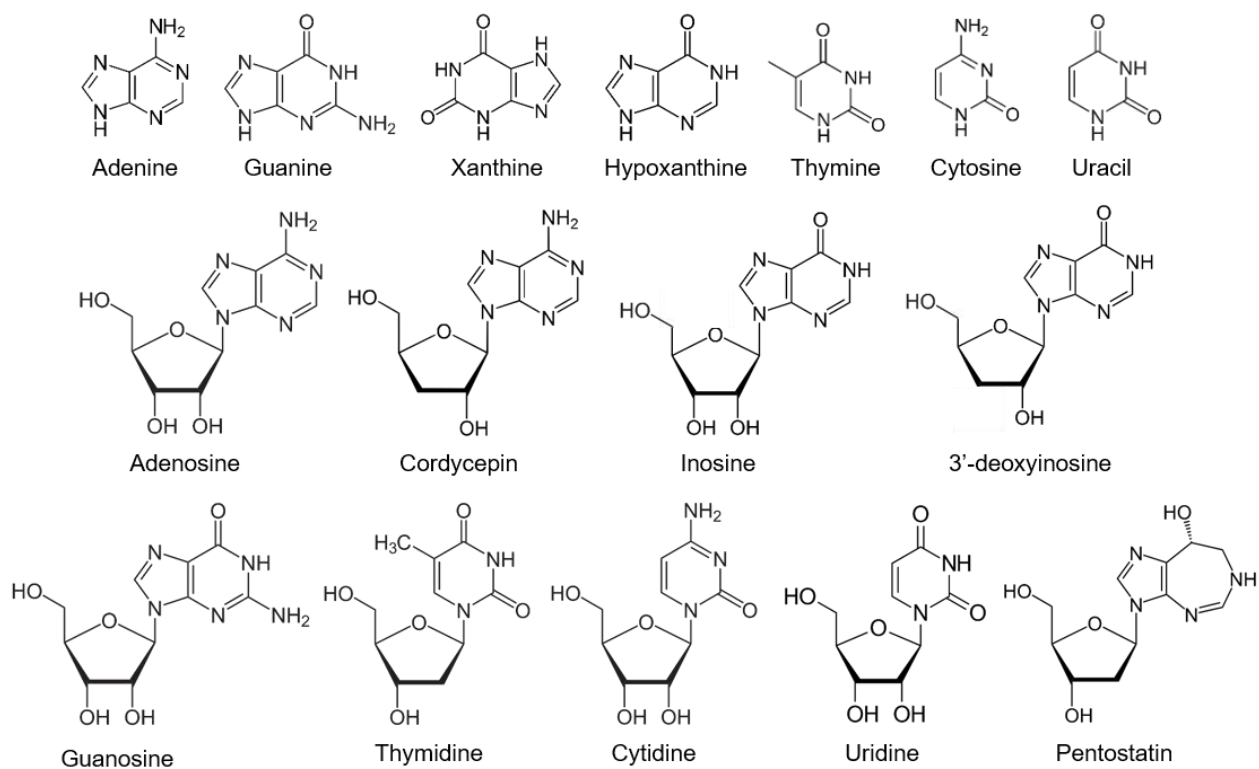


Figure 1.15: Structures of various nucleobases, nucleosides and derivatives and analogues of interest.

Table 1.10.1: Published mass spectrometry analyses of dried mycelial *Ophiocordyceps sinensis* and *militaris* extracts, targeting selected nucleobases and nucleosides [part 1 – including details of sample separation and extraction methods].

Study	Separation Method	Phases	Sample		
			Species	Extraction solvent	Extraction method
Zong <i>et al.</i> 2015	UHPLC	Formic acid (0.1%) + acetonitrile (A); water + acetonitrile (A)	<i>O. sinensis</i>	Methanol (10%)	Sonication
Zhao <i>et al.</i> 2013	HPLC (HILIC)	Ammonium acetate (10mM) + acetic acid (0.2%) (A), acetonitrile (100%, B)	<i>Cordyceps sp.</i>	Methanol (60%)	Sonication
Xie <i>et al.</i> 2010	HPLC	Ammonium acetate (A), methanol (B)	<i>O. sinensis</i>	Water	Sonication
Yang <i>et al.</i> 2010	Ion-pairing reversed-phase liquid chromatography	Pentadecafluorooctanoic acid (0.25mM, A), acetonitrile (100%, B)	<i>O. sinensis, C. militaris</i>	Water	Heating (95°C)
Yang <i>et al.</i> 2009	Capillary electrophoresis	Formic acid (100mM) + methanol (10%) (electrolyte)	<i>O. sinensis, C. militaris</i>	Water	Heating (95°C), sonication
Fan <i>et al.</i> 2006	HPLC	Ammonium acetate (5mM, A), methanol (100%, B)	<i>O. sinensis, C. militaris</i>	Methanol	Heating (160°C)
Guo <i>et al.</i> 2006	HPLC	Ammonium acetate (40mM, A), methanol (100%, B)	<i>O. sinensis</i>	Water, methanol (reconstitution)	Drying (35°C), sonication
Huang <i>et al.</i> 2004	HPLC	Methanol (12%) + formic acid (1.5%) (A)	<i>O. sinensis</i>	Methanol, water (reconstitution)	Drying by vacuum
Huang <i>et al.</i> 2003	HPLC	Methanol (14%) + formic acid (1%) (A)	<i>O. sinensis, C. militaris</i>	Water	Sonication

Table 1.10.2: ... [part 2 – including details of mass spectrometry method].

Study	Mass spectrometry method				LOD (cordycepin)	Metabolites detected
	Ionisation	Mass analyser	Machine	Identification by		
Zong <i>et al.</i> 2015	Electrospray ionisation	QqQ	Agilent 6460 Triple Quadrupole Tandem MS	RT, accurate mass, and fragmentation	0.04ng/mL	Adenine, adenosine, 2'-chloroadenosine, cordycepin, cytosine, guanine, guanosine, hypoxanthine, inosine, thymine, thymidine, uracil, uridine, 2'-deoxyuridine
Zhao <i>et al.</i> 2013	Electrospray ionisation	Q-TOF, QqQ	Agilent G6520 Q-TOF MS, Agilent G6420A MS	RT, accurate mass, and fragmentation	0.21ng/mL	Adenine, adenosine, 2'-chloroadenosine, cordycepin, cytosine, cytidine, guanine, guanosine, xanthine, hypoxanthine, inosine, thymine, thymidine, uracil, uridine, 2'-deoxyuridine
Xie <i>et al.</i> 2010	Electrospray ionisation	Quadrupole	Shimadzu LCMS-2010	RT and accurate mass	0.1µg/mL	Adenine, adenosine, cordycepin, thymine
Yang <i>et al.</i> 2010	Electrospray ionisation	Quadrupole	Agilent LC/MSD Trap	RT and accurate mass	0.04µg/mL	Adenine, adenosine, adenosine-5'-monophosphate, cordycepin, cytosine, cytidine, guanine, guanine-5'-monophosphate, guanosine, hypoxanthine, inosine, thymine, thymidine, uracil, uridine, uridine-5'-monophosphate
Yang <i>et al.</i> 2009	Electrospray ionisation	Quadrupole	Agilent Trap XCT	RT and accurate mass	0.12µg/mL	Adenine, adenosine, cordycepin, cytosine, 5-chlorocytosine, cytidine, guanine, guanosine, hypoxanthine, inosine, thymidine, uridine, 2'-deoxyuridine, arabinoside
Fan <i>et al.</i> 2006	Electrospray ionisation	QqQ	Agilent 1100 LC/MSD Trap	RT, accurate mass, and fragmentation	1.16µg/mL	Adenine, adenosine, cordycepin, cytosine, cytidine, guanine, guanosine, hypoxanthine, inosine, thymine, thymidine, uracil, uridine, 2'-deoxyuridine
Guo <i>et al.</i> 2006	Electrospray ionisation	Quadrupole	Shimadzu LCMS-2010	RT and accurate mass	0.1µg/mL	Adenine, adenosine, 2'-chloroadenosine, cordycepin, guanine, hypoxanthine, thymine, uracil, uridine
Huang <i>et al.</i> 2004	Electrospray ionisation	Quadrupole	Shimadzu LCMS-2010	RT and accurate mass		Adenine, adenosine, uridine
Huang <i>et al.</i> 2003	Electrospray ionisation	Quadrupole	Shimadzu LCMS-2010	RT and accurate mass	0.1µg/mL	Adenine, adenosine, cordycepin, hypoxanthine

Modern Advanced Metabolomics Studies and “Omics”

Recent high impact advanced applications of metabolomics include activity metabolomics to diagnose bioactive molecules, studies on cancers, and discovery of novel metabolic pathways [Rinschen *et al.* 2019; Guijas *et al.* 2018; Seo *et al.* 2018; Sun *et al.* 2019; Pareek *et al.* 2020]. The practise of integrating high-throughput datasets, or “omics” to increase understanding of biological effects and processes is an emerging field, and has been termed integrated omics. Examples of omics are presented in table 1.11, with various studies relating to cancer biology, one of the areas of research in which it has been most used.

Table 1.11: Types of omics, with recent example studies relating to cancer biology

Omics term	Concerns	Example Study
Genomics	DNA genome	Mateo <i>et al.</i> (2020) – prostate cancer
Epigenomics	Epigenetic elements	Serafini <i>et al.</i> (2020) – head and neck cancers
Methylomics	Epigenetics involving methylation	Silva <i>et al.</i> (2020) – prostate cancer
Transcriptomics	RNA transcripts	Ho <i>et al.</i> (2019) – liver cancer
Proteomics	Proteins	Enroth <i>et al.</i> (2019) – ovarian cancer
Glycomics	Sugars	Peng <i>et al.</i> (2019) – breast cancer
Metabolomics	Metabolites (by MS)	Jacyna <i>et al.</i> (2019) – bladder cancer
Lipodomics	Lipids	Wang <i>et al.</i> (2020) – colorectal cancer
Metabonomics	Metabolites (by NMR)	Li <i>et al.</i> (2019) – ovarian cancer

Metabolomics has been described as the omics most proximate to the phenotype [Guijas *et al.* 2018]. Linking metabolomics with genomics, proteomics and other high throughput datasets can help isolate metabolites of interest for further study, in a process known as metabolomics activity screening [Guijas *et al.* 2018]. Hence the metabolomic regulation of processes within organisms – such as macrophage immune activity, maturation of oligodendrocytes, and development of cancers – can be ascertained [Guijas *et al.* 2018; Rinschen *et al.* 2019]. Activity screening of metabolites is an extension of the study of metabolites as bioactivity markers – used for example as a diagnostic tool for cancers [e.g. Seo *et al.* 2018; Sun *et al.* 2019]. Metabolite activity screening has been applied to diseases

such as arthritis and asthma, as well as immunometabolism, and studies on ageing in model organisms [Rischen *et al.* 2019].

1.4 STUDYING INSECT HOSTS OF *CORDYCEPS*

1.4.1 Diversity of *C. militaris* Insect Hosts

The previously discovered insect hosts of *Cordyceps sensu lato* in the orders Coleoptera (beetles) and Lepidoptera (butterflies and moths) was comprehensively reviewed [Shrestha *et al.* 2016]. These orders contain the vast majority of host species known for this group of fungi. *C. militaris* is one of only two species observed to parasitise host species from both orders; and is also the only one to parasitise two other insect orders, Hymenoptera (wasps and relatives) and Diptera (flies) [Shrestha *et al.* 2016]. Of all the 92 fungal species assessed by the authors, *C. militaris* was found to have the greatest known host range, consisting of 32 species, within 13 families of both insect orders considered [Shrestha *et al.* 2016]. The lepidopteran host species are listed in table 1.12.

Table 1.12: Known natural lepidopteran hosts of *Cordyceps militaris* [from Shrestha *et al.* 2016]. Families in bold are exclusive to *C. militaris*.

Infraorder	Superfamily, Family	Species
Exoporia	Hepialoidea, Hepialidae	<i>Hepialus</i> sp.
Heteroneura	Noctuoidea, Erebidae	<i>Calliteara pudibunda</i> , <i>Leucoma salicis</i>
	Noctuoidea, Noctuidae	<i>Arcte coerula</i> , <i>Colocasia coryli</i> , <i>Euxoa ochrogaster</i> , <i>Panolis flammea</i>
	Noctuoidea, Notodontidae	<i>Fentonia ocypete</i> , <i>Lampronadata cristata</i> , <i>Phalera assimilis</i> , <i>Phalera bucephala</i> , <i>Syntypistis punctatella</i>
	Drepanoidea, Drepanidae	<i>Achlya flavicornis</i> , <i>Ochropacha duplaris</i> , <i>Tethea ocularis</i> , <i>Tetheella fluctuosa</i>
	Geometroidea, Geometridae	<i>Biston panterinaria</i> , <i>Lycia hirtaria</i> , <i>Triphosa</i> sp.
	Bombycoidea, Bombycidae	<i>Bombyx mori</i>
	Bombycoidea, Endromidae	<i>Andraca bipunctata</i>
	Bombycoidea, Saturniidae	<i>Anisota senatoria</i>
	Bombycoidea, Sphingidae	<i>Callambulyx tatarinovii</i> , <i>Laothoe populi</i> , <i>Marumba sperchius</i> , <i>Mimas tiliae</i> , <i>Hyles euphorbiae</i> , <i>Sphinx pinastri</i>
	Lasiocampoidea, Lasiocampidae	<i>Dendrolimus pini</i> , <i>Dendrolimus superans</i> , <i>Macrothylacia rubi</i>

1.4.2 Use and Adaptation of Insect Models for Infection: *Galleria mellonella*

In the pursuit of convenient infection models for fungal diseases of humans, invertebrates, including insects, have been used as model species. This strategy has particularly been used in research focussing on dimorphic fungi – those which occupy yeast and hyphal forms in different stages of their life cycle [Singulani *et al.* 2018]. The circumvention of ethical problems, physical experimental difficulties, time consumption and high costs are the key advantages of using invertebrate models [Champion *et al.* 2018]. Hence pathogens such as *Blastomyces dermatitidis*, *Histoplasma capsulatum*, and *Paracoccidioides* have been studied using host species such as *Caenorhabditis elegans* and *Galleria mellonella* [Singulani *et al.* 2018].

The greater wax moth, *Galleria mellonella*, is a pest of bees important in honey production due to its feeding on wax, pollen, and honey in hives [Kwadha *et al.* 2017]. It has a life cycle which is measured in weeks and can be reared at a range of suitable temperatures (20-30°C) [Ramarao *et al.* 2012]. Owing to the convenient size of *G. mellonella* caterpillars

(approximately 2cm in length and 250mg in weight) they can be easily handled and given defined accurate doses of infection material by injection [Ramarao *et al.* 2012]. As well as having been used to study fungal pathogens such as *Candida albicans*, *Aspergillus fumigatus*, and *Fusarium oxysporum*, caterpillars of this species have also been hosts to bacteria such as *Pseudomonas aeruginosa*, *Serratia marcescens*, and *Staphylococcus aureus* in experimental studies [Ramarao *et al.* 2012]. The popularity of this model has led to a refinement of the rearing of the caterpillars and moths and standardised methods for their use experimentally [e.g. Jorjao *et al.* 2018; Champion *et al.* 2018]. These methods, including the injection of material directly into the haemolymph of the caterpillar, have been used in this project for the study of *Cordyceps militaris* (see chapter 2). Furthermore, the genome of *G. mellonella* has been sequenced [Lange *et al.* 2018; Kong *et al.* 2019], making this species an ideal choice for a lepidopteran host model in this project.

Additionally, several immune response factors in *G. mellonella* have been described. For example, inducible metalloproteinase inhibitors were induced by invading bacterial pathogens to combat metalloproteinase virulence factors [Altincicek *et al.* 2007], antifungal factors gallerimycin, galiomicin, and lysozyme by the fungal pathogen *Beauveria bassiana* [Wojda *et al.* 2009]. Gallerimycin, an antimicrobial peptide, was even found to confer resistance to plant pathogens *Erysiphe* and *Sclerotinia* when expressed in tobacco [Langen *et al.* 2007].

An observable sign of immune response in *G. mellonella* caterpillars is melanisation. This process occurs following the detection of fungal pathogens [Chambers *et al.* 2012], and melanisation of the areas surrounding the foreign tissues is initiated by haemocytes. Encapsulation of fungal cells also occurs in the haemocoel [Cereneus *et al.* 2008]. Following a prophenoloxidase cascade, melanin is formed from the oxidation of phenolic molecules [Lu *et al.* 2014]. Active phenoloxidase catalyses this oxidation, which is in turn formed from prophenoloxidases via a serine protease cascade [Chandler 2016]. In spore injection experimental models, phenoloxidase activity can be significantly elevated within as little as 12 hours [Dubovskiy *et al.* 2013], and therefore melanisation can be a rapid observable immune

response. Melanin production however can also occur around wounds – so for example in injection-based assays, it is best to record only full body melanisation as an immune response in insect models.

An entomopathogenic relative of *C. militaris* – *Metarhizium anisopliae* – was tested on *G. mellonella* caterpillars, in an early study [Vilcinskas *et al.* 1997]. The authors showed responses by plasmatocytes, a type of haemocytic cell, to metabolites destruxin A and E *in vitro* and similar effects were observed in caterpillars infected with the fungus [Vilcinskas *et al.* 1997]. Other types of haemocytes include prohaemocytes, coagulocytes, oenocytoids, spherulocytes, and granular cells [Singulani *et al.* 2018]. These cells are able to perform functions such as phagocytosis, encapsulation and nodulation to resist pathogens as part of a complex insect immune system bearing some similarities to the mammalian innate immune system [Pereira *et al.* 2018]. For instance, haemocytes, much like neutrophils, are activated by binding to Toll-like receptors. This induces a NF- κ B-like pathway resulting in the release of anti-microbial peptides [Browne *et al.* 2013].

1.4.3 Exploring the Effects of Cordycepin on Insect Models

There may be potential for the exploitation of cordycepin and *Cordyceps militaris* for insect pest control in the absence of direct infection, given properties the fungus may have in its capacity as an entomopathogen. Despite this, there have been relatively few studies investigating the effects of fungal extracts or of cordycepin itself on insect mortality. Kryukov and colleagues found that Colorado potato beetles (*Leptinotarsa decemlineata*) fed with a solid culture suspension of *C. militaris* showed increased susceptibility to *Beauveria bassiana* infection. There was a decreased number of haemocytes in the haemolymph of treated beetles, especially of granulocytes and plasmatocytes – immunocompetent cells [Kryukov *et al.* 2014]. Elsewhere it has been noted before that *Beauveria* and *Metarhizium* toxins cause reduced haemocyte activity [Huxham *et al.* 1989; Kryukov *et al.* 2014; Samuels *et al.* 1988].

Only a handful of studies have examined effects of cordycepin on arthropods – these are summarised in table 1.13. Notably, Woolley *et al.* demonstrated evidence for the reduction in expression of immune-related genes in insect models caused by cordycepin. In *Drosophila melanogaster* Schneider 2 (S2) cells, following the stimulation by addition of curdlan (a β -1,3-linked glucose-based polysaccharide, used to simulate fungal infection) to media, the upregulation of the immune gene *Metchnikowin* observed after 4 hours was reduced when 25 $\mu\text{g}/\text{mL}$ cordycepin was also added. A similar effect was found in *Galleria mellonella* larvae, after injected with conidia or *Cordyceps militaris* or *Beauveria bassiana*. The upregulation of immune response genes *Lysozyme*, *IMPI*, and *Gallerimycin* observed after 72 hours were reduced when 3mg/mL cordycepin was also added to the injection serum. This was also the case with genes *Lysozyme* and *IMPI* after 48 hours, and the two genes even showed reduced upregulation following the sham (negative control) injection treatment [Woolley *et al.* 2020]. Two recent studies have shown that cordycepin reduces the survival after coinjection with spores of *C. militaris*, as well as a similar effects with related species *Beauveria bassiana* and *Metarhizium anisopliae*, which themselves do not produce cordycepin [Woolley *et al.* 2020; Kato *et al.* 2021].

Duncan and colleagues showed an effect of cordycepin on overall translation following recovery from heat shock treatments at 35°C in S2 cells (cultured at 22-24°C). SDS-PAGE analyses showed that the addition of 10, 50 and 100 μM cordycepin prior to heat shock treatments resulted in reduced restoration of protein production at 2, 3, and 4 hours post heat shock. A more detailed experiment, using ^{35}S -labelled methionine, showed additions of 100 μM cordycepin before, immediately after, and 1 hour after heat shock treatment caused reduced restoration of translation at time points of 0.5, 1, 2, 3, and 4 hours post heat shock. Further evidence of this hindrance of translation was provided through sedimentation analyses, showing a reduced decrease in 80S monosomes (therefore indicating a reduced increase in polysomes) 60 minutes after heat shock treatment when 50 μM cordycepin was added prior to heat shock [Duncan 1995].

Hence at least some effects of cordycepin on translation, and expression of immune genes in insect models are known, but not widely explored. The effects of small molecules present in *Cordyceps* and related entomopathogenic fungi on insect immunology is an area which requires more research, in order to ascertain the potential for fungal exploitation in agricultural field settings.

Table 1.13: Studies examining effects of cordycepin on arthropods.

Arthropod model system	Cordycepin dose; exposure method	Observed effect	Reference
<i>Chironomus pallidivittatus</i> (midge) salivary glands	39.8 μ M (10 μ g/mL); addition to media	Reduction in formed Balbiani rings on polytene chromosomes at 40 mins	Gopalan 1973
<i>Hyalophora cecropia</i> (cecropia moth) colleterial tubules	398 (100 μ g/mL); addition to media	Reduced protein synthesis in parenchymal tissue between 2 and 8 hours	Grayson & Berry 1973
<i>Laspeyresia pomonella</i> (codling moth) CP-1268 cells	59.7 μ M (15 μ g/mL); addition to media	Reduced incorporation of 3 H-labelled uridine (proxy for RNA synthesis) between 90 and 210 mins	Gallagher & Hartig 1976
<i>Drosophila melanogaster</i> S2 cells	200 μ M; addition to media 10 mins before heat shock	Reduced production of heat shock protein (Hsp) during heat shock	Duncan 1995
<i>Drosophila melanogaster</i> S2 cells	10, 50 and 100 μ M; addition to media 10 mins before 30 min heat shock	Reduced restoration of protein production at 2, 3 and 4 hours (SDS-PAGE) after heat shock	Duncan 1995
<i>Drosophila melanogaster</i> S2 cells	50 μ M; addition to media 10 mins before 60 min heat shock	Reduced restoration of translation at 60 mins after heat shock (sedimentation of polysomes and 80S monosome)	Duncan 1995
<i>Drosophila melanogaster</i> S2 cells	100 μ M; addition to media before and after 30 min heat shock, and 1 hour during recovery	Reduced restoration of translation at 0.5, 1, 2, 3, 4 after and during heat shock (SDS PAGE with 35 S-methionine-labelled proteins)	Duncan 1995
Mitochondria isolated from <i>Artemia franciscana</i> (brine shrimp) embryos	199 μ M and 1.99 mM (50 and 500 μ g/mL); addition to media	Reduced transcription rate (incorporation of 35 P-labelled UTP)	Eads & Hand 1999
<i>Plutella xylostella</i> (diamondback moth) larvae	2.07 mM (500 mg/L); food (<i>Brassica oleracea</i>) leaves dipped in solution	Mortality at 2 and 4 days after treatment; problem – no negative control	Kim <i>et al.</i> 2002
<i>Plutella xylostella</i> (diamondback moth) larvae	1.24 mM (300 mg/L); food (<i>Brassica oleracea</i>) leaves dipped in solution	Mortality at 2 and 4 days after treatment; problem – no negative control	Kim <i>et al.</i> 2002

<i>Drosophila melanogaster</i> S2r+ cells	99.5 μ M (25 μ g/mL); addition to media	Reduced <i>Metchnikowin</i> upregulation following application of curdlan at 4 hours	Woolley <i>et al.</i> 2020
<i>Galleria mellonella</i> (greater wax moth) larvae	11.9 mM (3 mg/mL); injection	Reduced survival time when coinjected with 10 and 100 spores of <i>Cordyceps militaris</i> compared to no cordycepin (spores only)	Woolley <i>et al.</i> 2020
<i>Galleria mellonella</i> (greater wax moth) larvae	11.9 mM (3 mg/mL); injection	Reduced survival time when coinjected with 10 and 100 spores of <i>Beauveria bassiana</i> compared to no cordycepin (spores only)	Woolley <i>et al.</i> 2020
<i>Galleria mellonella</i> (greater wax moth) larvae	11.9 mM (3 mg/mL); injection	Reduced upregulation of <i>Lysozyme</i> , <i>IMPI</i> and <i>Gallerimycin</i> at 72 hours when coinjected with <i>C. militaris</i> compared to no cordycepin (spores only)	Woolley <i>et al.</i> 2020
<i>Galleria mellonella</i> (greater wax moth) larvae	11.9 mM (3 mg/mL); injection	Reduced upregulation of <i>Lysozyme</i> , <i>IMPI</i> and <i>Gallerimycin</i> at 72 hours when coinjected with <i>B. bassiana</i> compared to no cordycepin (spores only)	Woolley <i>et al.</i> 2020
<i>Galleria mellonella</i> (greater wax moth) larvae	11.9 mM (3 mg/mL); injection	Reduced upregulation of <i>Lysozyme</i> and <i>IMPI</i> at 48 hours when coinjected with <i>C. militaris</i> compared to no cordycepin (spores only)	Woolley <i>et al.</i> 2020
<i>Galleria mellonella</i> (greater wax moth) larvae	11.9 mM (3 mg/mL); injection	Reduced upregulation of <i>Lysozyme</i> and <i>IMPI</i> at 48 hours when coinjected with <i>B. bassiana</i> compared to no cordycepin (spores only)	Woolley <i>et al.</i> 2020
<i>Galleria mellonella</i> (greater wax moth) larvae	11.9 mM (3 mg/mL); injection	Reduced upregulation of <i>Lysozyme</i> and <i>IMPI</i> at 48 hours compared to no cordycepin (sham injection)	Woolley <i>et al.</i> 2020
<i>Galleria mellonella</i> (greater wax moth) larvae	12.5 mM (3.14 mg/mL) injection	Reduced survival time when coinjected with 25 spores of <i>Cordyceps militaris</i> compared to no cordycepin (spores only)	Kato <i>et al.</i> 2021
<i>Galleria mellonella</i> (greater wax moth) larvae	12.5 mM (3.14 mg/mL) injection	Reduced survival time when coinjected with 25 spores of <i>Beauveria bassiana</i> compared to no cordycepin (spores only)	Kato <i>et al.</i> 2021
<i>Galleria mellonella</i> (greater wax moth) larvae	12.5 mM (3.14 mg/mL) injection	Reduced survival time when coinjected with 25 spores of <i>Metarhizium anisopliae</i> compared to no cordycepin (spores only)	Kato <i>et al.</i> 2021

1.5 PROJECT AIMS AND OUTCOMES

The principle purpose of my PhD was to examine the role of cordycepin in the biology of the fungus *Cordyceps militaris*. From this came three aims. Chronologically, the first aim was to investigate the implications of the phenomenon of culture degeneration, in which cordycepin production is reduced, on *C. militaris*. The second aim was to investigate what function, if any, cordycepin plays in the process of infection of the insect host. Finally, the third aim was to investigate why coupled cordycepin and pentostatin production has been favoured by natural selection in this species, and how it could have evolved.

To meet the first aim, culture degeneration was investigated using a *C. militaris* isolate from which two strains had been produced: a parental control strain (PCS) and a degenerated strain (DS). The degenerated strain was found not only to have reduced cordycepin and pentostatin production, as expected, but also reduced expression of genes involved in sexual development, and changes in other metabolites relating to the citrate cycle and purine synthesis.

Host models for infection were used to meet the second aim. After much method development, an effective model system was used to assess the effects of degeneration on host infection. This system consisted of injecting conidia of the *CM2* isolate PCS and DS into *Galleria mellonella* caterpillars and observing responsiveness, full melanisation, and fungal emergence from the insects on a daily basis. Here it was demonstrated that the degenerated strain produced a lesser pathogenic response in the host, with slower fungal colonisation in almost all and reduced melanisation in some experiments. Fungal emergence of this strain was enhanced when cordycepin and pentostatin were additionally injected into the host – suggesting an aid to the infection process by these secondary metabolites.

Gene expression analyses were also performed on cell model systems of extracted haemolymph from injected *G. mellonella* caterpillars and *Drosophila melanogaster* S2 cells.

Cordycepin was shown to suppress the upregulation of immune response genes in both models. Pentostatin was shown in one case to enhance the effect of a lower dose of cordycepin, which is consistent with its reported function as the protector molecule to cordycepin.

During a range of attempts to reverse degeneration and rescue cordycepin production in the degenerated strain, experiments involving the extraction and culture of the fungus after injection of spores into *G. mellonella* caterpillars showed enhanced expression of sexual development-related and cordycepin/pentostatin synthesis genes early in the infection process. Although the reversal of degeneration was not achieved in this project, these results support the suggestion that sexual development gene expression and cordycepin production are correlated features of the host infection process by this entomopathogenic fungus.

Finally, to meet the third aim, a bioinformatics study of the cordycepin/pentostatin biosynthesis gene cluster (genes *Cns1*, 2 and 3) was carried out – to investigate the evolutionary origins of cordycepin production. BLAST-based searches on hundreds of sequenced genomes uncovered intact homologue clusters for this synthesis in only a handful of mostly unrelated fungal species, several of which were plant pathogens. These findings suggest that cordycepin and pentostatin coproduction is rare in the fungal kingdom and that horizontal gene transfer has occurred between species. It is also likely that cordycepin, a kind of blunt molecular instrument, fulfils a variety of related purposes in the life histories of different possessors.

The findings of this PhD shed new light on the biological roles of cordycepin in the organism which produces it; as well as providing novel insights into the problem of culture degeneration.

CHAPTER 2: MATERIAL AND METHODS**2.1 Material and Methods Overview**

This PhD project spans a range of disciplines, including mycology, entomology, analytical chemistry, and molecular biology. Accordingly, a variety of different methods have been used – involving molecular biological techniques, fungal culturing, animal cell culture experiments, live caterpillar studies, and combined chromatography and mass spectrometry protocols with targeted and untargeted metabolomics analyses. Reagents, chemicals, and media used in the project are listed in table 2.1; computer software used is listed in table 2.2.

Table 2.1: Reagents, chemicals and media used

Reagent/Material	Use(s)	Supplier
Wizard® Genomic DNA Purification Kit - Cell lysis solution - Nuclei lysis solution - Protein precipitation solution	DNA extraction/purification	Promega
Reliaprep® RNA Cell Miniprep System - BL + TG buffer - RNA wash solution - DNase I - Yellow core buffer - MnCl ₂ (0.09M) - Column wash solution	RNA extraction - caterpillars	Promega
GeneJET® RNA Purification Kit - RNA lysis solution - Proteinase K - Wash buffer 1 - Wash buffer 2	RNA extraction - fungi	ThermoFisher
SuperScript® III First-Strand Synthesis System - Random hexamers - dNTPs - First Strand Buffer - Dithiothreitol (DTT) - Superscript III	Reverse transcription	ThermoFisher
GoTaq® qPCR Master Mix	Quantitative polymerase chain reaction (qPCR)	Promega
GoTaq® G2 polymerase, (with - buffer - dNTPs - MgCl ₂)	PCR	Promega

SYBR® Safe	Gel Electrophoresis	Invitrogen
Agarose	Gel Electrophoresis	Sigma-Aldrich/Merck
Distilled, deionised water (ddH ₂ O)	General use	
Methanol (LC-MS grade)	LC-MS (sample preparation; solvent)	VWR
Ethanol (HPLC grade)	DNA extraction	VWR
Isopropanol (HPLC grade)	DNA and RNA extraction	VWR
Chloroform (LC-MS grade)	LC-MS (sample preparation; solvent)	VWR
Acetonitrile (LC-MS grade)	LC-MS (phases)	VWR
Ammonium Carbonate	LC-MS (phases)	VWR
Pierce LTQ ESI Positive Ion Calibration Solution (modified)	LC-MS (calibration)	ThermoFisher
Pierce ESI Negative Ion Calibration Solution (modified)	LC-MS (calibration)	ThermoFisher
Potato-dextrose broth	Fungal culture	Sigma-Aldrich/Merck
Agar	Fungal culture	Thermo-Fisher
Silk pupa powder	Fungal culture	MycoMedica
Schneider's <i>Drosophila</i> Medium	<i>Drosophila melanogaster</i> Schneider 2 cell culture	ThermoFisher
Dimethyl sulfoxide (DMSO)	Cell culture experiments	Sigma-Aldrich/Merck
Trypan Blue (0.4%)	Cell counting	ThermoFisher
Curdlan	Cell culture experiments	Sigma-Aldrich/Merck
Lipopolysaccharide (LPS)	Cell culture experiments	Sigma-Aldrich/Merck
Foetal Bovine Serum (FBS)	Cell culture	Gibco (ThermoFisher)
Phosphate-buffered saline (PBS)	RNA extraction; caterpillar injections	Gibco (ThermoFisher)
Oligonucleotides/Primers	General use	Sigma-Aldrich/Merck

Table 2.2: Computer software used

Software name	Use
Microsoft Office Excel® 2016	General data analysis and calculations
GraphPad Prism® 7	Preparation of data figures and statistical analysis
R version 4.0.0	Advanced data figures (e.g. heatmaps)
Thermo Exactive Tune®	Operation of mass spectrometry method
Thermo Chromeleon®	Overview of LC-MS on the (Q-)Exactive mass spectrometer; operation of liquid chromatography method
Thermo XCalibur®	
XCMS [Tautenhahn <i>et al.</i> 2008]	Processing analysis of LC-MS raw data files
MzMatch [Scheltema <i>et al.</i> 2011]	
IDEOM [Creek <i>et al.</i> 2012]	Excel-based platform for LC-MS high-throughput metabolomics data
Thermo Compound Discoverer®	Identification of metabolites by mass spectra following LC-MS/MS
Thermo TraceFinder®	Absolute identification of metabolites using standards following LC-MS
Sartorius SIMCA-P® 4	Statistical analysis of metabolomics data – PCA and OPLS-DA
OligoCalc (online software) [Kibbe 2007]	Calculation of melting points and self-complementarity detection in primer design
BLAST flavours (online software) [blast.ncbi.nlm.nih.gov]	Searches of biological databases based on genetic data
Phylogeny.fr (online software)	Phylogenetic tree assembly

2.2 MOLECULAR BIOLOGICAL METHODS

2.2.1 DNA Extraction

Fungal DNA was extracted using the Wizard® Genomic DNA Purification Kit (Promega), using a modified method based on manufacturers' instructions, specifically using the protocol for DNA extraction from yeast samples. Fungal material was snap frozen and thawed three times in lysis buffer solution using liquid nitrogen and 30°C water bath, before incubation at 65°C for 30 minutes and protein precipitation. DNA pellets were formed and washed using isopropanol and 70% ethanol before resuspension with water. Quality of DNA samples was assessed

using the NanoDrop spectrophotometer (ThermoFisher), using A260/A280 ratios and concentration in ng/μL. Samples with A260/A280 ratios less than 1.8 were discarded, as were samples of under 50ng/μL.

2.2.2 RNA Extraction

Fungal samples. Fungal RNA was extracted using the GeneJET® RNA Purification Kit (ThermoFisher), according to manufacturers' instructions. Additionally, the lysis buffer was supplemented with 10% β-mercaptoethanol. Quality of RNA samples was assessed using the NanoDrop spectrophotometer (ThermoFisher), using A260/A280 ratios and concentration in ng/μL.

Insect samples. RNA from cell cultures (*Drosophila*) was extracted using the Reliaprep® RNA Cell Miniprep System (Promega), according to manufacturers' instructions. Following treatments and before extraction, cells were treated with ice-cold sterile PBS. Then BL+TG buffer was added to the cells, which were still adherent to the well plate, and dislodged lysed cells were removed for the rest of the protocol. Caterpillar RNA was extracted using the same kit and also according to instructions. Prior to this protocol, treated caterpillars were snap frozen in liquid nitrogen to induce quick death. Haemocytes were then removed from caterpillars, and added to 500μL BL+TG buffer. Three freeze thaw cycles, using liquid nitrogen and a water bath at 35°C were carried out, before the lysate was spun down by centrifugation at 13,000 xg and the supernatant removed for the rest of the protocol.

In all cases, the quality of RNA samples was assessed using the NanoDrop spectrophotometer (ThermoFisher), using A260/A280 ratios and concentration in ng/μL. Samples with A260/A280 ratios less than 2.0 were discarded, with the vast majority of samples above 2.1. Samples with a concentration of under 50ng/μL were also discarded. In addition to this, RNA samples were assessed for quality using the RNA ScreenTape® System (Agilent), on the Agilent TAPEStation® system [figure 2.1], initially to scrutinise RNA extraction method.

This was done by staff at the Deep Seq department at the University of Nottingham. Some samples assessed using this method do not show to have good 28S:18S rRNA ratios, but do have acceptable RIN (RNA integrity number) values [Schroeder *et al.* 2006]. Given the endogenous “hidden break” properties of insect 28S rRNA [Winnebeck *et al.* 2010], these are considered as high quality samples and not degraded. The 28S fragment of extracted insect rRNA samples is known to separate into two similarly-sized 18S-clustered fragments, via the disruption of hydrogen bonds [Winnebeck *et al.* 2010].

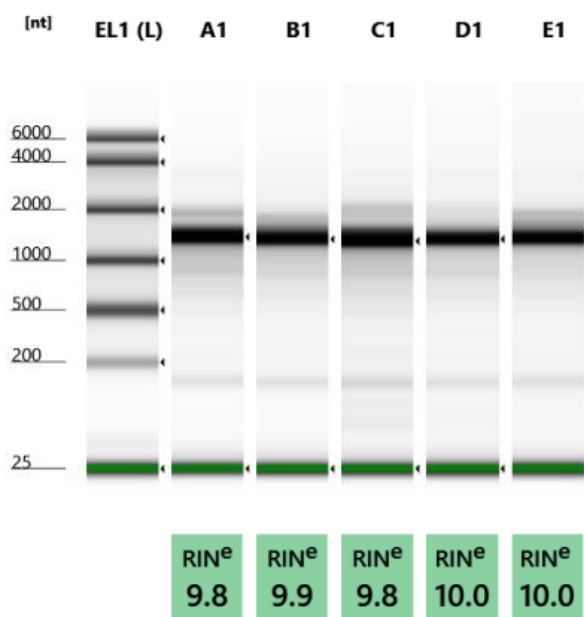


Figure 2.1: RNA ScreenTape results for a set of typical *Galleria mellonella* RNA extraction samples. Each sample has a clear band representing the 18S rRNA fragment.

2.2.3 Polymerase Chain Reaction (PCR) and Gel Electrophoresis

Standard PCR protocol – for example for screening fungal DNA with ITS or *MAT* loci primers was performed using GoTaq® G2 polymerase (Promega). 1 µL (50ng) template DNA was used in each case, with 1.25µM polymerase, 0.5 µM (final concentration) of each primer, and 1.5 mM MgCl₂, 0.2 mM dNTP mix (total reaction volume of 50 µL). The programme used on the thermocycler was 5 minutes at 95°C, followed by 40 cycles of 1 minute at 95°C, 30 seconds at 58°C and 2 minutes at 72°C, with a final elongation period of 10 minutes at 72°C.

RAPD (random amplification of polymorphic DNA) PCR reactions were performed using the same polymerase as above, but with a lower (1ng) amount of genomic DNA. The programme used on the thermocycler was 5 minutes at 95°C, followed by 45 cycles of 30 seconds at 95°C, 40 seconds at 37°C and 80 seconds at 72°C, with a final elongation period of 5 minutes at 72°C.

PCR products were run at 90 volts on 1.5% agarose gels in TBE buffer, stained with SYBR Safe® for visualisation under UV.

Primers used in PCRs are presented in table 2.3.

Gene	Sequence(s) (5'-3')	Organism	Reference
ITS (Internal transcribed spacer) 1 and 4	CTTGGTCATTTAGAGGAAGTAA TCCTCCGCTTATTGATATGC	<i>C. militaris</i>	White <i>et al.</i> (1990)
RAPD (Random amplification of polymorphic DNA)	A12: TCGGCGATAG A16: AGCCAGCGAA C7: GTCCCGAGCA B18: CCACAGCAGT S22: TGCCGAGCTG S62: GTGAGGCGTC	<i>C. militaris</i>	Sun <i>et al.</i> (2017)
<i>MAT 1-1-1</i>	GGAACACAGATCGAGCGACACTG CGTATAGTGGAAGTCTTCATGAGG	<i>C. militaris</i>	This study
<i>MAT 1-2-1</i>	CTCAGTATCGACGGTCTCATCTACC CCAGTGCCGGACATCAAATGTCCG	<i>C. militaris</i>	This study
<i>Cns1</i>	CCATGAACGAGAACGCTTATCC GCTCAAGCCGGACAAGACC	<i>C. militaris</i>	This study
<i>Cns2</i>	CTTGTCCTACCAGCGCCG GCACTCGGAAATGCCCGG	<i>C. militaris</i>	This study
<i>Cns3</i>	CGAGTCAACCGCCTACACC CGTGAAGAGGGACGTCTCG	<i>C. militaris</i>	This study
<i>Cns4</i>	GCACTCGGCATCACCTGG CTCTTGTTGCCATGGTCTCG	<i>C. militaris</i>	This study

2.2.4 Reverse Transcription and Quantitative PCR (RT-qPCR)

Following isolation of RNA, samples were converted to cDNA by reverse transcription, using the SuperScript® III First Strand Synthesis System (ThermoFisher). 200 ng RNA was used in each case, with 120 ng random hexamers, first strand buffer, 5 mM DTT, and 0.5 µL

SuperScript® Reverse Transcriptase enzyme. After the reaction, cDNA samples were diluted 10 times using 180 µL water.

The Qiagen Rotor-Gene Q qPCR machine (Qiagen) was used for qPCR. The GoTaq® qPCR Master Mix (Promega) was used, containing SYBR Green dye. 4 µL cDNA was used in each case, with 0.5 µM (final concentration) of each primer, and 5 µL master mix (total reaction volume of 10 µL). The programme used on the thermocycler was 5 minutes at 95°C, followed by 40 cycles of 30 seconds at 95°C, 30 seconds at 58°C and 60 seconds at 72°C.

Analysis of qPCR data. In all cases, three biological replicates were used for each treatment, and for each of these, three technical (pipetting) replicates were used. For the purposes of statistical comparisons, averages of technical replicates constitute individual biological replicates. Ct values from qPCR runs for genes of interest were compared against reference genes. In the case of fungal qPCRs, values from three reference genes were averaged. Differences between Ct values from genes of interest and reference gene averages were transformed into fold change values (2^{-Ct}), and finally these were normalised against a control sample.

Primers used in qPCRs are presented in table 2.4.

Table 2.4: Primers used in qPCRs

Gene/Locus	Sequences	Organism	Reference
<i>Actin (Act)</i> Reference gene	CGAAGACGTTGCCGCTCTGG CGGAGGCTGAGAATGCC	<i>C. militaris</i>	This study
<i>Calmodulin (Cal)</i> Reference gene	GCTTGCGCCCTCTCGCTGC CTCTGACTCGGAAGGGTTCTGGCC	<i>C. militaris</i>	This study
<i>Glyceraldehyde Phosphate Dehydrogenase (Gapdh)</i> Reference gene	CGTCAAGGTTGGCATCAACGG GCCGTTGACGACGAGATCG	<i>C. militaris</i>	This study
<i>Ribosomal Protein S3 (Rps3)</i>	TCCCAACTCTTGACCGACGA AGTGGTTGCGCCATCCATAC	<i>C. militaris</i>	This study
<i>Cordycepin/pentostatin synthesis cluster gene 1 (Cns1)</i>	GCTTATCCGACTACATTTCCATCC CCAGCCGCTCCAGGTGC	<i>C. militaris</i>	This study

<i>Cns2</i>	CGCCGGTGTCTCCAGAC CGAGGCGTGTGACACGC	<i>C. militaris</i>	This study
<i>Cns3</i>	CGAGTCAACCGCCTACACC GTAGGACTGGGGCAGCGG	<i>C. militaris</i>	This study
<i>Cn4</i>	GCCGGACAAAGAGAAACGAC CCAAGAGCATCTCTCCCGG	<i>C. militaris</i>	This study
<i>Loss of aflR- Expression A (LaeA)</i>	GGCTGTGCATCTGAACAAAATCC CGAGGGTAGCCAATGAATTTTCGACC	<i>C. militaris</i>	This study
<i>Velvet A (VeA)</i>	CCAGTGCCCAGTGCCAGTTG GCAATGGGCGAGGGCGAG	<i>C. militaris</i>	This study
<i>Variability of Spores A (VosA)</i>	CTCTTCATACACATCACCAAAGGC CTGTTGGCGCACCTCAAGG	<i>C. militaris</i>	This study
<i>Mating type a pheromone receptor (PreA)</i>	CGTTGTACCTTTGTTGCCAAGG GCAGACCAGGTTGGCCACG	<i>C. militaris</i>	This study
<i>Mating type alpha pheromone receptor (PreB)</i>	CGTCGTTTGACCGCTTCGC CGACGCAGAGCGCGAG	<i>C. militaris</i>	This study
<i>MAP kinase kinase Ste7 (Ste7)</i>	GATGGTCAACTCGAGATCGGG GTTGACAATGTAATCCGAGTGACAG	<i>C. militaris</i>	This study
<i>Transcription Factor SteA (SteA)</i>	GCTTTCTGCTCCCTACCGG GAAAGTCGAGAACTGGCTCTTG	<i>C. militaris</i>	This study
<i>MAT 1-2-1</i>	CTCAGTATCGACGGTCTCATCTACC CCAGTGCCGGACATCAAATGTCG	<i>C. militaris</i>	This study
<i>Ribosomal Gene S7e (S7e) Reference gene</i>	TCCCAACTCTTGACCGACGA AGTGTTGCGCCATCCATAC	<i>G. mellonella</i>	Wojda & Jakubowicz (2007)
<i>Lysozyme (Lyso)</i>	ATGTGCCAATGCCAAGTTG GTGGCTAGGCTTGGGAAGAAT	<i>G. mellonella</i>	Altincicek & Vilcinskas (2006)
<i>Gallerimycin (Gale)</i>	TATCATTGGCCTTCTTGGCTG GCACTCGTAAAATACACATCCGG	<i>G. mellonella</i>	Wojda & Jakubowicz (2007)
<i>Galiomicin (Gali)</i>	TCGTATCGTCACCGCAAATG GCCGCAATGACCACCTTTATA	<i>G. mellonella</i>	Wojda <i>et al.</i> (2009)
<i>Insect metalloproteinase inhibitor (IMPI)</i>	AGATGGCTATGCAAGGGATG AGGACCTGTGCAGCATTCT	<i>G. mellonella</i>	Altincicek & Vilcinskas (2006)
<i>Ribosomal protein RP49</i>	GACGCTTCAAGGGACAGTATCTG AAACGCGGTTCTGCATGAG	<i>D. melanogaster</i>	Goibert <i>et al.</i> (2003)
<i>Attacin A</i>	AGGTTTCCTTAACCTCCAATC CATGACCAGCATTGTTGTAG	<i>D. melanogaster</i>	Jin <i>et al.</i> (2008)
<i>Adenosine Deaminase (ADA)</i>	CCACGGAGTTGGCGATTTCG CCAAGCTGGGCACTGTTCC	<i>D. melanogaster</i>	This study

2.2.5 Design and Validation of Primers

Primers were designed manually based on sequence data – but checked using OligoCalc online software [Kibbe 2007], for self-complementarity and to calculate melting points. Those

used for qPCR were designed with approximately 200 base-pair sized products in mind. Primers were then ordered from Merck in dry format, and prior to use diluted to 10mM. Validation of primers was performed using serial dilution analysis, and with the running of qPCR products agarose gels to check for the band size expected.

2.3 LIQUID CHROMATOGRAPHY- MASS SPECTROMETRY (LC-MS)



Figure 2.2: The LC-MS system set up prior to running samples. Left: Thermo Exactive® mass spectrometer; right: Accela® HPLC.

Liquid chromatography-mass spectrometry (LC-MS) analysis of samples was chosen as the method to chemically assess fungal material with detection of metabolites by mass/charge (m/z) ratio. LC-MS is a more selective method for the identification of small molecules than UV detection, and typically has data outputs with lower background interference from solvents. Given the chemical diversity of the fungal extracts, my particular interest in nucleosides and related biomolecules, and also the opportunity for high-throughput and untargeted analyses,

a HILIC (hydrophilic interaction liquid chromatography) column and the Thermo Exactive® Orbitrap mass spectrometer were the chosen instruments for this [figure 2.1], available at the Centre for Analytical Biosciences (CAB). This was due to the high resolution and selectivity of this setup in particular for polar compounds.

2.3.1 Preparation of Samples

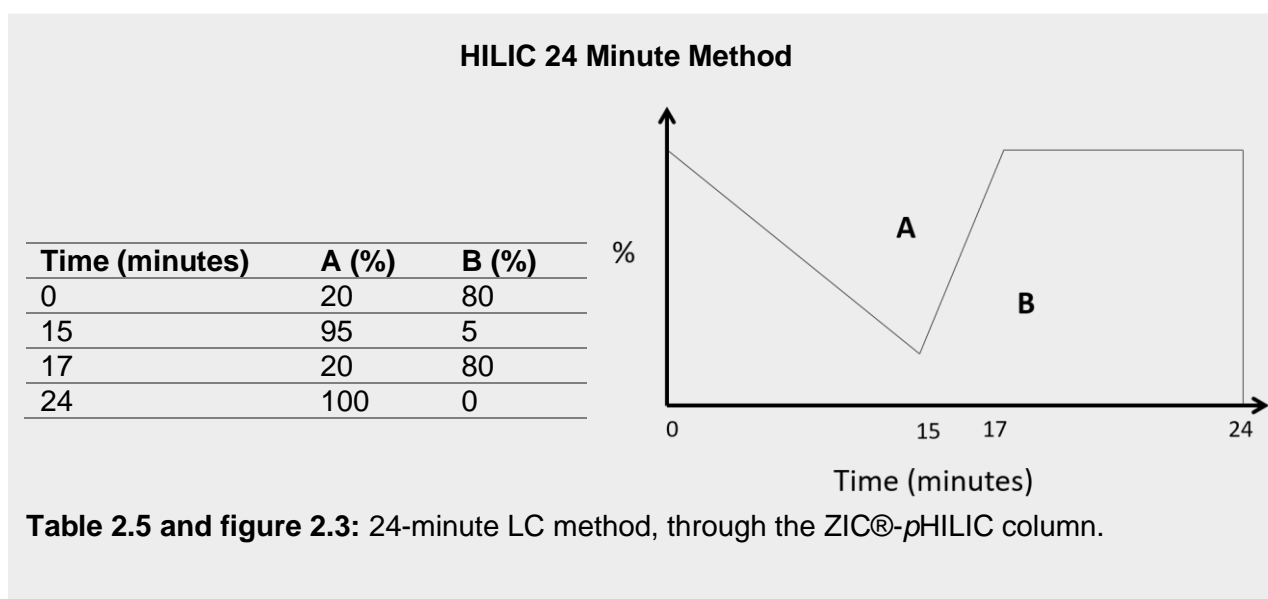
Samples were prepared from the removal of 30 mg of fungal culture from the agar plates, taking care to include no media at all. A freeze-thaw protocol similar to that used by Schatschneider *et al.* was used throughout, with a solvent of methanol:water:chloroform (1:1:2 ratio) [Schatschneider *et al.* 2018]. Following 24 hours at -20°C, the samples were centrifuged and the aqueous phase (1:1 methanol:water solvent) was removed for analysis. Three biological replicates, from separate plates, were used per treatment group. Once prepared, samples were stored at -80°C until LC-MS analysis. As well as analytical samples, blank samples were prepared using solvent only, QC (quality control) samples were prepared using mixtures of equal volumes from all analytical samples, and spiked QC samples were included by the addition of standards to QC samples.

Standards of cordycepin and pentostatin were prepared at 1, 5, 10, 25, 50, and 100 µM in the solvent. Use of these standard mixtures allowed for quantification of cordycepin and pentostatin in samples, by fitting to the resulting calibration curve (discussed later), in targeted LC-MS analyses. In untargeted LC-MS analyses, previously five prepared standard mixtures, containing 250 well-known metabolites as done previously [e.g. Schatschneider *et al.* 2018]. This technique allowed identification based on both *m/z* and retention times of large numbers of metabolites in a single LC-MS run.

2.3.2 Liquid Chromatography

Hydrophilic interaction liquid chromatography (HILIC) was employed for separation of compounds prior to mass spectrometry. Having the use of an eluent with a high concentration organic solvent (in this case 100% acetonitrile) in a highly soluble aqueous buffer (20 mM ammonium carbonate) allowed compounds to be separated on the basis of both electrostatic interactions by polar compounds, and hydrophilic partitioning. These interactions occurred between compounds in the samples and the stationary phase, consisting of a polymer with a sulfobetaine functional group, within the ZIC-pHILIC® column (Sequant, Merck) [Merck: ZIC-pHILIC manual].

The column was assembled according to manufacturer's instructions, within the Accela® (ThermoFisher) autosampler and LC pump system, and an isocratic solution of 20:80 20mM ammonium carbonate (pH 9.1) (A) : 100% acetonitrile (B). A flow rate of 300µL was used and a temperature of 45°C in the column oven was maintained. Regarding ratios of A:B in the mobile phase, a 24 minute-per-sample method was used, as done previously [Schatschneider *et al.* 2018] – as shown in table 2.5 and figure 2.3.



2.3.3 Mass Spectrometry

The Thermo Exactive® Orbitrap mass spectrometer was used for the most part, in targeted and untargeted MS runs. The Thermo Q-Exactive® MS was used for higher-level identification of metabolites using tandem MS (MS/MS) – this was performed on QC samples from previous runs. Before use, mass spectrometers were calibrated with modified versions of the Pierce ESI positive and negative solutions (ThermoFisher). The mass spectrometers are detailed in figure 2.4.

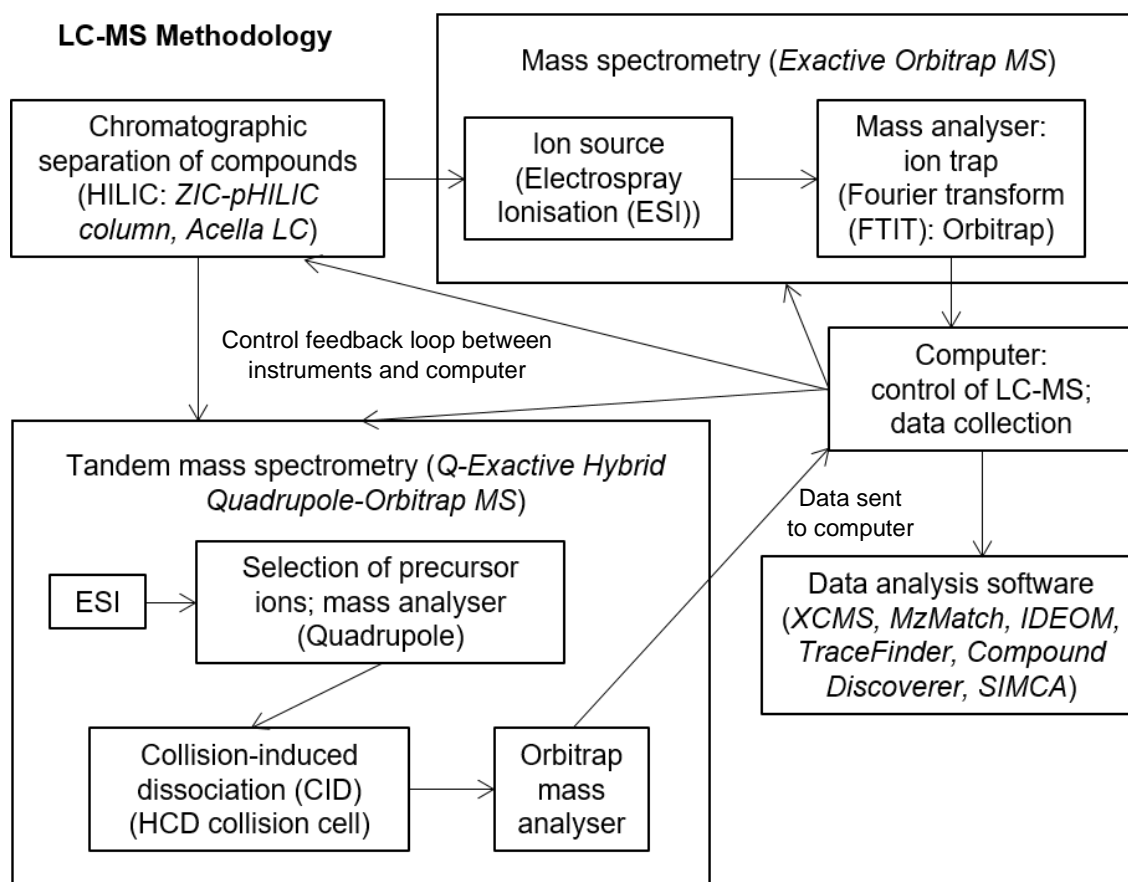


Figure 2.4: Diagram of LC-MS methodology. After separation of compounds in samples using the ZIC-pHILIC® column, flow through was fed into the mass spectrometer. In each case, ESI was used as the ionisation technique. **Exactive MS.** Ions from the resulting charged droplets formed by ESI were collected in a C trap®, from which they were injected into the orbitrap mass analyser in high speed pulses. The Orbitrap is a type of Fourier transform ion trap (FTIT) mass analyser, in which ions orbit and oscillate around an inner electrode. The complex ion paths formed by this process project an image current to the outer detectors, which is interpreted to obtain m/z values. **Q-Exactive MS.** This mass spectrometer was used to perform tandem mass spectrometry (MS/MS), in order to identify metabolites of interest to a higher level of confidence by using fragmentation patterns in mass spectra. The Q-Exactive contains two mass analysers: the first (MS1) being a quadrupole mass filter, which contains four electrical current and radio frequency-conducting rods; and the second (MS2) being an Orbitrap mass analyser. The role of the Orbitrap mass analyser in the Q-Exactive differed from that of the Exactive in that only precursor ions selected in MS1 were passed through it, and after collection in a C trap combined with a argon-containing HCD collision cell. In the collision cell, fragmentation of ions occurred, in the process of collision-induced dissociation.

2.3.4 Settings and Steps in Performing an LC-MS Run – ZIC-pHILIC and Exactive MS

The LC-MS system was controlled electronically using a linked desktop computer, with the Thermo Tune® and Xcalibur® softwares (ThermoFisher). Most runs were performed using the Accela HPLC and Exactive MS system. In the cases where the UltiMate 3000 HPLC and Q-Exactive MS system was used, Chomeleon® software (ThermoFisher) was used to control the HPLC instead of Xcalibur.

Sample preparation prior to LC-MS run is described in the methods sections of results chapters. 50% LC-MS-grade methanol (diluted with ddH₂O) was used as a sample solvent throughout.

Broadly speaking, the standard operating producer for running the LC-MS system consisting of the Thermo Accela® LC system with SeQuant ZIC®-pHILIC (Merck) column and Thermo Exactive® mass spectrometer can be divided into five main processes. These are (i) the preparation of samples and phases; (ii) calibration of mass spectrometer; (iii) HPLC settings and purging the system; (iv) conditioning the column; and (v) creating the sequence and starting the run.

(i) Preparation of samples and phases. Sample preparation methods are described in the proceeding chapters where appropriate. Samples were stored at -80°C prior to the LC-MS run. Mobile phases used to run through the column in the HPLC system were 20 mM ammonium carbonate (at pH 9.1) – phase A – and 100% acetonitrile – phase B. The wash solution for the system was defined as phase A. Lines were set up accordingly.

(ii) Calibration of the mass spectrometer. The mass spectrometer was calibrated using modified versions of the Pierce ESI positive and negative solutions (ThermoFisher). To cover small metabolites in the calibration mass range, contaminants with low masses were included in the mixture – these were C₂H₆NO₂ (m/z 76.0393) for the positive mode and C₃H₅O₃ (m/z = 89.0244) for the negative mode. Calibrations were performed using positive and negative modes and a calibration Tune file on the Thermo Tunes software. A 500 µL Hamilton syringe

was used to pump 10-20 μL solution per minute into the mass spectrometer. Calibration was set once total ion count (TIC) was lower than 5 per cent.

(iii) HPLC Settings and purging the system. Using the Xcalibur software, settings for the Accela HPLC system were put in place. Autosampler tray and oven temperatures were set at 4°C and 45°C respectively. The needle and syringe were washed prior to the run. Purging (removing bubbles) of the system was performed.

(iv) Conditioning the column. After purging, the ZIC-pHILIC column was attached and conditioned, with the running ratio and flow rate of phases A and B – 20% A and 80% B with flow rate 300 μL per minute – for at least half an hour in advance of the start of the LC-MS run.

(v) Creating the sequence and starting the run. The final step in the standard operating procedure for LC-MS setup for the creation of the sample sequence using the Xcalibur software. In all runs, QC (quality control) samples, both spiked and non-spiked with standards were used; and in targeted runs, standard samples containing metabolites of interest cordycepin and pentostatin, at 1, 5, 10, 25, 50, and 100 μM were used. Five mixtures (named A,B,C,D,E) of 250 standards were used for the untargeted run, as done previously [Schatschneider *et al.* 2018]. The sequence of samples injected followed recommendations [Want *et al.* 2010], as presented in figure 2.5. QC samples were interspaced between five randomised treatment group samples at a time, and repeated QC samples injected at the start of the run.

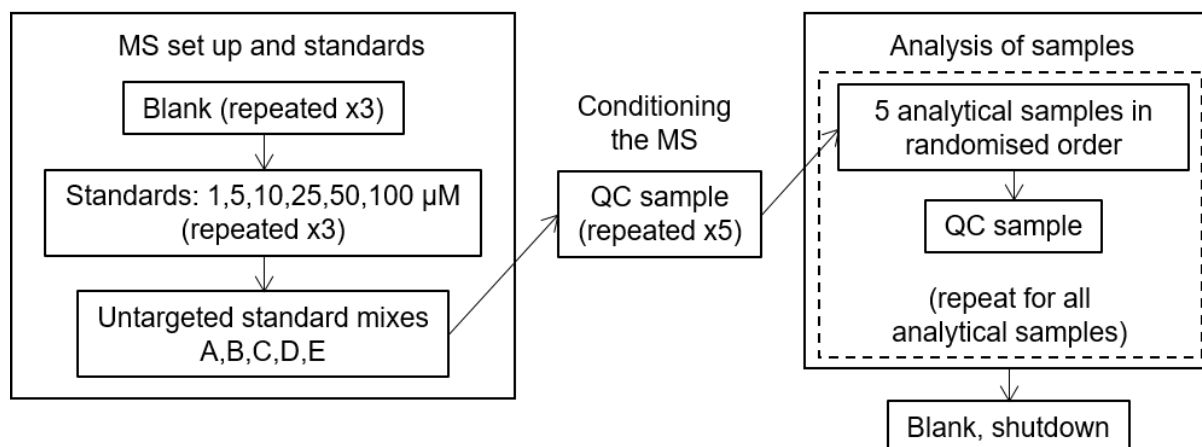


Figure 2.5: Sequence of samples used in LC-MS runs [after Want *et al.* 2010].

2.3.5 Analysis of LC-MS Data

Levels of identification of metabolites.

When present in standard samples in the same run, metabolites were identified based on accurate masses (calculated from mass:charge ratios (m/z values)) and retention times of these standards (Metabolomic Standards Initiative Level 1 identification). Other metabolites were identified at a lower level of confidence (putative identification), based on m/z and predicted retention times, as performed by IDEOM software under the parameters provided by default [Creek *et al.* 2012] (Metabolomic Standards Initiative Level 2 identification) [Sumner *et al.* 2007; Sumner *et al.* 2014]. IDEOM also performed noise filtering of samples, and softwares XCMS [Tautenhahn *et al.* 2008] and MzMatch [Scheltema *et al.* 2011] were used following untargeted MS runs, for picking peaks and the matching and annotation of peaks respectively, as done in previous studies [e.g. Kim *et al.* 2015]. The highest level of metabolite identification was achieved following tandem MS (MS/MS) runs using the Q-Exactive MS. Mass spectra depicting fragmentation products were used to identify several metabolites of interest. This was performed on Compound Discoverer® (Thermo) software.

Absolute and relative quantification of metabolites. Following targeted runs on the Exactive MS, outputs of standards for compounds of interest (notably cordycepin and pentostatin) were used for the absolute quantification of levels of these compounds in analytical samples. The software used for these analyses was TraceFinder® (Thermo), and calibration curves were fitted from standard samples. Only calibration curves with R squared values of 0.99 or above were deemed acceptable for use – and standard sample repeats were included or excluded to produce well-fitting curves. Care was taken to produce samples that would fit to curves on the straight part of the curve – i.e. with using dilutions to predicted concentrations of 10–50 μM . This avoided quantification issues caused by saturation of detection at higher concentrations. Examples of this are depicted in figure 2.6. By this method, peak areas from sample chromatograms at retention times matching the compounds in standards were used and converted to values for concentrations.

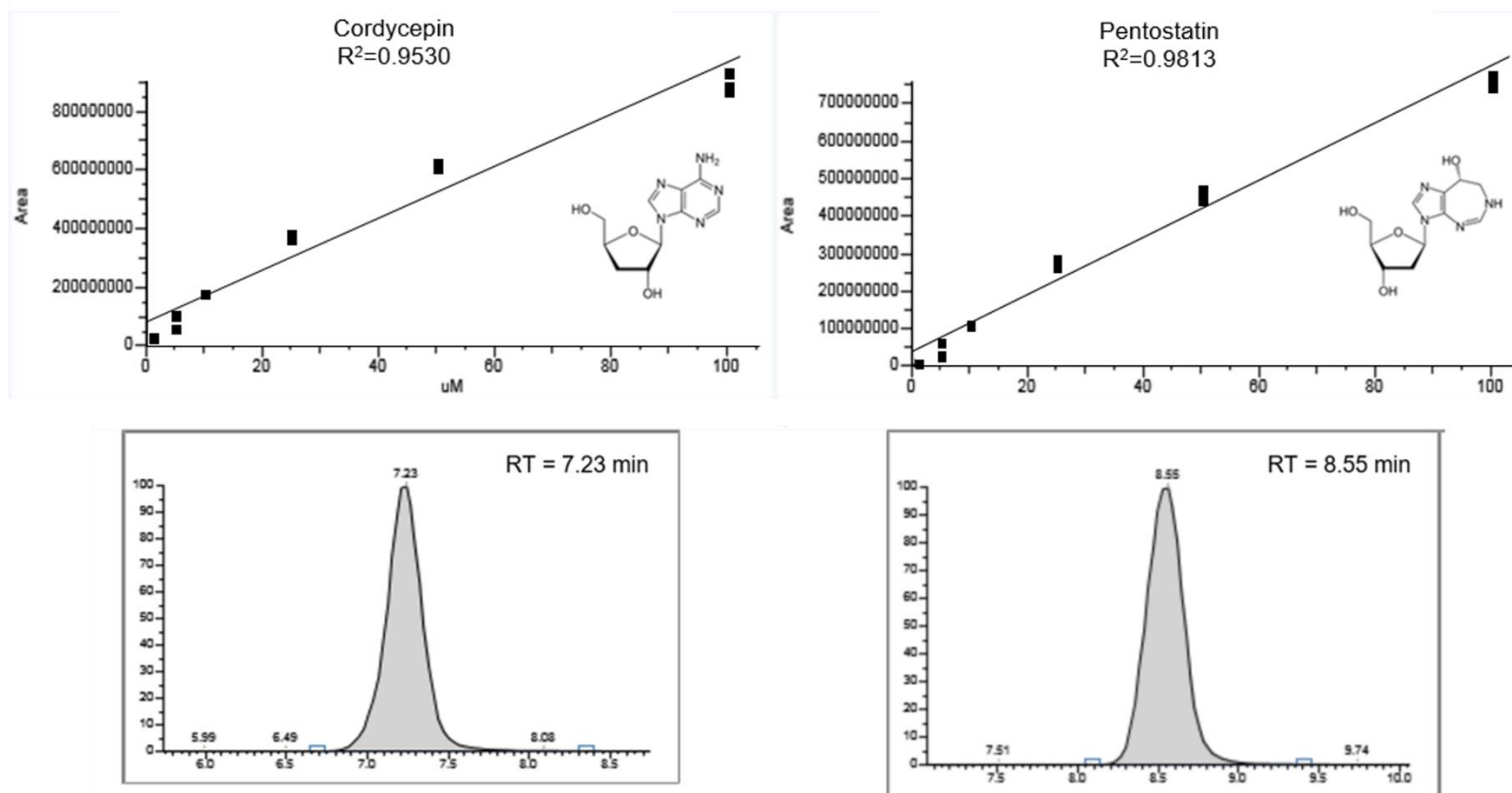


Figure 2.6: Calibration lines and chromatogram peaks for cordycepin and pentostatin, as shown in TraceFinder® software.

Relative concentration was calculated based on peak areas at relevant retention times in untargeted runs, using sample outputs from the five mixtures of standards, following untargeted runs on the Exactive MS. Additionally, relative concentrations of putatively-identified metabolites were also calculated, using IDEOM software.

Presenting untargeted metabolomics data. Figures used to present data from untargeted LC-MS runs were constructed using GraphPad Prism®, R® version 4.0.0. and SIMCA-P® version 4 softwares. This included pie charts, heatmaps, and multivariate analysis (principle component analysis (PCA) and orthogonal partial least squares-discriminant analysis (OPLS-DA)) respectively. Significant differences in metabolite levels were determined by both t-tests with false discovery rate (FDR) corrections and having VIP values >1 following orthogonal partial least squares-discriminant analysis (OPLS-DA) using SIMCA-P software.

2.4 FUNGAL CULTURE AND MICROBIOLOGICAL METHODS

2.4.1 Establishment of Fungal Cultures

Fungal strains were predominantly grown on potato dextrose agar (PDA). This media was chosen for a few reasons. Firstly, it is a common media for culturing fungi, including *C. militaris* as seen in relevant literature. Secondly, this choice of media produced growth rates allowing for data to be collected over a period of several days. Thirdly, PDA was the media used previously for the culture of the *C. militaris* strain subject to the degeneration experiments (see below). Throughout, PDA cultures were grown under dark conditions on parafilm-covered 9 cm diameter Petri dishes at 25°C, and were subject to further methods after two weeks of growth.

For a major part of the project, the strain *CM2* (MycMedica) was the subject of experiments, given its great production of cordycepin and the phenomenon of degeneration observed in

subcultured substrains. Strains *CM2* and *CM16*, were isolated by Andrej Gregori at MycoMedica, from *C. militaris* stromata collected from the wild in China and Slovenia respectively. In this case, ascospores from perithecia were isolated and established cultures on PDA plates [figure 2.7].

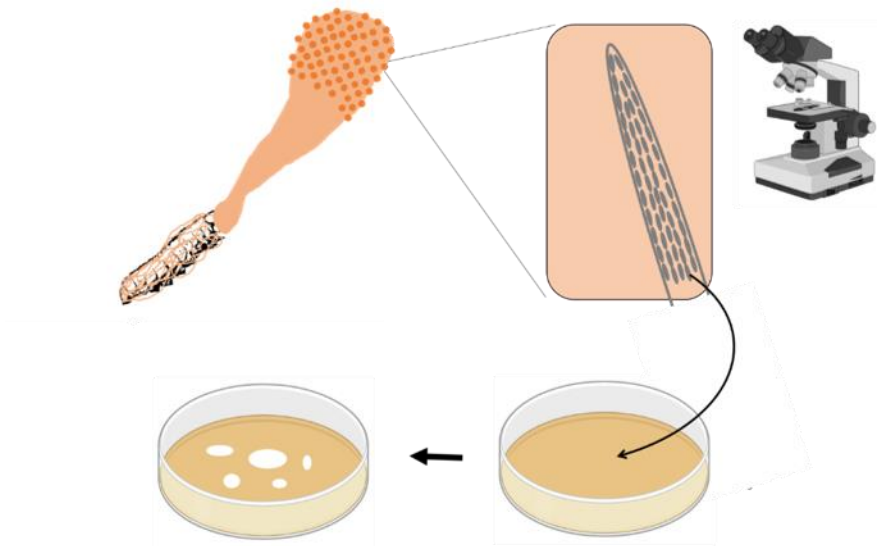


Figure 2.7: Establishing new fungal cultures from stromata. Ascospores (pictured on the right) are isolated from the perithecia of stromata, and produce new cultures on agar.

2.4.2 Subculturing on Agar

To investigate effects of subculturing in degeneration of *C. militaris*, the strain *CM2* was successively subcultured on PDA, during a period of over 2 years, at MycoMedica labs, Podkoren, Kranjska Gora, Slovenia, resulting in a low cordycepin-producing substrain. Director Dr. Andrej Gregori asked me to investigate the causes and characteristics of this new substrain in comparison to the original parental (S1) strain. The process of subculturing from the first culture (S1) was also repeated. In each case, a sterile scalpel was used to cut and transfer a 0.5 x 0.5 cm square edge piece of agar culture onto a fresh plate. Figure 2.8 depicts subculturing methods for PDA and also PDB (broth) which was used to prepare inoculum for insect experiments (discussed later).

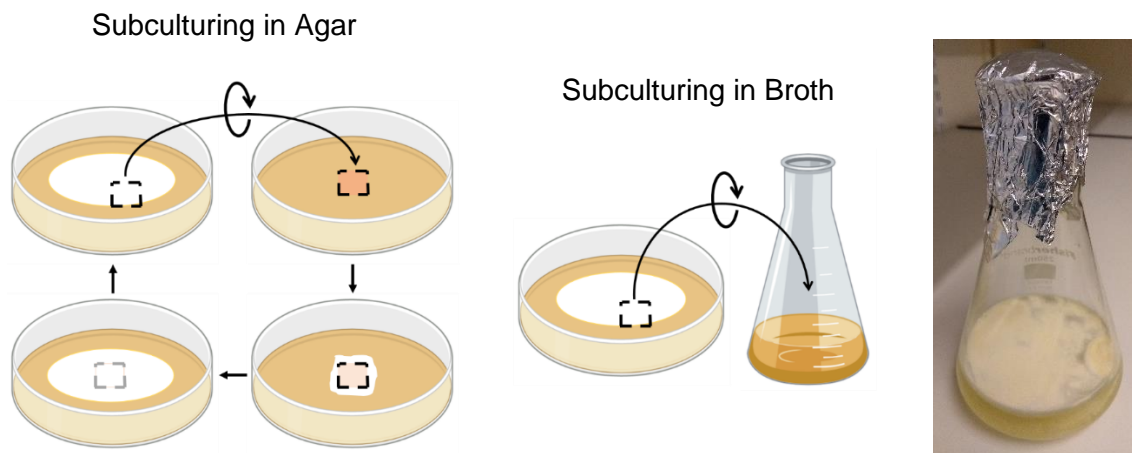


Figure 2.8: Subculturing *C. militaris* cultures on agar and in broth. Right: PDB culture after four weeks of growth

2.4.3 Single Spore Isolate Cultures

To prepare single spore isolate cultures [figure 2.9], fungal culture material collected from two week-old PDA cultures were added to sterile phosphate-buffered saline (PBS), and this suspension was diluted 1000 times in more sterile PBS. 100 μ L of the diluted suspension was spread on new PDA plates and monitored for growth of single spore cultures. After five days of growth, single spore cultures were subject to experimental treatments.

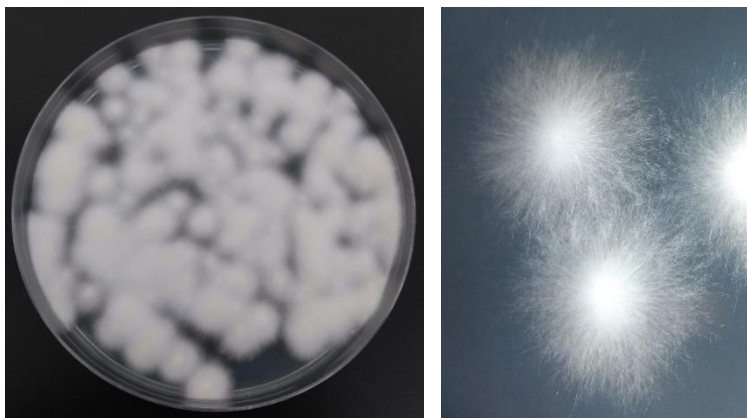


Figure 2.9: Single spore isolate cultures (*CM2* strains) after seven days (left) and five days (right) of growth.

2.4.4 Liquid Broth Cultures

Cultures of *C. militaris* in 100 mL PDB were used to prepare inoculum for insect host experiments, and were set up by subculturing from PDA plates. These were grown in foil-sealed conical flasks in static conditions at 27°C under constant light, for four weeks.

2.4.5 Measuring Fungal Growth

Fungal growth rates were assessed by measuring growth of fungal subcultures on PDA after 20 days (radius in mm); and by colony forming unit (CFU) analysis – counting colonies formed after 3 days using the same methods as used to obtain single spore isolates.

2.4.6 Preparing Inoculum and Extracts for Host Assays

For experimental use, in the case of caterpillar experiments, fungal cultures were grown for four weeks (in the case of broth cultures) or two weeks (agar cultures). Media and fungal material was extracted from broth and agar cultures as appropriate. When required, spores were counted using a haemocytometer. When spore-only treatments were required, spore suspensions taken from cultures were spun down using a centrifuge at 13000 xg for 10 minutes, washed with sterile phosphate-buffered saline (PBS), spun again, and resuspended in PBS. Typically PBS was used in blank samples. The preparations of fungal spore suspensions and extracts used on insect host experiments are detailed later.

2.4.7. Fungal Species Verification and Strain Characterisation

For comparisons between strains and confirmation of cultures belonging to the same *C. militaris* strain, RAPD PCRs were performed and run on agarose gels. ITS PCRs were used, with subsequent sequencing, to confirm species identity. The presence of *Cns* genes and mating-type loci in cultures was also tested using sequencing of PCR products. Sequencing was performed by Source Bioscience Ltd.

2.5 ANIMAL CELL CULTURE

2.5.1 *Drosophila melanogaster* Schneider 2 Cells

Drosophila melanogaster macrophage-like Schneider 2 cells were cultured in Schneider's *Drosophila* media (ThermoFisher), [figure 2.10] supplemented with L-Glutamate and 10% foetal bovine serum (FBS) (ThermoFisher), in T20 flasks. These were incubated at 25°C. Prior to experimental treatment, when at 80% confluence, cells were seeded into 6-well plates, with approximately 3×10^6 cells per well. Cells were counted using a haemocytometer following staining by Trypan Blue (ThermoFisher). 24 hours before treatment, media was replaced with fresh media without FBS, starving the cells. For maintenance of cell cultures, 1 mL cells were transferred to new flasks, with 19 mL fresh media. No more than 40 passages were permitted, and experimental replicates were performed within the same passage. Gene expression in treated cells was assessed at four hours after exposure.

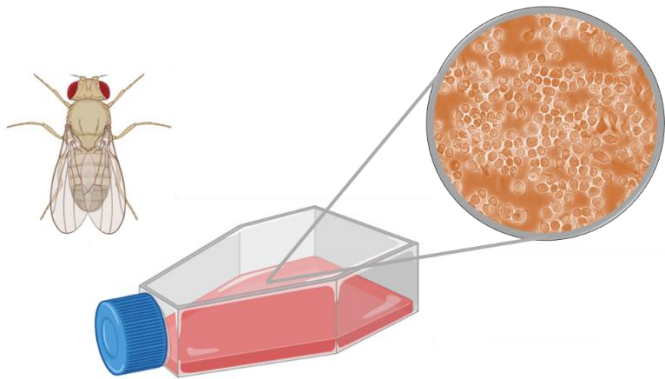


Figure 2.10: *Drosophila melanogaster* Schneider 2 Cells in culture.

2.5.2 Cell Culture Gene Expression Assays

Following treatments, cell cultures were placed on ice and had media removed. The adherent cells were washed with ice-cold sterile PBS. Then RNA was extracted using the Reliaprep® RNA Cell Miniprep System (Promega), according to manufacturers' instructions. RT-qPCR was subsequently performed to assess gene expression.

2.6 CATERPILLAR EXPERIMENTS

2.6.1 Caterpillar Rearing and Conditions

Greater wax moths (*Galleria mellonella*) were reared according to previously-established protocols for this model species (particularly Ramarao *et al.* 2012 and Jorjao *et al.* 2018). The moths were reared in a dark enclosed room, covered with muslin and at a temperature of approximately 25°C. Newly hatched larvae (caterpillars) were placed in boxes with regularly replaced (every two days) bran and honey food mixture. As larvae progressed along the six larval stages for this species, they were separated to match density and food intake. Once at pupation stage, pupae were separated from other larvae and left in separate boxes until emergence into adult moths around a fortnight later. Adult moths laid eggs in suspended 4-layered paper and these were placed in separate boxes until larval hatching.

2.6.2 Caterpillar Assays

The methods for treatments of *G. mellonella* as an insect host model for fungal infection are detailed in figures 2.11-12 and table 2.6. These include injections with fungal material and metabolites cordycepin and pentostatin, exposure to fungal cultures, and spore soaking. Readouts consisted of daily observations or gene expression assays involving RT-qPCR at

two hours post exposure. Caterpillars at a length 1.8 – 2.2 cm and weight 250 – 290 mg were selected randomly for experimental treatments, and placed in Petri dishes, with 5 caterpillars per dish. Injections of caterpillars were positioned behind the last left proleg, using sterile 0.3 mL 30 g 8 mm BD Microfine syringes and needles (UKMEDI). Daily assay treatments were recorded blindly throughout, using codes provided by a fellow lab member, the identities of which in each case were revealed only at the end of the experiment.

Insect Host Assay Treatment Methods

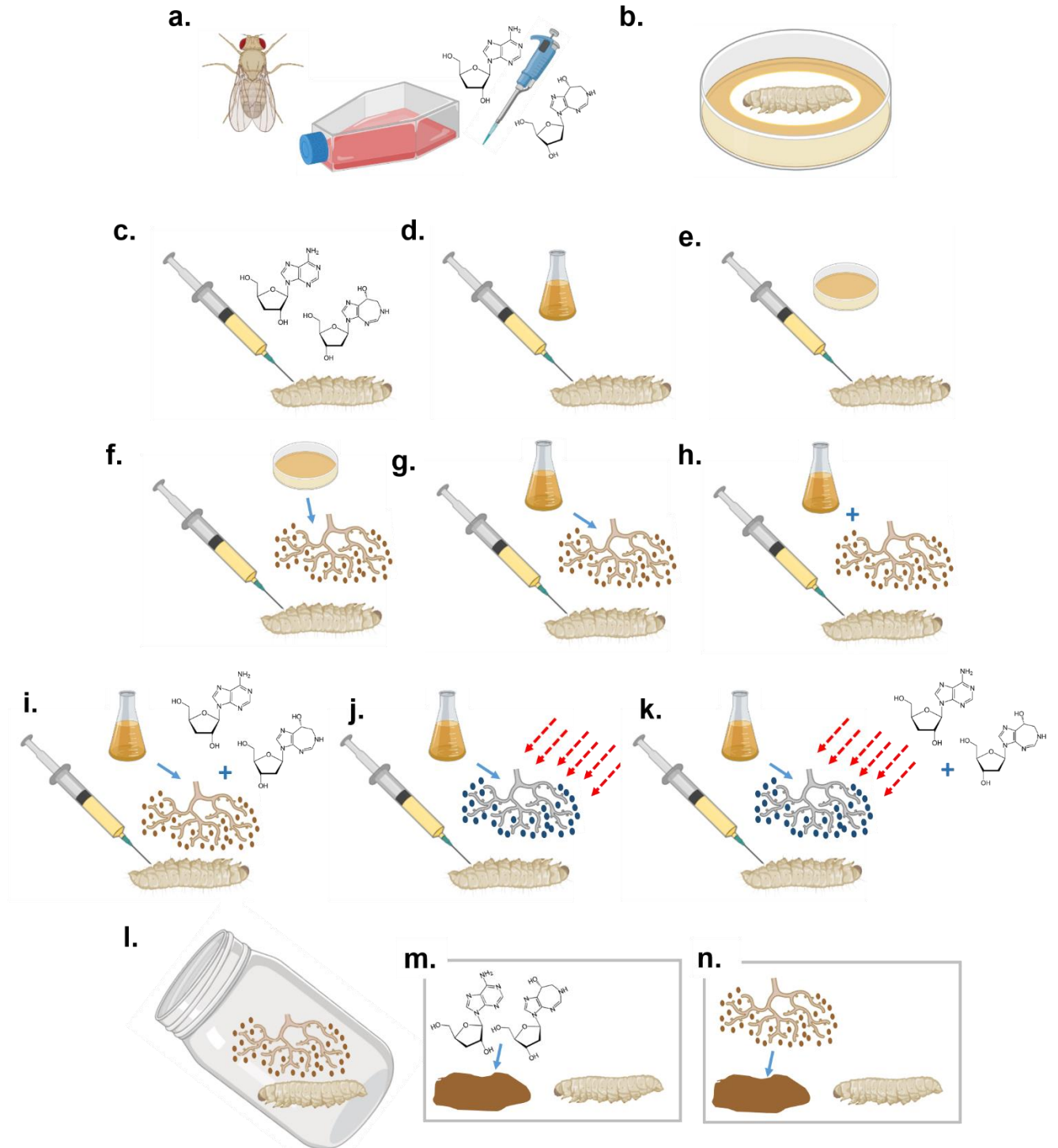


Figure 2.10: Treatments used for inoculation with fungal material and/or introduction of metabolites suspensions or fungal extracts to insect host models for subsequent assays. *Drosophila melanogaster* S2 cell culture assays were performed, with treatments of addition of pure cordycepin and pentostatin (a). Serums used for injection treatments on live *Galleria mellonella* caterpillars included pure cordycepin and pentostatin in solution (c), washed spores in solution (f, g), extracted media from fungal cultures (d), metabolite extractions from fungal culture material (e), washed irradiated spores (j), and combinations of extracted media with spores (h), and washed spores with cordycepin and pentostatin (i). Other treatment methods used on caterpillars included soaking with washed spores (k), exposure to fungal cultures on agar (b), and the introduction of washed spores and cordycepin and pentostatin to caterpillars' food – honey (l, m).

Insect Host Assay Readouts

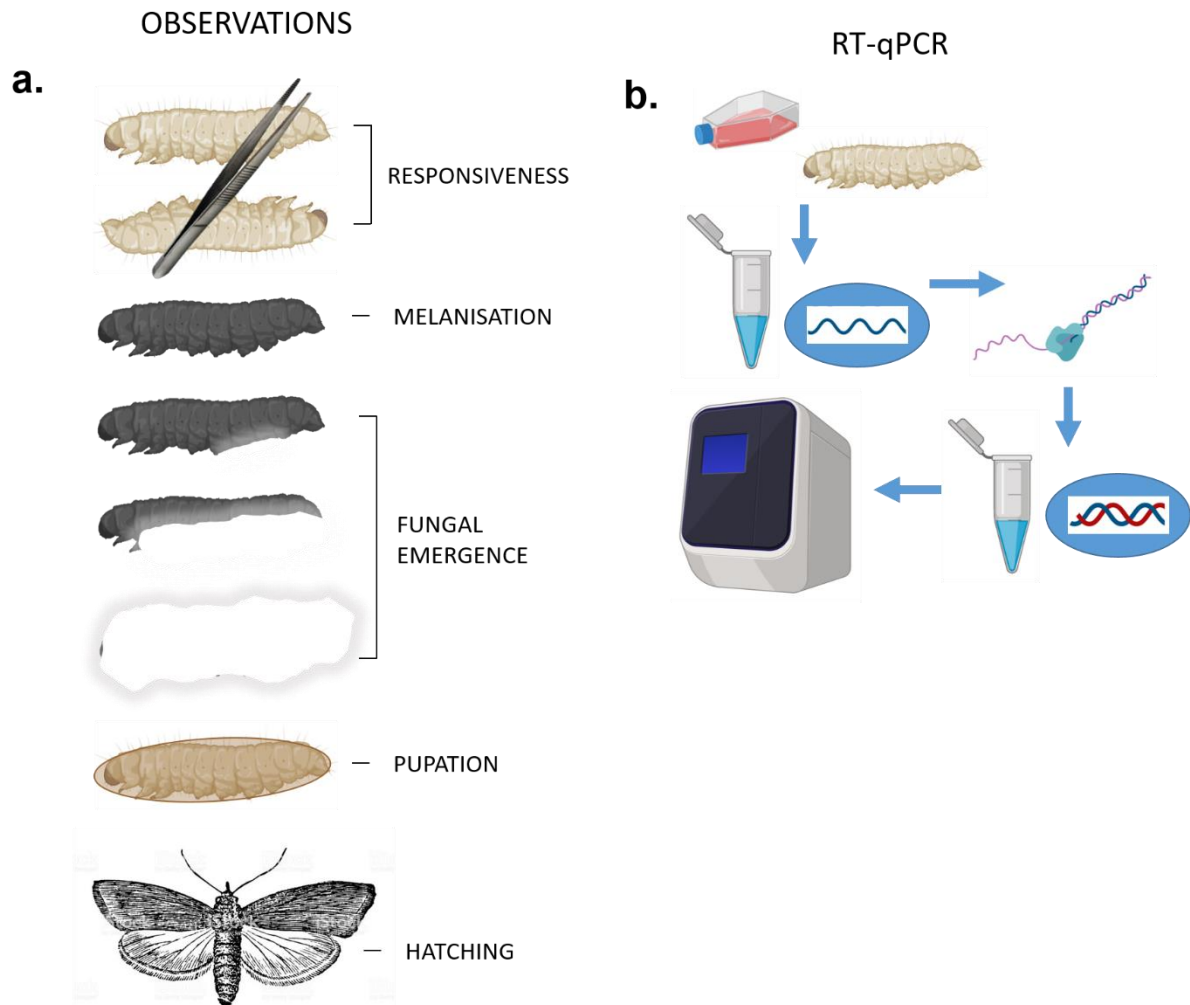


Figure 2.11: Data collection read-outs in *Galleria mellonella* host assays. These included daily observations, mainly of responsiveness, melanisation, and fungal emergence; or gene expression analysis by RT-qPCR following treatment. Details of individual experiments are listed in table 2.6.

Table 2.6: Experiments involving Greater Wax Moth (*Galleria mellonella*) Caterpillars. Featured in chapters 4, 5, and 7.

No.	Experiment Name	Treatment Method(s)	Fungal Strains	Details of spores used	Cordycepin/ Pentostatin	Relevant Readouts
1	Pure compounds injections, stimulation with curdlan (gene expression)	Injection (100 µL)			100 µM Cpn., 1.5 nM Ptn.	Gene expression at 2 hours (RT-qPCR)
2	Fungal extract injections, stimulation with curdlan (gene expression)	Injection (100 µL)	CM2 (PCS & DS)	None; extracted media from liquid cultures		Gene expression at 2 hours (RT-qPCR)
3	Pure compounds injections (live assay)	Injection (100 µL)			10, 50, 100 µM Cpn., 1.5 nM Ptn.	Responsiveness, melanisation, sensitivity to 0.04g and 0.16g Von Frey hairs
4	Fungal agar cultures spores injections	Injection (100 µL)	CM2 (PCS & DS)	1000 spores/caterpillar from agar cultures		Responsiveness, melanisation, fungal emergence
5	Fungal liquid cultures spores injections	Injection (100 µL)	CM2 (PCS & DS)	100,000 spores/caterpillar from liquid cultures		Responsiveness, melanisation, fungal emergence
6	Fungal liquid cultures spores and extract injections	Injection (100 µL)	CM2 (PCS & DS)	100,000 spores/caterpillar from liquid cultures, and extracted media		Melanisation, fungal emergence
7	Fungal liquid cultures spores and pure compounds injections	Injection (100 µL)	CM2 (PCS & DS)	1000 spores/caterpillar from liquid cultures	50 µM Cpn., 1.5 nM Ptn.	Responsiveness, melanisation, fungal emergence
8	Fungal agar culture exposure	Culture exposure	CM2 (PCS & DS)	Not measured		Responsiveness, melanisation, pupation, hatching
9	Fungal spores ingestion	Ingestion	CM2 (PCS & DS)	1000 spores/mL in food (honey)		Melanisation
10	Fungal liquid cultures spores injections (titration)	Injection (100 µL)	CM2 (PCS)	10, 100, 1000, 10000 spores/caterpillar from liquid cultures		Responsiveness, melanisation, fungal emergence

11	Fungal liquid cultures extract injections	Injection (100 µL)	CM2 (PCS & DS)	None; extracted media from liquid cultures		Responsiveness, melanisation
12	Fungal spores soaking and pure compounds ingestion	Soaking in fungal spores; ingestion	CM2 (PCS & DS)	1000 spores/mL in soaking liquid	100 µM Cpn., 1.5 nM Ptn. in food (honey)	Melanisation
13	Pure compounds ingestion and spores injection	Ingestion; injection (30 µL)	CM2 (PCS & DS)	50 spores/caterpillar from liquid cultures	100 µM Cpn., 1.5 nM Ptn. in food (honey)	Melanisation
14	Fungal liquid cultures spores injections (assemblages time course)	Injection (30 µL); extraction of haemolymph	CM2 (DS)	1000 spores/caterpillar	50 µM Cpn.	Bacterial colonies and <i>C. militaris</i> colonies isolated from haemolymph
15	Fungal liquid cultures spores injections (subcultures)	Injection (100 µL)	CM2 (PCS - subcultures)	1000 spores/caterpillar from liquid cultures		Responsiveness, melanisation, fungal emergence
16	Fungal liquid cultures spores and extract injections (different isolates)	Injection (100 µL)	CM2, CM16, CBS 128.25, KCTC 6064, TBRC 6804, NBRC 9787, BCRC 32219	100,000 spores/caterpillar from liquid cultures, and extracted media		Melanisation, fungal emergence

CHAPTER 3: CULTURE DEGENERATION IN *CORDYCEPS MILITARIS*

Culture degeneration, in which fungal strains lose desirable characteristics during subcultivation, is a major issue in fungal biotechnology. In *Cordyceps militaris* it is marked by and is of significant importance due to reduced production of cordycepin [Yin *et al.* 2017]. However, the effects of degeneration on the biology of this species have not widely been studied. The *Cordyceps militaris* isolate *CM2* was subcultivated through 14 passages over a period of two years on potato dextrose agar (PDA) [at MycoMedica by Andrej Gregori], resulting in a degenerated strain (DS). This strain had reported lower cordycepin production ability than the original, parental control strain (PCS). To investigate the process of degeneration, characteristics of the two strains were compared, including growth, production of cordycepin and pentostatin, overall metabolite production, and expression of genes of interest including those relating to sexual development. Major differences in gene expression and metabolite production were found, suggesting that a coordinated change in gene expression is involved in the degeneration process.

It is worth noting that to avoid confusion, from now on, *C. militaris* will be referred as an isolate, and the *CM2* parental control and degenerated cultures will be referred to as strains.

3.1 COMPARISON OF PARENTAL CONTROL AND DEGENERATED STRAINS

3.1.1 Growth of Cultures

Firstly, the two strains were compared using genetic screens, to confirm both the identities of species and isolate and exclude the possibility of culture contamination with other fungi. The parental control (PCS) and degenerated (DS) strains of the *Cordyceps militaris* *CM2* isolate

(which was originally collected from the wild in China), were demonstrated to both be of the species *C. militaris* of the same isolate using both ITS and RAPD PCR screens [see chapter 7]. Secondly, to exclude the possibility of differences in growth rates biasing results, the growth of the two strains were also compared. This was done by measuring radial growth rate and colony forming unit (CFU) analysis on potato dextrose agar (PDA). No significant difference in growth between the strains was detected [figure 3.1]. In addition, both strains, growing on PDA and potato dextrose broth (PDB) [figure 3.2] were also observed under a light microscope. Figure 3.3 shows hyphae and conidia from these observations. Similar structures of vegetative hyphae and conidia were observed in both strains.

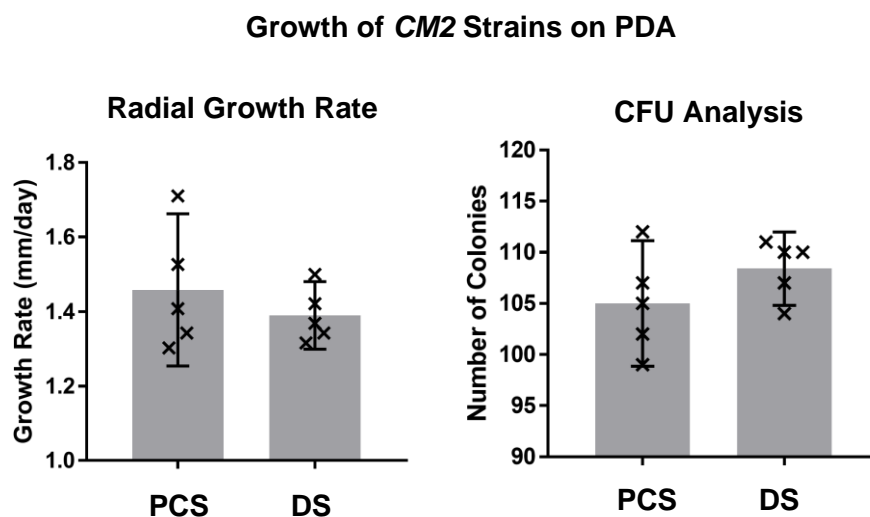


Figure 3.1: Growth rates of *CM2* parental control (PCS) and degenerated (DS) strains. Left: radial growth rate after 20 days from subculture on potato dextrose agar (PDA); right: colony forming unit (CFU) analysis on PDA. CFUs were obtained by spreading 100 μ L of 1000 times-diluted two week-old PDA cultures in phosphate-buffered saline. Error bars show 95% confidence intervals of means, from five biological replicates.

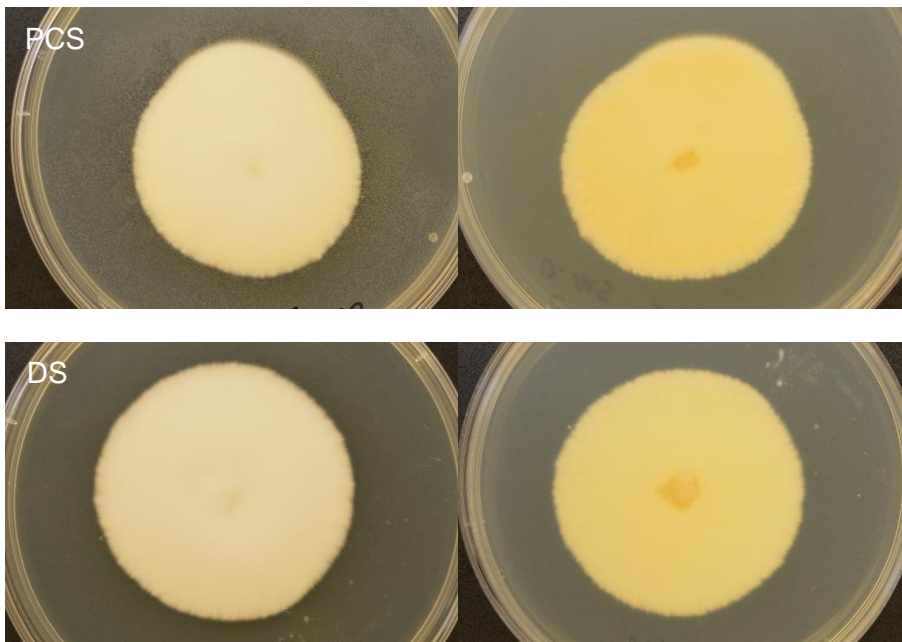


Figure 3.2: Cultures of *Cordyceps militaris* CM2 strain on potato dextrose agar. Top: parental control strain; bottom: degenerated strain; photos taken from top (left) and bottom (right) of cultures.

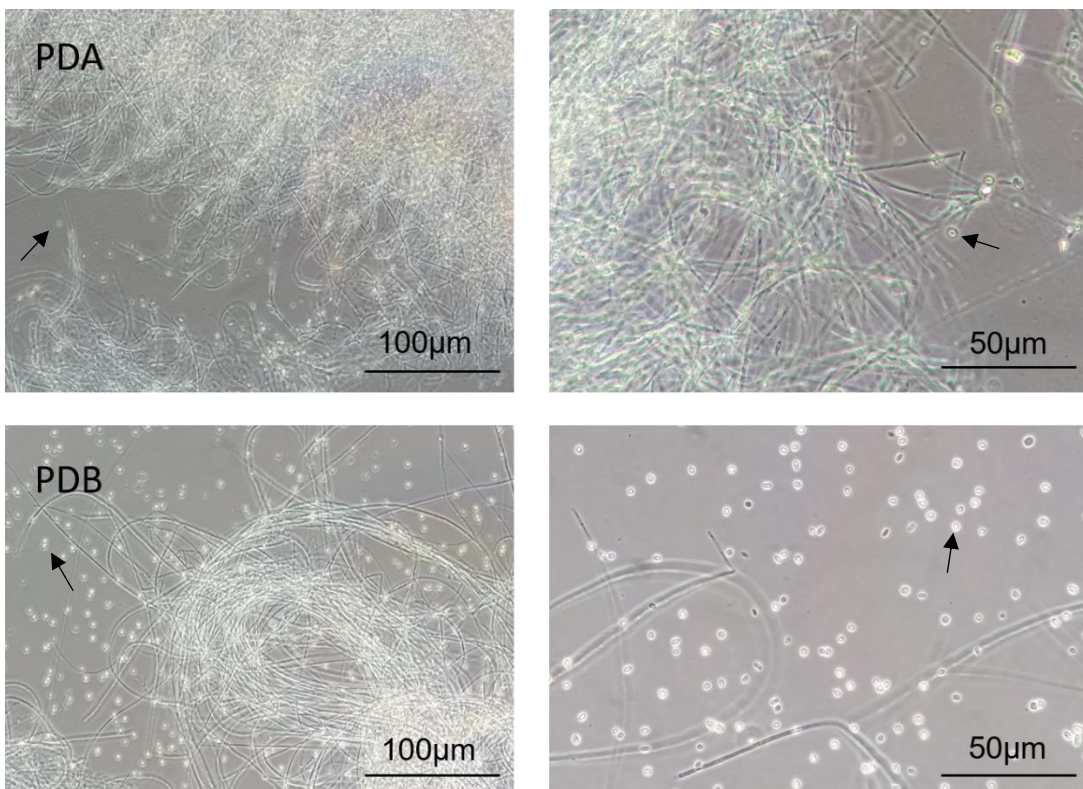


Figure 3.3: Light micrographs of *Cordyceps militaris* CM2 strains. These cultures were grown on potato dextrose agar (PDA, top) and broth (PDB, bottom), showing conidia and hyphae. Arrows are pointing to conidia; bars indicate scale.

In previous experiments, performed with the help of Dr. Andrej Gregori at MycoMedica, both strains of the *CM2* isolate were demonstrated to form stroma-like bodies when grown on rice-based media [figure 3.4]. These were much more abundant and larger in the PCS cultures, but in both cases they were sterile and did not bear perithecia (sexual fruiting bodies) or indeed any asci. PCR-based analysis showed both strains to possess only one mating type [see supplementary material]. These findings confirm that *C. militaris* is a heterothallic species, as previously described [Shrestha *et al.* 2004, Zheng *et al.* 2011], but also previously disputed [Wen *et al.* 2017]. Therefore the *CM2* isolate, from which both the PCS and DS strains were derived, presents an effectively clonal system for study.



Figure 3.4: Cultures of *Cordyceps militaris* *CM2* strains on rice-based media. Left: parental control strain (PCS); middle: degenerated strain (DS); right: pseudostromata (right) of *CM2* next to a fertile stromata bearing perithecia from a different *C. militaris* strain (left). [Carried out by Andrej Gregori, MycoMedica.]

3.1.2 Cordycepin and Pentostatin Production in Cultures

To verify that the degenerated strain on *CM2* produced less cordycepin than the parental control strain, targeted LC-MS analysis was performed on both strains. Significantly-lower production of cordycepin in the degenerated strain was detected in extracts from three cultures of each strain on PDA. The pentostatin, the protector molecule for cordycepin, was also found

to have significantly reduced production in the degenerated strain [figure 3.5]. These differences were supported by t-tests ($df = 4$, $t = 30.8$, $p < 0.0001$).

It was possible that cordycepin excreted by these fungal cultures into agar, which would have been missed in extracts of the fungal material only [figure 3.5]. To assess this, a further LC-MS analysis was performed on agar, with three technical replicates from each of three independent cultures [figure 3.6]. There was significantly less cordycepin produced by the degenerated strain detected in fungal material according to t-tests with Bonferroni corrections ($df = 56$, $t = 9.298$, $p < 0.0001$). There was also significantly-less cordycepin detected in extractions from agar taken directly below the degenerated strain fungal culture samples than those of the parental control strain ($df = 56$, $t = 8.191$, $p < 0.0001$). These agar extractions contained less cordycepin than the fungal extractions [figure 3.6]. In this LC-MS run, technical replicates and culture replicates of the same strains showed gave consistent outputs of cordycepin [figure 3.6]. This indicates that cordycepin production is highly reproducible across separate cultures.

The identification of cordycepin and pentostatin was confirmed using mass spectra obtained following fragmentation using LC-MS/MS (tandem mass spectrometry) in the case of cordycepin, compared to those of the authentic standard samples [figure 3.7]. This, combined with accurate mass and comparison of retention times, provides a high confidence in identification of these two metabolites.

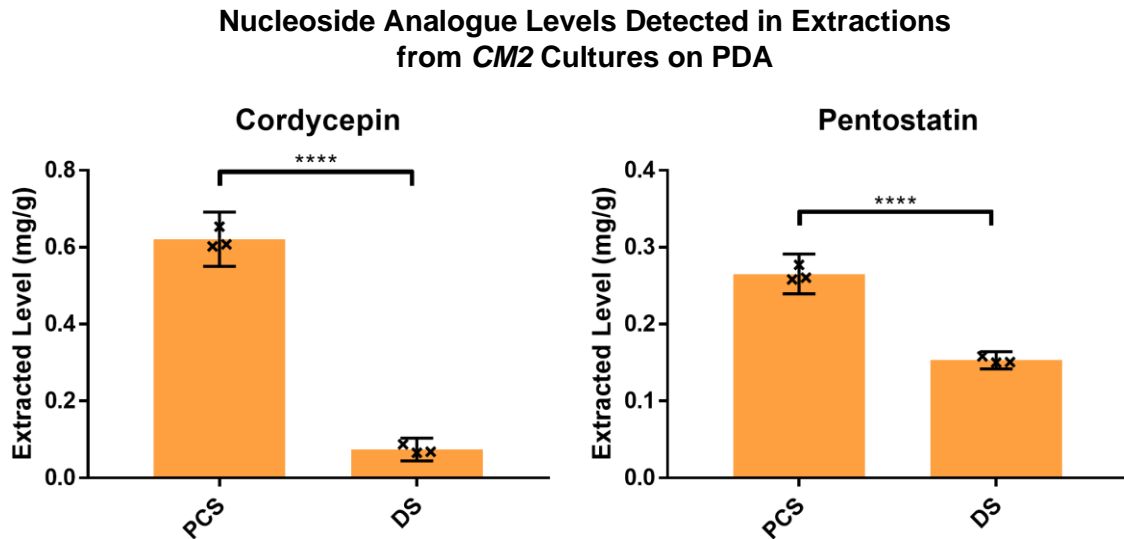


Figure 3.5: Cordycepin and pentostatin levels in *CM2* strains detected by LC-MS. These levels were detected in fungal extractions from parental control (PCS) and degenerated (DS) strains of *CM2*. Three biological replicates are used, with error bars showing 95% confidence intervals. P values are indicated by brackets: **** = $p < 0.0001$ – as determined by t-tests.

Cordycepin Levels Detected in Extractions from *CM2* Cultures and Agar on PDA

Fig. 3.6.1: Technical Replicates

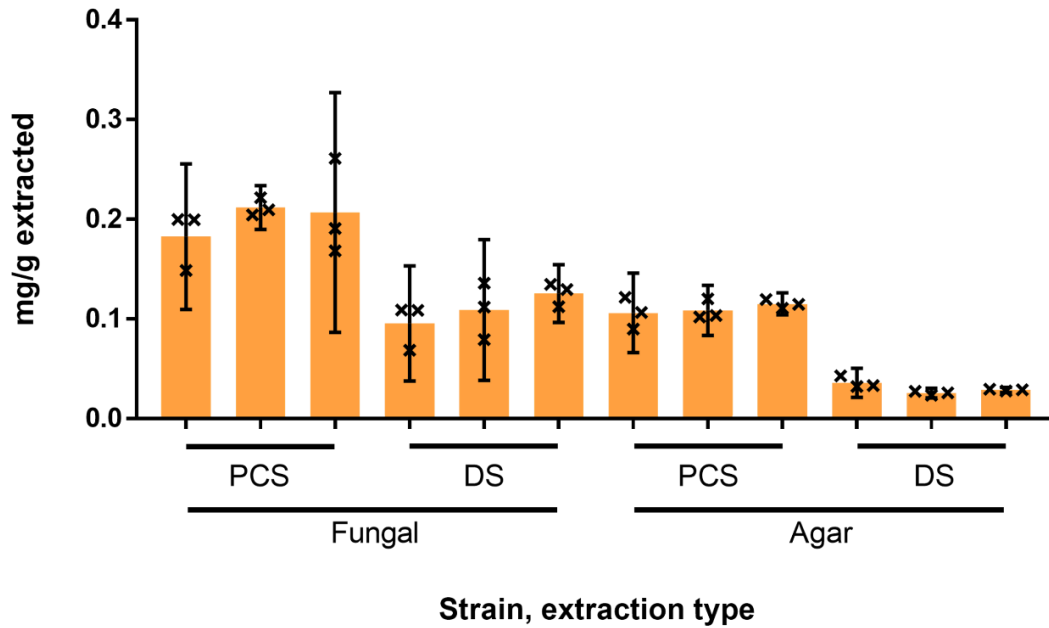


Fig. 3.6.2: Biological Replicates

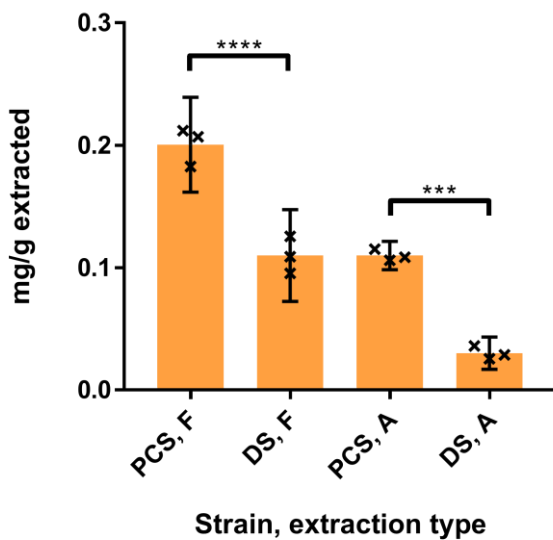


Figure 3.6: Cordycepin levels in fungal (F) and agar (A) extractions from *CM2* strains detected by LC-MS. These levels were detected in (PCS) and degenerated (DS) strains of *CM2*. Technical replicates (figure 3.6.1) were samples taken separately from the same plate; biological replicates (figure 3.6.2) are the mean values from three technical replicates in each case. Cordycepin is measured here by mg/g(fungal material). Error bars show 95% confidence intervals. P values are indicated by brackets: *** = $p < 0.001$, **** = $p < 0.0001$ – as determined by t-tests with Bonferroni corrections.

LC-MS(/MS): Fragmentation Spectra of Cordycepin and Pentostatin

Fig. 3.7.1: QC Samples

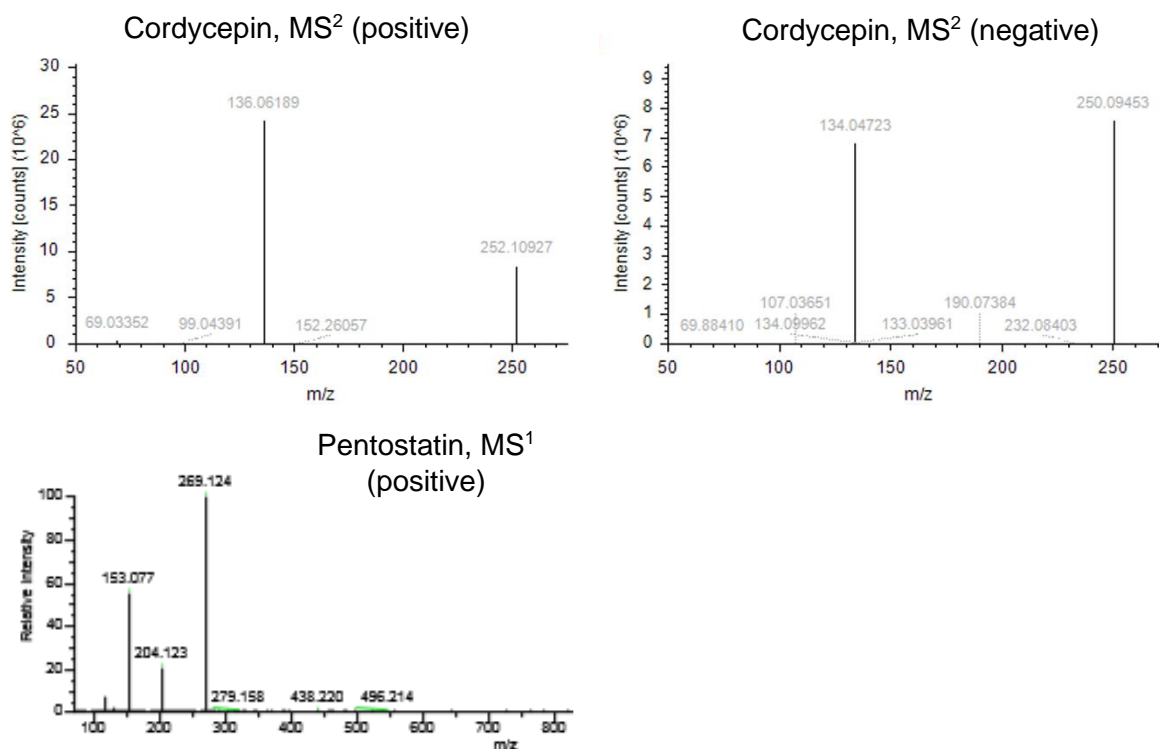


Fig. 3.7.2: Authentic Standards

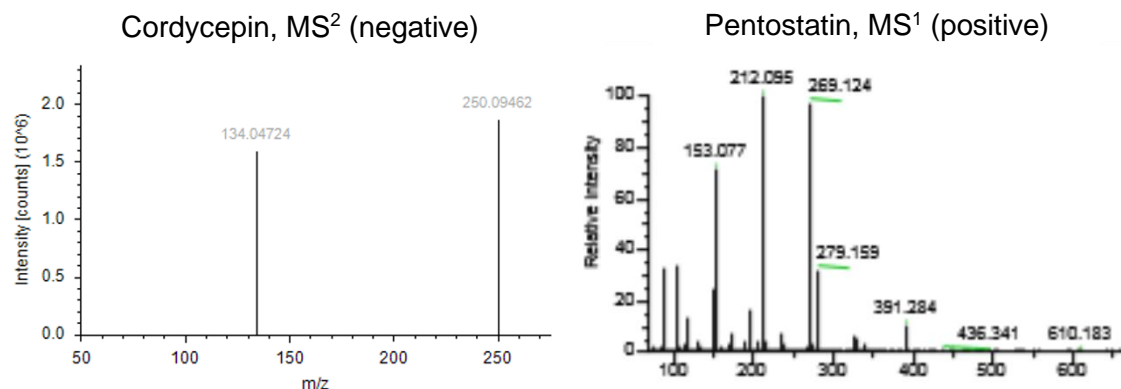


Figure 3.7: Fragmentation spectra of cordycepin and pentostatin. These were obtained following tandem MS (LC-MS/MS), and non-tandem MS in the case of pentostatin. The metabolites were detected in both *CM2* parental control and degenerated strain fungal extract samples. Mass spectra shown are from QC samples (fig. 3.7.1), with comparison to samples of authentic standards (fig. 3.7.2) – confirming Metabolomics Standards Initiative Level 1 identification of cordycepin and pentostatin.

3.1.3 Metabolomics of Cultures

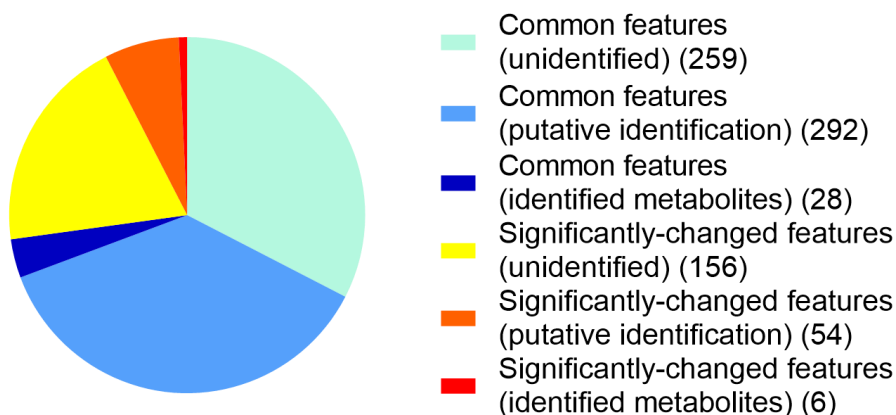
To investigate possible changes in wider metabolites during degeneration, untargeted LC-MS analysis of extracts from *CM2* cultures on PDA was carried out. Seven biological replicates were used. Identified and putatively-identified metabolites represented just under half of total detected features as well as base peak features (49.8% and 47.8% respectively) [figure 3.8]. Totals of 815 and 718 identified and putatively-identified metabolites were detected in PCS and DS samples respectively [figures 3.9.1-2]. These were obtained from features in the total data based on accurate mass and retention times compared to authentic standards (Metabolomics Standards Initiative level 1 identification) or by using predicted retention times (Metabolomics Standards Initiative level 2 identification/ putative identification) [Sumner *et al.* 2007; Sumner *et al.* 2014]. Relative concentrations of the identified metabolites in PCS and DS samples, with logarithmic adjustment, are shown in a heatmap [figure 3.10].

60 metabolites were found to have significantly different levels in the PCS and DS samples, according to t-tests with false discovery rate (FDR) corrections and an orthogonal partial least squares-discriminant analysis (OPLS-DA) model (with VIP values > 1). This represented 7.36% and 8.36% of identified/putatively-identified metabolites in PCS and DS samples respectively. Of the described classes of metabolites in figure 3.9, the best represented by the significantly-different metabolites is carbohydrate metabolism (18.3%) [figure 3.9.3]. Relative concentrations of these metabolites in PCS and DS samples, with logarithmic adjustment, are shown in another heatmap [figure 3.11], and the metabolites are listed in table 3.1. Some metabolites involved in the citrate cycle and in purine metabolism has significantly-lower levels in DS compared to PCS samples – such as citrate, pyruvate, and adenine [figure 3.12]. The latter is consistent with the reduced output of cordycepin in DS cultures, as cordycepin is a purine and has been proposed to be generated through the purine metabolism pathway via adenosine [Xia *et al.* 2017]. The changes in citrate cycle metabolites suggest a reduced energetic output.

Multivariate analyses show clustering of samples from the same treatment groups [figure 3.13]. Principle component analyses show tight clustering of quality control (QC) samples in the middle of the plot for the first run [figure 3.13.1] – indicating consistent performance of the instrument throughout the run.

Fig. 3.8.1

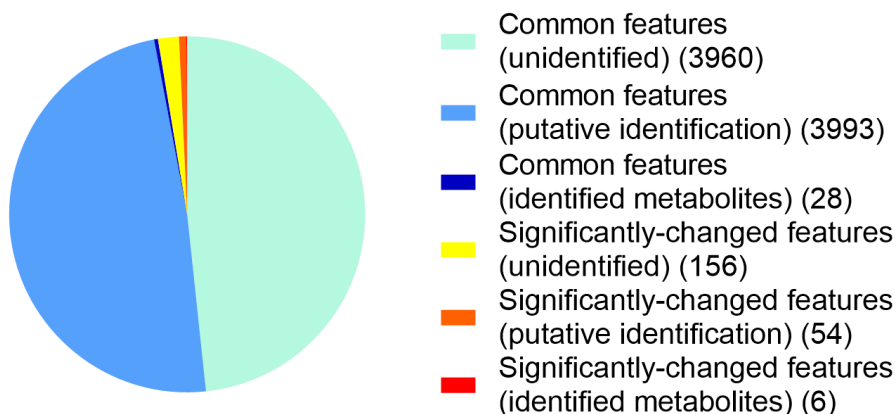
Untargeted Metabolomics: Base Peaks



Total = 795

Fig. 3.8.2

Untargeted Metabolomics: Total Detected Features



Total = 8197

Figure 3.8: Features detected in *CM2* parental control and degenerated strains on PDA by untargeted LC-MS. Features detected from base peaks (fig. 3.7.1) and total detected features (fig. 3.7.2). Features contributed to Level 1 and 2 identification. Metabolites were extracted from fungal material. There were seven biological replicates, taken from separate agar plates. Untargeted data was processed using XCMS, MzMatch, and IDEOM. Identification of metabolites (Level 1) was achieved using accurate mass and retention time based on authentic standards. Level 2 putative identification of metabolites was achieved using accurate mass and predicted retention times without the use of standards. Significantly-different metabolites were determined using t-tests with false discovery rate (FDR) corrections and having VIP values > 1 following orthogonal partial least squares-discriminant analysis (OPLS-DA) using SIMCA-P (v4) software.

Fig. 3.9.1

Total Metabolites Detected: PCS on PDA

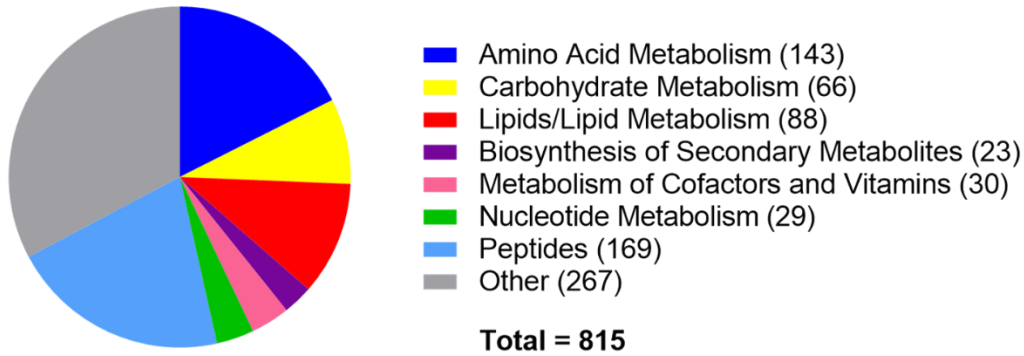


Fig. 3.9.2

Total Metabolites Detected: DS on PDA

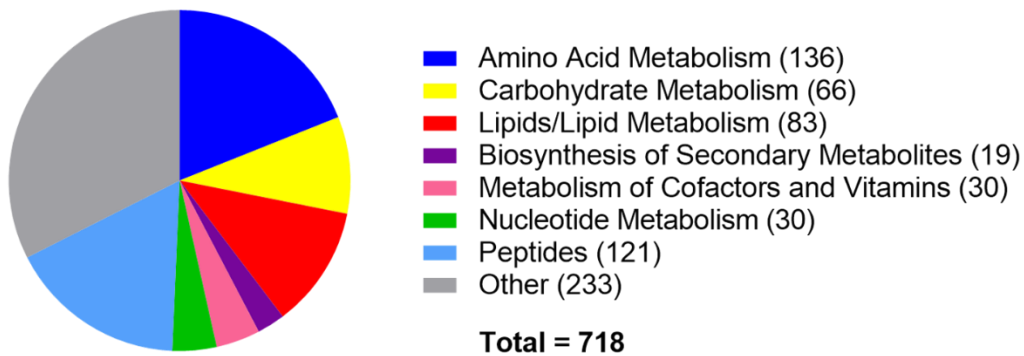


Fig. 3.9.3

Significantly-Different Metabolites: PCS vs. DS on PDA

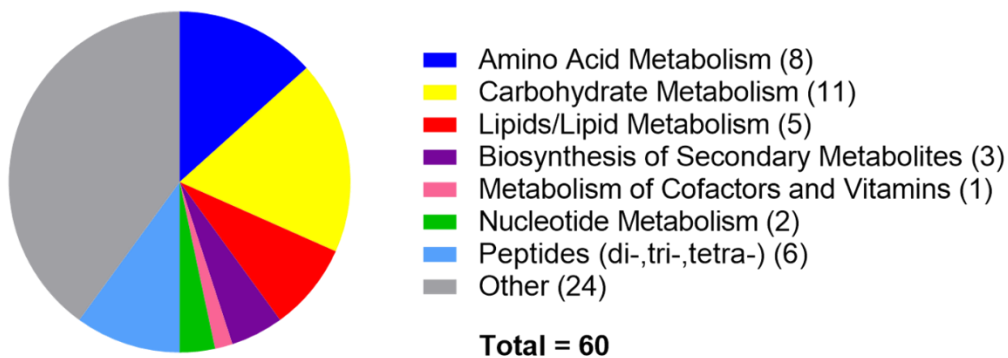


Figure 3.9: Total metabolites (Levels 1 and 2 identification) detected in *CM2* parental control (PCS) and degenerated (DS) strains on PDA by untargeted LC-MS. See legend of figure 3.8 for further details

Figure 3.10: Heatmap – Identified Metabolites from CM2 PCS, DS on PDA; Fungal Extractions

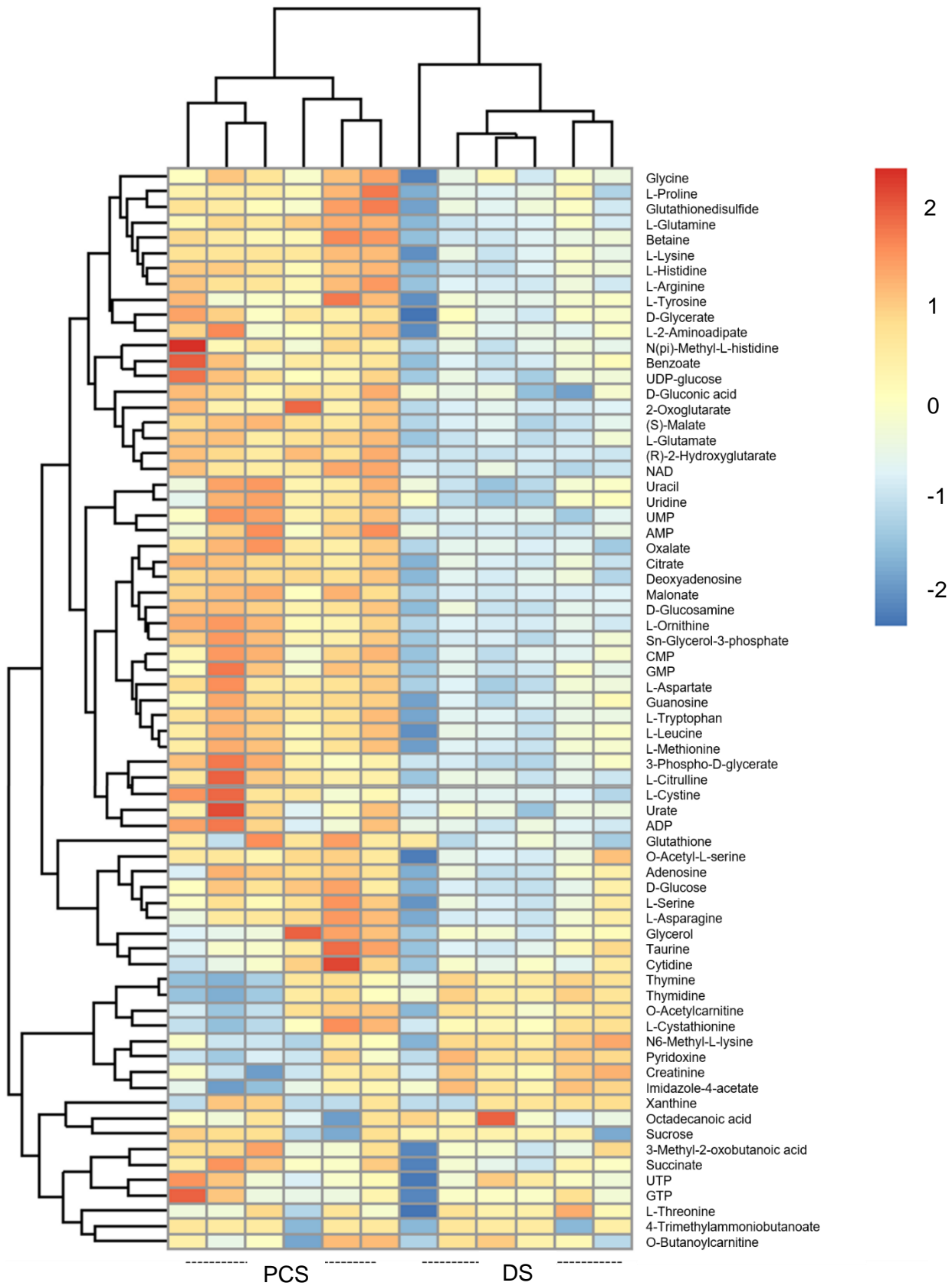
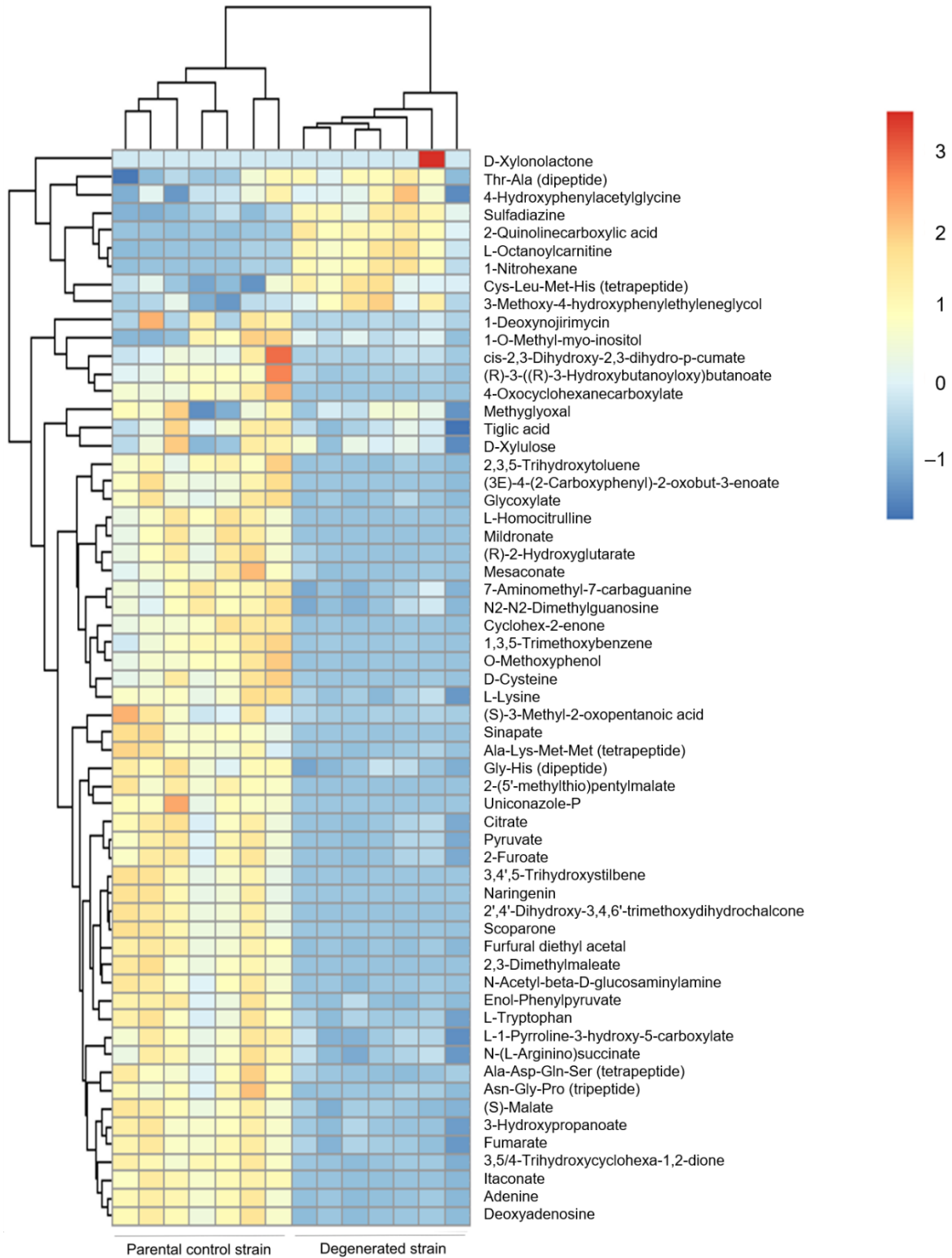


Figure 3.11: Heatmap – Significantly-Different Metabolites from CM2 PCS, DS on PDA; Fungal Extractions



Heatmap figures (3.10 and 3.11) – from previous pages

Figure 3.10: Heatmap featuring identified metabolites in an untargeted LC-MS run of extracts from *CM2* parental control (PCS) and degenerated (DS) strains on potato dextrose agar (PDA). Metabolites were extracted from fungal material. Six biological replicates are shown, taken from separate agar plates. This analysis is based upon relative concentrations of metabolites identified using accurate mass and retention times based on authentic standards, following XCMS, MzMatch, and IDEOM processing of data. Concentrations were transformed prior to heatmap construction using a logarithm with base 10. This figure was produced using R version 4.0.0 software, with the heatmap package (“pheatmap”).

Figure 3.11: Heatmap featuring significantly-different metabolites in an untargeted LC-MS run of extracts from *CM2* parental control (PCS) and degenerated (DS) strains on PDA. Metabolites were extracted from fungal material. There were seven biological replicates, taken from separate plates. This analysis is based upon relative concentrations of metabolites identified using accurate mass and retention times based on authentic standards (Level 1 identified metabolites) or predicted retention time without the use of standards (Level 2/ putative identification), following XCMS, MzMatch, and IDEOM processing of data. Significantly-different metabolites were determined using t-tests with false discovery rate (FDR) corrections and having VIP values > 1 following orthogonal partial least squares-discriminant analysis (OPLS-DA) using SIMCA-P (v4) software. The figure was produced in the same manner as figure 3.10.

Table 3.1: Significantly-different metabolites (Levels 1 and 2 identification) detected from untargeted LC-MS run of extracts from CM2 parental control and degenerated strains on PDA.

Metabolite classes: AAM (amino acid metabolism), BSM (biosynthesis of secondary metabolites), peptides, CM (carbohydrate metabolism), LLM (lipids and lipid metabolism), MCF (metabolism of cofactors and vitamins), NM (nucleotide metabolism).

<i>m/z</i>	Metabolite	Class	Pathway
90.03174	3-Hydroxypropanoate	AAM	beta-Alanine metabolism__Propanoate metabolism
121.0198	D-Cysteine	AAM	Cysteine metabolism
129.0427	L-1-Pyrroline-3-hydroxy-5-carboxylate	AAM	Arginine and proline metabolism
146.1054	L-Lysine	AAM	Lysine biosynthesis__Lysine degradation__Biotin metabolism__Alkaloid biosynthesis II
148.0371	(R)-2-Hydroxyglutarate	AAM	glutamate degradation V (via hydroxyglutarate)
186.0293	enol-Phenylpyruvate	AAM	Phenylalanine metabolism
204.0899	L-Tryptophan	AAM	Tryptophan metabolism__Phenylalanine, tyrosine and tryptophan biosynthesis__Indole and ipecac alkaloid biosynthesis
290.1228	N-(L-Arginino)succinate	AAM	Arginine and proline metabolism__Alanine and aspartate metabolism
168.0787	1,3,5-trimethoxybenzene	BSM	1,3,5-trimethoxybenzene biosynthesis
224.0686	Sinapate	BSM	Phenylpropanoid biosynthesis
228.0789	3,4',5-Trihydroxystilbene	BSM	Phenylpropanoid biosynthesis
190.0953	Thr-Ala	Peptides	
212.0909	Gly-His	Peptides	
419.1643	Ala-Asp-Gln-Ser	Peptides	
479.2246	Ala-Lys-Met-Met	Peptides	
502.2043	Cys-Leu-Met-His	Peptides	
286.1279	Asn-Gly-Pro	Peptides	
88.01607	Pyruvate	CM	Glycolysis / Gluconeogenesis__Citrate cycle (TCA cycle)__Pentose phosphate pathway__Ascorbate and aldarate metabolism__Biosynthesis of steroids__Alanine and aspartate metabolism__Glycine, serine and threonine metabolism
130.0267	Itaconate	CM	C5-Branched dibasic acid metabolism
134.0215	(S)-Malate	CM	
160.0372	3,5/4-Trihydroxycyclohexa-1,2-dione	CM	Inositol phosphate metabolism
190.0842	(R)-3-((R)-3-Hydroxybutanoyloxy)butanoate	CM	Butanoate metabolism
192.027	Citrate	CM	Citrate cycle (TCA cycle)__Glutamate metabolism__Alanine and aspartate metabolism__Glyoxylate and dicarboxylate metabolism__Reductive carboxylate cycle (CO2 fixation)
194.0789	1-O-Methyl-myo-inositol	CM	Inositol phosphate metabolism
74.00025	Glyoxylate	CM	Glyoxylate and dicarboxylate metabolism
116.011	Fumarate	CM	Citrate cycle (TCA cycle)__Pyruvate metabolism__Butanoate metabolism__Pyrimidine metabolism
130.0266	Mesaconate	CM	Glyoxylate and dicarboxylate metabolism__Benzoate degradation

150.0527	D-Xylulose	CM	Pentose and glucuronate interconversions__Thiamine metabolism__Terpenoid backbone biosynthesis
100.0525	Tiglic acid	LLM	Fatty Acids and Conjugates
287.2098	L-Octanoylcarnitine	LLM	Fatty acyl carnitines
130.0631	(S)-3-Methyl-2-oxopentanoic acid	LLM	Fatty Acids and Conjugates
272.0687	[Fv] Naringenin	LLM	Flavonoids
304.0949	[Fv hydroxy,methoxy(4:0)] 3,4,4',alpha-Tetrahydroxy-2'-methoxydihydrochalcone	LLM	Flavonoids
144.0422	2,3-Dimethylmaleate	MCF	Nicotinate and nicotinamide metabolism
135.0545	Adenine	NM	Purine metabolism
251.1019	Deoxyadenosine	NM	Purine metabolism
<i>Unspecified class metabolites:</i>			
m/z	Metabolite	m/z	Metabolite
96.05762	Cyclohex-2-enone	198.0893	cis-2,3-Dihydroxy-2,3-dihydro-p-cumate
112.0161	2-Furoate	250.0876	2-(5'-methylthio)pentylmalate
124.0525	o-Methoxyphenol	291.1143	uniconazole-P
131.0946	1-nitrohexane	311.1233	N2-N2-Dimethylguanosine
163.0844	1-deoxynojirimycin	72.02096	Methylglyoxal
179.0807	7-Aminomethyl-7-carbaguanine	142.0631	4-Oxocyclohexanecarboxylate
189.1113	L-Homocitrulline	146.1056	mildronate
206.058	Scoparone	170.0944	Furfural diethyl acetal
220.1059	N-Acetyl-beta-D-glucosaminyllamine	173.0478	2-Quinolinecarboxylic acid
237.0638	(3E)-4-(2-Carboxyphenyl)-2-oxobut-3-enoate	209.0689	4-Hydroxyphenylacetyl glycine
250.0513	Sulfadiazine	140.0473	2,3,5-Trihydroxytoluene
184.0735	3-Methoxy-4-hydroxyphenylethyleneglycol	148.0372	D-Xylonolactone

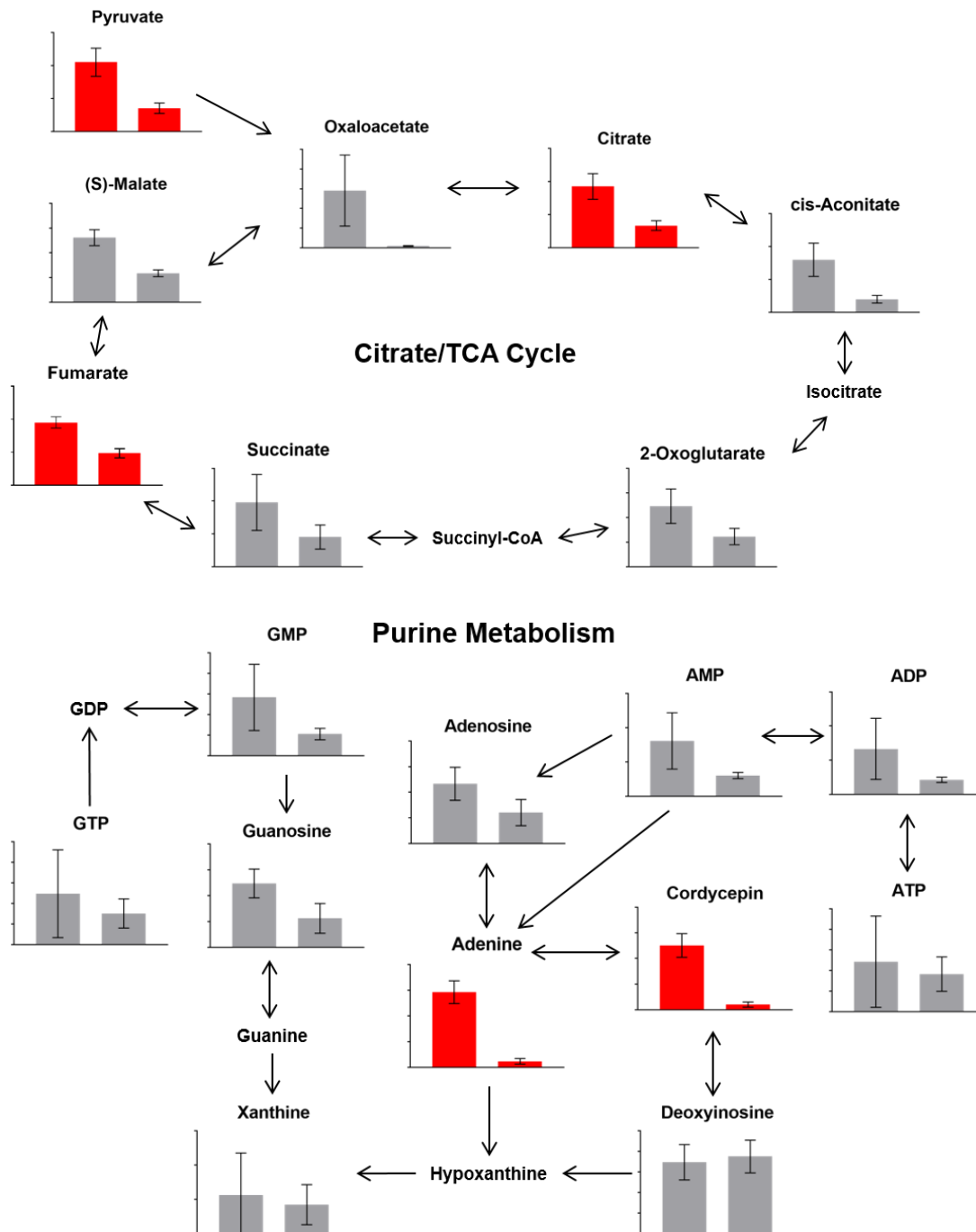


Figure 3.12: Citrate cycle and purine metabolism pathways, as described by the KEGG database, with compared concentrations of metabolites detected *CM2* strains by untargeted LC-MS. Bar graphs show mean values of relative concentrations, with error bars showing 95% confidence intervals. Parental control (PCS) and degenerated (DS) strains are represented by bars on the left and right respectively. Red graphs represent significant differences in metabolite levels between the strains, as determined by both t-tests with false discovery rate (FDR) corrections and having VIP values >1 following orthogonal partial least squares-discriminant analysis (OPLS-DA) using SIMCA-P (v4) software. Arrows between the graphs represent pathway steps.

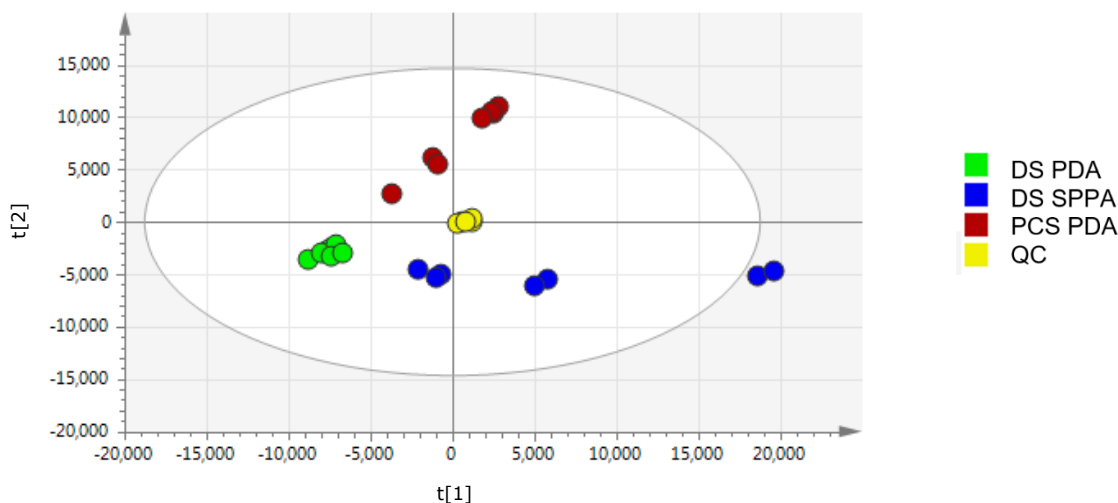
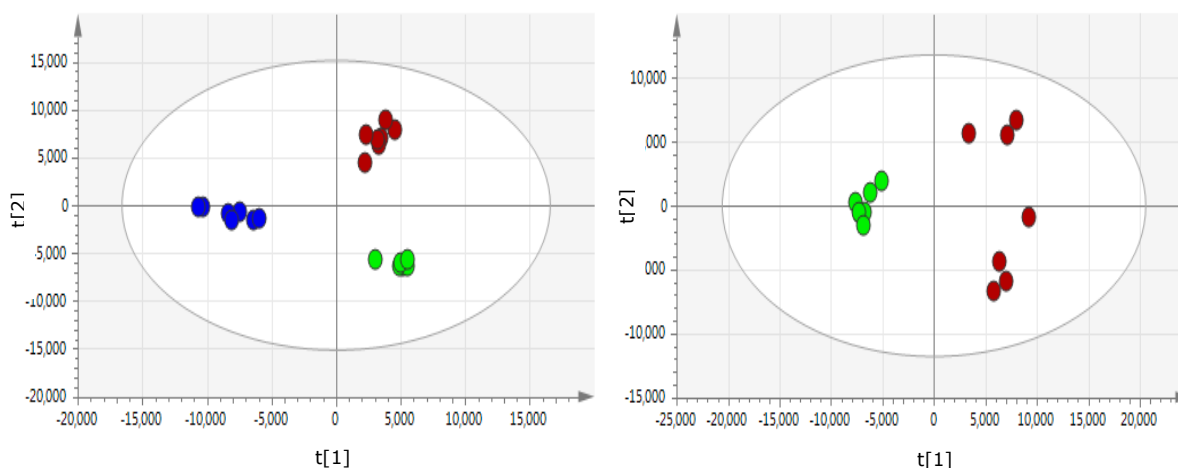
Fig. 3.13.1 PCA – *CM2* PCS, DS on PDA, DS on SPPA**Fig. 3.13.2** OPLS-DA – *CM2* PCS, DS on PDA, DS on SPPA

Figure 3.13: Multivariate analysis plots for detected metabolites (Levels 1 and 2 identification) in *CM2* strains by untargeted LC-MS. Principle component analysis (PCA, fig. 3.13.1) and orthogonal partial least squares-discriminant analysis (OPLS-DA, fig. 3.13.2) plots are shown. *CM2* parental control (PCS) and degenerated (DS) strains on potato dextrose agar (PDA) as well as DS on silk pupa-powder agar (SPPA) were used [experiments on SPPA are featured in chapter 6]. QC samples are also shown (PCA only). There were seven biological replicates, taken from separate agar plates. These multivariate analyses are based upon relative concentrations of all identified and putatively-identified metabolites following XCMS, MzMatch, and IDEOM processing of data. These figures were produced using SIMCA-P (v4) software.

3.1.4 Gene Expression in Cultures

To assess possible gene expression changes during degeneration, genes of interest were selected for RT-qPCR analyses of potato dextrose agar cultures of the parental control and degenerated strains of the *CM2* isolate. These included previously described genes in the cordycepin/pentostatin biosynthesis cluster – *Cns1*, 2, 3, and 4. *Cns1*, *Cns2*, and *Cns3* are involved in the proposed biosynthesis pathway for cordycepin, whilst *Cns3* and *Cns4* are involved in the biosynthesis and export of pentostatin respectively [Xia *et al.* 2017]. Genes involved in sexual development were also selected, to investigate whether or not degeneration is related to a shift away from the sexual phase. The rationale for this was that successful infection of the insect host results in the sexual reproduction and the formation of fertile stromata; and cordycepin production has been suggested to be involved in aiding host infection [Wellham *et al.* 2019; Woolley *et al.* 2020]. These genes included velvet genes *VeA* (*Velvet A*), *VosA* (*Variability of spores A*), and their master regulator *LaeA* (*Loss of aflR Expression A*). The velvet genes are highly conserved regulators of fungal sexual development and secondary metabolism. Genes downstream of these, *Ste7* and *SteA*, were also selected. In addition, mating-type gene *MAT1-2-1* and downstream gene *PreB* were selected for RT-qPCR analysis. Control genes *Gapdh* (*Glyceraldehyde Phosphate Dehydrogenase*), *Act* (*Actin*), *Cal* (*Camodulin*), and *Rps3* (*Ribosomal Protein S3*) were used for comparison to the genes of the interest.

The majority of these genes of interest were found to be significantly downregulated in the degenerated strain compared to the parental control strain, in comparison with the control [figure 3.14]. Downregulated genes included three of those in the cordycepin/pentostatin biosynthesis gene cluster, *Cns1* (df = 4, t = 27.27, p < 0.0001), *Cns3* (df = 4, t = 10.61, p = 0.0004), and *Cns4* (df = 4, t = 63.97, p < 0.0001). This is consistent with the lower production of cordycepin and pentostatin by the degenerated strain. There were also significantly-lower levels of expression in sexual development-related genes – *LaeA* (df = 4, t = 20.23, p < 0.0001), *VeA* (df = 4, t = 14.28, p = 0.0001), *VosA* (df = 4, t = 22.68, p < 0.0001), *PreB* (df =

4, $t = 85.23$, $p < 0.0001$), *Ste7* ($df = 4$, $t = 20.14$, $p < 0.0001$), and *SteA* ($df = 4$, $t = 59.7$, $p < 0.0001$). However, the mating-type gene *MAT 1-2-1* was upregulated in DS ($df = 4$, $t = 12.95$, $p = 0.0002$).

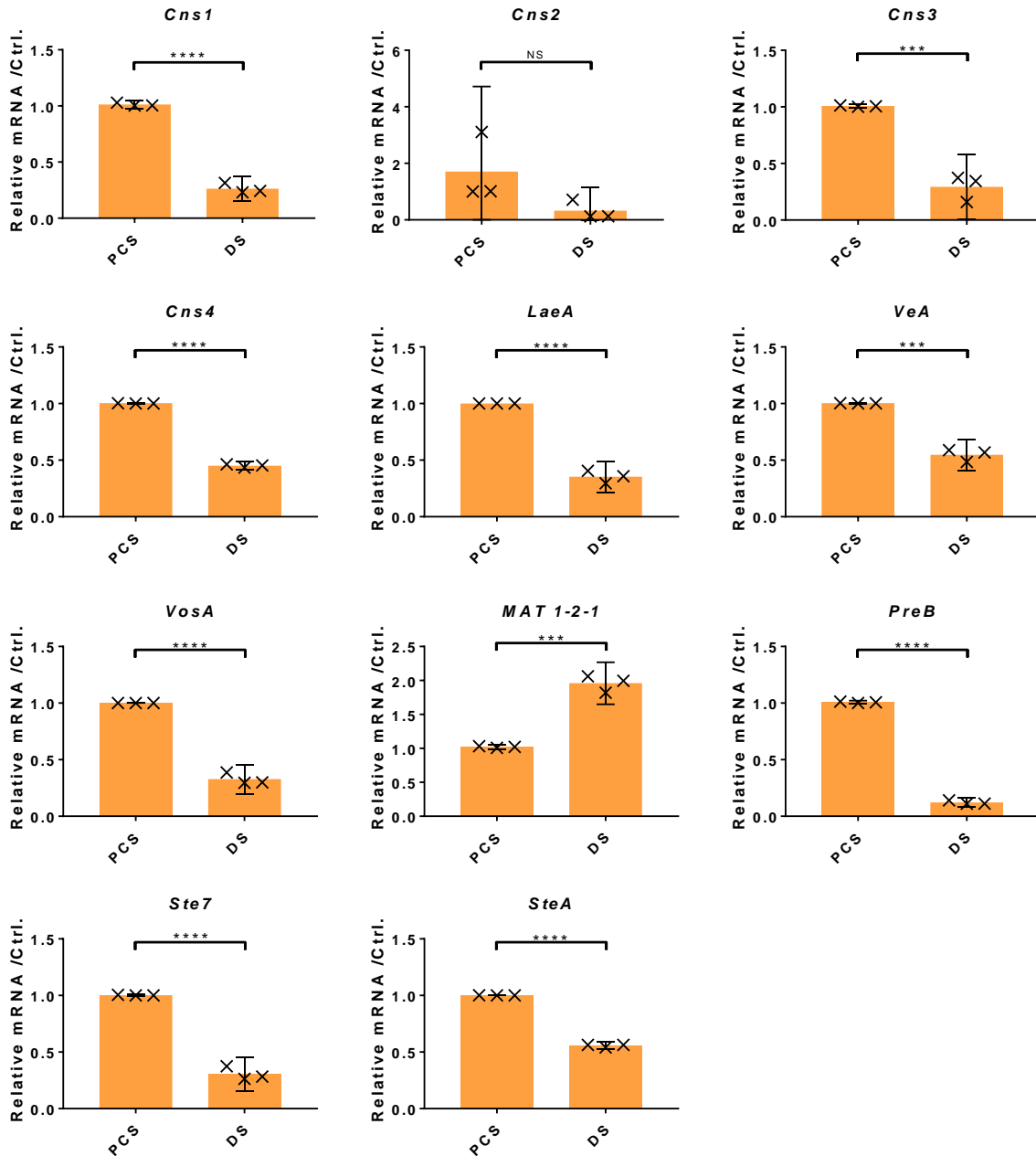
Gene Expression in *CM2* Strains on PDA

Figure 3.14: Relative mRNA levels of genes of interest in parental control (PCS) and degenerated (DS) strains of *CM2* cultured on PDA. Gene expression was normalised against the average of four controls, *Gapdh*, *Actin*, *Calmodulin* and *Rps3*. Error bars show 95% confidence intervals, and labels show differences between means as calculated using t-tests. * p < 0.05; ** p < 0.01; *** p < 0.001; **** p < 0.0001. Genes included are the cordycepin and pentostatin synthesis gene cluster (*Cns1-4*), velvet and related genes (*LaeA*, *VeA*, *VosA*), or other sexual development-related genes (*MAT 1-2-1*, *PreB*, *Ste7*, *SteA*). Three biological replicates, with each point representing an average of three technical replicates are shown.

3.2 DISCUSSION

Through repeated subcultivation of the CM2 *C. militaris* isolate over two years on PDA, degeneration has occurred, with a decrease in production of cordycepin and its protector molecule pentostatin. Simultaneously reductions in other metabolites relating to purine metabolism and the citrate cycle, and in the expression of genes relating to sexual development occurred. These results suggest that the effects of degeneration are more complex than and not restricted to just a decline in secondary metabolites of interest.

The reduced expression of sexual development-related genes in the degenerated strain compared to the parental control strain indicate that with the degeneration process, facilitated by cultivation on agar, there has been a shift away from the characteristics of the teleomorph (sexual phase) towards the vegetative state. Specifically, these down-regulated genes include the velvet genes *VeA* (*Velvet A*) and *VosA* (*Variability of Spores A*). These genes, conserved in ascomycetes, encode members of the velvet family of proteins, and were initially discovered in the *Aspergillus* species [Bayram & Braus 2012]. Velvet proteins are known to act in complexes, and other examples of velvet genes include *VelB* and *VelC* [Bayram & Braus 2012]. They play roles in the regulation of both secondary metabolism and sexual development, with responses to light and other abiotic stimuli [Kim *et al.* 2002; Ni & Yu 2007; Bayram & Braus 2012]. *Ste7* and *SteA*, genes downstream of the velvet genes and encoding a MAP kinase kinase and a transcription factor respectively [Paoletti *et al.* 2007; Vallim *et al.* 2000], also had reduced expression in DS. Mating-type gene *MAT1-2-1* however had increased expression in DS, although the downstream G-protein coupled receptor-encoding [Dyer *et al.* 2003] gene *PreB* was downregulated. Also down regulated was *LaeA* (*Loss of aflR-Expression A*), a non-velvet master regulator gene, which controls velvet gene expression [Bayram *et al.* 2010]. *LaeA* encodes a methyltransferase [Bayram *et al.* 2010]. Therefore, a change in the high-level regulation of gene expression by *LaeA*, and perhaps other master regulators, could explain the simultaneous changes in both sexual development-

related gene expression and secondary metabolite (cordycepin and pentostatin) production occurring with degeneration. Given that LaeA is a methyltransferase, it is possible that epigenetic changes are responsible for the degeneration phenotype.

If a shift away from the teleomorph towards the vegetative state has taken place through degeneration of this *C. militaris* isolate, this raises the question of whether or not the degenerated strain also shows a reduced pathogenicity in the insect host. The logic behind this is that in this species, sexual development – manifesting ultimately in the formation of stromata bearing sexual fruiting bodies (perithecia) with sexual spores in asci – occurs after the colonisation of the insect host [Webster & Weber 2007]. This is investigated in chapter 5.

Much of the results and analyses in chapters 3 and 5 have been published in a peer-reviewed paper [Wellham *et al.* 2021].

CHAPTER 4: METHODS FOR USE OF *CORDYCEPS MILITARIS* HOST MODELS

In light of the findings of chapter 3, we wanted to test both the effects of culture degeneration on fungal pathogenicity, and for the effects of cordycepin and pentostatin on the infection of the host by *Cordyceps militaris*. To do this, some method development was required, to be able to reliably use a live host model system. *Galleria mellonella* (wax moth) caterpillars were chosen for use as the model, owing to their small size and convenience in large sample sizes, and use as a model organism in previous fungal infection studies. Several methods were attempted for the use of the caterpillars as the *C. militaris* host model system. Relevant findings from the most appropriate methods are described in chapter 5. This chapter details the method development with some other methods tested.

4.1 *CORDYCEPS MILITARIS* HOST MODEL METHODS

The *Galleria mellonella* caterpillar assays relied on the daily recording of observations, by the naked eye, across large numbers of caterpillars (typically 60 per treatment group). While the key advantage of this was the easy means of observation, and ability to obtain a data sets with large sample sizes, it also had disadvantages – which were revealed by the experimental data from different methods tried. Observation readouts of responsiveness, full melanisation, and fungal emergence were available for data collection. These were used as a proxy for survival (or moribund status), immune response of the host, and fungal growth respectively. In the case of injection experiments, mostly 100 μ L was used as the injection volume, and the injection site was behind the last left proleg. While 100 μ L is a large injection volume compared

to more typically used 10-20 μL , it was chosen due to the ability of more precise injection of this volume into large numbers of caterpillars on each occasion by hand.

4.1.1 Injection of Concentrations of Cordycepin into Caterpillars

It has previously been proposed that cordycepin functions as the proximate death-causing factor in the early stages of *Cordyceps* host infection [Kim *et al.* 2002]. Therefore an experiment was carried out here involving the injection of pure cordycepin and pentostatin into caterpillars to investigate this. However, even after injections of 100 μL suspensions of up to 100 μM cordycepin (1 μmol per caterpillar), the majority of *G. mellonella* caterpillars survived after two weeks (60% remained responsive) [figure 4.1]. Cordycepin and pentostatin did not affect melanisation rates and levels in caterpillars compared to the blank control treatment [figure 4.2]. Proportions of caterpillar sensitivity were tested after injections of pure cordycepin and pentostatin. A more precise measurement of responsiveness in caterpillars was attempted – namely the use of application of very light pressure with Von Frey hairs. A gradual rise and fall in numbers of caterpillars sensitive to 0.04g Von Frey hairs, peaking around one week after injection was observed in the control group – perhaps an effect analogous to allodynia (enhanced sensitivity and pain) resulting from the injury caused by needle penetration [figure 4.3]. This pattern was not present in caterpillars injected with 50 and μM cordycepin, with very low proportions showing sensitivity, as was the case with injected pentostatin. The use of Von Frey hairs was not suitable for experiments involving fungal spores [data not shown], with losses of sensitivity in caterpillars precluding the usefulness of a more precise responsiveness measure.

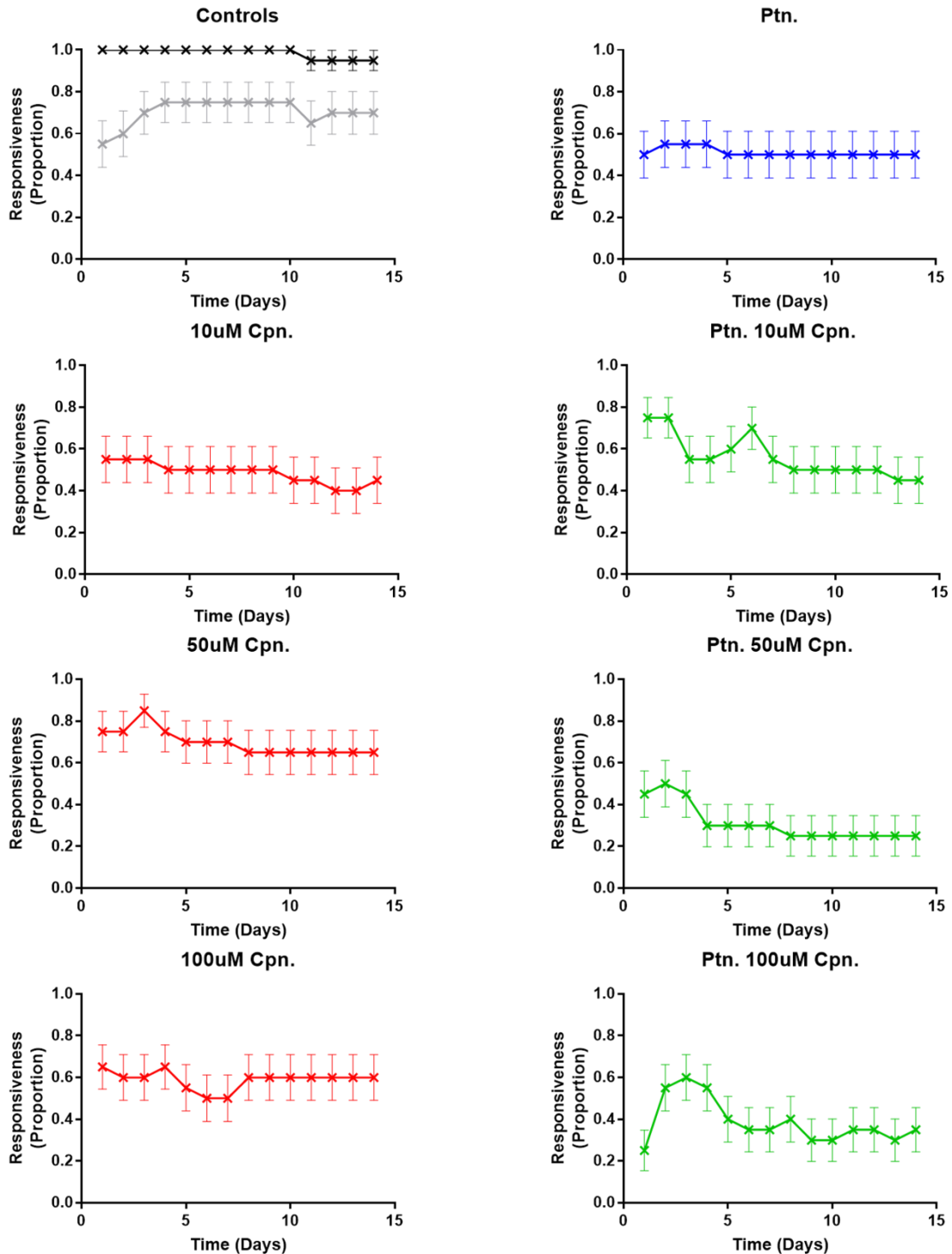
Figure 4.1.1: Pure Compounds Injections (Live Assay) – Responsiveness

Figure 4.1.1: Proportions of responsiveness observed in *Galleria mellonella* caterpillars following 100 μ L injections with varying concentrations of cordycepin (cpn) with (green) or without (red) added 1.5 nM pentostatin (ptn) in phosphate-buffered saline (PBS). There were also blank injected (PBS only, grey), uninjected (black) and pentostatin only in PBS (blue) controls. Error bars show 95% confidence intervals. Sample size = 20 caterpillars.

Figure 4.1.2: Pure Compounds Injections (Live Assay) – Responsiveness (Area Under the Curve)

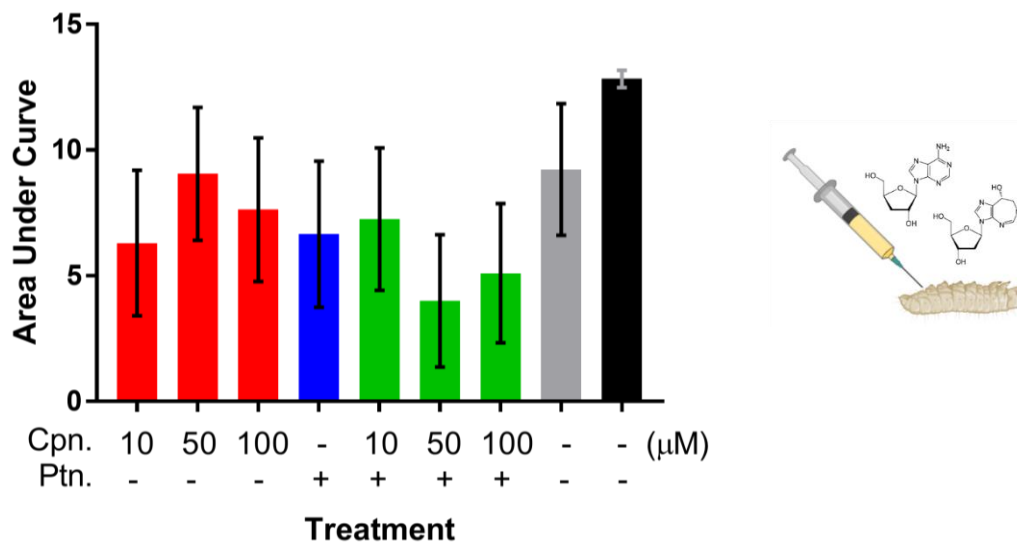


Figure 4.1.2: Proportions of responsiveness observed in *Galleria mellonella* caterpillars following 100 μ L injections with varying concentrations of cordycepin (cpn) with (green) or without (red) added 1.5 nM pentostatin (ptn) in phosphate-buffered saline (PBS) – area under the curve graph. Areas under the curves values apply to the full 14-day time period of the experiment. There were also blank injected (PBS only, grey), uninjected (black) and pentostatin only in PBS (blue) controls. Error bars show 95% confidence intervals. Asterisks (*) indicate significant differences between area under the curve means ($p < 0.05$). Sample size = 20 caterpillars.

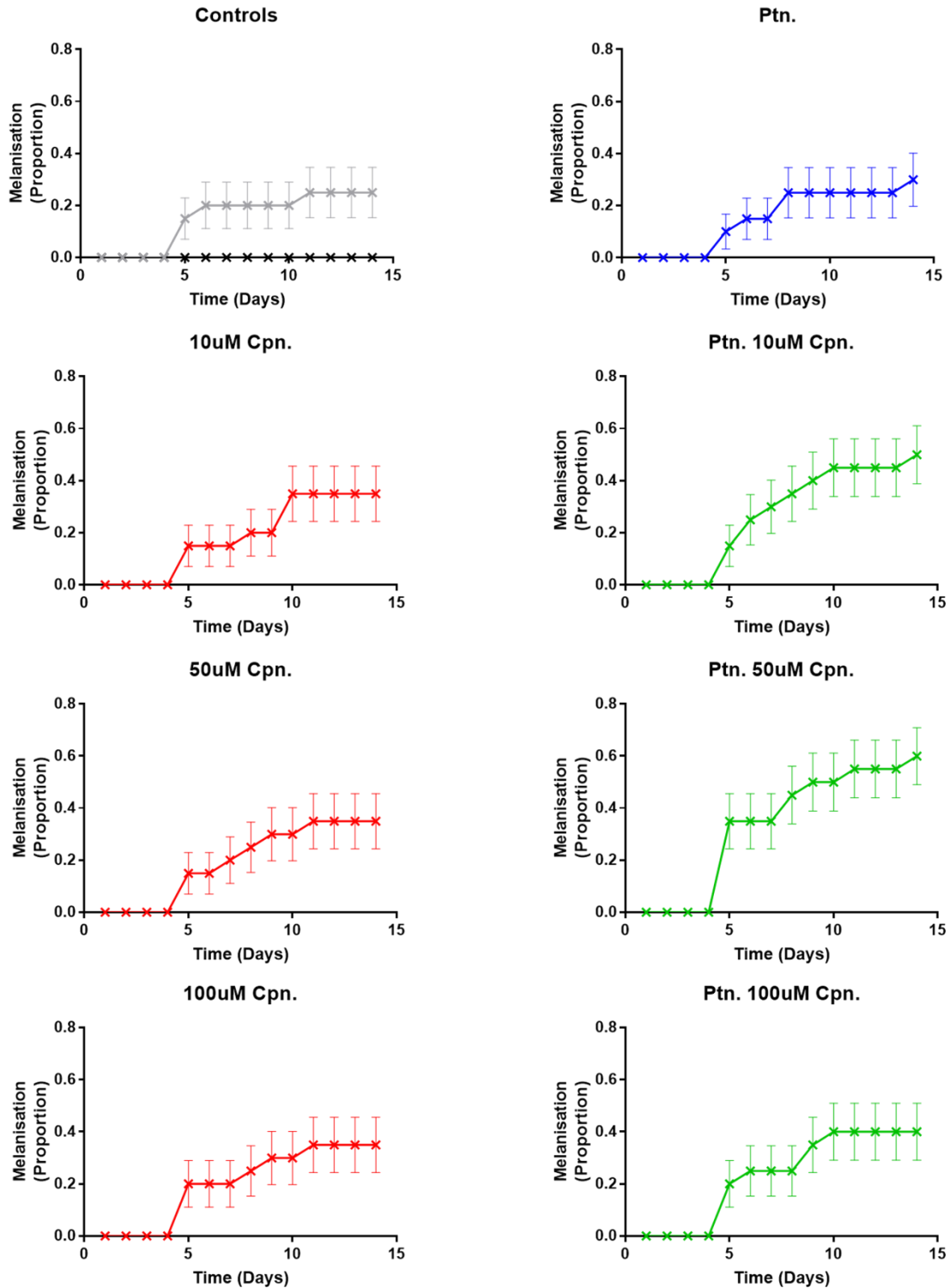
Figure 4.2.1: Pure Compounds Injections (Live Assay) – Melanisation

Figure 4.2.1: Proportions of full melanisation observed in *Galleria mellonella* caterpillars following 100 μ L injections with varying concentrations of cordycepin (cpn) with (green) or without (red) added 1.5 nM pentostatin (ptn) in phosphate-buffered saline (PBS). There were also blank injected (PBS only, grey), uninjected (black) and pentostatin only in PBS (blue) controls. Error bars show 95% confidence intervals. Sample size = 20 caterpillars.

Figure 4.2.2: Pure Compounds Injections (Live Assay) – Melanisation (Area Under the Curve)

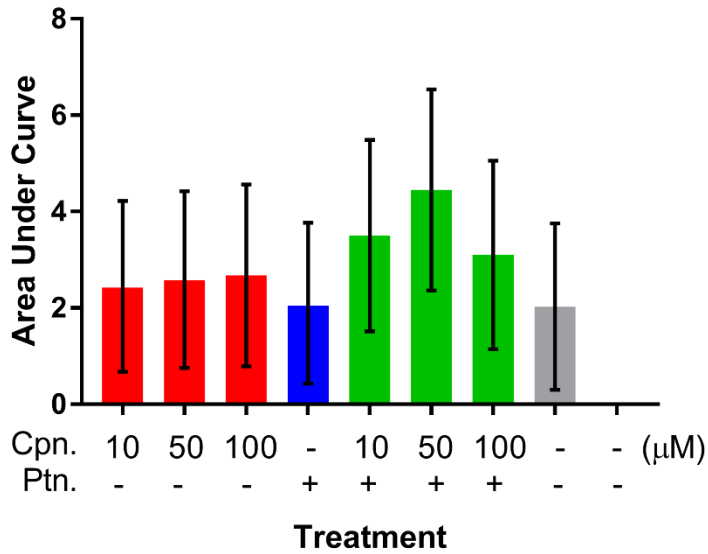


Figure 4.2.2: Proportions of full melanisation observed in *Galleria mellonella* caterpillars following 100 μL injections with varying concentrations of cordycepin (cpn) with (green) or without (red) added 1.5 nM pentostatin (ptn) in phosphate-buffered saline (PBS) – area under the curve graph. Areas under the curves values apply to the full 14-day time period of the experiment. There were also blank injected (PBS only, grey), uninjected (black) and pentostatin only in PBS (blue) controls. Error bars show 95% confidence intervals. Asterisks (*) indicate significant differences between area under the curve means ($p < 0.05$). Sample size = 20 caterpillars.

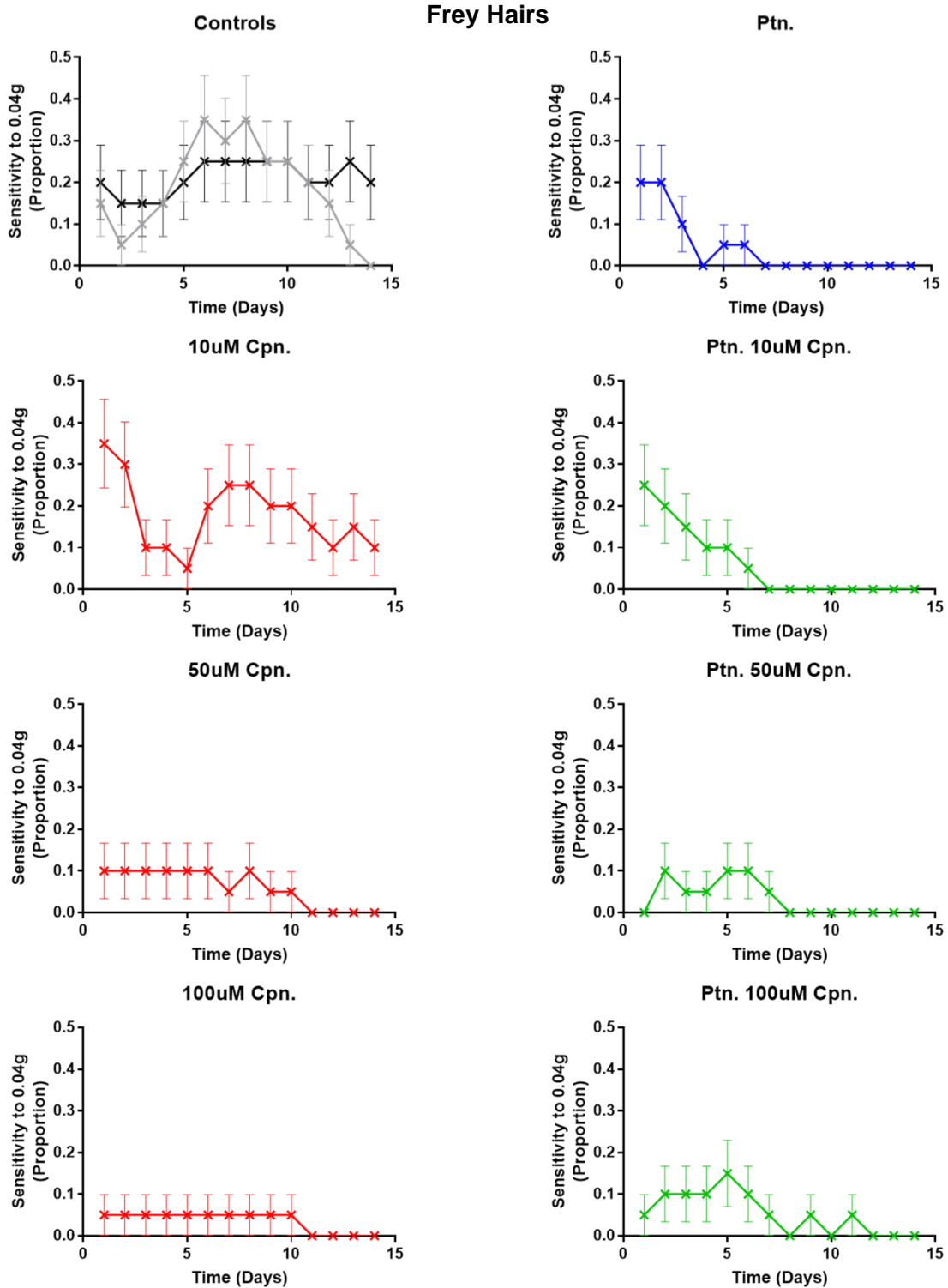
Figure 4.3.1: Pure Compounds Injections (Live Assay) – Sensitivity to 0.04g Von

Figure 4.3.1: Proportions of sensitivity to 0.04g Von Frey hairs observed in *Galleria mellonella* caterpillars following 100 μ L injections with varying concentrations of cordycepin (cpn) with (green) or without (red) added 1.5 nM pentostatin (ptn) in phosphate-buffered saline (PBS). There were also blank injected (PBS only, grey), uninjected (black) and pentostatin only in PBS (blue) controls. Error bars show 95% confidence intervals. Sample size = 20 caterpillars.

Figure 4.3.2: Pure Compounds Injections (Live Assay) – Sensitivity to 0.04g Von Frey Hairs (Area Under the Curve)

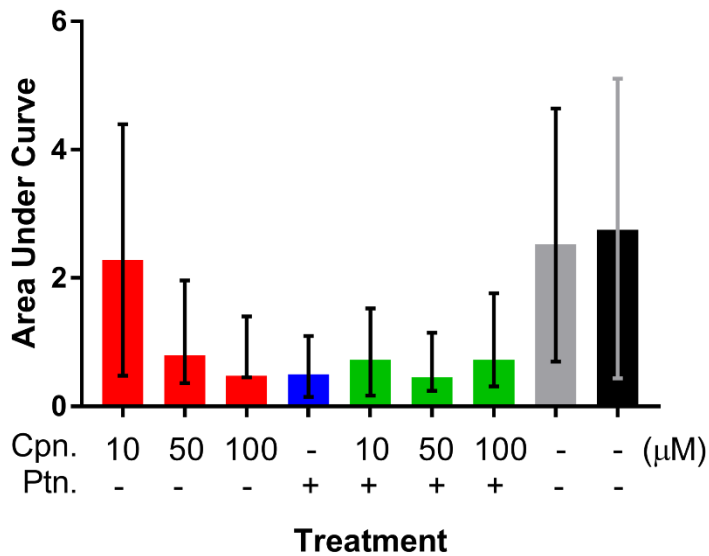


Figure 4.3.2: Proportions of sensitivity to 0.04g Von Frey hairs observed in *Galleria mellonella* caterpillars following 100 μL injections with varying concentrations of cordycepin (cpn) with (green) or without (red) added 1.5 nM pentostatin (ptn) in phosphate-buffered saline (PBS) – area under the curve graph. Areas under the curves values apply to the full 14-day time period of the experiment. There were also blank injected (PBS only, grey), uninjected (black) and pentostatin only in PBS (blue) controls. Error bars show 95% confidence intervals. Asterisks (*) indicate significant differences between area under the curve means ($p < 0.05$). Sample size = 20 caterpillars.

4.1.2 Alternative Methods for Using *Galleria mellonella*

Less invasive methods for introducing fungal material and/or cordycepin and pentostatin were desirable, to avoid the noise effects of injuries caused by injections in the data. Alternative methods of inoculation of caterpillars with fungal material were attempted – these included direct placement of caterpillars on solid agar cultures [figure 4.4; figure 4.5]; mixing of spores with caterpillar food (honey) [figure 4.6]; and soaking caterpillars with suspensions of spores [figure 4.12]. All three of these methods resulted in no observed fungal emergence at all, and no significant differences in melanisation were found between PCS and DS treatment groups [figure 4.5; figure 4.6; figure 4.12]. Another practical concern with these methods was the uncertainty regarding numbers of spores to which caterpillars were exposed – which for example was at the mercy of caterpillar movement on the agar plate, and feeding activity of caterpillars.

Injection of spores being the most reliable experimental method for caterpillar assays, it was decided that a titration of injected spore number would be performed. Surprisingly, across four orders of magnitude – from 10 to 10,000 spores used per injection – there were not significant differences in proportions of melanisation or fungal emergence over time [figure 4.8; figure 4.9].

An experimental method was carried out to investigate possible effects of secreted metabolites from *C. militaris* cultures, and to compare between parental control and degenerated strains of the *CM2* isolate. When media from liquid cultures, without the spores, was injected into caterpillars, there were no significant differences in responsiveness [figure 4.10] or melanisation proportions [figure 4.11]. This contrasts with the observed differences in melanisation caused by secreted metabolites in the company of spores described later in chapter 5. This indicates that this increased insect immune response took place as the result of a genuine infection, although enhanced by secreted metabolites from the parental control strain compared to the degenerated strain.

Two additional methods for the introduction of pure cordycepin and pentostatin with spores to caterpillars were performed – these both involved adding cordycepin and pentostatin to caterpillar food, following spore injection [figure 4.13] or spore soaking [figure 4.12]. There were no significant effects of interest observed following these experiments.

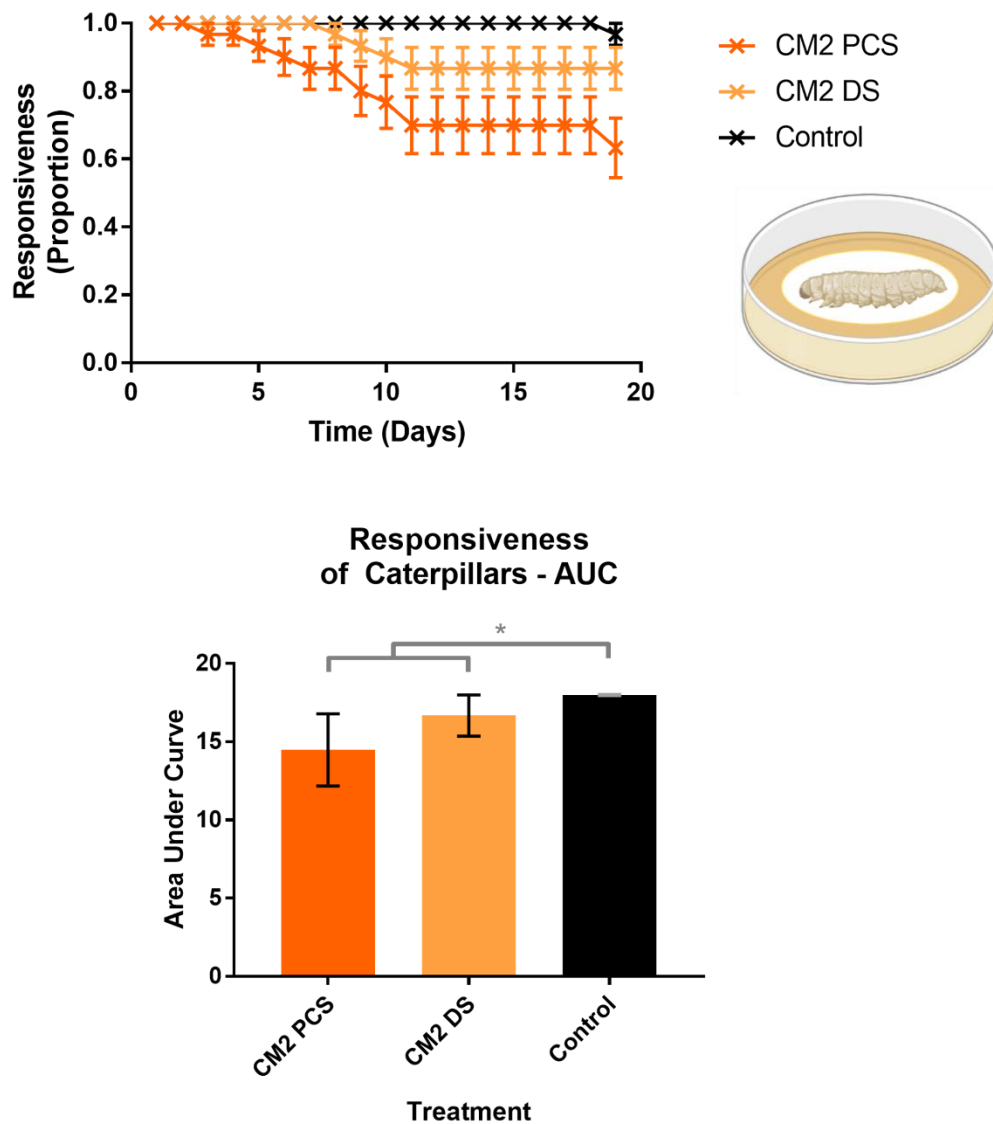
Figure 4.4: Fungal Agar Culture Exposure – Responsiveness

Figure 4.4: Proportions of responsiveness observed in *Galleria mellonella* caterpillars following exposure for 4 hours to potato dextrose agar (PDA) cultures. Parental control (PCS) and degenerated (DS) strain cultures of the *CM2 Cordyceps militaris* isolate, as well as an untreated control group were used. Error bars show 95% confidence intervals in both time course plots and area under the curve graphs. Asterisks (*) indicate significant differences between area under the curve means ($p < 0.05$). Sample size = 30 caterpillars.

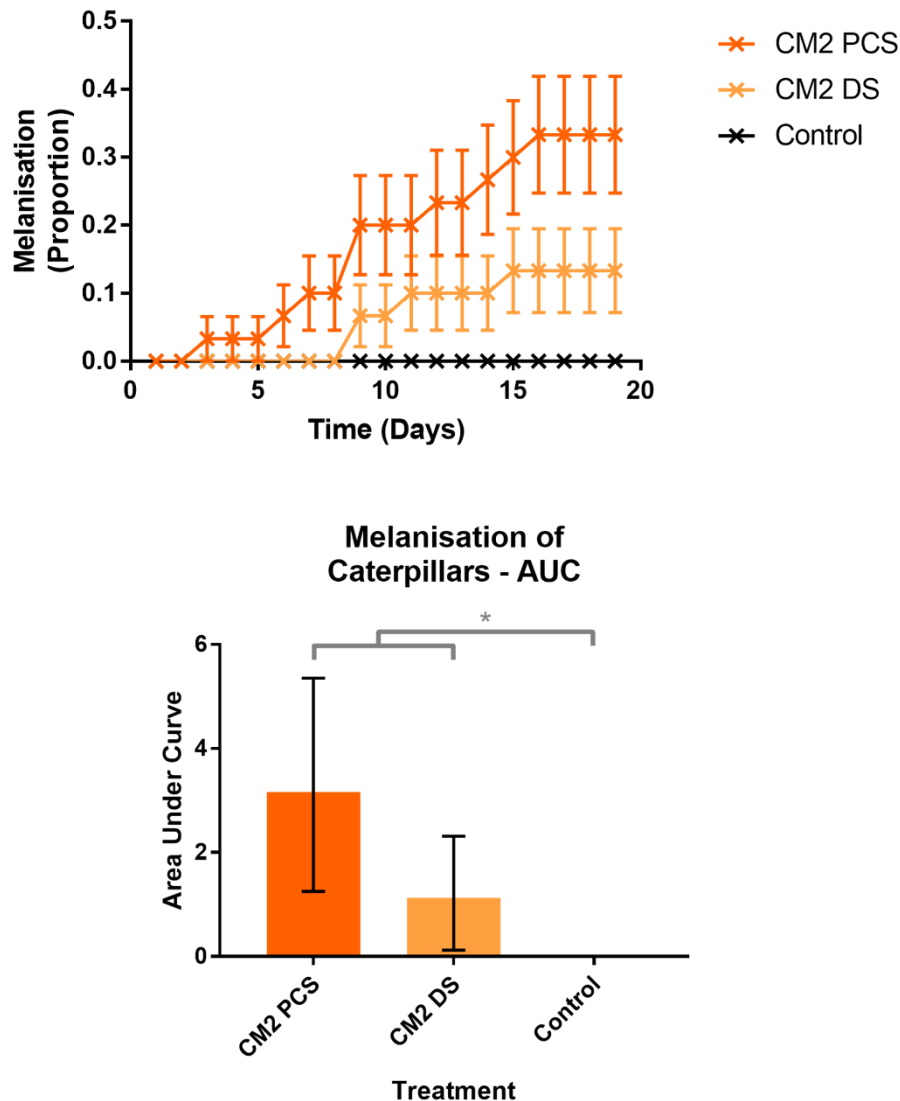
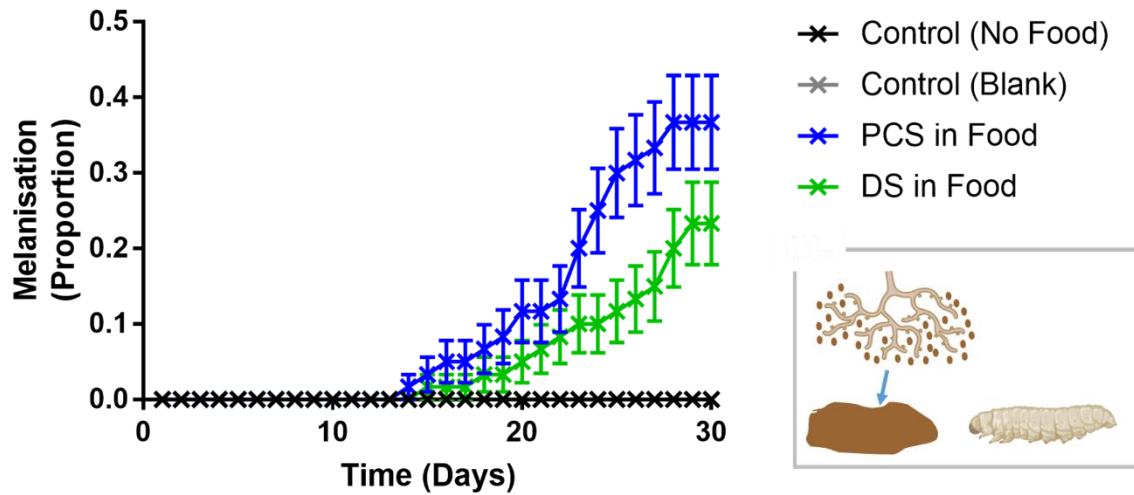
Figure 4.5: Fungal Agar Culture Exposure – Melanisation

Figure 4.5: Proportions of full melanisation observed in *Galleria mellonella* caterpillars following exposure for 4 hours to potato dextrose agar (PDA) cultures. Parental control (PCS) and degenerated (DS) strain cultures of the *CM2 Cordyceps militaris* isolate, as well as an untreated control group were used. Error bars show 95% confidence intervals in both time course plots and area under the curve graphs. Asterisks (*) indicate significant differences between area under the curve means ($p < 0.05$). Sample size = 30 caterpillars.

Figure 4.6: Fungal Spores Ingestion – Melanisation



Melanisation of Caterpillars - AUC

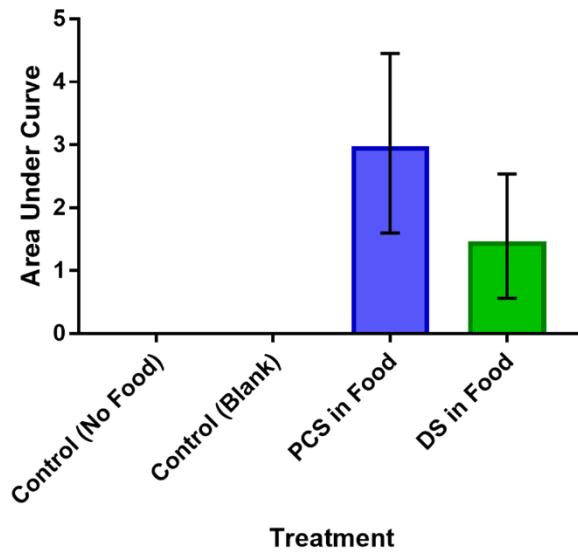


Figure 4.6: Proportions of full melanisation observed in *Galleria mellonella* caterpillars following the addition of 1000 spores/mL to food (honey). Washed spores from potato dextrose broth (PDB) cultures of parental control (PCS) and degenerated (DS) strain cultures of the *CM2 Cordyceps militaris* isolate were used. There were also blank (no spores in food) and no food control treatments. Error bars show 95% confidence intervals in both the time course plot and area under the curve graph. Sample size = 60 caterpillars.

Figure 4.7: Fungal Liquid Cultures Spores Injections (Titration) – Responsiveness

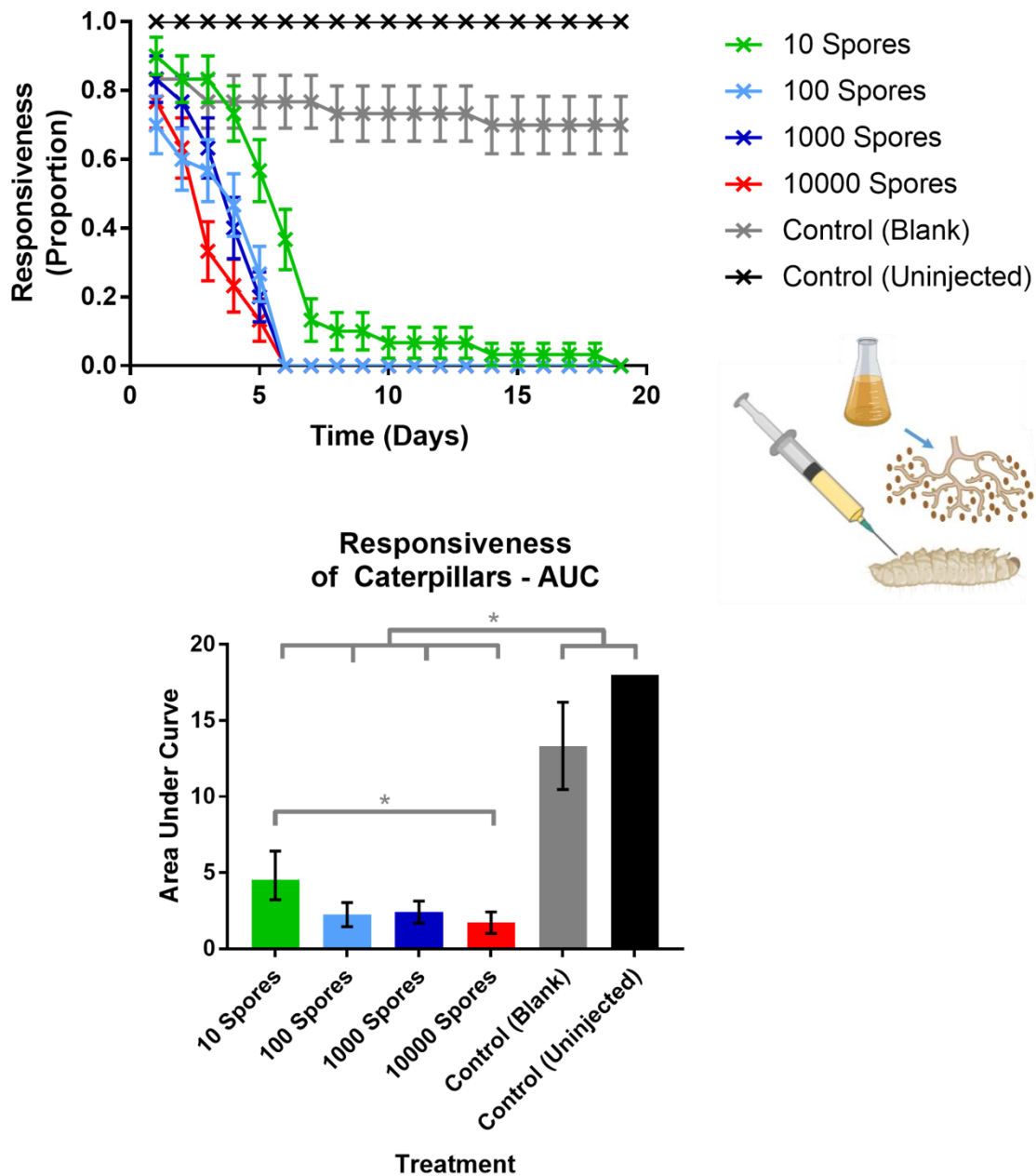


Figure 4.7: Proportions of responsiveness observed in *Galleria mellonella* caterpillars following 100 μ L injections with various doses of phosphate-buffered saline (PBS)-washed conidia. Potato dextrose broth (PDB)-grown cultures of the CM2 isolate were used, with spores doses from 10 – 10,000 spores per caterpillar. There were also blank injected (PBS only) and uninjected controls. The parental control strain (PCS) of CM2 was used. Error bars show 95% confidence intervals in both time course plots and area under the curve graphs. Asterisks (*) indicate significant differences between area under the curve means ($p < 0.05$). Sample size = 60 caterpillars.

Figure 4.8: Fungal Liquid Cultures Spores Injections (Titration) – Melanisation

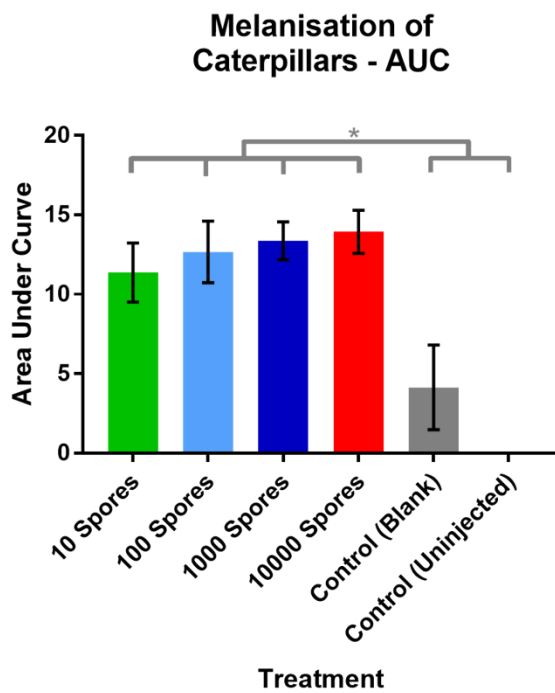
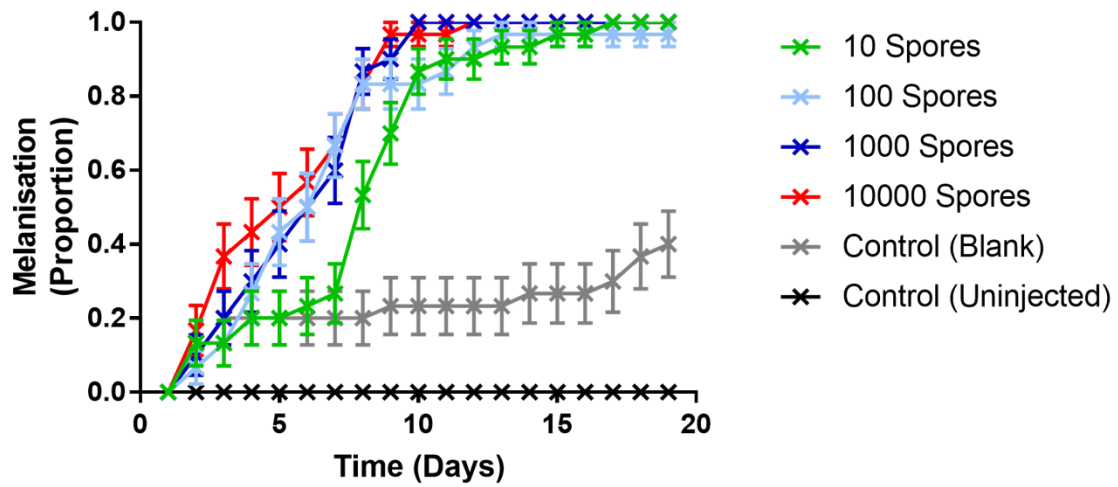
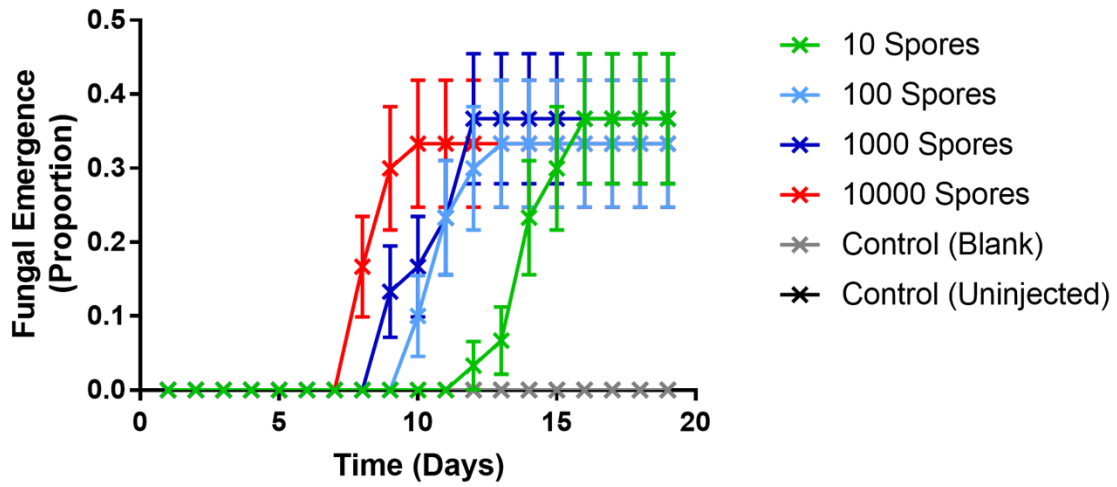


Figure 4.8: Proportions of full melanisation observed in *Galleria mellonella* caterpillars following 100 μ L injections with various doses of phosphate-buffered saline (PBS)-washed conidia. See the legend of figure 4.7 for further details

Figure 4.9: Fungal Liquid Cultures Spores Injections (Titration) – Fungal Emergence



Fungal Emergence from Caterpillars - AUC

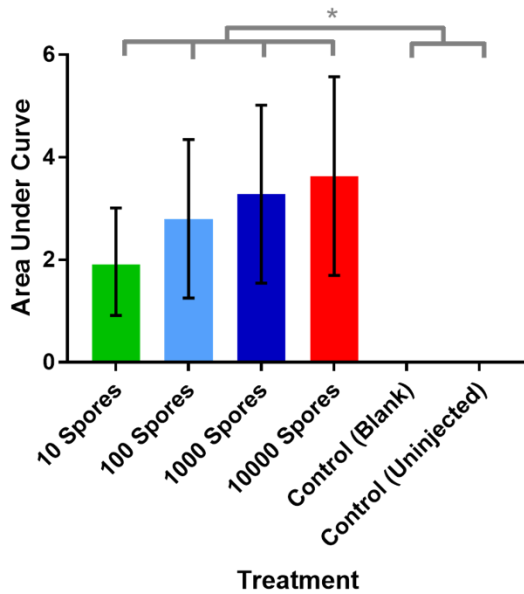


Figure 4.9: Proportions of fungal emergence observed in *Galleria mellonella* caterpillars following 100 μ L injections with various doses of phosphate-buffered saline (PBS)-washed conidia. See the legend of figure 4.7 for further details

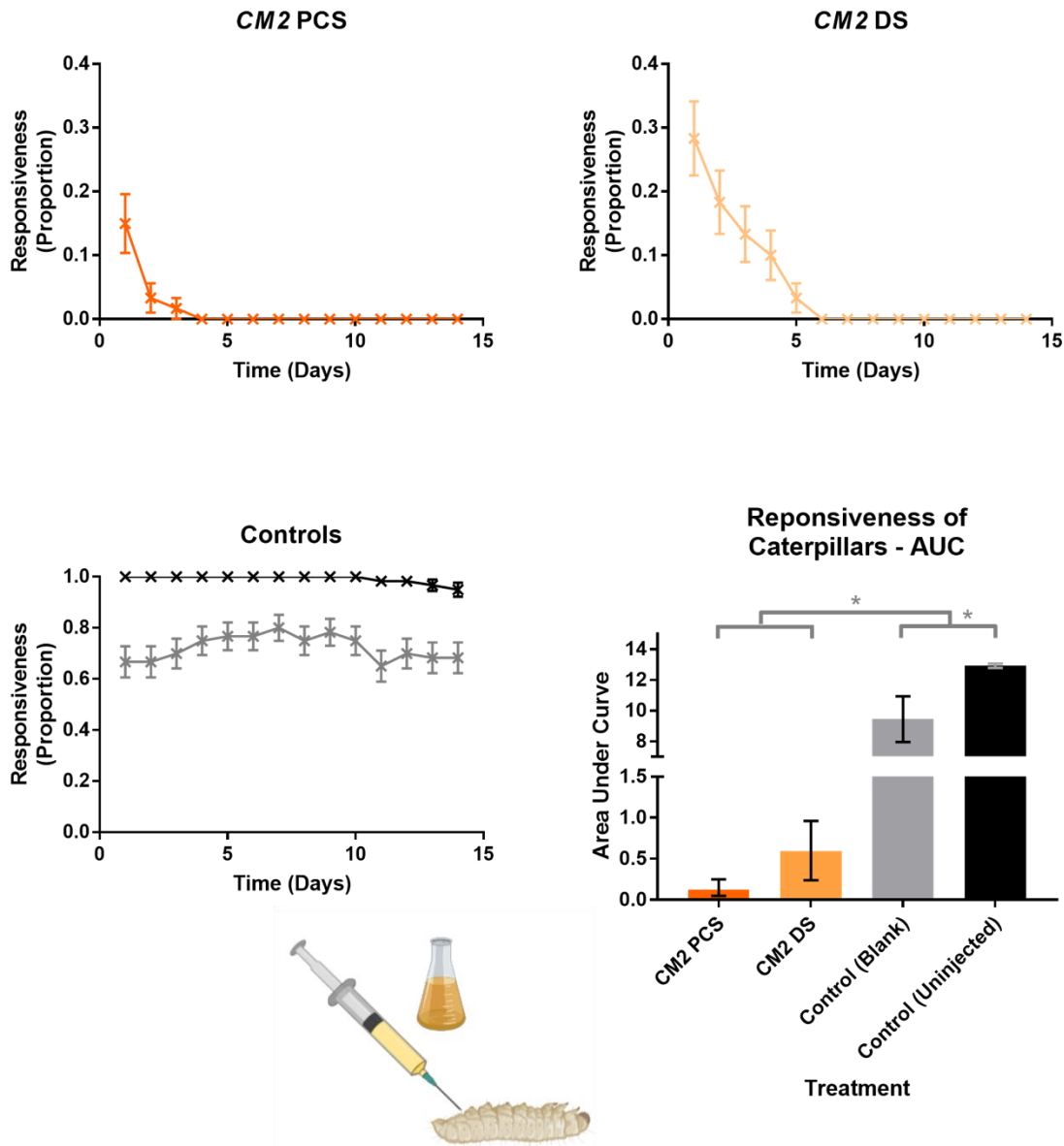
Figure 4.10: Fungal Liquid Cultures Extract Injections – Responsiveness

Figure 4.10: Proportions of responsiveness observed in *Galleria mellonella* caterpillars following 100 μ L injections with spent media from potato dextrose broth (PDB)-grown cultures. The parental control (PCS) and degenerated (DS) strains of the *Cordyceps militaris* CM2 isolate were used. There were also blank injected (fresh PDA media only) and uninjected controls. Error bars show 95% confidence intervals in both time course plots and area under the curve graphs. Asterisks (*) indicate significant differences between area under the curve means ($p < 0.05$). Sample size = 60 caterpillars.

Figure 4.11: Fungal Liquid Cultures Extract Injections – Melanisation

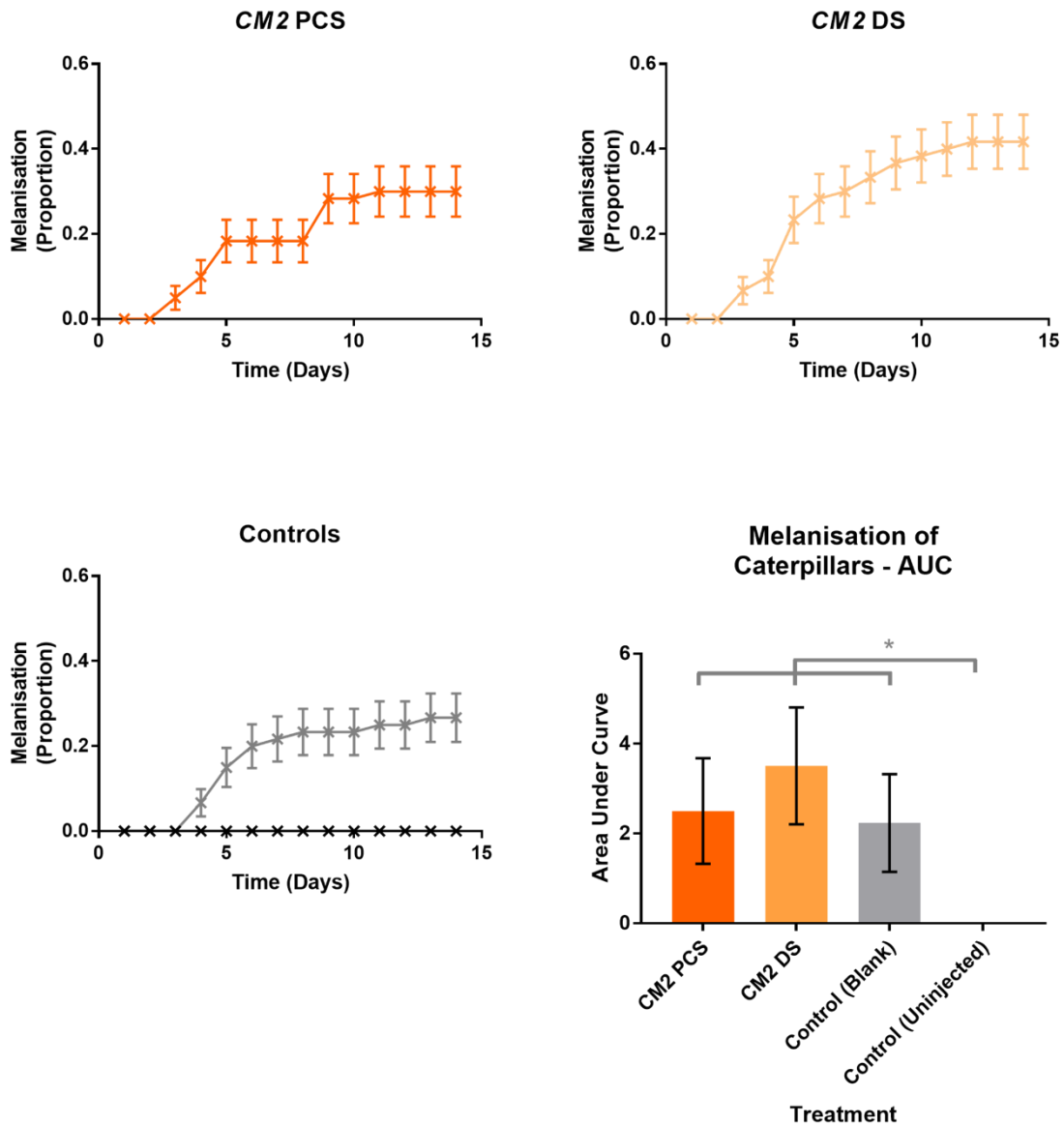


Figure 4.11: Proportions of full melanisation observed in *Galleria mellonella* caterpillars following 100 μ L injections with spent media from potato dextrose broth (PDB)-grown cultures. See the legend of figure 4.10 for further details.

Figure 4.12.1: Fungal Spores Soaking and Pure Compounds Ingestion – Melanisation

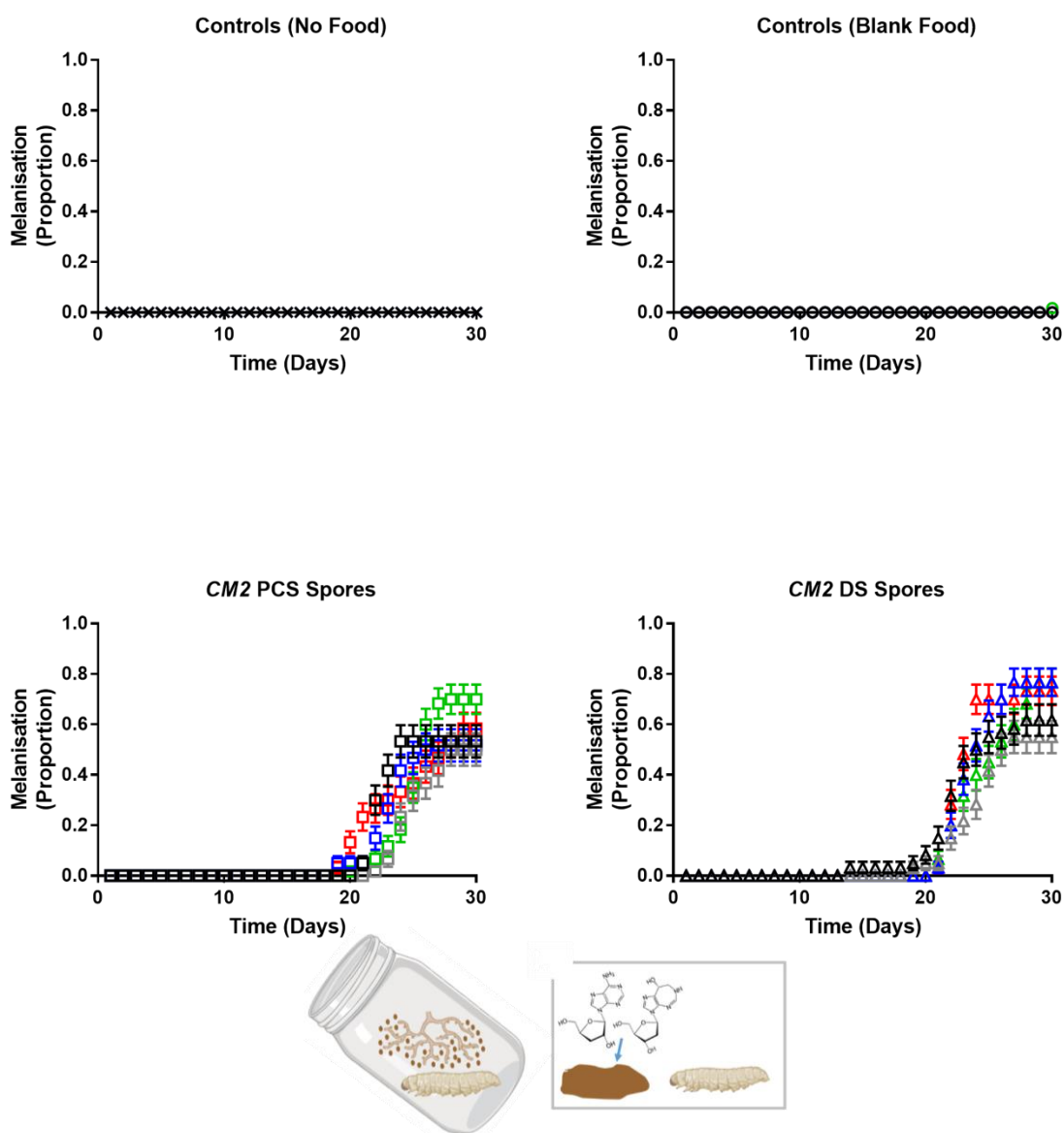


Figure 4.12.1: Proportions of full melanisation observed in *Galleria mellonella* caterpillars following soaking in suspensions of 1000 spores/mL from potato dextrose broth (PDB)-grown cultures and feeding with cordycepin and/or pentostatin. The parental control (PCS) and degenerated (DS) strains of the CM2 isolate were used. Spores were washed with and suspended in phosphate-buffered saline (PBS), and feeding of 100 μ M cordycepin (cpn, blue) or 1.5 nM pentostatin (ptn, green) or both (red) in honey took place. There were food controls of honey only (blank, grey) and no food (-, black), as well as soaking controls of PBS only (blank) and no soaking (-), and. Error bars show 95% confidence intervals. Sample size = 60 caterpillars.

Figure 4.12.2: Fungal Spores Soaking and Pure Compounds Ingestion – Melanisation (Area Under the Curve)

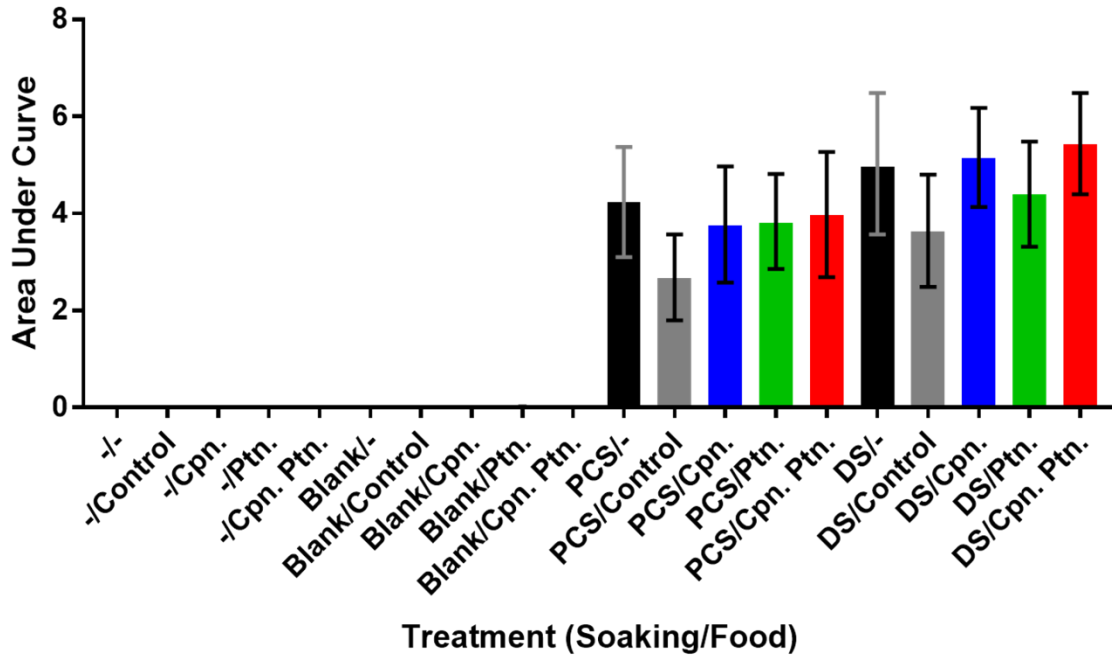


Figure 4.12.2: Proportions of full melanisation observed in *Galleria mellonella* caterpillars following soaking in suspensions of 1000 spores/mL from potato dextrose broth (PDB)-grown cultures and feeding with cordycepin and/or pentostatin – area under the curve graph. Error bars show 95% confidence intervals. Sample size = 60 caterpillars. See the legend of figure 4.12.1 for further details.

Figure 4.13.1: Pure Compounds Ingestion and Spores Injection – Melanisation

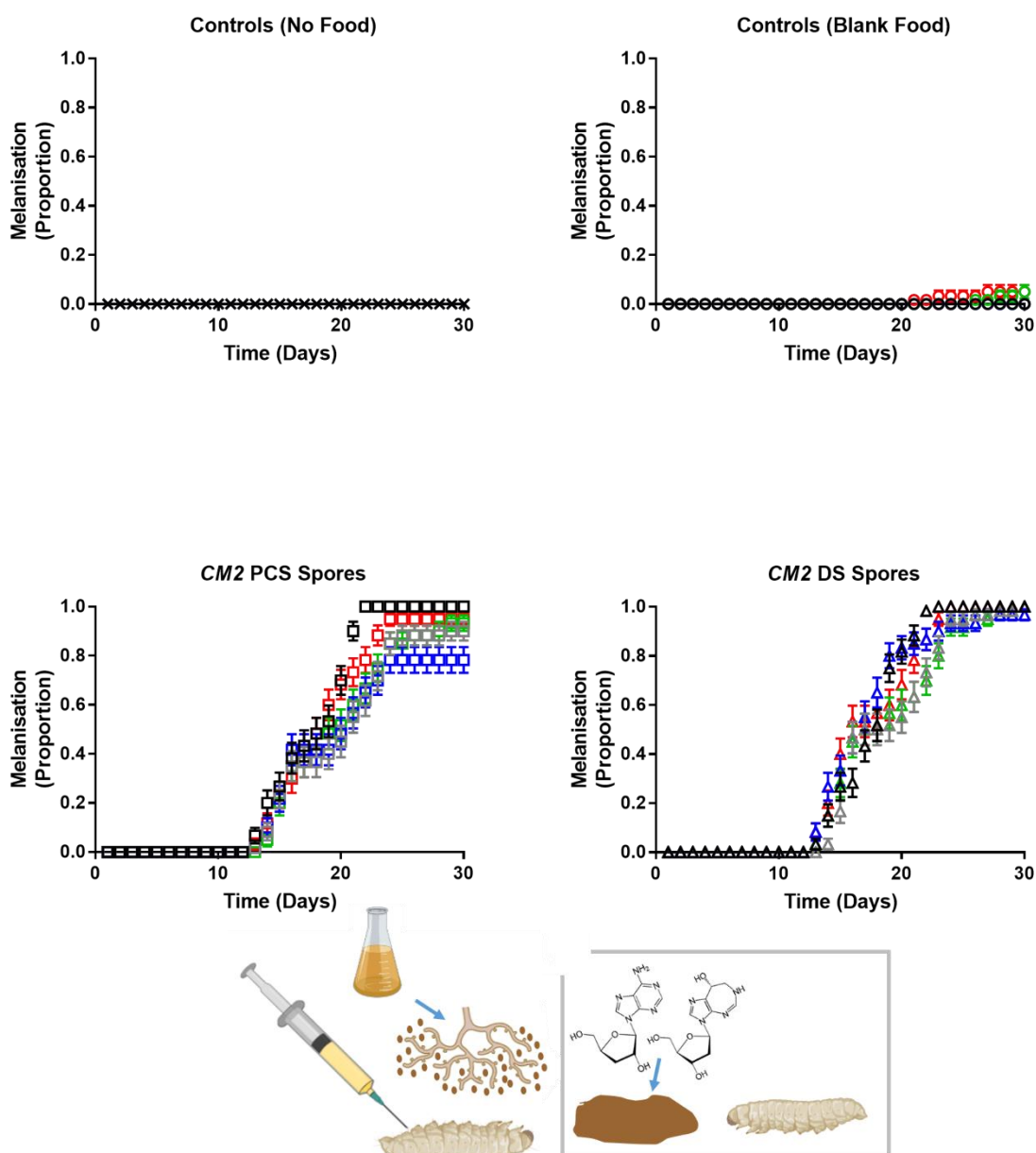


Figure 4.13.1: Proportions of full melanisation observed in *Galleria mellonella* caterpillars following 30 μL injections of washed spores from potato dextrose broth (PDB)-grown cultures and feeding with cordycepin and/or pentostatin. The parental control (PCS) and degenerated (DS) strains of the CM2 isolate were used. Spores were washed with and suspended in phosphate-buffered saline (PBS), and feeding of 100 μM cordycepin (cpn, blue) or 1.5 nM pentostatin (ptn, green) or both (red) in honey took place. There were food controls of PBS only (blank, grey) and no soaking (-, black), and injection controls of PBS only (blank) and uninjected caterpillars (-). Error bars show 95% confidence intervals. Sample size = 60 caterpillars.

Figure 4.13.2: Pure Compounds Ingestion and Spores Injection – Melanisation (Area Under the Curve)

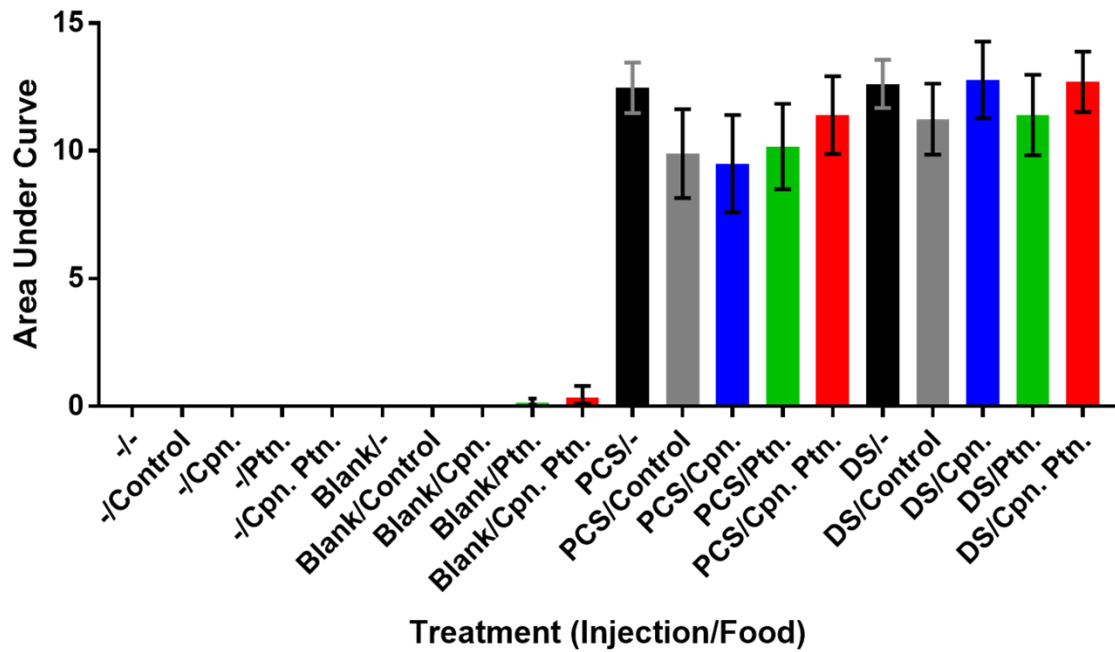


Figure 4.13.2: Proportions of full melanisation observed in *Galleria mellonella* caterpillars following 30 μ L injections of washed spores from potato dextrose broth (PDB)-grown cultures and feeding with cordycepin and/or pentostatin – area under the curve graph. Error bars show 95% confidence intervals. Sample size = 60 caterpillars. See the legend of figure 4.13.1 for further details.

4.2 DISCUSSION

The data from these methods reveal some disadvantages in using *Galleria mellonella* caterpillars as the *Cordyceps militaris* host model species. In particular, it was not possible to determine the point of death of caterpillars. Responsiveness could be described as a proxy for survival by first assumption – but this cannot be true because unresponsive caterpillars have been shown to regain responsiveness later [figure 4.1]. Furthermore, loss of responsiveness has frequently occurred before melanisation in caterpillars [multiple figures in chapters 4 and 5]. Being an observable insect immune response, melanisation is an active process which takes place while the host is alive, and occurs upon detection of the pathogen [Chambers *et al.* 2012]. Deaths would most likely have occurred soon after full melanisation. Together the observations of melanisation and fungal emergence (growth of hyphae out from the caterpillar) give an indication of host pathogenic response to the fungus.

It has been noted previously [Kryukov *et al.* 2020] that blackening of *Galleria mellonella* caterpillars can be caused by bacterial infection, resulting in decomposition. This was not the case here, as caterpillars described as fully melanised were firm to the touch; and many followed with fungal emergence. For example, when injected with spent PDB media and spores from cultures of the parental control strain, almost all (97%) caterpillars showed melanisation – and almost half (48%) became fully melanised [figure 5.11; figure 5.12].

It is worth also noting that in future experiments, humid conditions can be used to potentially aid fungal colonisation of caterpillars.

From the array of alternative methods attempted here, for both inoculation of caterpillars with spores and introduction of cordycepin and pentostatin – it is apparent that the injection methods used in experiments described in chapter 5 are the most effective in obtaining informative results. 100 µL injection volumes enabled precision with amounts of cordycepin and pentostatin, as well as numbers of spores in suspensions given to each caterpillar.

However, this relatively large injection volume may have contributed to melanisation rates in controls, which were nevertheless far below those in treatment groups. Observable readouts of responsiveness, melanisation, and fungal emergence enabled high numbers of replicates.

Despite extensive efforts here to establish less invasive and more quantitative systems for the study of *Cordyceps militaris* infection of *Galleria mellonella*, the methods used in the next chapter were the best available among those tested. Insights into the process of culture degeneration and effects in the context of the host, as well as the roles of cordycepin and pentostatin in infection were made using these.

CHAPTER 5: CORDYCEPIN AND DEGENERATION IN THE CONTEXT OF THE INSECT HOST

The role of cordycepin in the context of the fungus best known to produce it – *Cordyceps militaris* – has not been widely investigated. It has been proposed that this compound and its co-produced stabilising molecule pentostatin are involved in aiding the infection of the insect host by the fungus [Wellham *et al.* 2019]. Recent evidence for this was provided by demonstrating the reduced upregulation of immune-related genes in insect models by colleagues in Warwick [Woolley *et al.* 2020]. Further to this, reduced cordycepin production in a degenerated strain of the *C. militaris* isolate CM2 was accompanied by reduced sexual development-related gene expression (chapter 3). Given that the infection of the host directly precedes sexual development, one can hypothesise that degeneration also causes a reduction in pathogenicity. Here, insect host models of *Drosophila melanogaster* S2 cells, cells from haemolymph of *Galleria mellonella* caterpillars, and whole *G. mellonella* caterpillars were used to investigate the effects of culture degeneration on pathogenic response to *Cordyceps militaris*, as well as the potential roles of cordycepin and pentostatin in the host.

5.1 CORYCEPIN AND DEGENERATION – EFFECTS ON THE HOST

5.1.1 Pure Cordycepin/ Pentostatin and Insect Host Immunity

To examine the effects of cordycepin and pentostatin on immunity of the insect host, model systems were used, consisting of *Drosophila melanogaster* S2 cells and injected *Galleria mellonella* caterpillars with haemolymph extracted afterwards. To stimulate mock fungal infection [Jin *et al.* 2008], curdlan was used in both models. The expression of immune response genes was assessed by RT-qPCR compared to a reference housekeeping gene in

each case. Solutions of pure cordycepin and pentostatin were added additionally, to test for effects on the upregulation of immune response genes by curdlan.

In *Drosophila* S2 cells, curdlan stimulated upregulation of *Attacin A* compared to both the untreated negative control (df = 48, t = 6.153, p < 0.0001) and the solvent (DMSO only) negative control (df = 48, t = 6.108, p < 0.0001) [figure 5.1; table 5.1]. Lipopolysaccharide (LPS) achieved a similar effect [figure 5.2]. When injected into *G. mellonella* caterpillars, curdlan stimulated upregulation of *Lysozyme*, compared to the equivalent controls of uninjected (df = 14, t = 12.44, p < 0.0001) and blank (PBS only) (df = 14, t = 6.968, p = 0.0001) injected caterpillars [figure 5.3]. This was not the case with other genes considered – *Gallerimycin* [figure 5.3], *Galiomicin*, and *IMPI* [data not shown].

Cordycepin suppresses the host's immune response. In both model systems, suppressive effects of added cordycepin on immune response gene upregulation by curdlan were observed. Expression of genes *Attacin A* and *Lysozyme* in the S2 cells and caterpillars respectively are discussed below. *Attacin A* encodes an antimicrobial peptide, known to be upregulated in response to fungal infection [Jin *et al.* 2008], and with recent precedent of assessment in S2 cells in response to curdlan [Woolley *et al.* 2020]. *Lysozyme* has antibacterial properties by targeting peptidoglycan, but also acts as an antifungal – although the mechanism behind this activity is not well characterised. It has been demonstrated to cause apoptosis in *Candida albicans* via binding the protoplasts [Sowa-Jasilek *et al.* 2016]. *Lysozyme*, selected alongside three other immune-related genes in *G. mellonella* based on previous work with *C. militaris* [Woolley *et al.* 2020], is particularly discussed due to its upregulation with curdlan treatments in the experiments here.

Attacin A expression in *D. melanogaster* S2 cells after four hours was significantly lower when 20, 50, and 100 µM cordycepin were added compared to curdlan and solvent alone (df = 48; t = 4.732, 5.807, 5.858, p = 0.0055, 0.0001, 0.0001 respectively) [figure 5.1; table 5.1]. In a further experiment on the S2 cells involving LPS stimulation rather than curdlan, to stimulate

mock bacterial infection, the addition of 100 μ M cordycepin suppressed the upregulation of *Attacin A* compared to the LPS and solvent control (df = 12, t = 4.497, p = 0.011) [figure 5.2].

Curdlan-stimulated *Lysozyme* expression after two hours was suppressed when 50 μ M cordycepin was added in injected *G. mellonella* caterpillars (df = 14, t = 4.795, p = 0.006) [figure 5.3]. These findings indicate that cordycepin plays a role in the suppression of the immune response of the early-stage infected host.

Pentostatin enhances the effect of cordycepin in the insect host. Pentostatin has been reported as the stabilising molecule for cordycepin [Xia *et al.* 2017]. Here, pentostatin was added to cordycepin treatments to test for possible enhancement of effects due to stabilising cordycepin in the host. When pure cordycepin and 1.5 nM pentostatin were added to curdlan-stimulated S2 cells, the suppression of *Attacin A* upregulation was again observed, this time also for cordycepin concentrations at a lower level of 10 μ M (df = 48, t = 5.43, p = 0.0005) [figure 5.1; table 5.1]. In *G. mellonella* caterpillars, expression levels of *Lysozyme* were even lower when injected with additional pentostatin, compared to curdlan-cordycepin injections without pentostatin (df = 14, t = 5.01, p = 0.004) [figure 5.3]. This indicates that pentostatin functions to enhance cordycepin function in the host, consistent with its description as a stabilising protector molecule for cordycepin [Xia *et al.* 2017]. However it was not possible from the data to obtain any evidence of an effect on the host for pentostatin on its own.

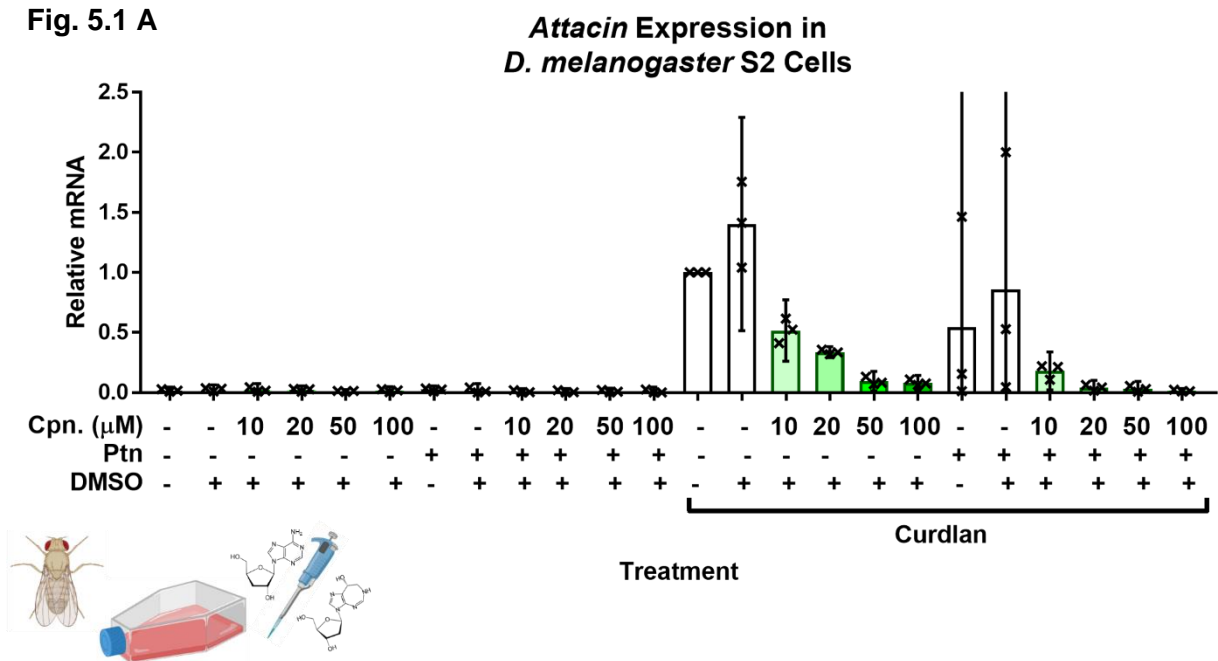
Figure 5.1: *Drosophila melanogaster* S2 Cell Gene Expression Assays

Figure 5.1: Relative expression of *Attacin A* in *Drosophila melanogaster* S2 cells following stimulation curdlan (cdl), with or without pre-treatment of cordycepin (cpn) of various concentrations and 1.5nM pentostatin (ptn). DMSO = dimethyl sulfoxide, the solvent used for cordycepin and pentostatin. Cells were sampled four hours after treatment. Expression levels are relative to the control gene *Ribosomal Protein 49 (Rp49)*, and all values were normalised to the curdlan-only treatment. Error bars show 95% confidence intervals, and comparisons between means as calculated using t-test, with Bonferroni corrections, are shown in table 5.1. Three biological replicates, with each point representing an average from three technical replicates are shown.

Table 5.1: Significances of differences determined by t-tests with Bonferroni corrections, for treatment groups in the *Drosophila melanogaster* S2 cell culture *Attacin A* gene expression assays [figure 5.1]. Abbreviations: cdl. = curdlan, cpn. = cordycepin, ptn. = pentostatin, DMSO = dimethyl sulfoxide.

Gene Expression: <i>Attacin A</i>	Cdl. Ctrl.	Cdl. DMSO		
Negative control	*	****	Ptn. 50 μ M Cpn.	* ****
DMSO	*	****	Ptn. 100 μ M Cpn.	* ****
10 μ M Cpn.	*	****	Cdl. 10 μ M Cpn.	NS NS
20 μ M Cpn.	*	****	Cdl. 20 μ M Cpn.	NS **
50 μ M Cpn.	*	****	Cdl. 50 μ M Cpn.	NS ***
100 μ M Cpn.	*	****	Cdl. 100 μ M Cpn.	* ***
Ptn.	*	****	Cdl. Ptn.	NS NS
Ptn. DMSO	*	****	Cdl. Ptn. 10 μ M Cpn.	NS ***
Ptn. 10 μ M Cpn.	*	****	Cdl. Ptn. 20 μ M Cpn.	* ****
Ptn. 20 μ M Cpn.	*	****	Cdl. Ptn. 50 μ M Cpn.	* ****
			Cdl. Ptn. 100 μ M Cpn.	* ****

Figure 5.2: *Drosophila melanogaster* S2 Cell Gene Expression Assays (LPS Induction)

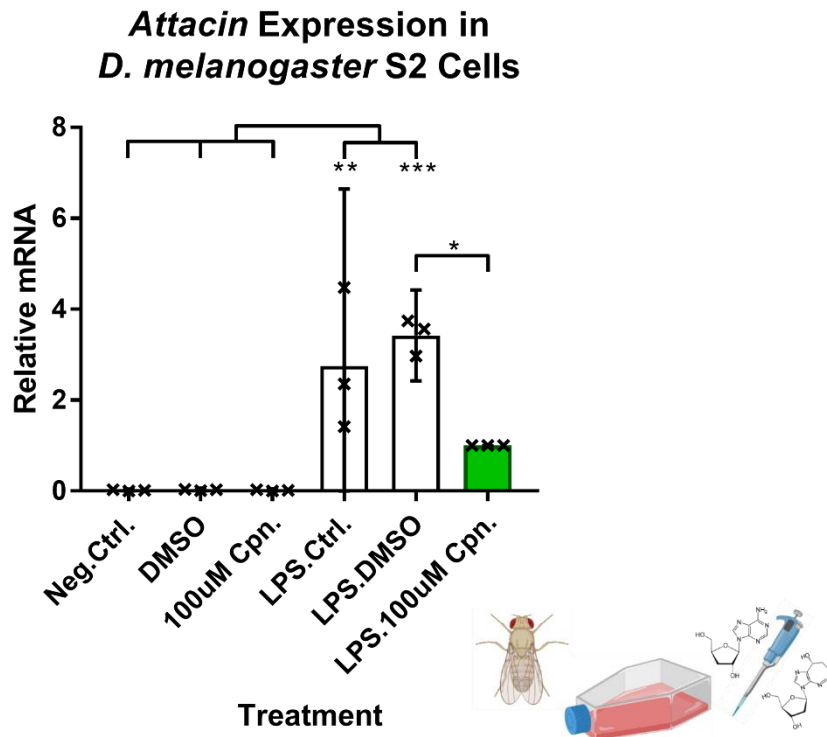


Figure 5.2: Relative expression of *Attacin A* in *Drosophila melanogaster* S2 cells following stimulation lipopolysaccharide (LPS), with or without pre-treatment of 100 μ M cordycepin (cpn). DMSO = dimethyl sulfoxide, the solvent used for cordycepin. Cells were sampled four hours after treatment. Expression levels are relative to the control gene *Ribosomal Protein 49* (*Rp49*). Error bars show 95% confidence intervals, and labels show differences between means as calculated using t-test, with Bonferroni corrections. * $p < 0.05$; ** $p < 0.01$; *** $p < 0.001$; **** $p < 0.0001$. Three biological replicates, with each point representing an average from three technical replicates are shown.

Figure 5.3: Pure Compounds Injections, and Fungal Extract Injections (Gene Expression)

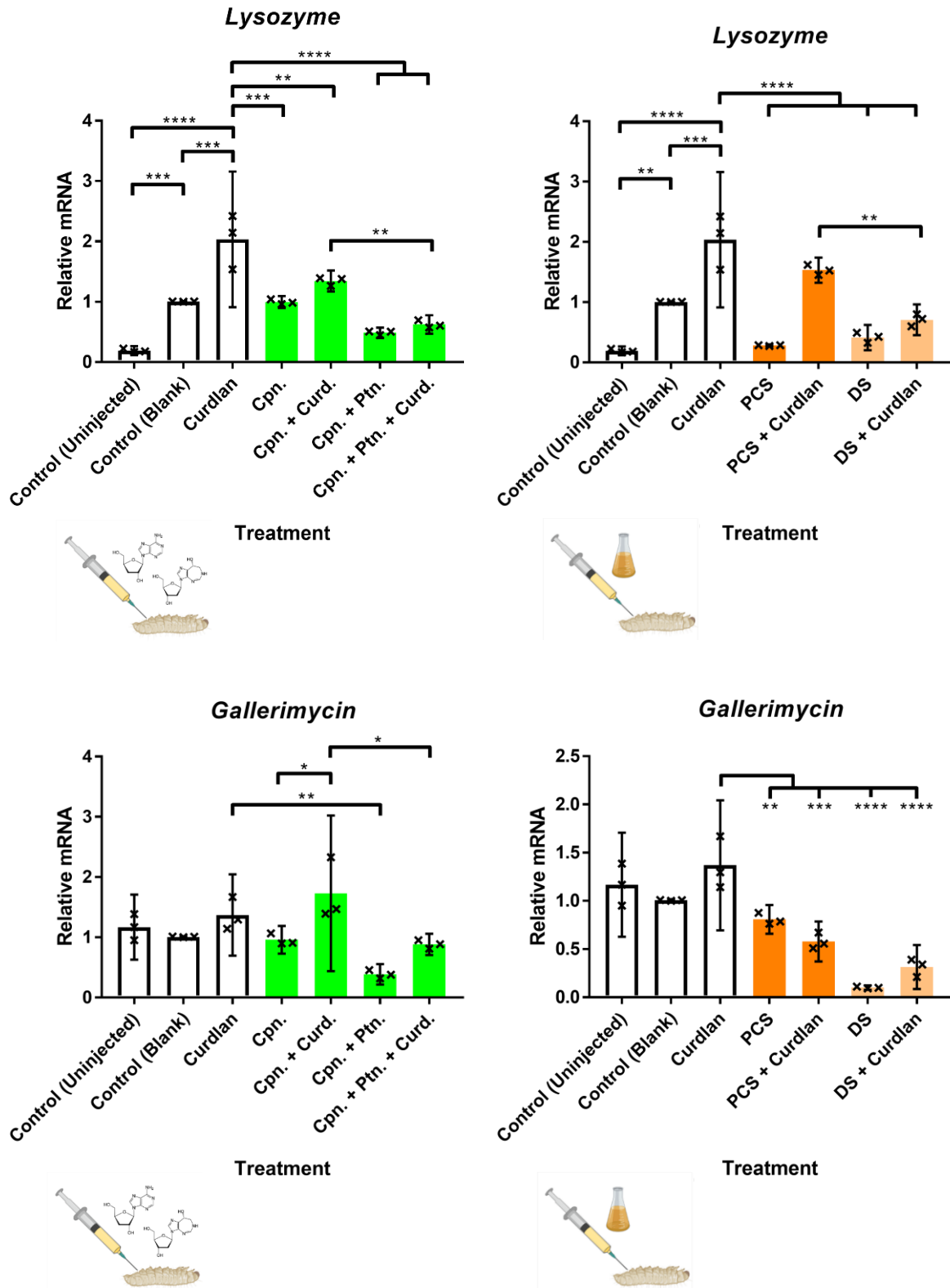


Figure 5.3: Relative expression of immune genes *Lysozyme* and *Gallerimycin* in cells from *Galleria mellonella* haemolymph following injection by curdlan, with or without cordycepin treatment and with or without spent media. Potato dextrose broth cultures (PDB) of the *CM2* isolate were used. PCS = parental control strain; DS = degenerated strain; curd = curdlan; cpn = cordycepin. Control treatments of uninjected caterpillars, and blank injections (fresh PDB only), and cordycepin with or without pentostatin in PDB were used. Haemolymph was extracted from caterpillars two hours after injection. Expression levels are relative to the control gene *S7e*. Error bars show 95% confidence intervals, and labels show differences between means as calculated using t-test, with Bonferroni corrections. * $p < 0.05$; ** $p < 0.01$; *** $p < 0.001$; **** $p < 0.0001$. Three biological replicates, with each point representing an average from three technical replicates are shown.

5.1.2 Degeneration and the Insect Host

To explore potential effects of strain degeneration on pathogenic response and the interaction of *C. militaris* with the host, experiments involving comparisons of the parental control strain (PCS) and degenerated strain (DS) of the *CM2* isolate were performed. These involved injections of *G. mellonella* caterpillars with either spores from liquid or solid agar-grown cultures, media (containing secreted metabolites) from liquid cultures, as well as additional pure cordycepin and pentostatin. Differences between results for different treatments were analysed by Bonferroni-adjusted log-rank (Mantel-Cox) tests.

As expected following findings in chapter 4, throughout the experiments, caterpillars injected with spores showed rapid rates in loss of responsiveness [figure 5.4; figure 5.7; figure 5.10; figure 5.13], and these were very similar in the parental control and degenerated strains. High proportions of responsiveness in control treated caterpillars indicate high efficacy of inoculation methods used.

Degeneration is accompanied by reduced fungal growth in the host. Fungal growth within the host was compared between the parental control and degenerated strains of the *CM2* isolate by observing emergence of hyphae from caterpillars following injections with spores. In several experiments, fungal emergence occurred at a faster rate and with greater success for the parental control strain (PCS) compared to the degenerated strain (DS). This was the case when spores from solid agar plates ($df = 1$, $X^2 = 7.405$, $p = 0.039$) [figure 5.6], and washed spores from liquid cultures ($df = 1$, $X^2 = 26.01$, $p < 0.001$) [figure 5.15], and spores with media from liquid cultures ($df = 1$, $X^2 = 14.6$, $p < 0.001$) [figure 5.12] were injected. (The difference was not significant however when a higher dose of 100,000 washed spores from liquid cultures were injected [figure 5.9].) Proportions of caterpillars showing fungal emergence by the end of the experiments were consistently much higher in for the parental control strain. For example, when spores and spent liquid media were injected, this was 48% for PCS versus 22% for DS. For spores only injections this was 35% versus 15% and 16% versus 5% for liquid and agar-based cultures respectively [figure 5.6; figure 5.9; figure 5.12]. These consistent differences

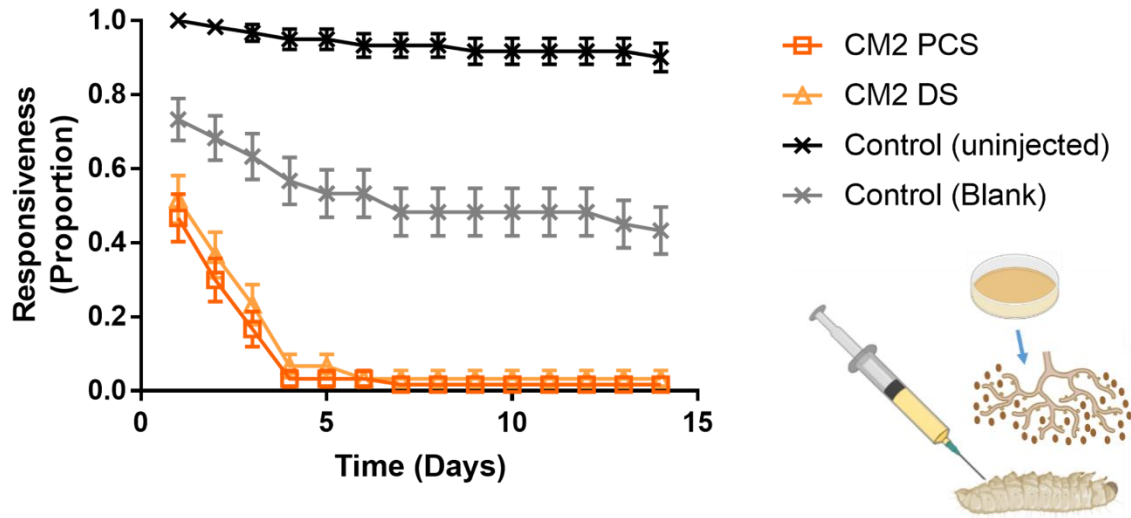
indicate that the degenerated strain produces a lesser pathogenic response than the parental control strain. It should be noted that hyphal emergence from caterpillars was used as a proxy for fungal growth in the host, and that growth without emergence from cadavers was also a possibility.

Lower virulence in the degenerated strain could be due to cordycepin/pentostatin production. To assess the effects of cordycepin and pentostatin in the context of degeneration, injections of washed PCS and DS liquid cultures spores were also compared with and without cordycepin (50 μ M) and pentostatin (1.5 nM) [figure 5.15]. When cordycepin and/or pentostatin were added to spore injections, the significant differences in fungal emergence, a proxy for virulence, from PCS and DS-treated caterpillars were no longer present. Between 17 and 20 days after injection, i.e. the end point of the experiment, addition of cordycepin, pentostatin, and both metabolites to degenerated spores significantly enhanced numbers of successful infections, measured by proportions of observed fungal emergence from caterpillars. For overall fungal emergence, the addition of cordycepin with pentostatin significantly enhanced the performance of the degenerated strain ($df = 1$, $X^2 = 11.91$, $p = 0.0468$). However this was not the case for the enhancement of cordycepin added without pentostatin, which was not significant. This indicates that lower production of cordycepin and pentostatin in the degenerated strain is at least in part a causal factor in its decreased virulence. Once again, supplementing added cordycepin with pentostatin appears also to enhance the effects of the former.

Degeneration is accompanied by reduced host immune suppression by secreted metabolites. To consider the effects of degeneration on the host immune response in these caterpillar experiments, the proportions of caterpillars observed with melanisation were recorded. When spores from solid agar cultures or washed spores from liquid cultures were injected into caterpillars, there was no significant difference in levels of melanisation between the parental control and degenerated strains [figure 5.5; figure 5.8]. Spores were also injected in combination with spent media from the same liquid cultures, to assess the effects of overall

secreted fungal metabolites on the host. When these were injected, melanisation was significantly greater in the parental control strain-treated caterpillars ($df = 1$, $X^2 = 16.14$, $p < 0.001$) [figure 5.11]. Here, 96% of caterpillars showed full melanisation over the course of the experiment in the PCS treatment versus 65% for DS. This indicates that differences in secreted metabolites present in the media of PCS and DS liquid cultures are responsible for differences in melanisation response.

Figure 5.4: Fungal Agar Cultures Spores Injections – Responsiveness



Responsiveness of Caterpillars - AUC

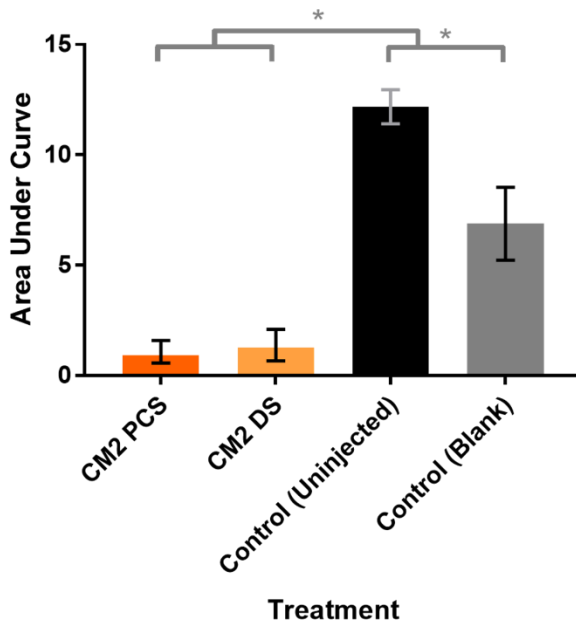


Figure 5.4: Proportions of responsiveness observed in *Galleria mellonella* caterpillars following injections with phosphate-buffered saline (PBS)-washed conidia from potato dextrose agar (PDA)-grown cultures of *Cordyceps militaris* CM2 isolate. Treatments of 100 μ L suspensions of 1000 washed conidia in PBS from parental control (PCS) and degenerated (DS) strains were used, as well as blank injected (PBS) and uninjected controls. PCS = parental control strain; DS = degenerated strain. Error bars show 95% confidence intervals in both time course plots and area under the curve graphs. Asterisks (*) indicate significant differences between area under the curve means ($p < 0.05$). Sample size = 60 caterpillars.

Figure 5.5: Fungal Agar Cultures Spores Injections – Melanisation

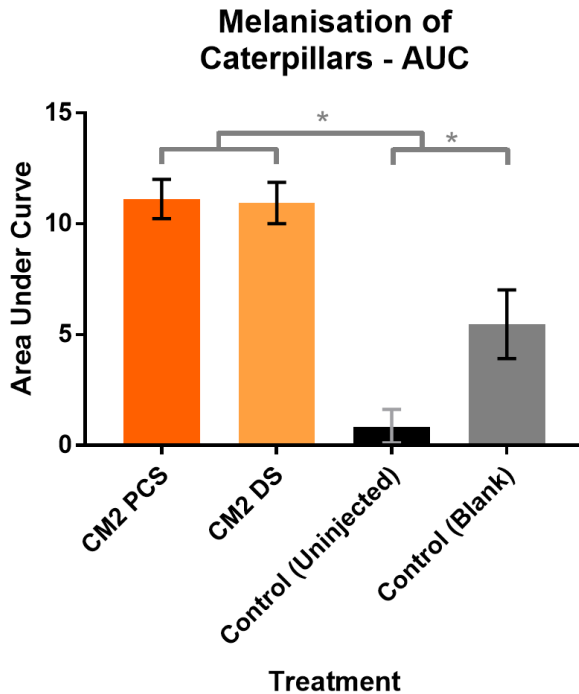
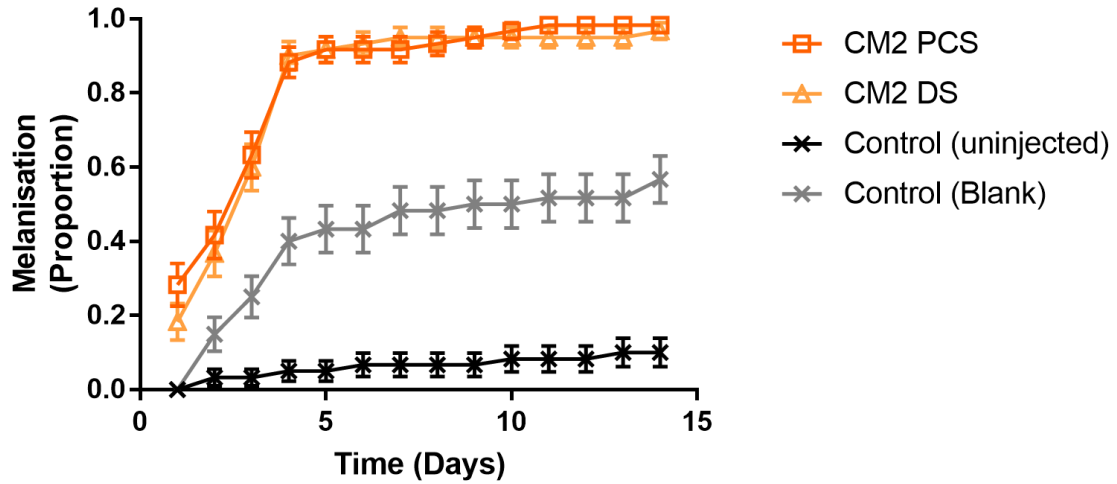


Figure 5.5: Proportions of full melanisation observed in *Galleria mellonella* caterpillars following injections with phosphate-buffered saline (PBS)-washed conidia from potato dextrose agar (PDA)-grown cultures of *Cordyceps militaris* CM2 isolate. See legend of figure 5.4 for further details.

Figure 5.6: Fungal Agar Cultures Spores Injections – Fungal Emergence

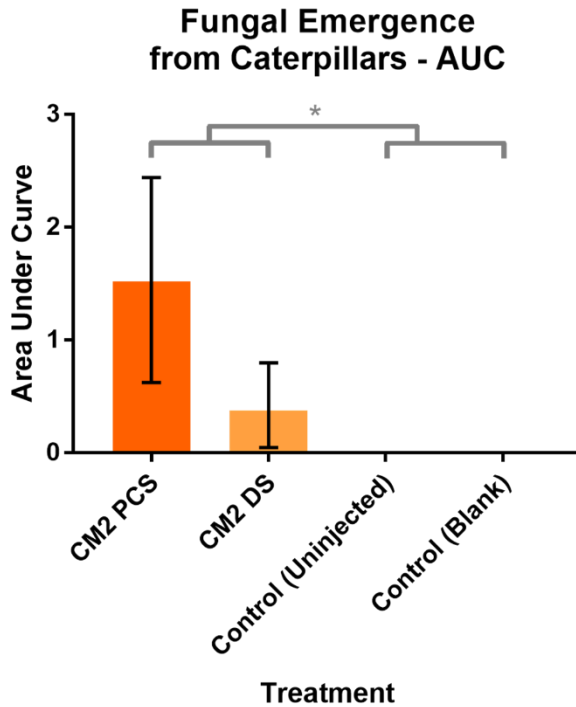
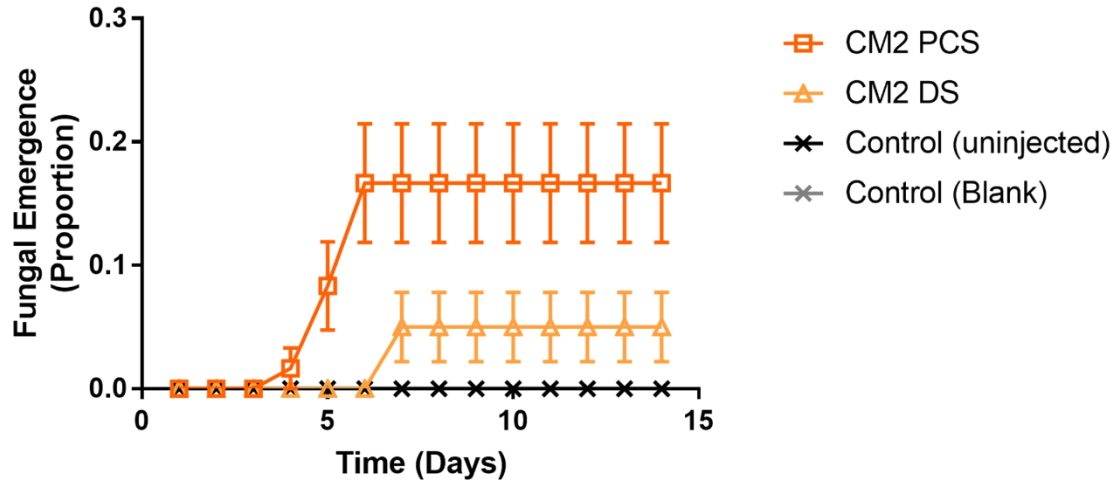


Figure 5.6: Proportions of fungal emergence observed in *Galleria mellonella* caterpillars following injections with phosphate-buffered saline (PBS)-washed conidia from potato dextrose agar (PDA)-grown cultures of *Cordyceps militaris* CM2 isolate. See legend of figure 5.4 for further details.

Figure 5.7: Fungal Liquid Cultures Spores Injections – Responsiveness

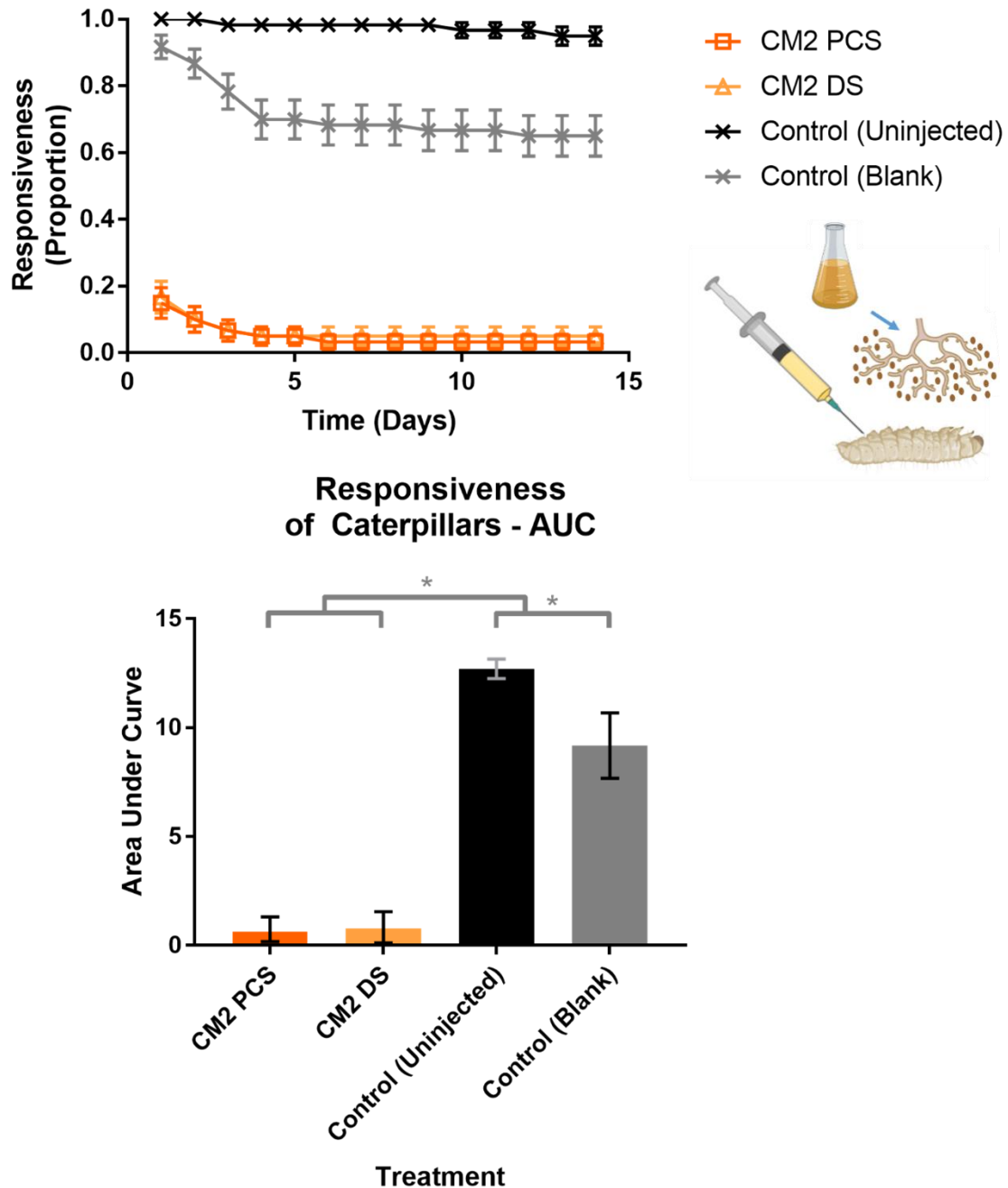


Figure 5.7: Proportions of responsiveness observed in *Galleria mellonella* caterpillars following injections with phosphate-buffered saline (PBS)-washed conidia from potato dextrose broth (PDB)-grown cultures of *Cordyceps militaris* CM2 isolate. Treatments of 100 μ L suspensions of 100,000 washed conidia in PBS from parental control (PCS) and degenerated (DS) strains were used, as well as blank injected (PBS) and uninjected controls. PCS = parental control strain; DS = degenerated strain. Error bars show 95% confidence intervals in both time course plots and area under the curve graphs. Asterisks (*) indicate significant differences between area under the curve means ($p < 0.05$). Sample size = 60 caterpillars.

Figure 5.8: Fungal Liquid Cultures Spores Injections – Melanisation

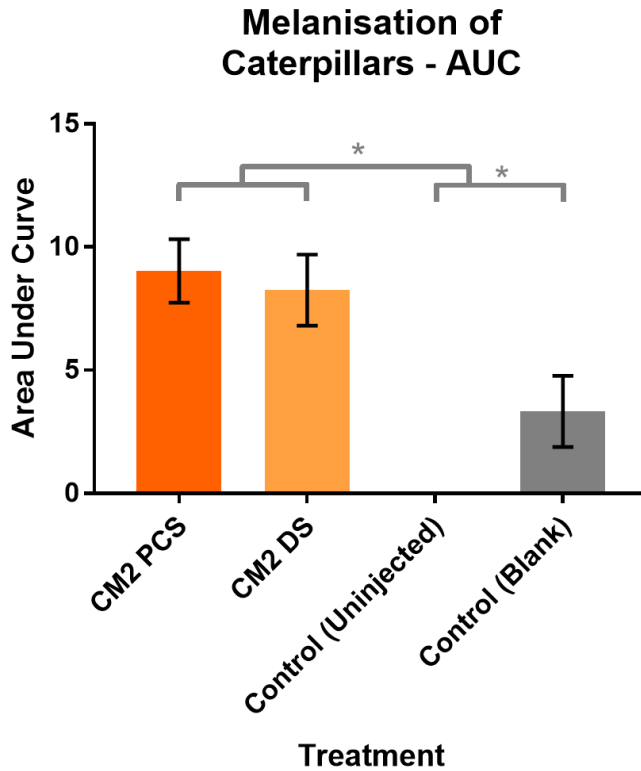
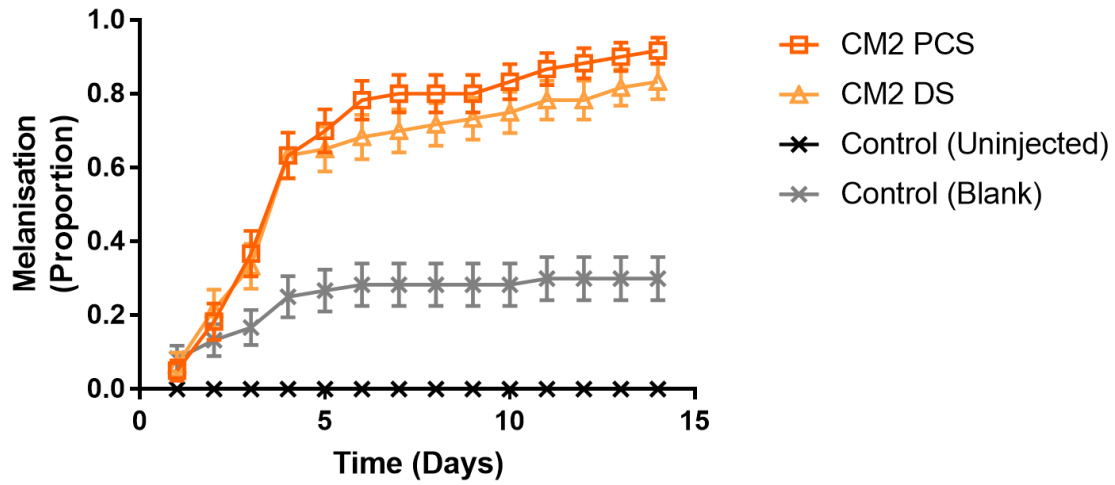


Figure 5.8: Proportions of full melanisation observed in *Galleria mellonella* caterpillars following injections with phosphate-buffered saline (PBS)-washed conidia from potato dextrose broth (PDB)-grown cultures of *Cordyceps militaris* CM2 isolate. See legend of figure 5.7 for further details.

Figure 5.9: Fungal Liquid Cultures Spores Injections – Fungal Emergence

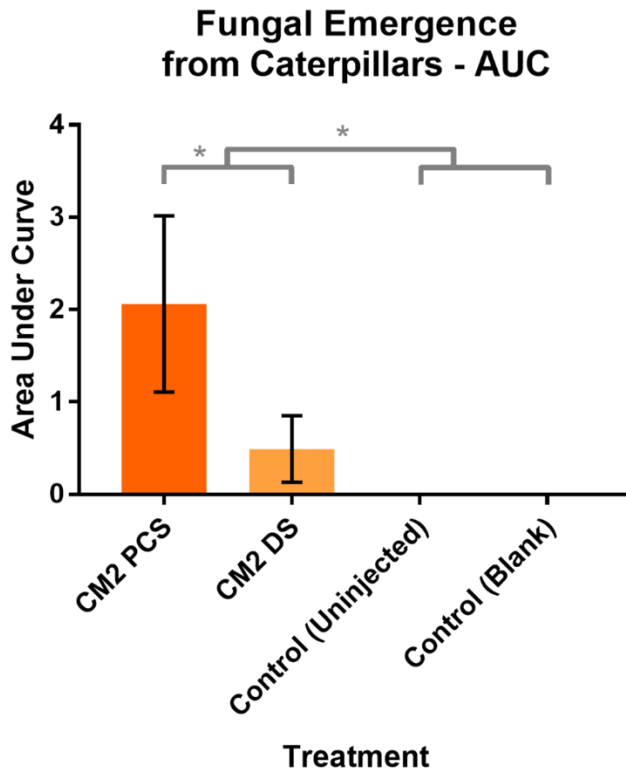
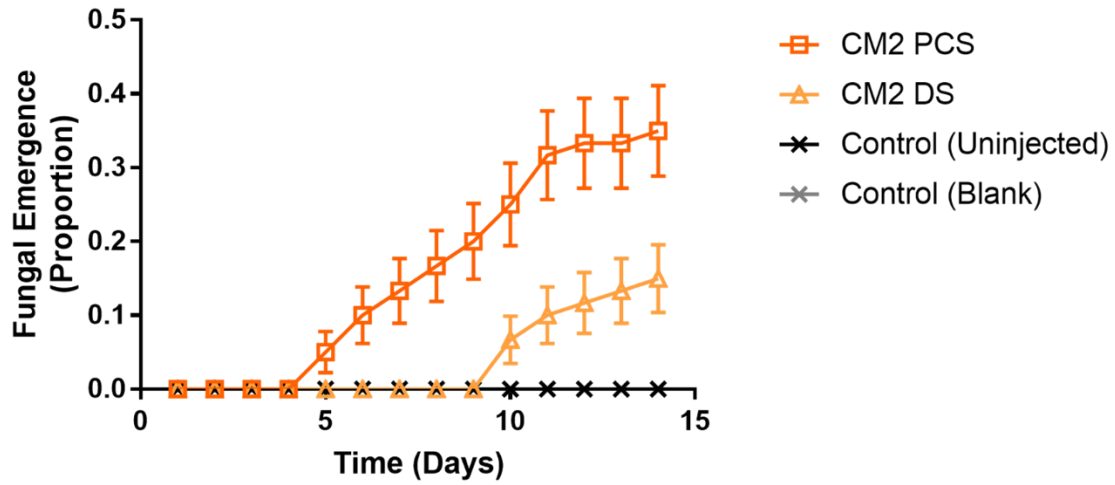


Figure 5.9: Proportions of fungal emergence observed in *Galleria mellonella* caterpillars following injections with phosphate-buffered saline (PBS)-washed conidia from potato dextrose broth (PDB)-grown cultures of *Cordyceps militaris* CM2 isolate. See legend of figure 5.7 for further details.

Figure 5.10: Fungal Liquid Cultures Spores and Extract Injections – Responsiveness

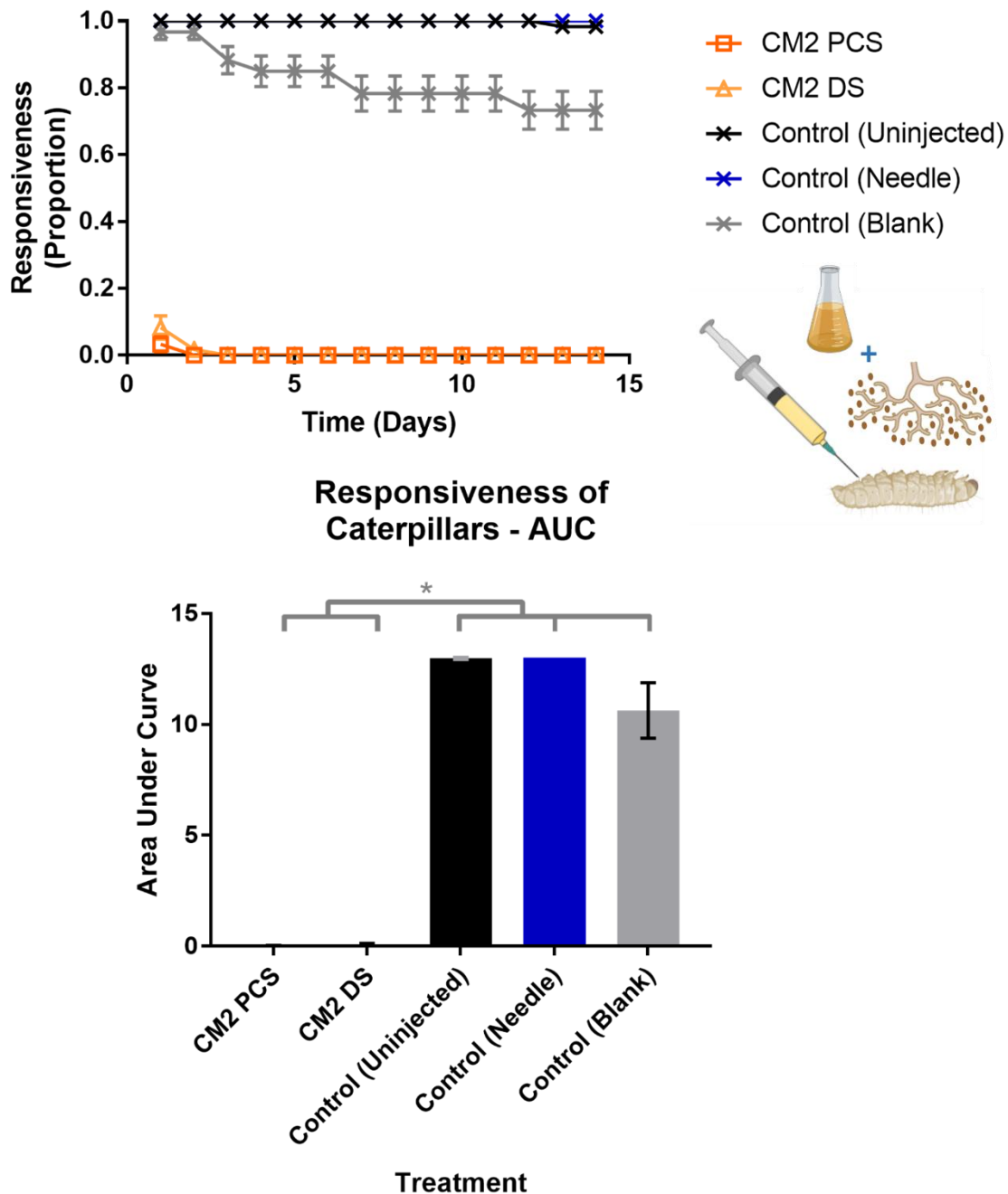


Figure 5.10: Proportions of responsiveness observed in *Galleria mellonella* caterpillars following injections with conidia and spent media from potato dextrose broth (PDB)-grown cultures of *Cordyceps militaris* CM2 isolate. Treatments of 100 μ L suspensions of 100,000 conidia in spent PDB from parental control (PCS) and degenerated (DS) strains were used, as well as blank injected (fresh PDA media only), needle-penetrated, and uninjected (no treatment) controls. PCS = parental control strain; DS = degenerated strain. Error bars show 95% confidence intervals in both time course plots and area under the curve graphs. Asterisks (*) indicate significant differences between area under the curve means ($p < 0.05$). Sample size = 60 caterpillars.

Figure 5.11: Fungal Liquid Cultures Spores and Extract Injections – Melanisation

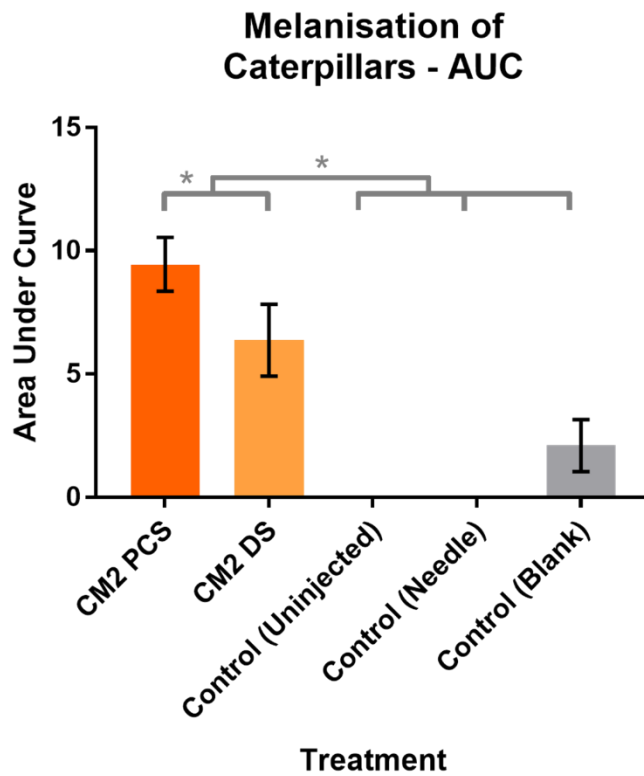
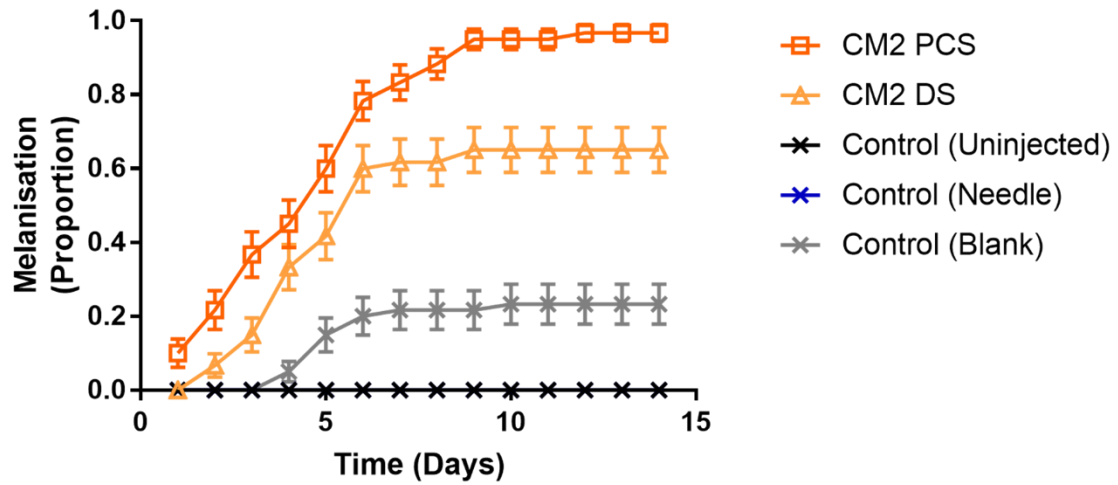
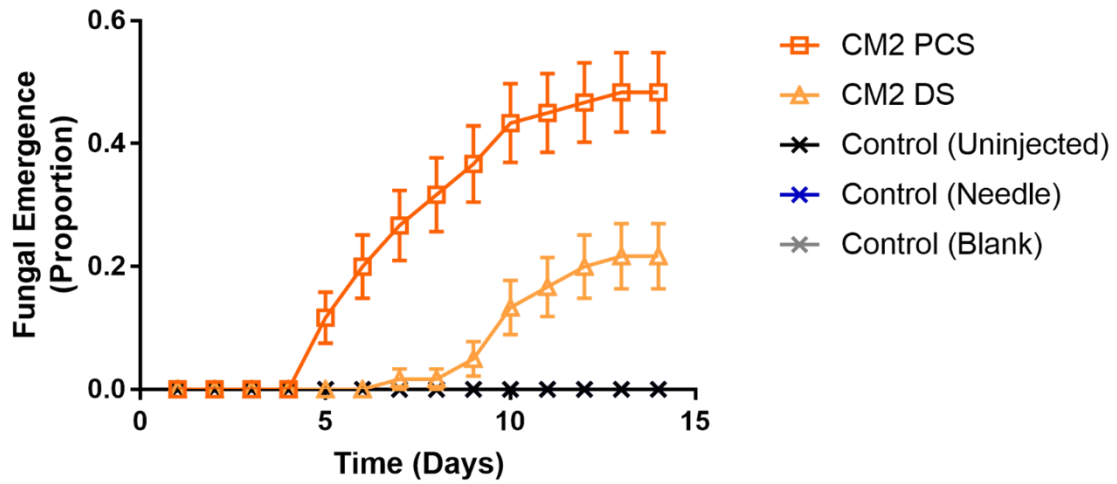


Figure 5.11: Proportions of full melanisation observed in *Galleria mellonella* caterpillars following injections with conidia and spent media from potato dextrose broth (PDB)-grown cultures of *Cordyceps militaris* CM2 isolate. See legend of figure 5.10 for further details.

Figure 5.12: Fungal Liquid Cultures Spores and Extract Injections – Fungal Emergence



Fungal Emergence from Caterpillars - AUC

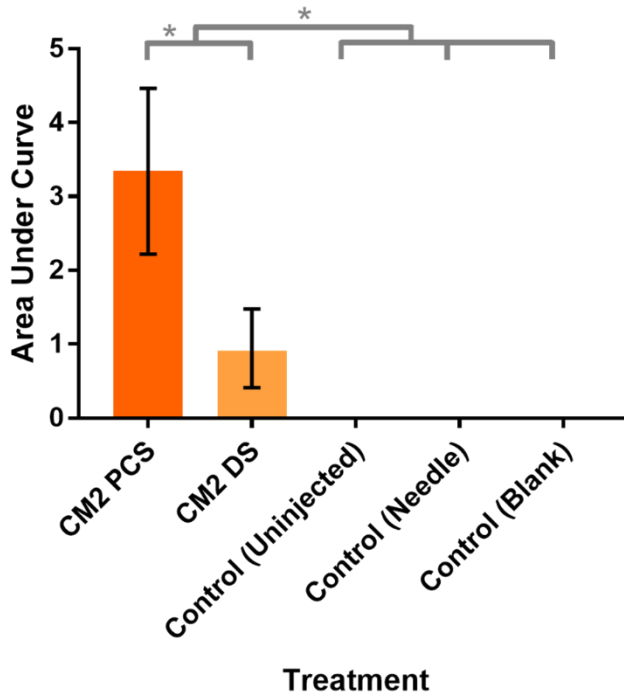


Figure 5.12: Proportions of fungal emergence observed in *Galleria mellonella* caterpillars following injections with conidia and spent media from potato dextrose broth (PDB)-grown cultures of *Cordyceps militaris* CM2 isolate. See legend of figure 5.10 for further details.

Figure 5.13.1: Fungal Liquid Cultures Spores and Pure Compounds Injections – Responsiveness

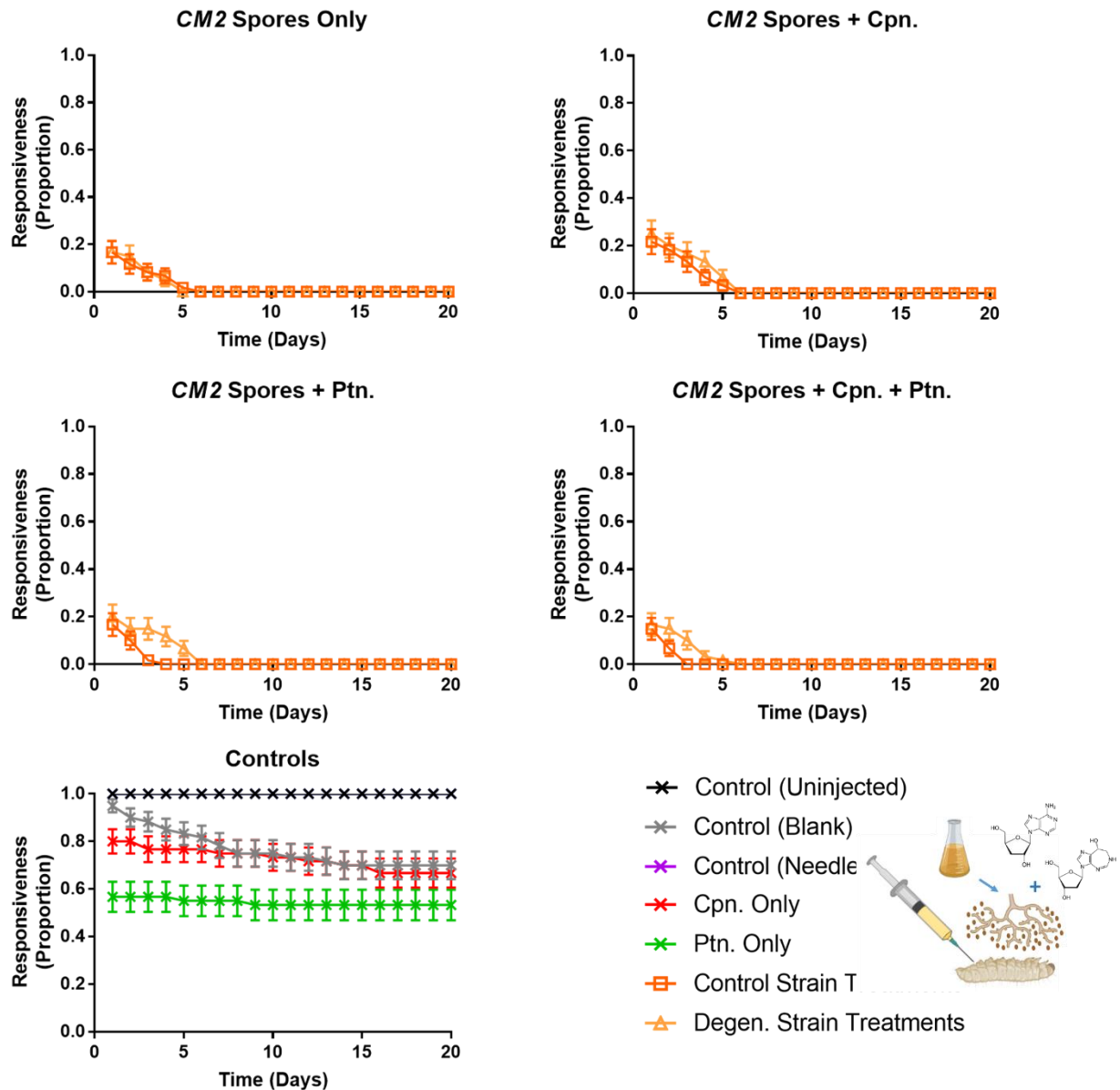


Figure 5.13.1: Proportions of responsiveness observed in *Galleria mellonella* caterpillars following injections with phosphate-buffered saline (PBS)-washed conidia from potato dextrose broth (PDB)-grown cultures of *Cordyceps militaris* CM2 isolate, supplemented with 50 μ M cordycepin (cpn.) and/or 1.5 nM pentostatin (ptn.). Treatments of 100 μ L suspensions of 1000 washed conidia in PBS from parental control (PCS) and degenerated (DS) strains were used in isolation, and with added cordycepin and/or pentostatin. There were also blank injected (PBS only), needle-penetrated, cordycepin in PBS, pentostatin in PBS, and uninjected controls. PCS = parental control strain; DS = degenerated strain. Error bars show 95% confidence intervals. Sample size = 60 caterpillars.

Figure 5.13.2: Fungal Liquid Cultures Spores and Pure Compounds Injections – Responsiveness (Area Under the Curve)

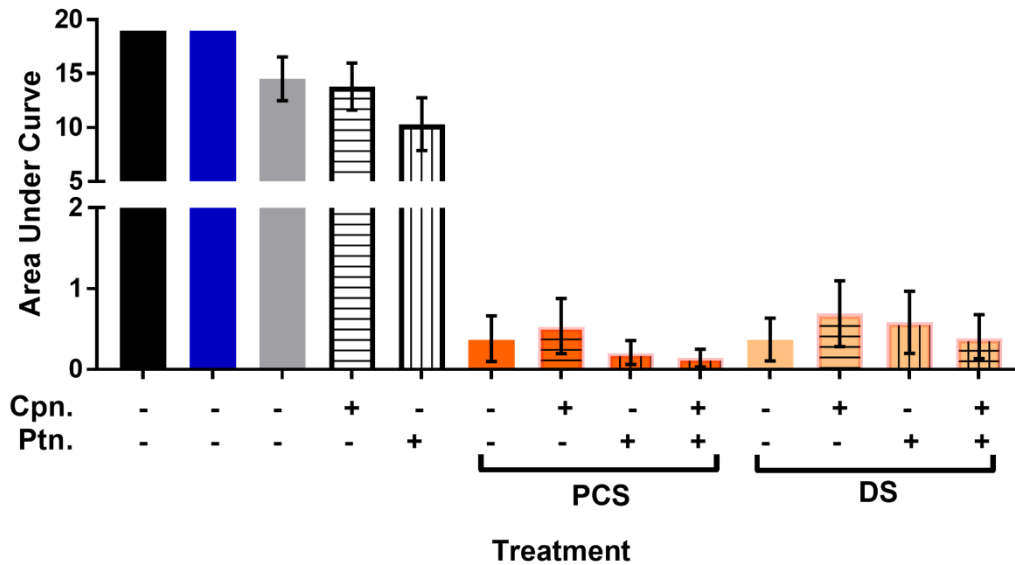


Figure 5.13.2: Proportions of responsiveness observed in *Galleria mellonella* caterpillars following injections with phosphate-buffered saline (PBS)-washed conidia from potato dextrose broth (PDB)-grown cultures of *Cordyceps militaris* CM2 isolate, supplemented with 50 μ M cordycepin (cpn.) and/or 1.5 nM pentostatin (ptn.) – area under the curve graph. Error bars show 95% confidence intervals. Asterisks (*) indicate significant differences between area under the curve means ($p < 0.05$). See legend of figure 5.13.1 for further details.

Figure 5.14.1: Fungal Liquid Cultures Spores and Pure Compounds Injections – Melanisation

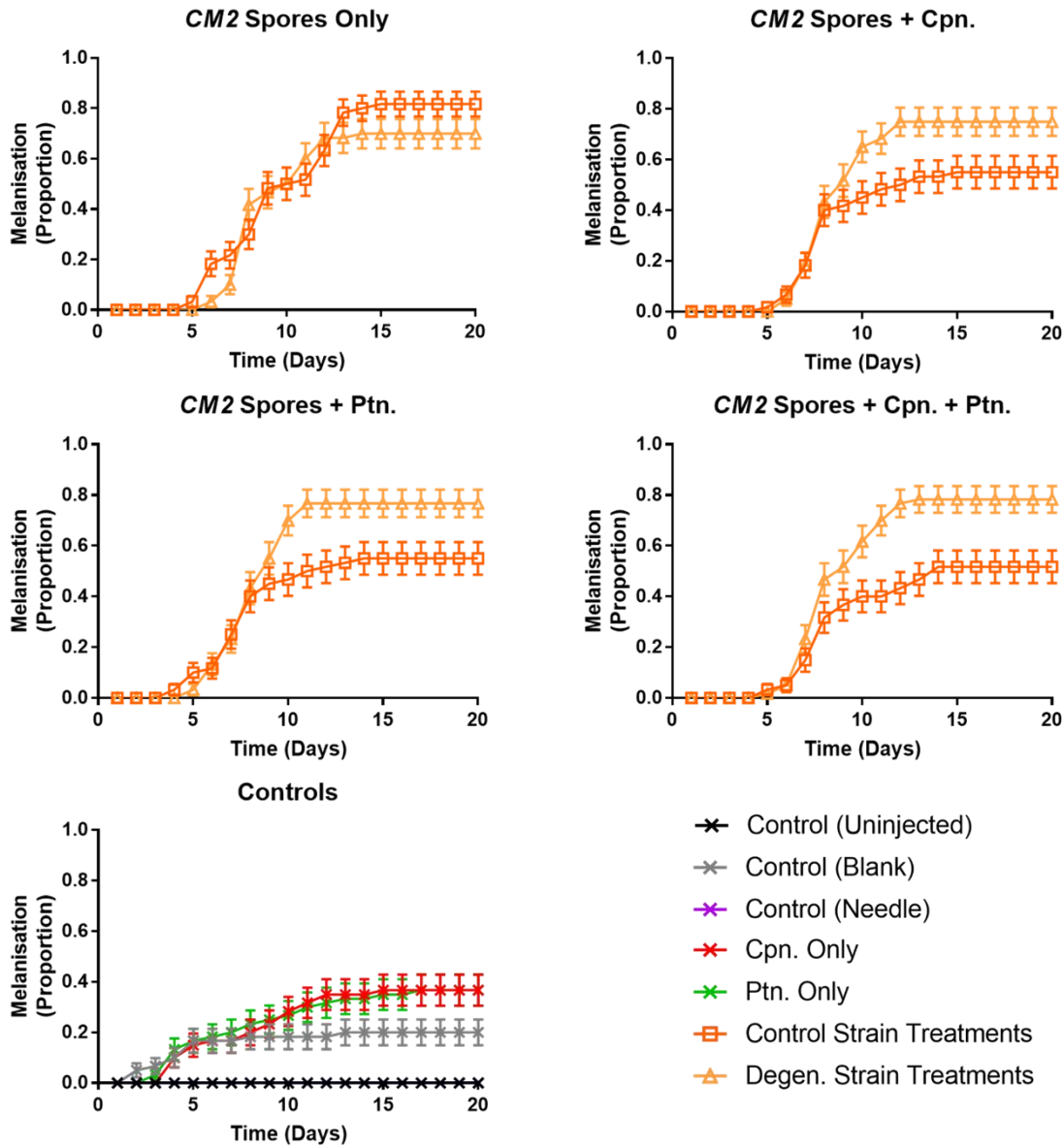


Figure 5.14.1: Proportions of full melanisation observed in *Galleria mellonella* caterpillars following injections with phosphate-buffered saline (PBS)-washed conidia from potato dextrose broth (PDB)-grown cultures of *Cordyceps militaris* CM2 isolate, supplemented with 50 μ M cordycepin (cpn.) and/or 1.5 nM pentostatin (ptn.). See legend of figure 5.13.1 for further details.

Figure 5.14.2: Fungal Liquid Cultures Spores and Pure Compounds Injections – Melanisation (Area Under the Curve)

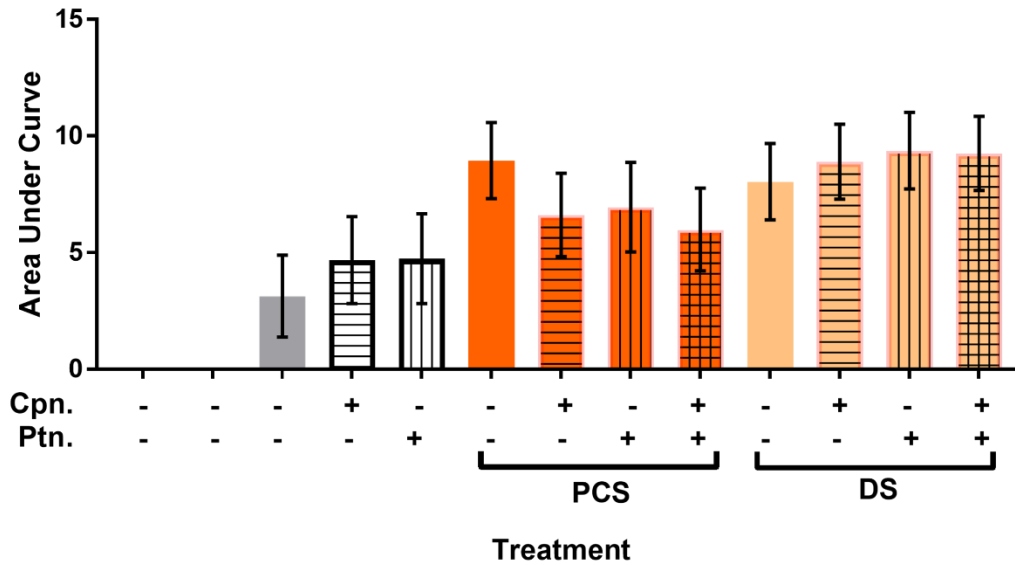


Figure 5.14.2: Proportions of full melanisation observed in *Galleria mellonella* caterpillars following injections with phosphate-buffered saline (PBS)-washed conidia from potato dextrose broth (PDB)-grown cultures of *Cordyceps militaris* CM2 isolate, supplemented with 50µM cordycepin (cpn.) and/or 1.5 nM pentostatin (ptn.) – area under the curve graph. See legend of figure 5.13.2 for further details.

Figure 5.15.1: Fungal Liquid Cultures Spores and Pure Compounds Injections – Fungal Emergence

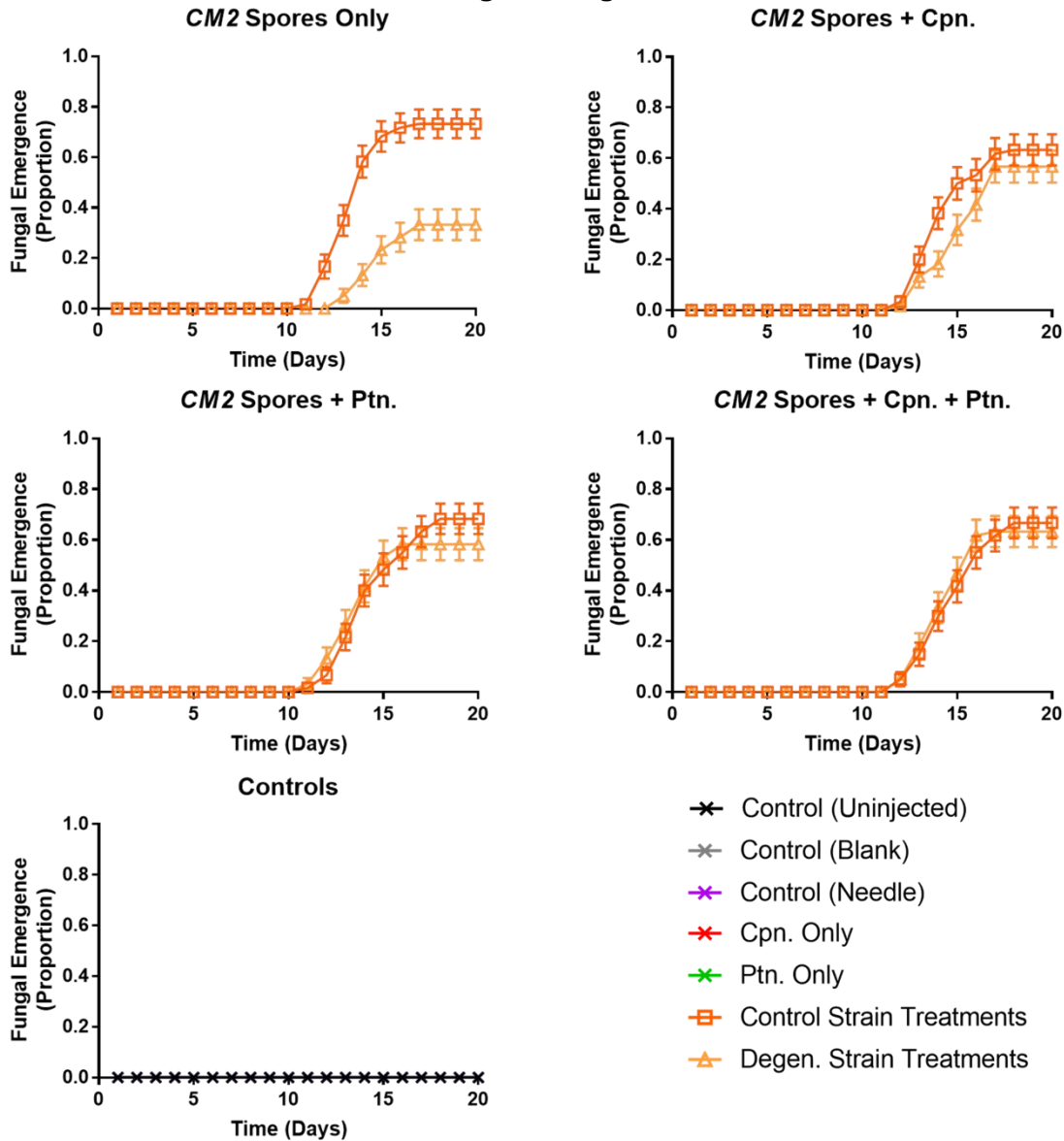


Figure 5.15.1: Proportions of fungal emergence observed in *Galleria mellonella* caterpillars following injections with phosphate-buffered saline (PBS)-washed conidia from potato dextrose broth (PDB)-grown cultures of *Cordyceps militaris* CM2 isolate, supplemented with 50 μ M cordycepin (cpn.) and/or 1.5 nM pentostatin (ptn.). See legend of figure 5.13.1 for further details.

Figure 5.15.2: Fungal Liquid Cultures Spores and Pure Compounds Injections – Fungal Emergence (Area Under the Curve)

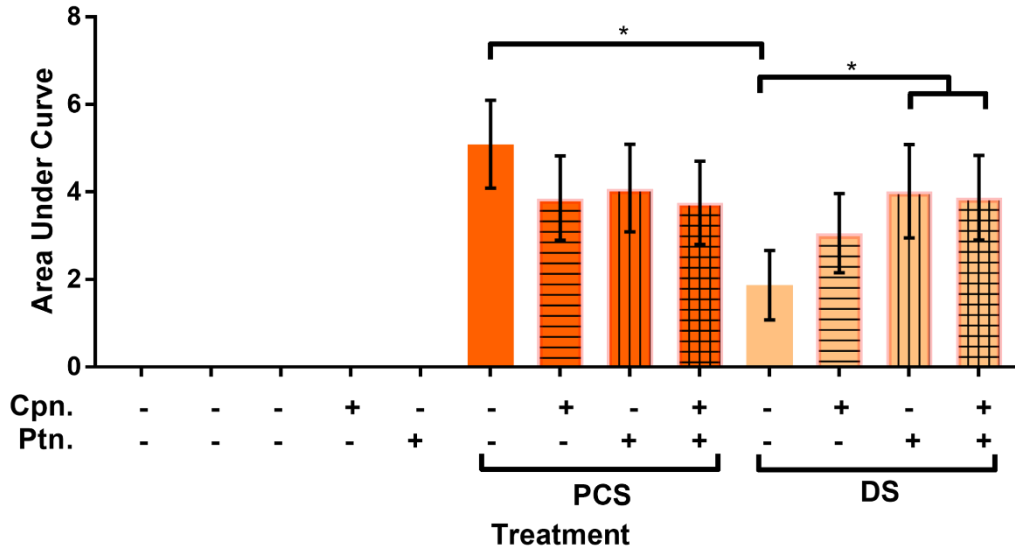


Figure 5.15.2: Proportions of fungal emergence observed in *Galleria mellonella* caterpillars following injections with phosphate-buffered saline (PBS)-washed conidia from potato dextrose broth (PDB)-grown cultures of *Cordyceps militaris* CM2 isolate, supplemented with 50µM cordycepin (cpn.) and/or 1.5 nM pentostatin (ptn.) – area under the curve graph. See legend of figure 5.13.2 for further details.

5.2 DISCUSSION

In the chapter 3, simultaneous decline in the production of secondary metabolites cordycepin and pentostatin, declines in other metabolites in purine metabolism and the citrate cycle, and decline in the expression of sexual development-related genes were demonstrated to occur with the degeneration of the *C. militaris* CM2 isolate following repeated subcultivation on PDA. The results in this chapter suggest that further to that, there is also a decline in the pathogenic response of the degenerated strain in the host – specifically in host response to infection (melanisation) and fungal virulence (fungal emergence from caterpillars). This was indicated by reduced proportions of *G. mellonella* caterpillars developing full melanisation and showing fungal hyphal emergence when subjected to the degenerated strain compared to the parental control strain. This reduced pathogenic response may be similar to the effects of strain attenuation in *Beauveria bassiana* and *Metarhizium anisopliae*, related entomopathogenic species which are used as bioinsecticides. Successive subcultivation in these species has resulted in reduced product viability of bioinsecticides, caused by a decline in virulence to model hosts [Safavi 2012; Ansari & Butt 2011]. There can be an array of factors affecting entomopathogenic fungal virulence [Chandler 2016].

Improved fungal growth of the degenerated strain was observed when washed spores were supplemented with both cordycepin and pentostatin, suggesting that these metabolites together may confer a pathogenic advantage to the fungus. This has been demonstrated in other studies. For example, reduced survival from *C. militaris* infections in both *G. mellonella* and silkworm (*Bombyx mori*) caterpillars were observed when cordycepin was introduced [Woolley *et al.* 2020; Kato *et al.* 2021]. There was also a pathogenic advantage for the non cordycepin-producing entomopathogenic species *B. bassiana* and *M. anisopliae* [Woolley *et al.* 2020; Kato *et al.* 2021]. One of these was published shortly before our paper [Wellham *et al.* 2021], also in the special edition of the Journal *Microorganisms* focusing on entomopathogenic fungi [Kato *et al.* 2021].

Considering the anti-inflammatory effects of cordycepin in mammalian cells, and the fact that the successful infection of a pathogen is often influenced by the ability to evade the host immune system [Schmid-Hempel 2009], we have hypothesised that cordycepin has a role in the repression of the immune system of the insect host [Wellham *et al.* 2019]. This is supported by the results of reduced expression of curdlan-stimulated immune genes *Attacin A* and *Lysozyme* in cordycepin-supplemented *Drosophila* S2 cells and injected *G. mellonella* caterpillars respectively. This corroborates with previous findings of reduced host immune genes by the addition of cordycepin in the same host models [Woolley *et al.* 2020]. Woolley *et al.* found reduced upregulation of immune gene *Metchnikowin* in *Drosophila* S2 cells stimulated with curdlan, and reduced upregulation of immune genes *Lysozyme*, *IMPI*, and *Gallerimycin* in *G. mellonella* caterpillars injected with *C. militaris* or *B. bassiana* spores – when supplemented with cordycepin [Woolley *et al.* 2020].

Pentostatin may also act to stabilise cordycepin in the insect host, enhancing its effect. This is suggested by the activity of a lower dose (10 μ M) of cordycepin supplemented with pentostatin in reducing the upregulation of *Attacin A* in the S2 cells – an effect which was not present in the treatment of the lower dose without pentostatin. This is consistent with the description of pentostatin as the protector molecule for cordycepin, with which it is co-produced from the same gene cluster [Xia *et al.* 2017].

These results suggest that the reduced pathogenic ability of the degenerated strain is at least partly due to reduced cordycepin and/or pentostatin production. More generally, there is evidence for the role of cordycepin in suppressing the immune system of the host, with the stabiliser pentostatin enhancing activity.

CHAPTER 6: FACTORS AFFECTING DEGENERATION OF CORDYCEPS MILITARIS AND REGENERATION ATTEMPTS

Several different attempts were made to find significant factors affecting degeneration in *Cordyceps militaris* and also attempts to reverse the process (regeneration). Efforts of the latter were assessed using treatments of the degenerated strain of the *CM2* isolate, and the former by treatments of the parental control strain. If successful, either of these findings could have important implications on *C. militaris* in biotechnology, as well as potential applications in understanding attenuation in other species. However, the attempts at regeneration were unsuccessful. These largely negative results are described here.

6.1 SERIAL SUBCULTURING

Given that the degenerated strain of the *CM2* isolate was attained, according to MycoMedica, by successive subcultivation over a long period of time, this process was investigated from scratch using the parental control strain. After successive subcultivation, subcultures 1-8 were compared by growth rates [figure 6.1], cordycepin and pentostatin production (subcultures 1, 2, 4, 6) [figure 6.2], and influence on the model host using *Galleria mellonella* caterpillar injection assays [figure 6.3; figure 6.4; figure 6.5]. In all cases, there were no significant differences detected between subcultures. There was no evidence of degeneration of the parental control strain or indication of reduced cordycepin production. Rates and levels of responsiveness, full melanisation, and fungal emergence were consistent across subcultures after caterpillars were injected with 1000 PBS-washed spores.

Radial Growth Rate – Serial Subculturing of CM2 Strains

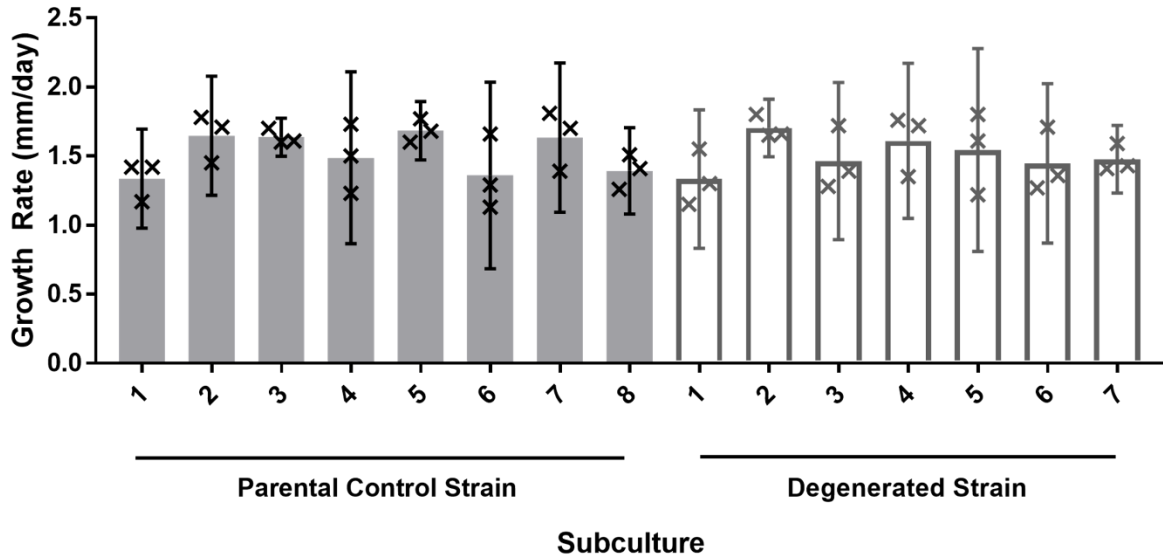


Figure 6.1: Radial growth rates of subcultures of CM2 parental control (grey bars) and degenerated (white bars) strains. Rates were based on measurements taken after 20 days of the growth of cultures on potato dextrose agar (PDA) plates, following serial subculturing. Error bars show 95% confidence intervals of means, from three biological replicates.

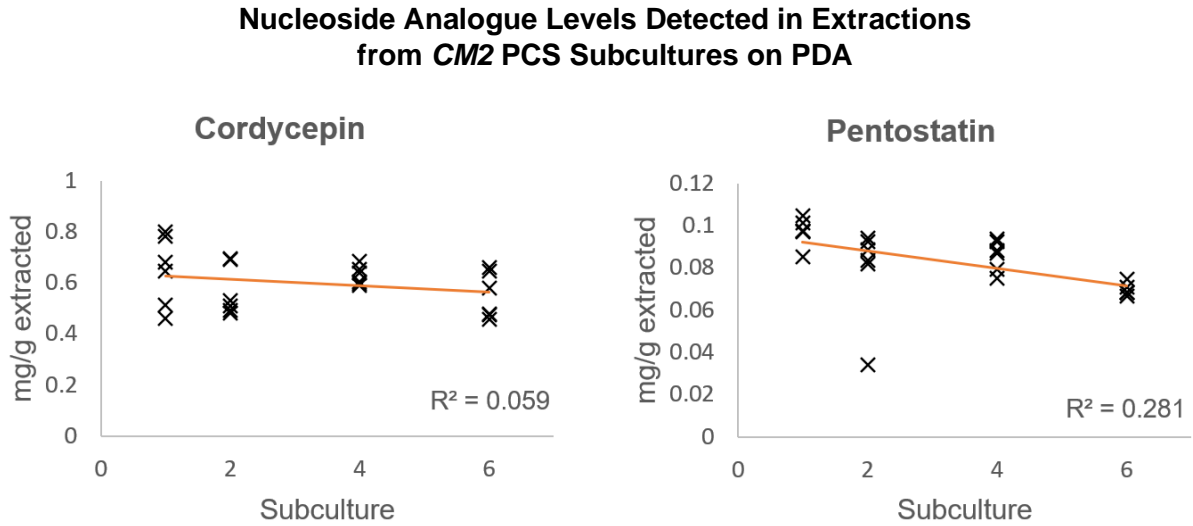


Figure 6.2: Cordycepin and pentostatin levels as detected in fungal extractions from subcultures of the parental control strain (PCS) of CM2 by targeted LC-MS analysis. Serial subculturing of the strain on PDA was performed, and extractions were taken from one week-old cultures. Six biological replicates are used, and linear trend line displayed.

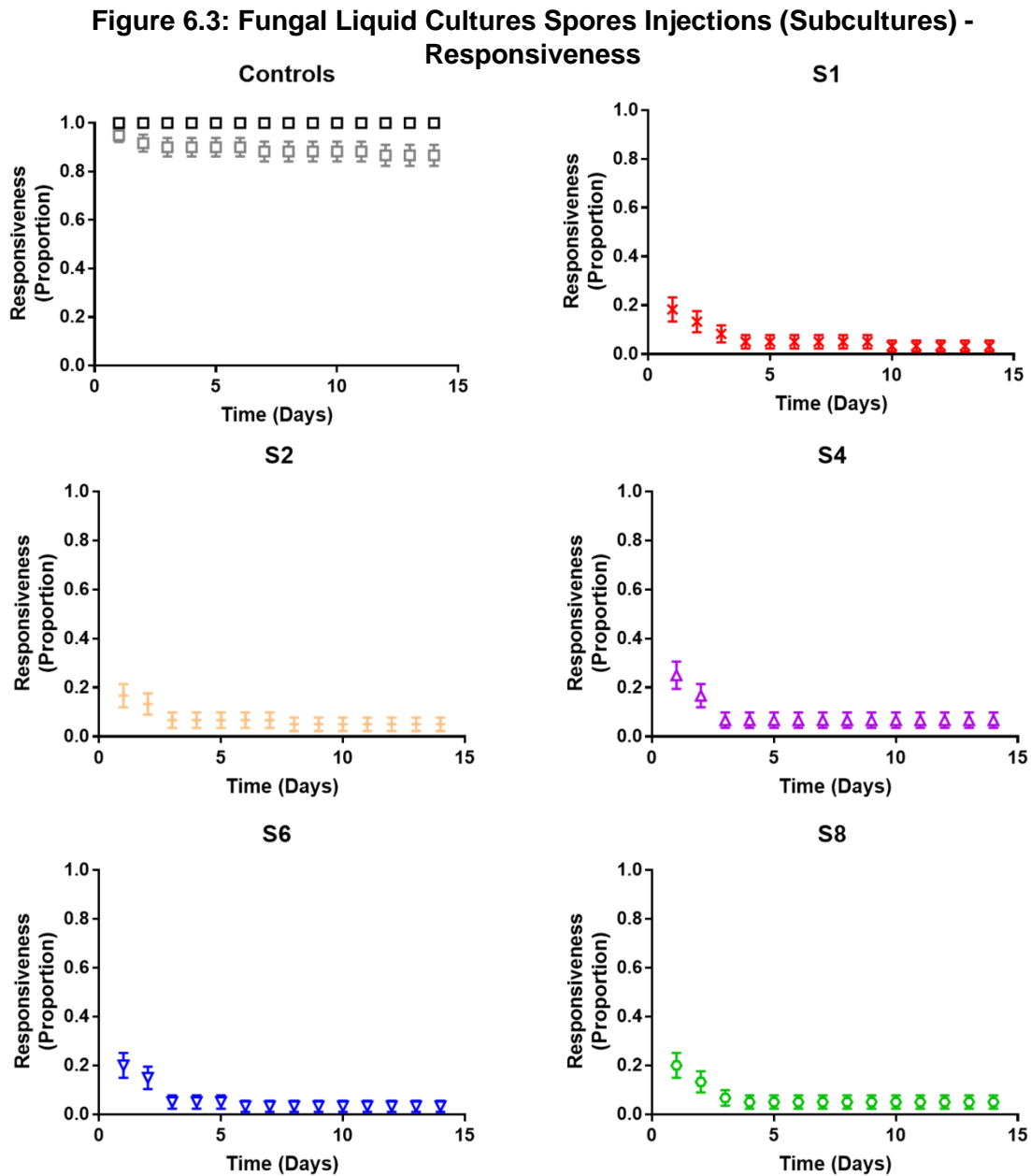


Figure 6.3: Proportions of responsiveness observed in *Galleria mellonella* caterpillars injected with washed spores from subcultures of the *CM2* parental control strain (PCS). Each caterpillar was injected with 1000 phosphate-buffered saline (PBS)-washed spores from four week-old potato dextrose broth (PDB) fungal cultures suspended in 100 μ L sterile PBS. 60 caterpillars in each treatment group were used, with observations recorded daily. Control treatments of no injection (uninjected, black), and PBS-only injected (blank, grey) were performed, along with injections of spores from the original PCS (S1), and strains obtained after serial subculturing on potato dextrose agar (S2, S4, S6, S8). Error bars show 95% confidence intervals, as calculated from the standard error values of proportions.

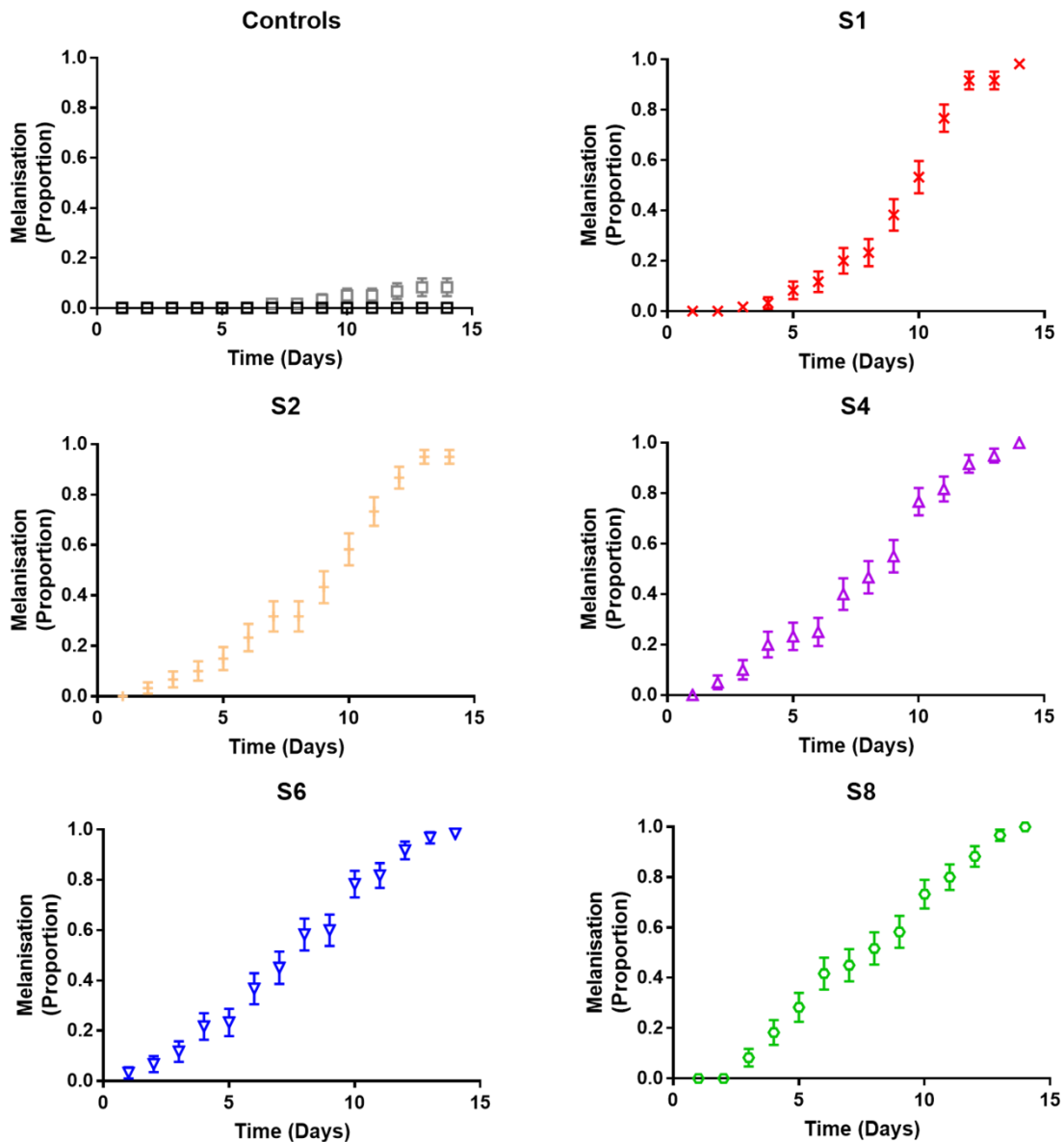
Figure 6.4: Fungal Liquid Cultures Spores Injections (Subcultures) - Melanisation

Figure 6.4: Proportions of full melanisation observed in *Galleria mellonella* caterpillars injected with washed spores from subcultures of the CM2 parental control strain (PCS). Each caterpillar was injected with 1000 phosphate-buffered saline (PBS)-washed spores from four week-old potato dextrose broth (PDB) fungal cultures suspended in 100 μ L sterile PBS. 60 caterpillars in each treatment group were used, with observations recorded daily. Control treatments of no injection (uninjected), and PBS-only injected (blank) were performed, along with injections of spores from the original PCS (S1), and strains obtained after serial subculturing on potato dextrose agar (S2, S4, S6, S8). Error bars show 95% confidence intervals, as calculated from the standard error values of proportions.

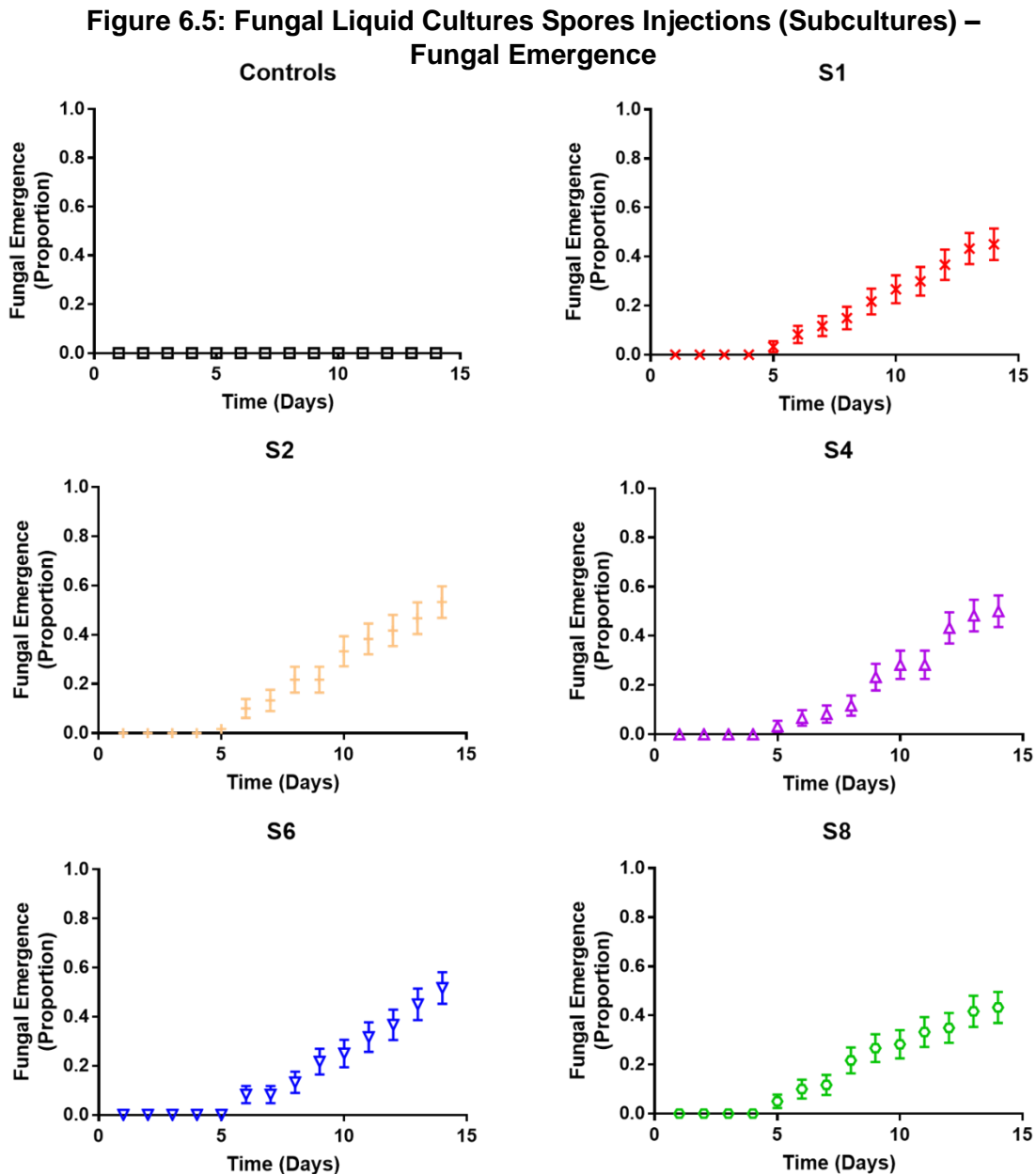


Figure 6.5: Proportions of fungal emergence observed in *Galleria mellonella* caterpillars injected with washed spores from subcultures of the *CM2* parental control strain (PCS). Each caterpillar was injected with 1000 phosphate-buffered saline (PBS)-washed spores from four week-old potato dextrose broth (PDB) fungal cultures suspended in 100 μ L sterile PBS. 60 caterpillars in each treatment group were used, with observations recorded daily. Control treatments of no injection (uninjected), and PBS-only injected (blank) were performed, along with injections of spores from the original PCS (S1), and strains obtained after serial subculturing on potato dextrose agar (S2, S4, S6, S8). Error bars show 95% confidence intervals, as calculated from the standard error values of proportions.

6.2 EXPOSURE TO THE HOST

Attention was turned to regeneration attempts with treatments to the degenerated strain of *CM2*. There were two strategies, both involving exposure of the fungus to the host. The rationale for this was to provoke a response in the fungus towards optimum behaviour for host infection. Given the hypothesis that cordycepin production aids host infection, and that reduced sexual development gene expression coincides with degeneration, exposure to the host was predicted to form a stimulus for the fungus to increase cordycepin production, potentially via regulatory processes involved in sexual changes as well. The host exposure strategies were (i) culturing on a host-based media type (silk pupa powder agar), and (ii) exposing to the live host via injection into *Galleria mellonella* caterpillars and subsequent extraction and culture on agar.

6.2.1 Cultures on Silk Pupa Powder Agar (SPPA)

To test the short term effects of growth on a host-based media type, parental control (PCS) and degenerated (DS) strain cultures grown on potato dextrose agar (PDA) and silk pupa powder agar (SPPA) were compared. Growth on SPPA did not increase cordycepin or pentostatin production in either strain [figure 6.6], and conversely there was a slight decrease on SPPA in cordycepin production by PCS. Untargeted LC-MS analysis was also performed to detect early indications of changes to the degenerated state of DS, using methods described earlier in chapter 3. Relatively few metabolites were significantly-changed in levels between the PDA and SPPA-grown cultures of DS – only a total of 36 identified and putatively-identified metabolites [figure 6.7; figure 6.8; table 6.1]. Distinct metabolic profiles of these two groups of samples are shown in figure 6.9, mostly due to downregulated metabolites in the SPPA samples [figure 6.8]. RT-qPCR analyses conducted in the same way as described in chapter 3 showed no significant differences between samples of the degenerated strain cultures on PDA and SPPA – but downregulation of *Cns1* and *VosA* in PCS cultures on SPPA [figure 6.10; figure 6.11]. It appears that culturing on SPPA has had little effect on the degenerated strain and a slightly negative effect on the parental control strain.

The degenerated strain was subcultured on SPPA over several passages in order to assess longer term effects of culture on this media type. DS subcultures 1-7 on the media were compared for cordycepin and pentostatin production [figure 6.12] as well as expression of cordycepin/pentostatin biosynthesis cluster genes (*Cns1-4*) [figure 6.13] and sexual development-related genes (*VeA*, *VosA*, *SteA*) [figure 6.14]. There were no significant changes detected.

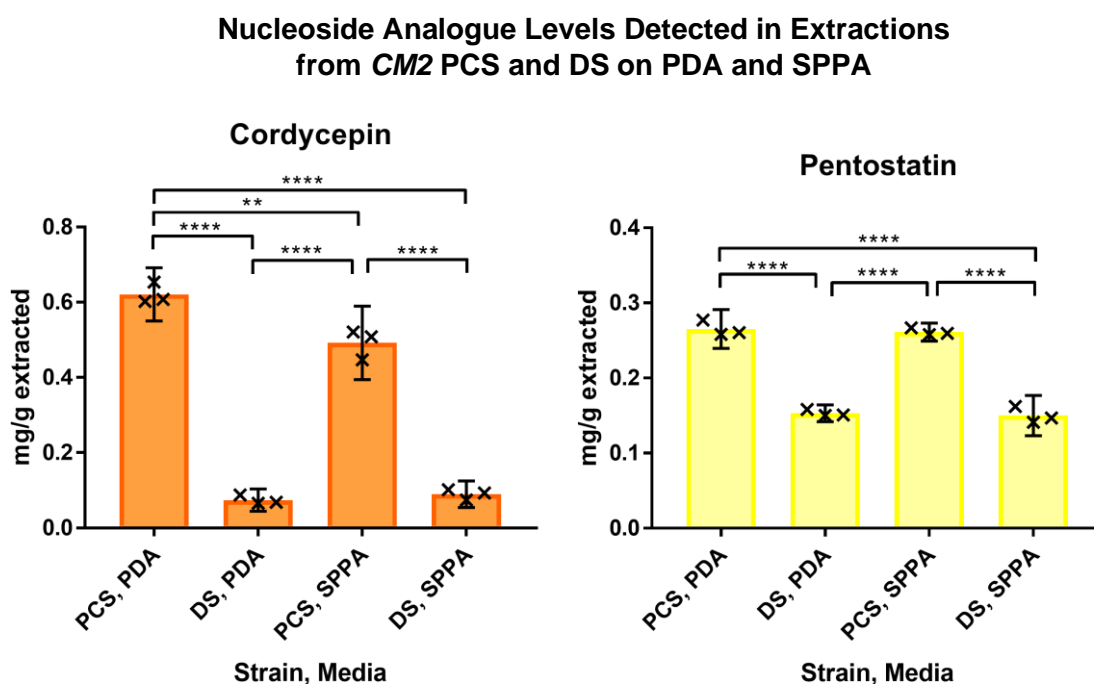


Figure 6.6: Cordycepin and pentostatin levels as detected in fungal extractions from subcultures of the parental control (PCS) and degenerated (DS) strains of *CM2* grown on potato dextrose agar (PDA) and silk pupa powder agar (SPPA) by targeted LC-MS analysis. Extractions were taken from one week-old cultures. Three biological replicates are used, with error bars showing 95% confidence intervals.

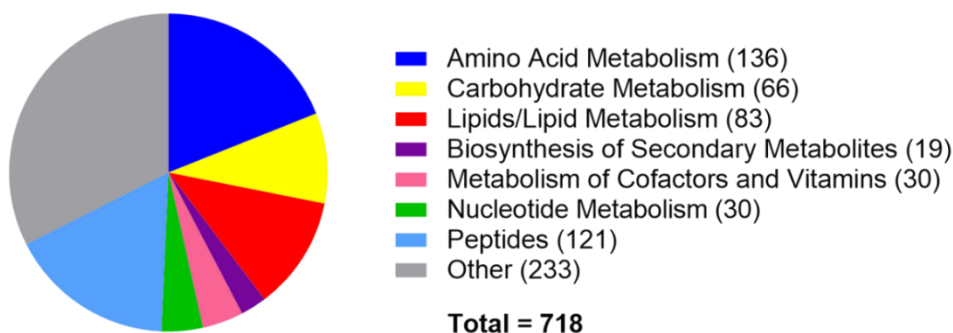
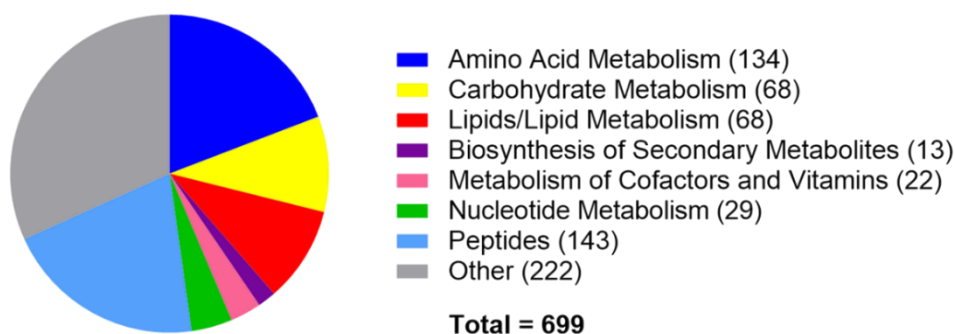
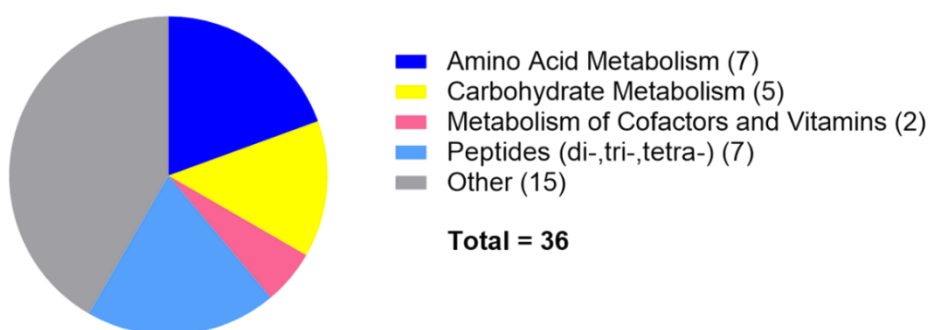
Fig. 6.7.1 Total Metabolites Detected: DS on PDA**Fig. 6.7.2 Total Metabolites Detected: DS on SPPA****Fig. 6.7.3 Significantly-Different Metabolites: DS on PDA vs. SPPA**

Figure 6.7: Total metabolites (Level 1 and 2 identification) detected in an untargeted LC-MS run of extracts from *CM2* degenerated control strain (DS) on potato dextrose agar (PDA) and silk pupa powder agar (SPPA). Other data from this LC-MS run are shown in chapter 3 (figures 3.7, 3.8). Metabolites were extracted from fungal material. There were seven biological replicates, taken from separate agar plates. Untargeted data was processed using XCMS, MzMatch, and IDEOM. Identification of metabolites (Level 1 identification) was achieved using accurate mass and retention time based on authentic standards. Putative identification of metabolites (Level 2 identification) was achieved using accurate mass and predicted retention times without the use of standards. Significantly-different metabolites (fig. 5.7.3) were determined using t-tests with false discovery rate (FDR) corrections and having VIP values > 1 following orthogonal partial least squares-discriminant analysis (OPLS-DA) using SIMCA-P (v4) software.

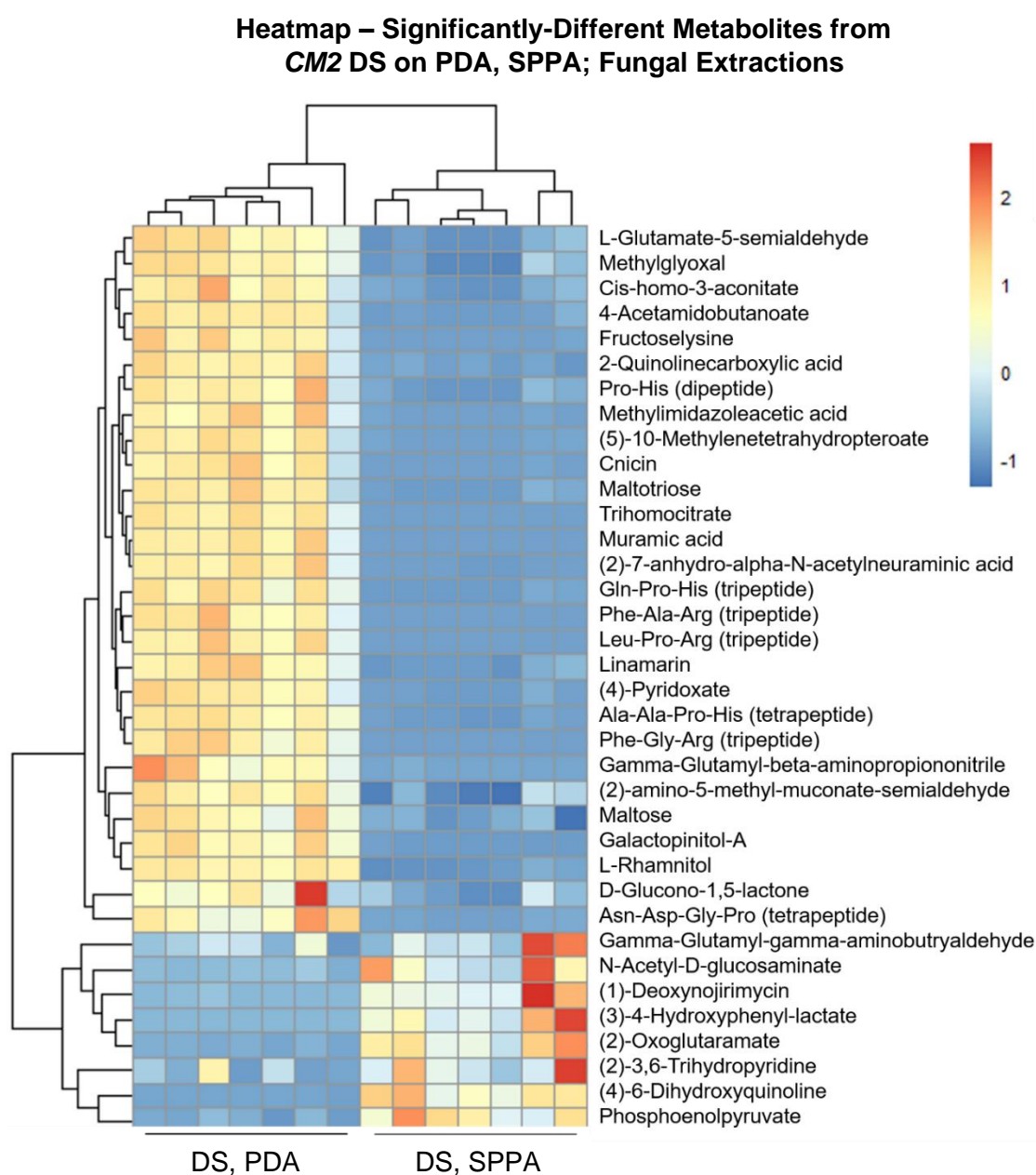


Figure 6.8: Heatmap featuring significantly-different metabolites in an untargeted LC-MS run of extracts from *CM2* degenerated strain (DS) cultures on potato dextrose agar (PDA) and silk pupa powder agar (SPPA). Significantly-different metabolites were determined using t-tests with false discovery rate (FDR) corrections and having VIP values > 1 following orthogonal partial least squares-discriminant analysis (OPLS-DA) using SIMCA-P (v4) software. Concentrations were transformed prior to heatmap construction using a logarithm with base 10. This figure was produced using R version 4.0.0 software, with the pheatmap package. See legend of figure 6.7 for further details.

Table 6.1: Significantly-different metabolites (Level 1 and 2 identification) detected from untargeted LC-MS run of extracts from CM2 degenerated strain cultures on potato dextrose agar and silk pupa powder agar. Metabolite classes: AAM (amino acid metabolism), CM (carbohydrate metabolism), MCF (metabolism of cofactors), NM (nucleotide metabolism), and peptides.

<i>m/z</i>	Metabolite	Class	Pathway
131.0582	L-Glutamate 5-semialdehyde	AAM	Arginine and proline metabolism
145.0739	4-Acetamidobutanoate	AAM	Arginine and proline metabolism
157.0851	Methylimidazoleacetic acid	AAM	Histidine metabolism
161.0477	4,6-Dihydroxyquinoline	AAM	Tryptophan metabolism
204.04	3-(4-Hydroxyphenyl)lactate	AAM	Tyrosine metabolism
216.1111	gamma-Glutamyl-gamma-aminobutyraldehyde	AAM	Arginine and proline metabolism
145.0375	2-Oxoglutaramate	AAM	Alanine, aspartate and glutamate metabolism
178.0477	D-Glucono-1,5-lactone	CM	Pentose phosphate pathway
504.1698	Maltotriose	CM	glycogen degradation I
167.9823	Phosphoenolpyruvate	CM	Glycolysis/Gluconeogenesis__Citrate cycle (TCA cycle)__Pyruvate metabolism__Glycerolipid metabolism__Purine metabolism__Pyrimidine metabolism
342.1165	Maltose	CM	Glycolysis/Gluconeogenesis__Starch and sucrose metabolism__amino sugar and nucleotide sugar metabolism
72.02095	Methylglyoxal	CM	Pyruvate metabolism__propanoate metabolism
183.0532	4-Pyridoxate	MCF	Vitamin B6 metabolism
216.0634	cis-(homo)3aconitate	MCF	coenzyme B biosynthesis
293.1477	Pro-His	Peptides	
394.1958	Ala-Ala-Pro-His	Peptides	
401.1537	Asn-Asp-Gly-Pro	Peptides	
380.1799	Gln-Pro-His	Peptides	
392.2164	Phe-Ala-Arg	Peptides	
406.2319	Leu-Pro-Arg	Peptides	
378.2007	Phe-Gly-Arg	Peptides	
<i>Unspecified class metabolites:</i>			
<i>m/z</i>	Metabolite	<i>m/z</i>	Metabolite
247.1057	Linamarin	291.0956	2,7-Anhydro-alpha-N-acetylneuraminic acid
308.1586	Fructoselysine	327.1321	5,10-methylenetetrahydropteroate
356.1321	galactopinitol A	173.0478	2-Quinolinecarboxylic acid
155.0582	2-amino-5-methyl-muconate semialdehyde	378.1682	Cnicin
163.0844	1-deoxynojirimycin	127.027	2,3,6-Trihydroxypyridine
166.084	L-rhamnitol	199.0957	gamma-Glutamyl-beta-aminopropionitrile
234.074	trihomocitrate	291.0956	2,7-Anhydro-alpha-N-acetylneuraminic acid
237.0849	N-Acetyl-D-glucosaminiate	327.1321	5,10-methylenetetrahydropteroate
251.1005	Muramic acid	173.0478	2-Quinolinecarboxylic acid

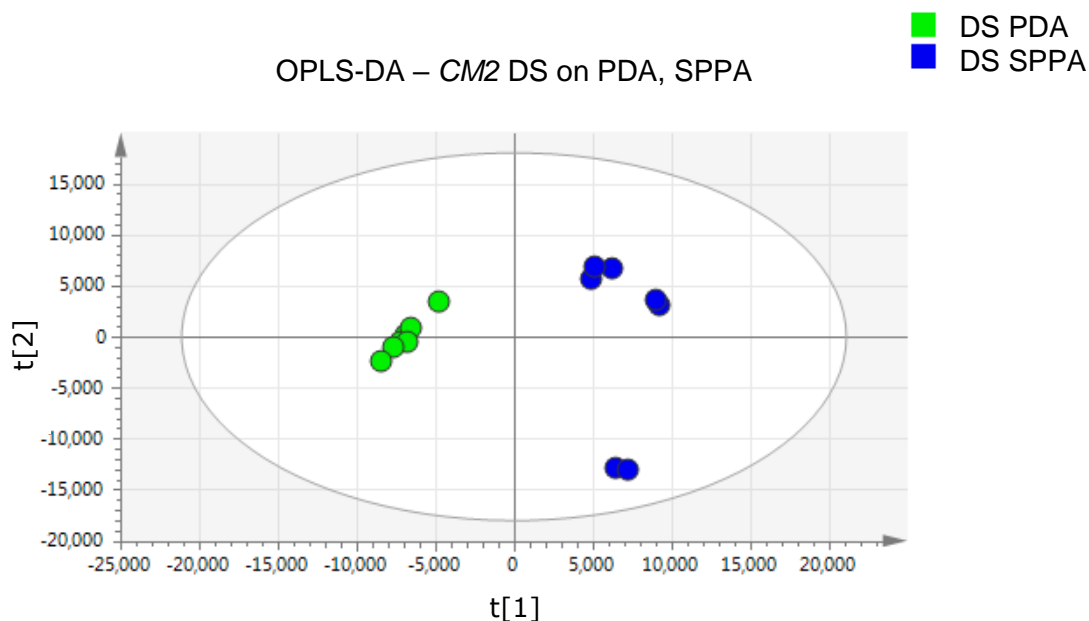


Figure 6.9: Orthogonal partial least squares-discriminant analysis (OPLS-DA) plots for an untargeted LC-MS run of extracts from CM2 degenerated strain (DS) cultures on potato dextrose agar (PDA) and silk pupa powder agar (SPPA). Other multivariate analysis plots from this same LC-MS run are shown in chapter 3 (figure 3.9). Metabolites were extracted from fungal material. There were seven biological replicates, taken from separate agar plates. These multivariate analyses are based upon relative concentrations of all identified and putatively-identified metabolites (Levels 1 and 2 identification) following XCMS, MzMatch, and IDEOM processing of data. These figures were produced using SIMCA-P (v4) software.

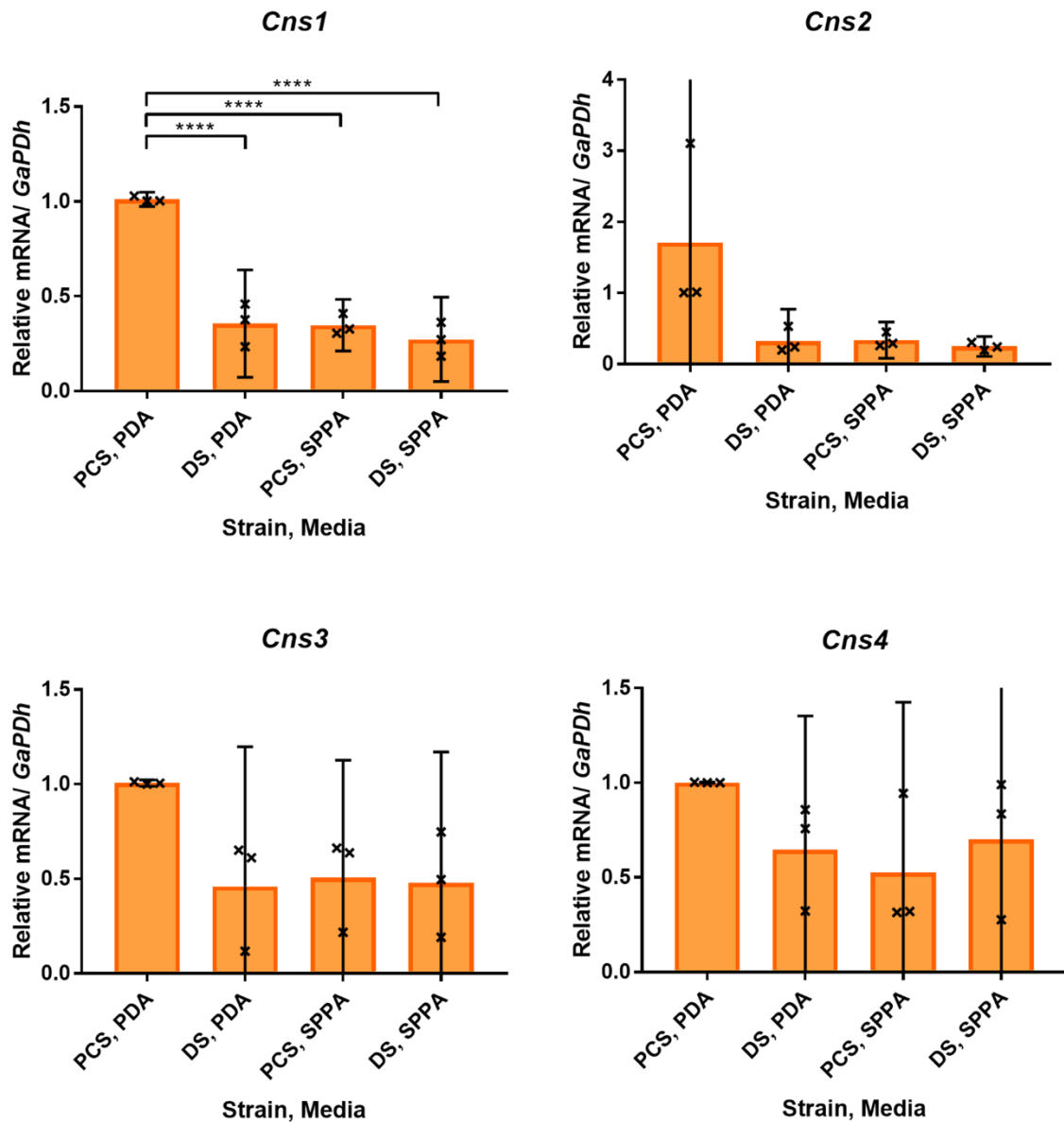
Gene Expression in *CM2* PCS and DS Cultures on PDA and SPPA – *Cns* Genes

Figure 6.10: Relative mRNA levels of cordycepin/pentostatin biosynthesis cluster (*Cns*) genes in parental control (PCS) and degenerated (DS) strains of *CM2* on potato dextrose agar (PDA) and silk pupa powder agar (SPPA). Gene expression was normalised against the expression of the control gene *Gapdh*. Error bars show 95% confidence intervals, and labels show differences between means as calculated using t-tests with Bonferroni corrections. * $p < 0.05$; ** $p < 0.01$; *** $p < 0.001$; **** $p < 0.0001$. Three biological replicates, with each point representing an average of three technical replicates are shown.

Gene Expression in CM2 PCS and DS Cultures on PDA and SPPA – Sexual Development-Related Genes

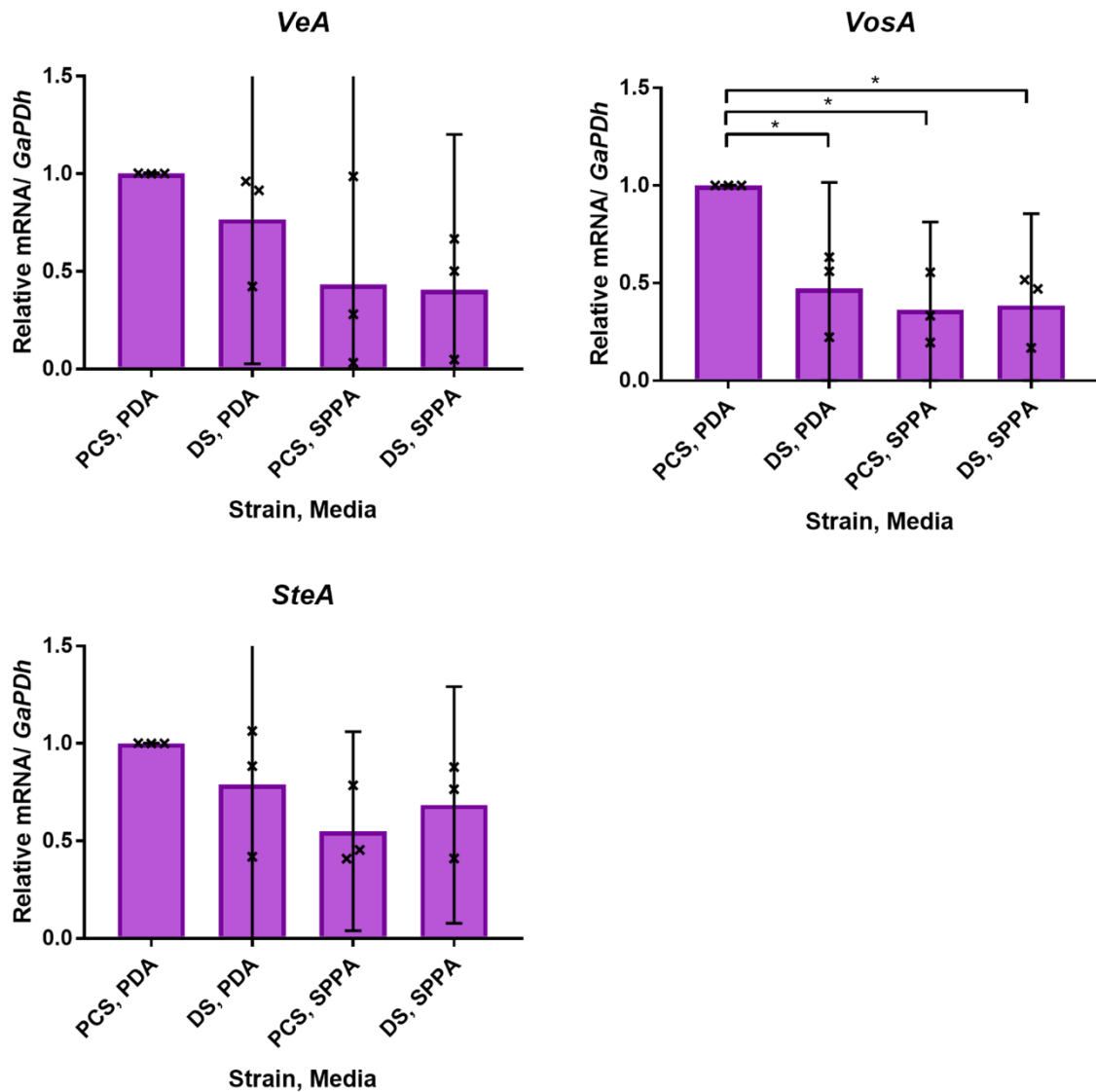


Figure 6.11: Relative mRNA levels of sexual development-related genes (*VeA*, *VosA*, *SteA*) in parental control (PCS) and degenerated (DS) strains of *CM2* on potato dextrose agar (PDA) and silk pupa powder agar (SPPA). Gene expression was normalised against the expression of the control gene *Gapdh*. Error bars show 95% confidence intervals, and labels show differences between means as calculated using t-tests with Bonferroni corrections. * $p < 0.05$. Three biological replicates, with each point representing an average of three technical replicates are shown.

Nucleoside Analogue Levels Detected in Extractions from *CM2* PCS and Subcultures of DS on SPPA

Fig. 6.12.1

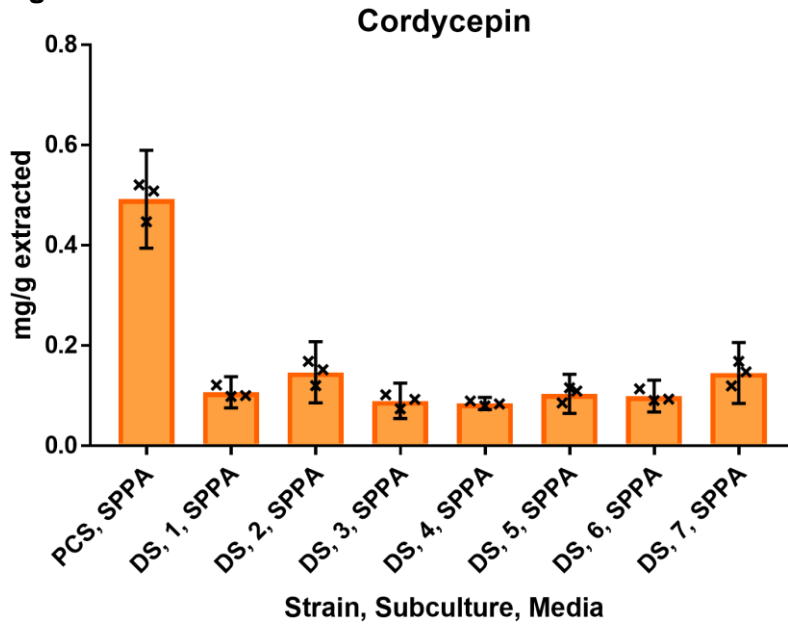


Fig. 6.12.2

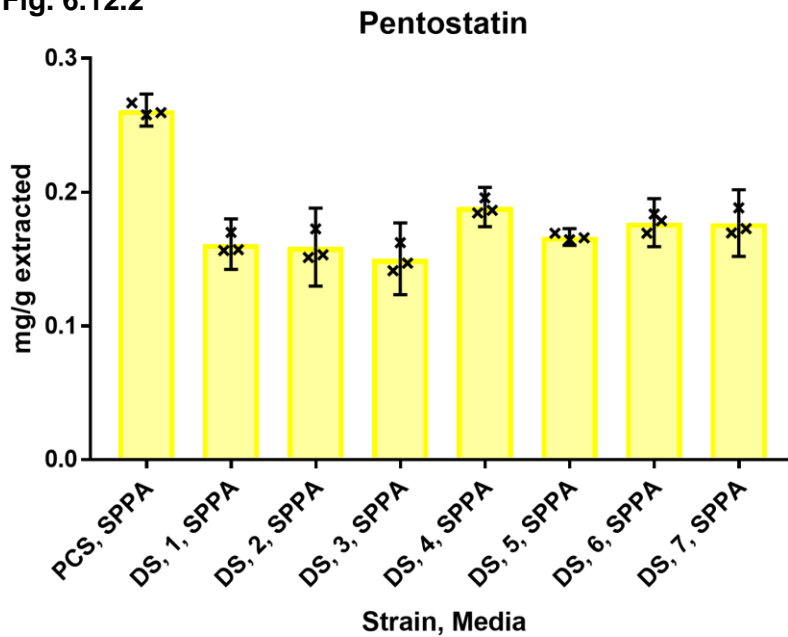


Figure 6.12: Cordycepin and pentostatin levels as detected in fungal extractions from the parental control strain (PCS) and subcultures of the degenerated strain (DS) of *CM2* on silk pupa powder agar (SPPA) by targeted LC-MS analysis. Serial subculturing of the degenerated strain on SPPA was performed, and extractions were taken from one week-old cultures. Three biological replicates are used, with error bars showing 95% confidence intervals.

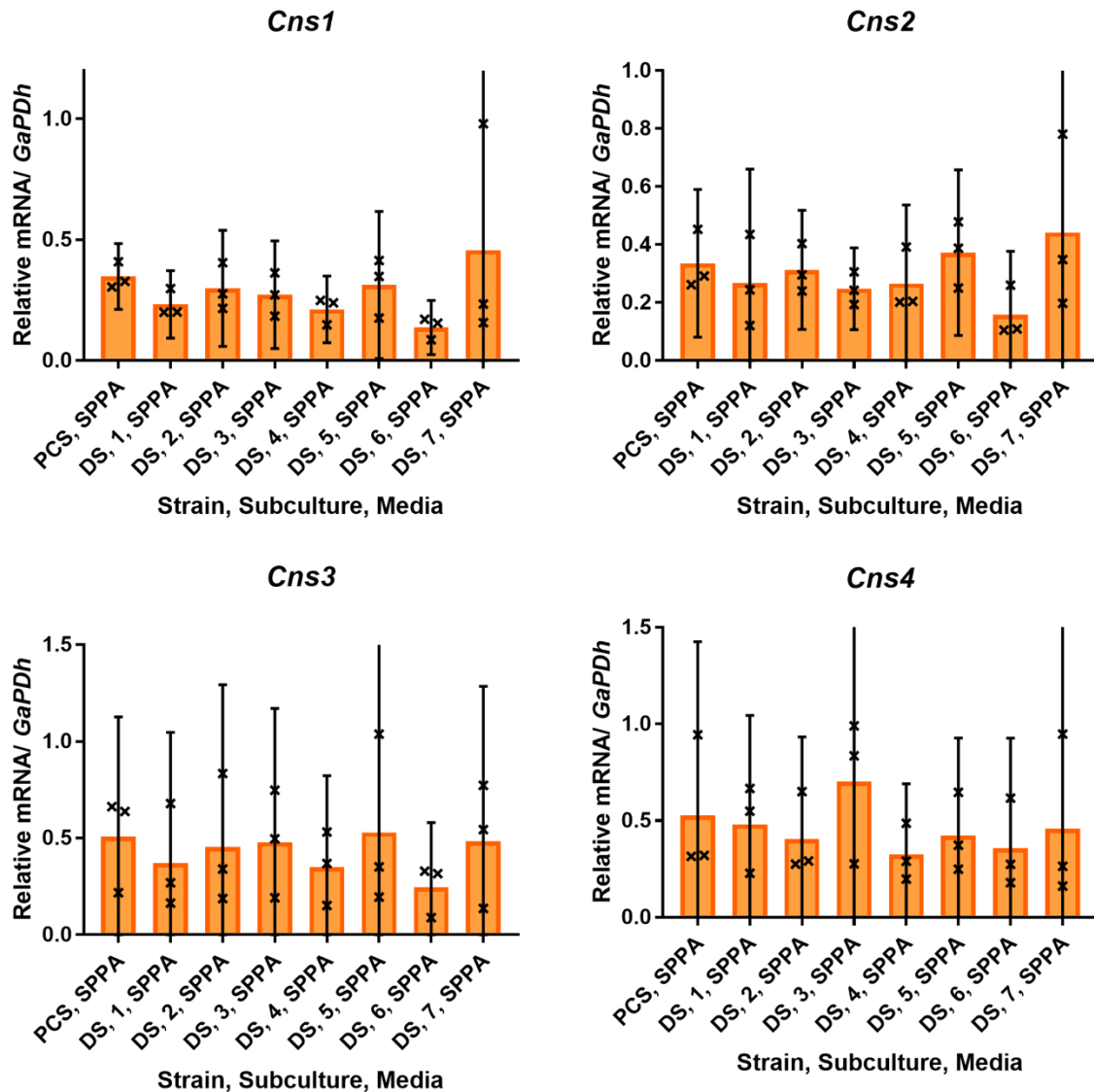
Gene Expression in CM2 PCS and Subcultures of DS on SPPA – *Cns* Genes

Figure 6.13: Relative mRNA levels of cordycepin/pentostatin biosynthesis cluster (*Cns*) genes in the parental control strain (PCS) and subcultures of the degenerated strain (DS) of CM2 on silk pupa powder agar (SPPA). Gene expression was normalised against the expression of the control gene *GaPDh*. Error bars show 95% confidence intervals. Three biological replicates, with each point representing an average of three technical replicates are shown.

Gene Expression in CM2 PCS and Subcultures of DS on SPPA – Sexual Development-Related Genes

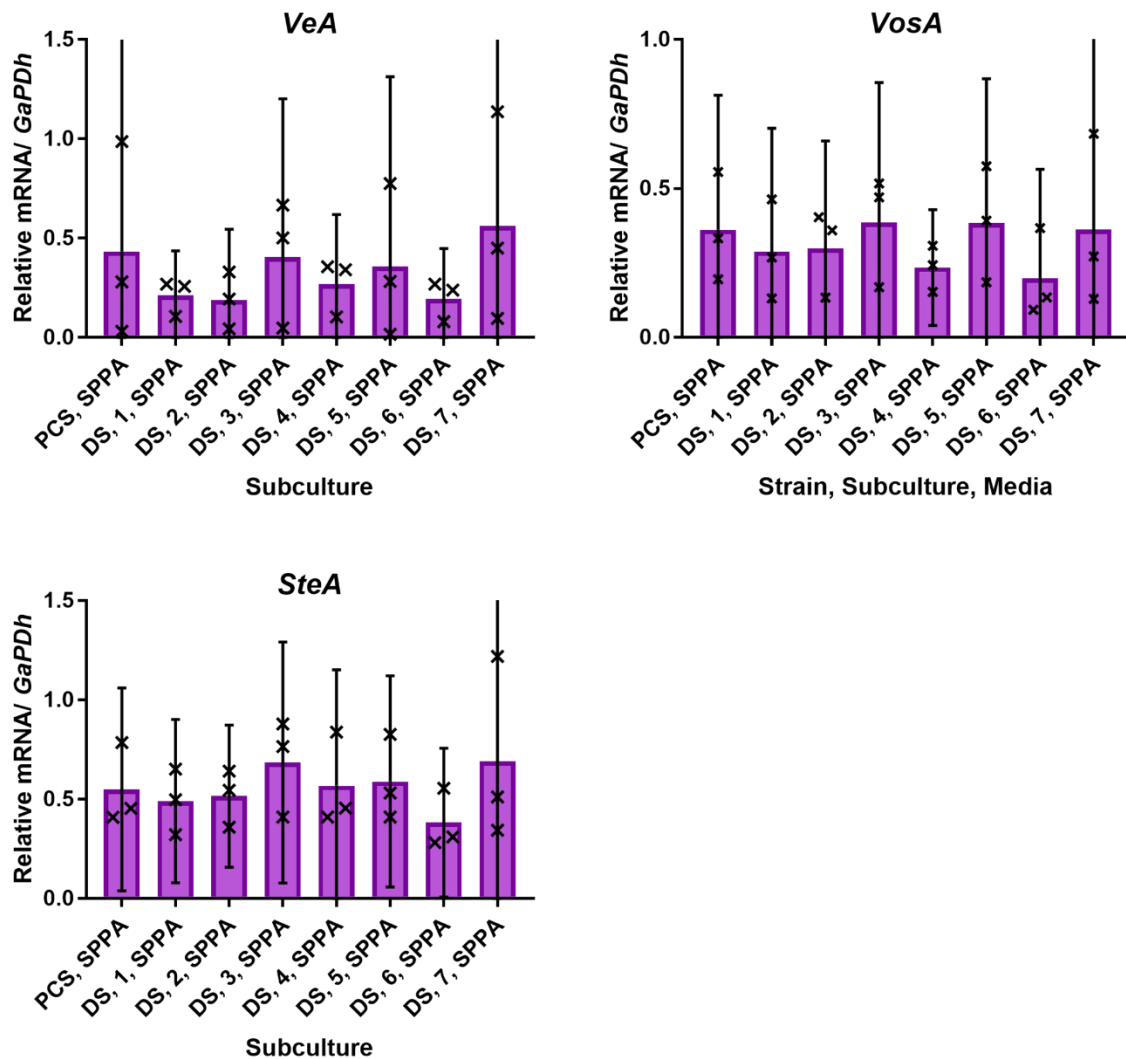


Figure 6.14: Relative mRNA levels of sexual development-related genes (*VeA*, *VosA*, *SteA*) in the parental control strain (PCS) and subcultures of the degenerated strain (DS) of CM2 on silk pupa powder agar (SPPA). Gene expression was normalised against the expression of the control gene *GaPDH*. Error bars show 95% confidence intervals. Three biological replicates, with each point representing an average of three technical replicates are shown.

6.2.2 Cultures Extracted from Spore-Injected Hosts

Exposure of *C. militaris* cultures to live hosts was investigated. This was done using the model system of injecting *Galleria mellonella* caterpillars with PBS-washed spores as described in chapter 5. After injection, the fungus was retrieved, by extraction from caterpillar haemolymph and culture once again on potato dextrose agar (PDA). This was tested at time points of one day and four days post injection, using both the parental control and degenerated strains of the *CM2* isolate.

RT-qPCR analyses were performed on extracted cultures compared to non-host exposed controls on PDA, focusing on the genes of interest considered and using the same controls as earlier experiments in chapter 3. At day one extraction, there was no consistent effect for PCS cultures, with some control samples showing higher expression of *Cns1* and *LaeA* than host-exposed samples [figure 6.15]. This was also the case for PCS at the time point of four days post injection [figure 6.18]. In the case of the degenerated strain at day one extraction, significant increases in gene expression compared to control samples were seen in host-exposed cultures [figure 6.16; figure 6.17]. This was the case in expression of cordycepin/pentostatin biosynthesis cluster genes *Cns1*, 2, 3, and 4, and sexual development-related genes *LaeA*, *VeA*, *VosA*, *PreB*, *SteA*, and *Ste7*. In one of the repeats, a mean upregulation of 471 times expression was observed for *Cns1*, and between 40 and 110 times expression for the other genes of interest. No effect was observed however at the four day time point [figure 6.19].

Subsequently, the same cultures showing upregulation with genes of interest – the DS cultures extracted at one day post injection – were analysed by targeted LC-MS [figure 6.20]. However, no significant changes in cordycepin production were detected compared to the controls. Therefore no strong evidence was gathered to suggest that this method can reverse the process of degeneration in *Cordyceps militaris*.

Gene Expression in CM2 PCS Cultures Isolated from Host Haemolymph – *Cns1* and *LaeA*

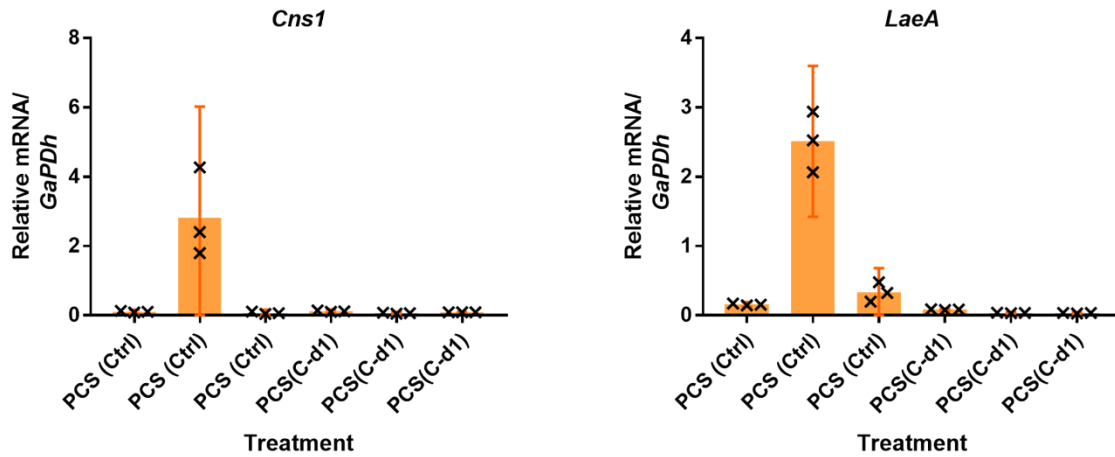


Figure 6.15: Relative mRNA levels of *Cns1* and *LaeA* in CM2 parental control strain (PCS) cultures isolated from haemolymph of spore-injected *Galleria mellonella*, one day after injection (C-d1). PCS control (ctrl) cultures were grown in PDA. Spores of PCS from four week-old potato dextrose broth (PDB) cultures were used for injection. Prior to injection, spores were washed in phosphate-buffered saline (PBS); they were injected in suspensions of sterile PBS. Gene expression was normalised against the expression of the control gene *GaPDh*. Each bar shows mean values for three technical replicates from one biological replicate. Error bars show 95% confidence intervals.

Gene Expression in *CM2* DS Cultures Isolated from Host Haemolymph – *Cns* Genes

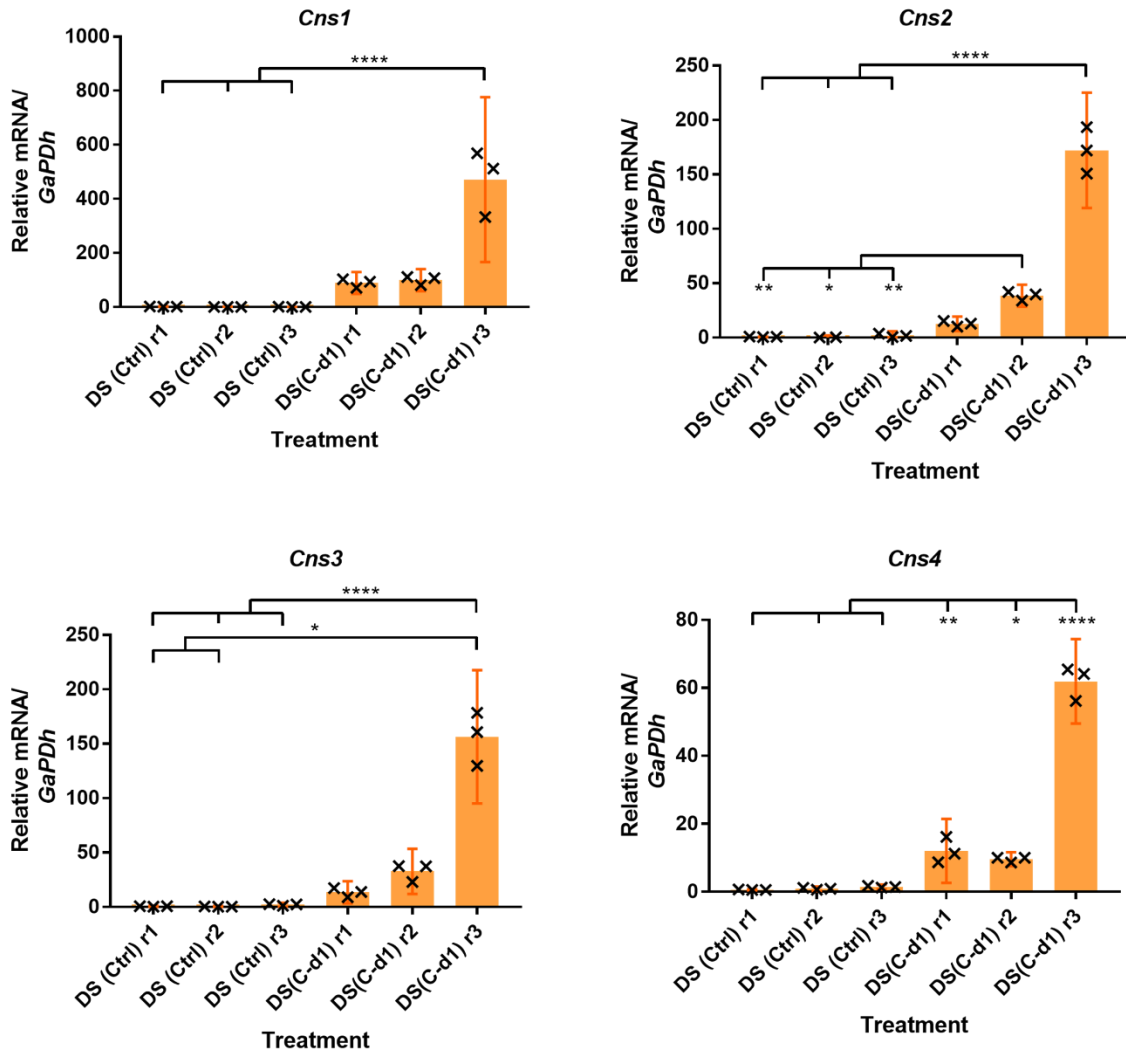


Figure 6.16: Relative mRNA levels of cordycepin/pentostatin biosynthesis cluster (*Cns*) genes in *CM2* degenerated strain (DS) cultures isolated from haemolymph of spore-injected *Galleria mellonella*, one day after injection (C-d1). DS control (ctrl) cultures were grown in PDA. Spores DS from four week-old potato dextrose broth (PDB) cultures were used for injection. Prior to injection, spores were washed in phosphate-buffered saline (PBS); they were injected in suspensions of sterile PBS. Gene expression was normalised against the expression of the control gene *GaPDH*. Each bar shows mean values for three technical replicates from one biological replicate. Error bars show 95% confidence intervals, and labels show differences between means as calculated using t-tests with Bonferroni corrections. * p < 0.05; ** p < 0.01; *** p < 0.001; **** p < 0.0001.

Gene Expression in CM2 DS Cultures Isolated from Host Haemolymph – Sexual Development-Related Genes

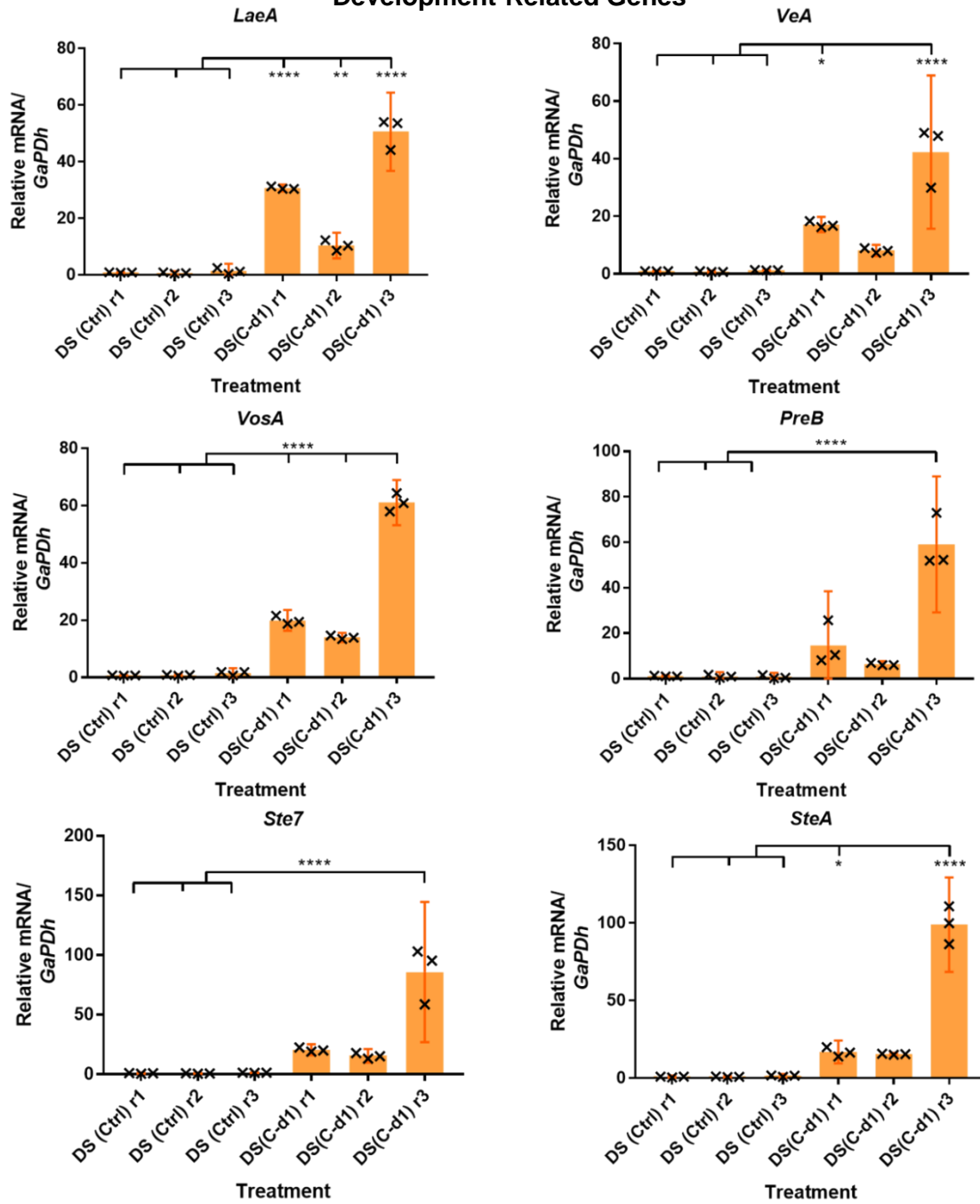


Figure 6.17: Relative mRNA levels of sexual development-related genes (*LaeA*, *VeA*, *VosA*, *PreB*, *Ste7* and *SteA*) in CM2 degenerated strain (DS) cultures isolated from haemolymph of spore-injected *Galleria mellonella*, one day after injection (C-d1). DS control (ctrl) cultures were grown in PDA. Spores DS from four week-old potato dextrose broth (PDB) cultures were used for injection. Prior to injection, spores were washed in phosphate-buffered saline (PBS); they were injected in suspensions of sterile PBS. Gene expression was normalised against the expression of the control gene *GaPDH*. Each bar shows mean values for three technical replicates from one biological replicate. Error bars show 95% confidence intervals, and labels show differences between means as calculated using t-tests with Bonferroni corrections. * $p < 0.05$; ** $p < 0.01$; *** $p < 0.001$; **** $p < 0.0001$.

Gene Expression in CM2 PCS Cultures Isolated from Host Haemolymph – *Cns1* and *LaeA*

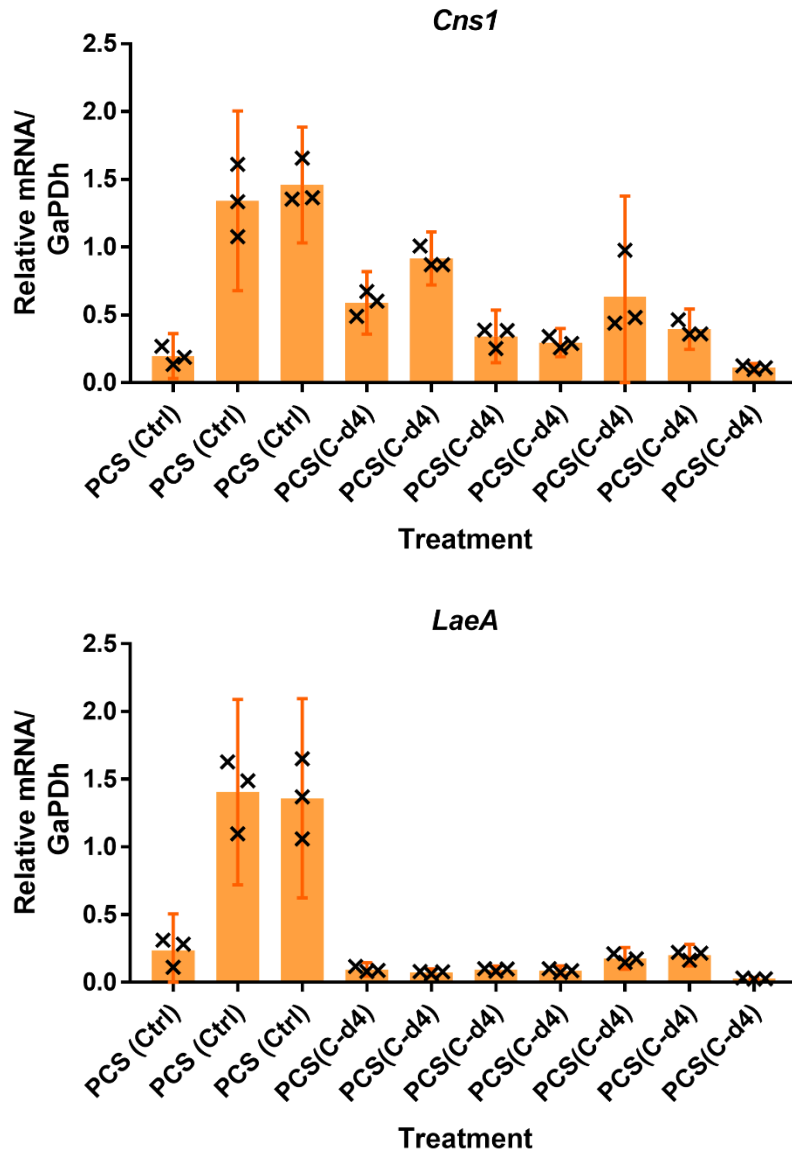


Figure 6.18: Relative mRNA levels of *Cns1* and *LaeA* in CM2 parental control strain (PCS) cultures isolated from haemolymph of spore-injected *Galleria mellonella*, four days after injection (C-d4). PCS control (ctrl) cultures were grown in PDA. Spores of PCS from four week-old potato dextrose broth (PDB) cultures were used for injection. Prior to injection, spores were washed in phosphate-buffered saline (PBS); they were injected in suspensions of sterile PBS. Gene expression was normalised against the expression of the control gene *GaPdH*. Each bar shows mean values for three technical replicates from one biological replicate. Error bars show 95% confidence intervals.

Gene Expression in *CM2* DS Cultures Isolated from Host Haemolymph – *Cns1* and *LaeA*

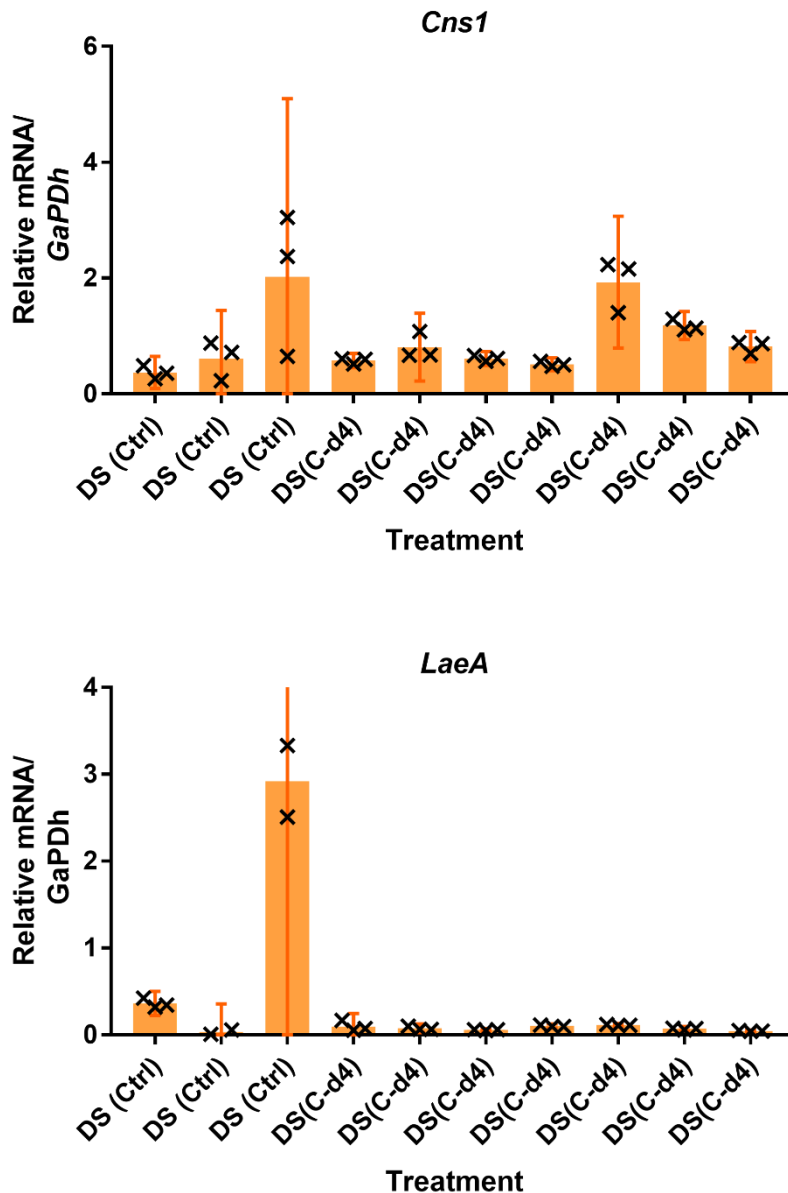


Figure 6.19: Relative mRNA levels of *Cns1* and *LaeA* in *CM2* degenerated strain (DS) cultures isolated from haemolymph of spore-injected *Galleria mellonella*, four days after injection (C-d4). DS control (ctrl) cultures were grown in PDA. Spores of PCS from four week-old potato dextrose broth (PDB) cultures were used for injection. Prior to injection, spores were washed in phosphate-buffered saline (PBS); they were injected in suspensions of sterile PBS. Gene expression was normalised against the expression of the control gene *GaPDH*. Each bar shows mean values for three technical replicates from one biological replicate. Error bars show 95% confidence intervals.

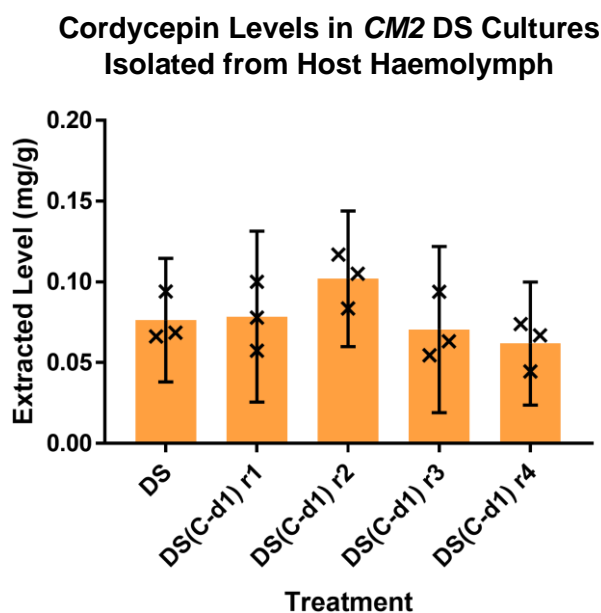


Figure 6.20: Cordycepin levels detected by LC-MS in fungal extractions from degenerated strain (DS) cultures cultures isolated from haemolymph of spore-injected *Galleria mellonella*, one day after injection (C-d1). DS control cultures were grown in PDA. Spores of PCS from four week-old potato dextrose broth (PDB) cultures were used for injection. Prior to injection, spores were washed in phosphate-buffered saline (PBS); they were injected in suspensions of sterile PBS. Each bar shows mean values for three biological replicates (cultures from separate plates. Four repeats of the injection and extraction process are shown (r1, 2, 3, 4). Error bars show 95% confidence intervals.

6.3 DISCUSSION

Although unsuccessful in attempts to illustrate causes of degeneration, or reverse the process by restoring cordycepin production in the degenerated strains, these results reveal a small insight into degeneration.

Firstly, it seems apparent that cordycepin production is relatively stable over multiple subcultures of *C. militaris* provided with controlled laboratory conditions. Perhaps a much longer period of time on agar, and other factors contributed to degeneration. Degeneration appears to be a slow and gradual process, albeit an important problem in biotechnology. It is

difficult to reverse, and potentially this is a gradual process in itself. The observation of the upregulation of cordycepin synthesis and sexual development-related genes by extraction of the fungus one day post injection for host haemolymph suggest that these genes of interest are important in the early stages of infection of the insect host.

Further research is required to tackle the problem of culture degeneration and properly understand factors influencing the process.

CHAPTER 7: DIVERSITY OF *CORDYCEPS MILITARIS* AND CORDYCEPIN PRODUCTION

Cordyceps militaris is a cosmopolitan species of entomopathogenic fungus, found in Europe, Asia and North America, with many host species [Shrestha *et al.* 2016]. To assess potential variability in the species, properties of several isolates of *Cordyceps militaris* were investigated and compared. Based on the results described earlier with the isolate *CM2*, one might expect that higher cordycepin-producing strains would produce greater pathogenic responses in *Galleria mellonella* infection assays. However, this did not occur, indicating that there are additional factors affecting infection of the insect host which are subject to variability across different populations of this species.

7.1 VARIATION BETWEEN *CORDYCEPS MILITARIS* ISOLATES

In a prospective study comparing nine available *C. militaris* isolates – growth rates, genetic properties, cordycepin production, metabolomics, and pathogenic response in *Galleria mellonella* caterpillars were investigated. This was to compare possible trends between these factors, as observed in *CM2* earlier. These isolates were obtained from culture collections, and originated from several countries in both Europe and Asia.

7.1.1 Growth of *Cordyceps militaris* Isolates

The growth rates of *C. militaris* isolates were assessed by measuring the size of potato dextrose agar (PDA) cultures over time. There were no significant differences between any two isolates for up to 20 days of growth.

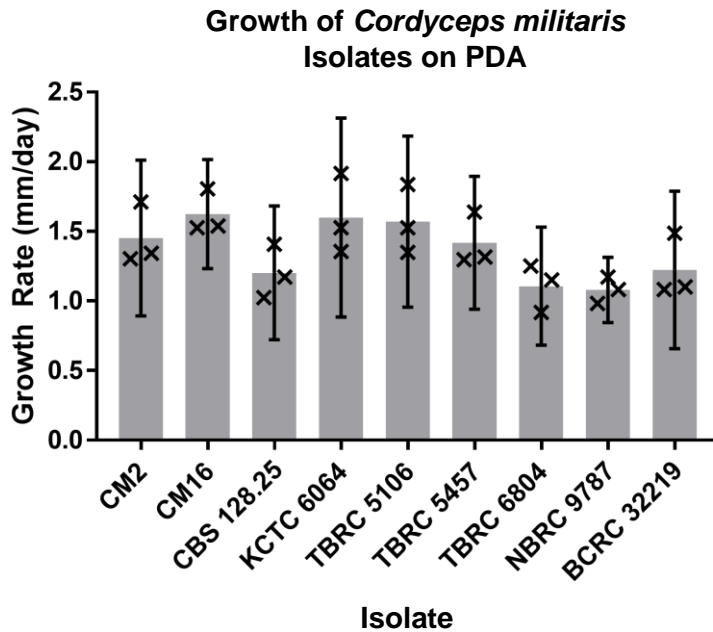


Figure 7.1: Growth rates of cultures of *Cordyceps militaris* isolates on PDA. Radial growth rate after 20 days from subculture. Error bars show 95% confidence intervals of means, from three biological replicates.

7.1.2 Genetic Screens of *Cordyceps militaris* Isolates

To distinguish between different isolates of *C. militaris*, several primers were used in RAPD PCR screens of *C. militaris* isolates DNA (data not shown) – of these, S62 [Sun *et al.* 2017] was the most reliable for producing bands. As shown in figure 7.2, distinctive sets of bands between different isolates were visible in the gel. As expected, the RAPD screen confirms the identity of the CM2 parental control and degenerated strains as belonging to the same isolate.

To assess the presence of matings types in isolates, mating-type loci (*MAT*) screens were also performed. Given that *C. militaris* is a heterothallic species, the gel in figure 7.3 indicates that some of these isolates consisted of a mixed culture of two or more strains with different mating types. In the case of the *CM2* isolate, only the *MAT1-2* mating-type locus was present. The *CM2* isolate, used in experiments investigating degeneration and pathogenicity in *Galleria mellonella* caterpillars, was therefore monokaryotic and functioned as a clonal organism.

The cordycepin/pentostatin synthesis cluster genes *Cns1-4* were found to be present in the genomes of the majority of the *C. militaris* isolates, and furthermore, *ITS* sequencing confirmed the species identity of all of these cultures as *C. militaris* [figure 7.4]. The *ITS* sequences were highly similar, and less than five nucleotide differences were present between any two isolates.

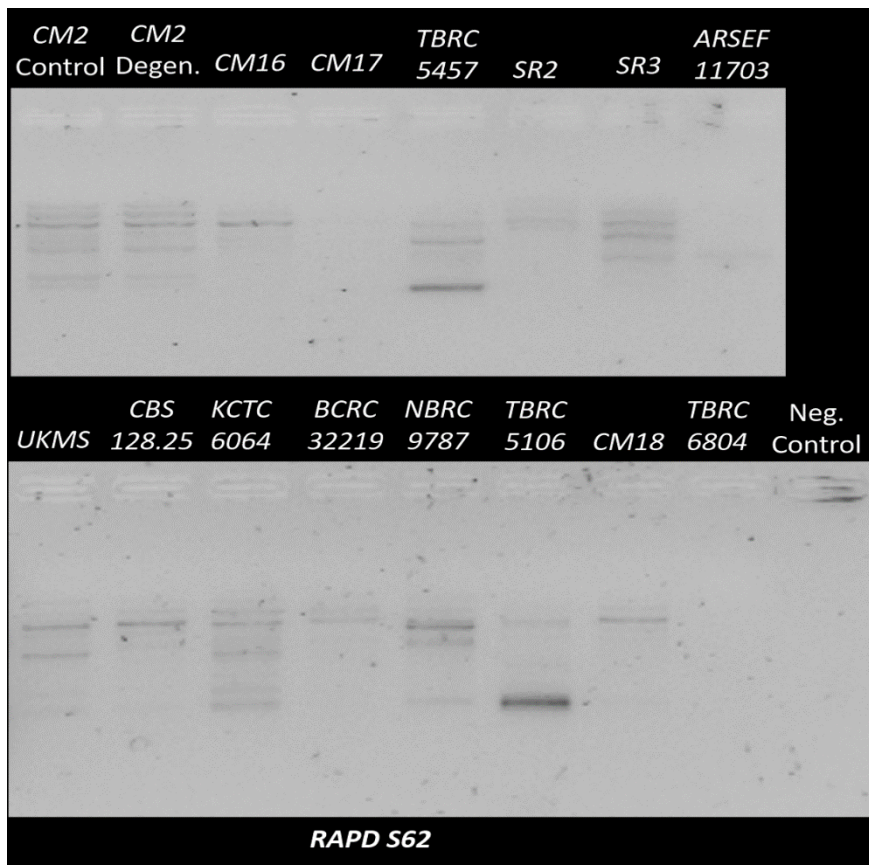


Figure 7.2: RAPD screens distinguish between different *C. militaris* isolates, using the *RAPD S62* primers. Negative of the image.

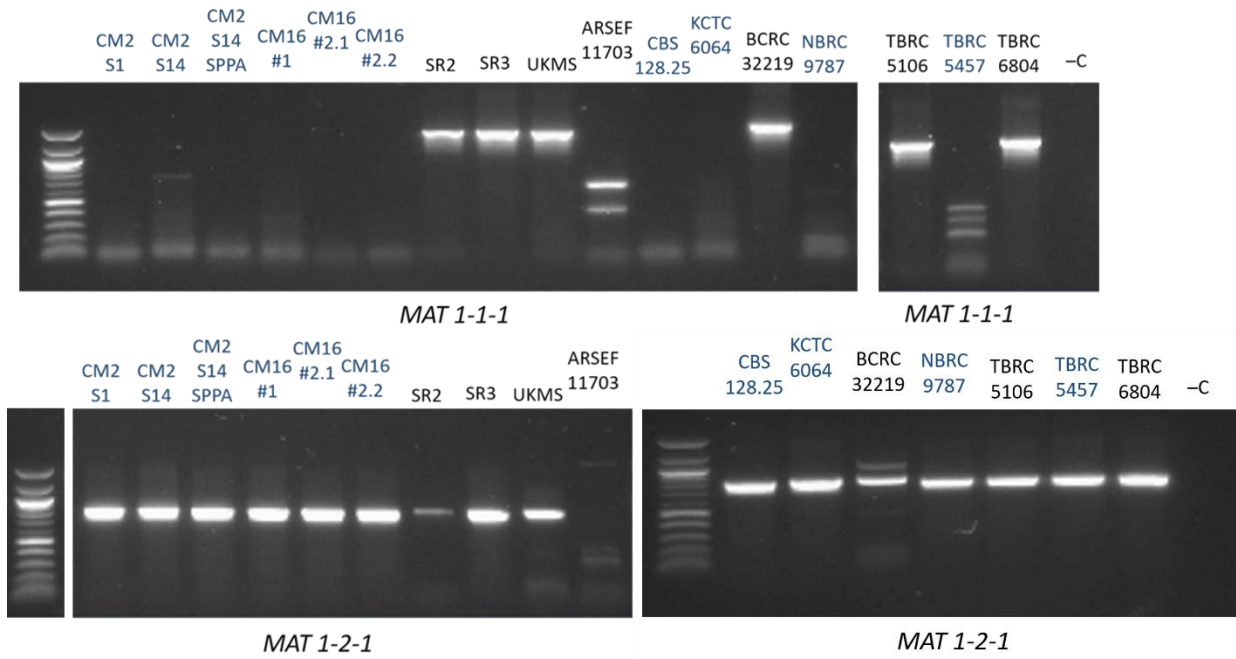


Figure 7.3: MAT screens of several *C. militaris* isolates. The marker used in lane 1 of both gels is a 100bp ladder, with major bands at 500 and 1000bp. -C = negative control.

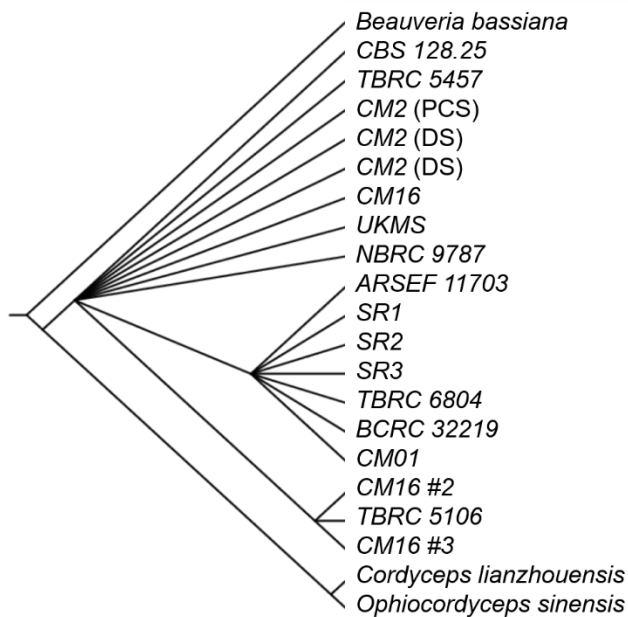


Figure 7.4: Phylogenetic tree constructed based on maximum parsimony with ITS sequences from the genomic DNA of 15 *C. militaris* isolates. *B. bassiana*, *C. lianzhouensis*, and *O. sinensis* were used as outgroups.

7.1.3 Cordycepin and Pentostatin Production and Metabolomics

Levels of cordycepin extracted from two week-old potato dextrose agar (PDA) cultures of seven *Cordyceps militaris* isolates measured by targeted LC-MS [figure 7.5], to assess the variation in output in different isolates. Of these isolates, the highest level of cordycepin detected was in *CM16*, a newly-isolated strain from Slovenia, and the lowest was in *CBS 128.25*, an isolate from the Westerdijk collection and originally isolated in the Netherlands. Untargeted LC-MS analysis was also performed on several isolates [see supplementary material].

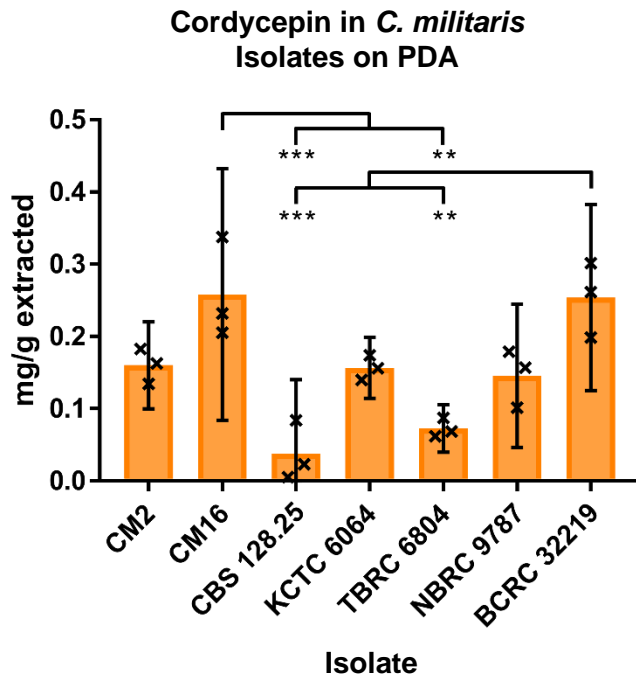


Figure 7.5: Cordycepin levels as detected in fungal extractions from cultures of *C. militaris* isolates on PDA, by targeted LC-MS. There are three biological replicates, from separate agar plates for each treatment. Error bars show 95% confidence intervals. P values are indicated by brackets: ** = $p < 0.01$, *** = $p < 0.001$ – as determined by t-tests with Bonferroni corrections.

7.1.4 Infection of *Galleria mellonella*

One can hypothesise that the higher cordycepin-producing isolates would produce a greater pathogenic response in the host. To test this, conidia and spent media of seven isolates of *C. militaris* were compared in the model host *Galleria mellonella* caterpillars, as described in chapter 5. Differences between results for different treatments were analysed by Bonferroni-adjusted log-rank (Mantel-Cox) tests.

Proportions of caterpillars over time showing full melanisation between the isolates were at similar levels [figure 7.7]. For all isolates, these were significantly greater than both the blank (df = 1, X^2 values between 36.48 and 83.36, $p < 0.01$) and uninjected (df = 1, X^2 values between 94.58 and 140.3, $p < 0.01$) controls. The highest levels of full melanisation were observed in caterpillars injected with spores from the *CM2* and *CM16* – these were both significantly greater than those for the lowest performing isolates *TBRC 6804*, *NBRC 9787*, and *BCRC 32219* (df = 1, X^2 values between 18.12 and 26.43, $p < 0.01$).

Conidia from all isolates except for *CBS 128.25* (which showed none at all) caused observable fungal emergence from injected caterpillars, which was not observed in the controls [figure 7.8]. The best fungal emergence response was seen in the *CM2* isolate, and this was significantly-greater than that in isolates *CBS 128.25* (df = 1, $X^2 = 48.4$, $p < 0.01$) and *CM16* (11.36, $X^2 = 11.36$, $p = 0.036$) according to the log-rank tests. It was also greater than the fungal emergence caused by the *KCTC 6064* and *NBRC 9787* isolates according to area under the curve 95% confidence intervals of means. The *CM16* isolate, shown earlier to have a particularly high detected level of cordycepin [figure 7.5], performed poorly in this respect, having lower levels of fungal emergence than the *CM2*, *TBRC 6804* (df = 1, $X^2 = 15.94$, $p < 0.01$), and *BCRC 32219* (df = 1, $X^2 = 14.1$, $p = 0.009$) isolates.

Figure 7.7.1: Fungal Liquid Cultures Spores and Extract Injections (Different Isolates) – Melanisation

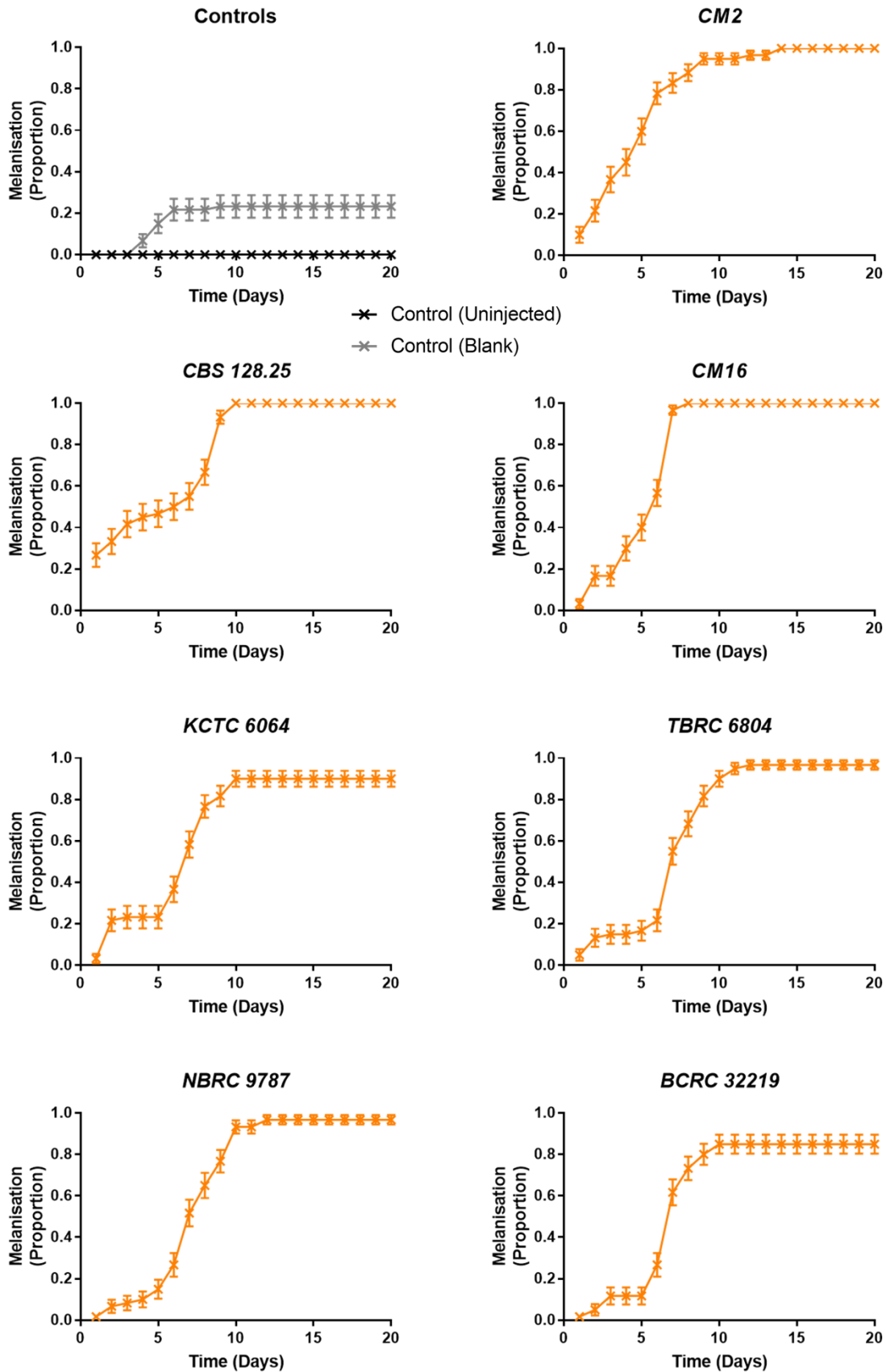


Figure 7.7.2: Fungal Liquid Cultures Spores and Extract Injections (Different Isolates) – Melanisation (Area Under the Curve)

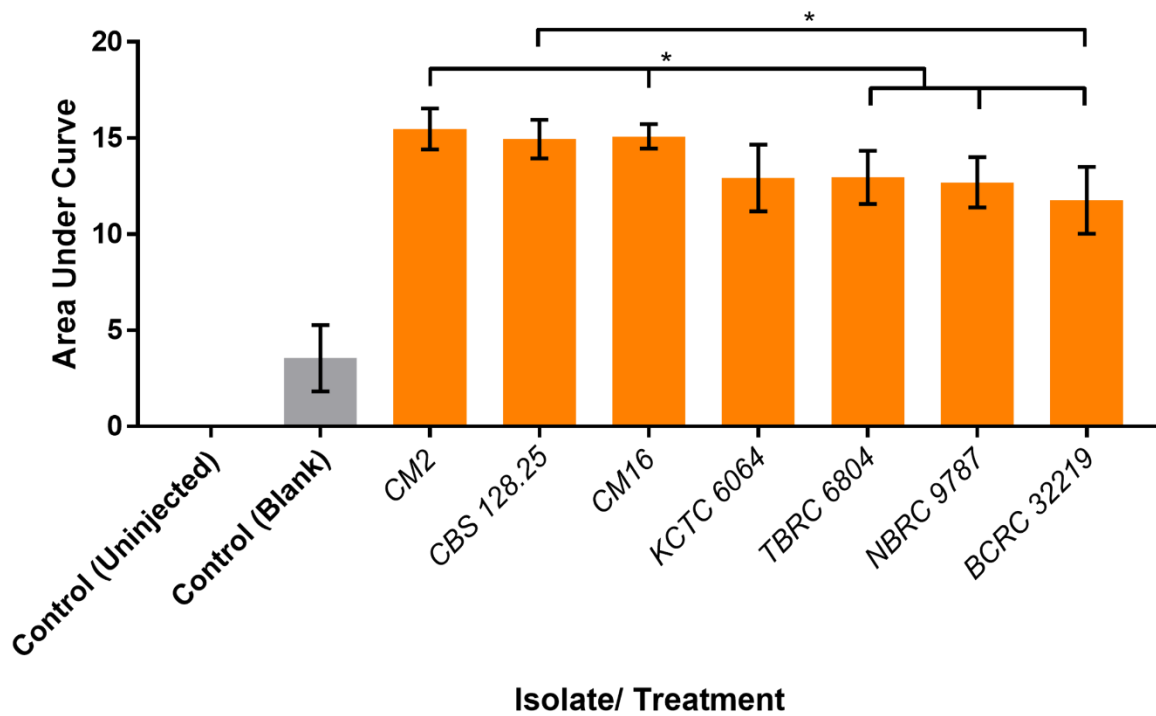


Figure 7.7: Proportions of full melanisation observed in *Galleria mellonella* caterpillars following 100 µL injections with spores and spent media from potato dextrose broth (PDB) cultures of several isolates of *Cordyceps militaris*. 100,000 conidia were injected into each caterpillar. There were also blank injected (sterile fresh media only) and uninjected controls. Error bars show 95% confidence intervals in both the time course plots and area under the curve graph. Asterisks (*) indicate significant differences between area under the curve means ($p < 0.05$). Sample size = 60 caterpillars.

Figure 7.8.1: Fungal Liquid Cultures Spores and Extract Injections (Different Isolates) – Fungal Emergence

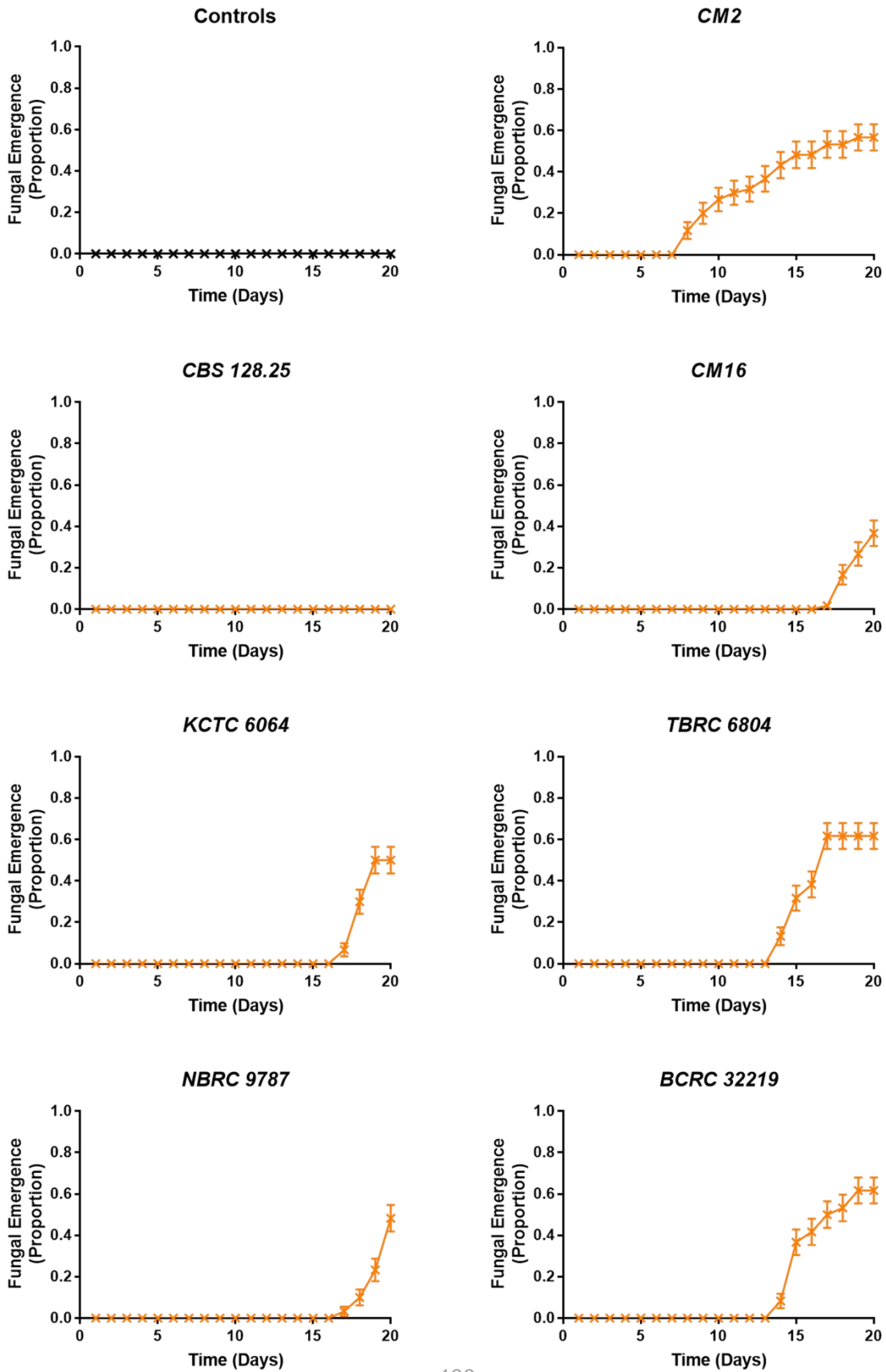


Figure 7.8.2: Fungal Liquid Cultures Spores and Extract Injections (Different Isolates) – Fungal Emergence (Area Under the Curve)

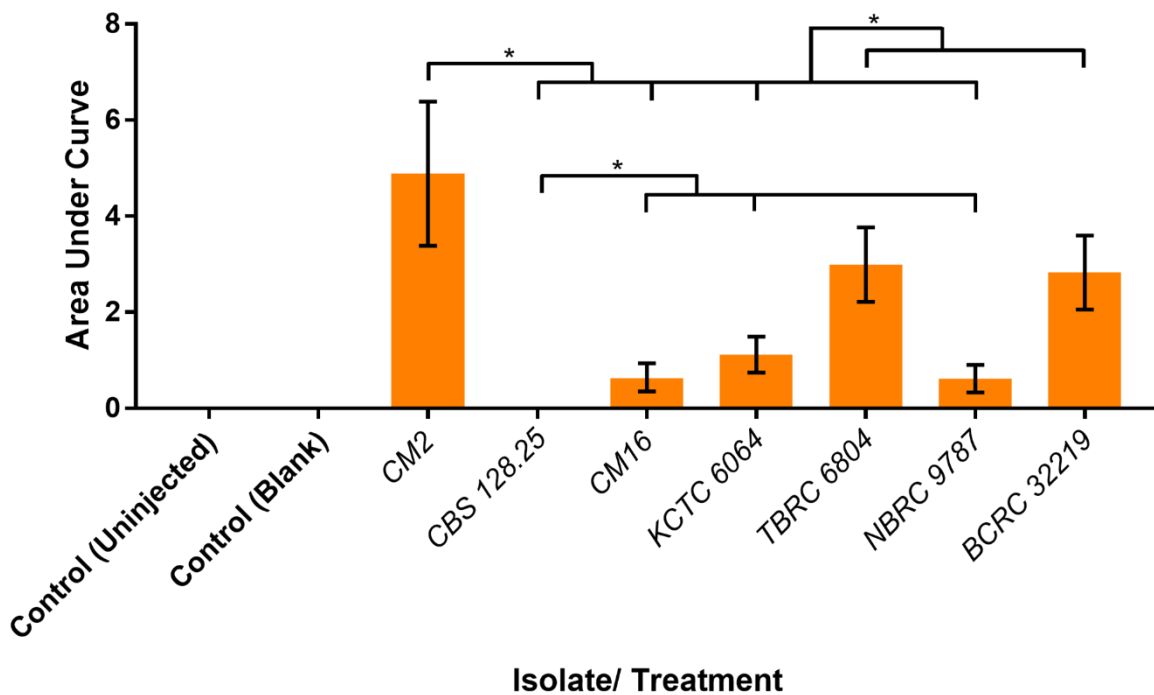


Figure 7.8: Proportions of fungal emergence observed in *Galleria mellonella* caterpillars following 100 µL injections with spores and spent media from potato dextrose broth (PDB) cultures of several isolates of *Cordyceps militaris*. 100,000 conidia were injected into each caterpillar. There were also blank injected (sterile fresh media only) and uninjected controls. Error bars show 95% confidence intervals in both the time course plots and area under the curve graph. Asterisks (*) indicate significant differences between area under the curve means ($p < 0.05$). Sample size = 60 caterpillars.

7.2 DISCUSSION

The growth, cordycepin production, and pathogenic response in a model host of several *Cordyceps militaris* isolates were compared.

Results from the experiments on isolates *CM2*, *CM16*, *CBS 128.25*, *KCTC 6064*, *TBRC 6804*, *NBRC 9787* and *BCRC 32219* did not present a consistent link between cordycepin production and pathogenic response in the *Galleria mellonella* host model – although *CM2* performed well in the caterpillar assays – producing high levels of fungal emergence to match its high cordycepin output – and *CBS 128.25* by contrast matched its low cordycepin production with a complete failure to cause fungal emergence. However, *CM16*, the greatest cordycepin producer, presented a comparatively-low proportion of fungal emergence from injected caterpillars; and all isolates caused relatively similar levels of full melanisation. Given the cosmopolitan nature of this species and indeed the isolates tested here – there may be an array of other factors influencing both secondary metabolite production and pathogenic performance as a result of varying selection pressures across different populations. There may be considerable differences in the ecology of this species in different locations and across different isolates.

CHAPTER 8: EVOLUTION OF CORDYCEPIN-PENTOSTATIN CO-PRODUCTION

We hypothesised that the trait of cordycepin and pentostatin co-production had been subject to horizontal gene transfer due to its rarity in fungal species in general and absence in other *Cordyceps* species [Wellham *et al.* 2019]. To test this, bioinformatics-based analyses of sequence data from the *Cns* gene cluster were carried out to gain insights into the evolution of the production of cordycepin and pentostatin in *C. militaris* and wider fungal taxa.

8.1 SEARCHING FOR EVIDENCE OF CORDYCEPIN PRODUCTION IN OTHER FUNGI

In studies by Xia *et al.* and Wu *et al.*, coupled biosynthesis strategies involving modified adenosines and pentostatin were described in *Cordyceps militaris* and the bacterium *Streptomyces antibioticus* respectively [Xia *et al.* 2017; Wu *et al.* 2017]. Given that the production of modified nucleosides and similar antibiotics represent secondary variations of highly-conserved eukaryotic metabolic pathways, this protector-protégé system may be a more widespread strategy for the manipulation of other organisms by fungi than expected. Given also that bioinformatics-based tests performed by Xia *et al.* only managed to find evidence for the cordycepin-pentostatin synthesis (*Cns*1-4) gene cluster in three phylogenetically-distanced fungal species, there is a possibility that horizontal gene transfer (i.e. between organisms of different species), and/or rapid plasticity of gene arrangement could play important roles in the evolution of this strategy. Here, BLAST-based bioinformatics techniques have been used to search for further *in silico* evidence for *Cns*1-4 gene homologues in other ascomycete species, as well as across the fungal kingdom.

8.1.1 Searches for Homologues of *Cordyceps militaris* Cns1-4 Using BLASTp

The protein BLAST (BLASTp) tool was used to search the non-redundant protein sequences (nr) database on the NCBI website, with inputs of each of the Cns1-4 protein amino acid sequences. These protein sequences were produced from the translation of nucleotide sequences of genes *Cns1-4* – these are shown in table 8.1. As proposed by Xia and colleagues, Cns1, Cns2 and Cns3 are involved in the synthesis pathway for cordycepin, and Cns3 (a bifunctional protein) is also involved in the synthesis of pentostatin. Cns4 is an exporter of pentostatin.

Table 8.1: Nucleotide sequences used to obtain inputs used in BLASTp searches for Cns1-4 homologues.

Protein name	Gene number	Accession number
Cns1 “oxidoreductase domain containing”	CCM_04436	XM_006669584.1
Cns2 “phosphoribosyl-aminoimidazole-succinocarboxamide synthase”	CCM_04437	XM_006669585.1
Cns3 “hypothetical protein”	CCM_04438	XM_006669586.1
Cns4 “ABC multidrug transporter”	CCM_04439	XM_006669587.1

BLASTp search results were filtered, with only matches possessing an e value of less than 0.01 included.

Overall, the results corroborate the findings of Xia and colleagues – with clear evidence for the existence of homologous genes for all four genes (Cns1-4) in the species *Acremonium chrysogenum* and *Aspergillus nidulans* only [Xia *et al.* 2017]. In the case of Cns1, there were only matches for these species, as well as *C. militaris*, with query coverages above 80%. Being a particularly-well studied group of ascomycetes, the *Aspergillus* species represent a large proportion of matches, particularly in the case of Cns2; this in itself may be an artefact of the attention the aspergilli receive. *A. nidulans* stands out clearly from the other *Aspergillus* matches – out of 47 matches for Cns2, only *A. nidulans* has an identity match above 80%,

with the others below 60%. These other *Aspergillus* species included *A. parasiticus*, *A. flavus*, *A. niger*, *A. carbonarius*, *A. tubingensis* and others.

Cns2, Cns3, and Cns4 matches are phylogenetically broadly spread throughout the ascomycete phylum, with representatives in several major classes – Sordariomycetes, Eurotiomycetes, Leotiomycetes, and Dothideomycetes. Many matches are described as hypothetical proteins, particularly those of higher query coverage and identity match scores – and therefore have not been investigated for their specific functions and structural domain homologies. However, some matches have described functions and structures. This was explored further using searches of protein domain databases.

8.1.2 Cns1-4 Protein Structures and Functions

To investigate protein structures with regards to known domains, the Cns1-4 protein sequences were put into the search tool for the Pfam database [El-Gebali *et al.* 2019] as well as the Conserved Domain Database (CDD) [<https://www.ncbi.nlm.nih.gov/cdd/>].

These results are shown in table 8.2 and figure 8.1. Protein domains listed in the CDD, corresponding to matches for Cns1-4 are detailed in table 8.2, as well as similar domains. Figure 8.1 corroborates with the findings of Xia *et al.* and has been presented in a similar format to the diagram shown in the paper [Xia *et al.* 2017]. Cns4 is an ATP-binding cassette protein, possessing a set of ABC domains, all of which are highly conserved and preponderant throughout the eukaryotes, involved in the export/import of a great variety of metabolites.

Cns1-3 and Biosynthesis Pathways

Cns1 is an oxidoreductase, and possesses an NADP-binding Rossmann fold domain – similar to that on Gfo/Idh/MocA family proteins. This family of proteins are responsible for catalysing redox reactions between pyranoses (such as glucose and fructose) and NADP⁺/NADPH. Xia *et al.* provided mass spectrometric evidence for the role of Cns1 in catalysing the final step in the synthesis of cordycepin, in which 2'-carboxy-3'-deoxyadenosine (2'-C-3' dA) is reduced via the oxidation of NADPH [figure 8.2] [Xia *et al.* 2017]. These has been proposed a similar role for Pen I/J/H, a set of oxidoreductases [figure 8.3] – the genes for which are present in the vidarabine-pentostatin biosynthesis cluster [Wu *et al.* 2017]. Wu and colleagues propose that one or more of the proteins catalyse both redox reactions which convert adenosine to vidarabine, via the oxidised intermediate 2'-keto-deoxyadenosine (2'-keto dA) [Wu *et al.* 2017]. It seems likely that Cns1 and related oxidoreductases play roles in the synthesis of adenosine analogues, given the presence of the genes for them in species producing these secondary metabolites.

Cns3 is a protein with two separate domains of interest. The nucleotide kinase (NK) domain, located towards the N terminus, has been proposed to catalyse the conversion of adenosine to 3'-cyclic AMP (3'-AMP) [Xia *et al.* 2017]. The NK family of proteins are well-known for transferring phosphate groups to nucleoside and nucleotide analogues [Deville-Bonne *et al.* 2008]. The other domain is the HisG domain, located towards the C terminus. This domain is possessed by ATP phosphoribosyltransferases involved in the early steps of the highly-conserved L-histidine biosynthesis pathway. The synthesis of pentostatin has been suggested to be similar to these steps [Hanvey *et al.* 1988], and hence the C-terminal domain of Cns3 has been described as responsible for the biosynthesis of pentostatin [Xia *et al.* 2017; Wu *et al.* 2017].

Cns2 is highly similar in structure to SAICAR (phosphoribosyl-aminoimidazole-succinocarboxamide) synthase, and possesses a metal-dependent phosphohydrolase domain. It has been proposed to catalyse the conversion of 3'-AMP to 2'-C-3'-dA by the removal of a phosphate group [Xia *et al.* 2017]. It is possible either that Cns2 is itself the SAICAR synthase protein functional in *C. militaris* and other species, the gene for which has been arranged into the cordycepin-pentostatin synthesis cluster. Alternatively, the *Cns2* gene could have been created following a gene duplication event of the *SAICAR synthase* gene and subsequent subfunctionalisation. To determine this, a simple nucleotide blast (BLASTn) was carried out on the DNA sequence of the *Cns2* gene, against the sequenced genome of the CM01 isolate of *C. militaris* [Zheng *et al.* 2011]. There were two loci detected, with 96.95 per cent sequence similarity. Therefore this supports the hypothesis of gene duplication and subfunctionalisation.

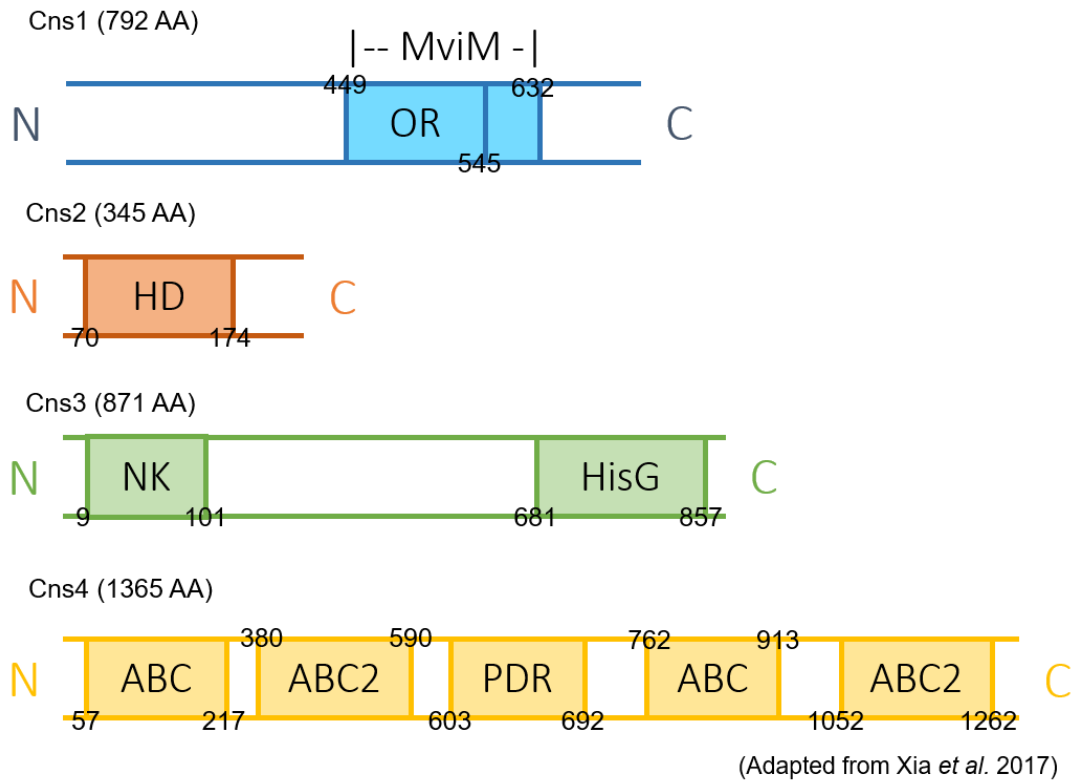


Figure 8.1: Protein domains on *Cordyceps militaris* Cns1-4 proteins as identified via searches using Pfam [El-Gebali *et al.* 2019] and CDD [adapted from Xia *et al.* 2017]. For details of abbreviations, see table 8.2.

Table 8.2: Protein families and domains identified with CDD and Pfam, or bearing similarities to Cns1-4 from BLASTp results

Protein	Domain/Protein Family	Functions/ comments	Reference
Cns1	MviM (including OR): oxidoreductase, with NADP-binding Rossmann-fold domain (also described as Gfo/Idh/MocA family)	Typically pyranose oxidoreductases, NADP dependent. Gfo: glucose-fructose OR; Idh: inositol 2-dehydrogenase; MocA: rhizopine catabolism protein	Rowland <i>et al.</i> 1994; Kingston <i>et al.</i> 1996; Taberman <i>et al.</i> 2016
Cns2	HD: metal-dependent phosphohydrolase	Often associated with helicases and nucleotidyltransferases; conserved HD amino acid pair	Aravind <i>et al.</i> 1998; Yakunin <i>et al.</i> 2004
Cns2 (similarity)	SAICAR (phosphoribosyl-aminoimidazole-succinocarboxamide) synthase	A highly-conserved enzyme acting early in purine biosynthesis; adds succinate to CAIR at the carboxylic acid group, creating a carboxamide group	Levdikov <i>et al.</i> 1998
Cns3	NK: nucleoside/nucleotide kinase	Used for transfer of phosphate groups to nucleoside/nucleotide analogues, in viral treatment for example	Deville-Bonne <i>et al.</i> 2008
Cns3	HisG: ATP phosphoribosyltransferase	HisG is an enzyme acting early in the biosynthesis of histidine; short form of the domain in Cns3	Cho <i>et al.</i> 2008
Cns3 (similarity)	Phosphoribosyl-AMP cyclohydrolase	An enzyme acting early in the biosynthesis of histidine	Minson & Creaser 1969
Cns4	ABC: ATP-binding cassette domain	Highly conserved domain; binds ATP for subsequent hydrolysis to transport of substrates across membranes by ABC transporter protein	Hung <i>et al.</i> 1998
Cns4	ABC2: ABC class 2	Found in drug resistance transport proteins of bacteria such as <i>Streptomyces</i> ; related to but distinct from the ABC domain	Reizer <i>et al.</i> 1992
Cns4	PDR: pleiotropic drug resistance	A class of ABC transporters providing resistance to drugs in bacteria	Gauthier <i>et al.</i> 2003
Cns4 (similarity)	P-loop-containing NTPase	A class of nucleotide trisphosphatases, containing a proline-loop structure	Aravind <i>et al.</i> 2004

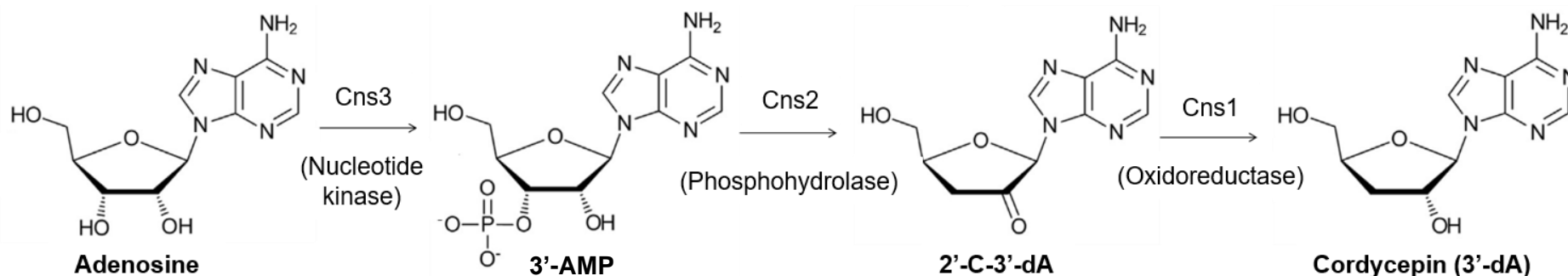
Previously Proposed Syntheses of Modified Adenosine Nucleoside Analogues [adapted from Xia *et al.* 2017 and Wu *et al.* 2017]

Figure 8.2: Pathway for cordycepin synthesis described by Xia *et al.* (2017). This pathway is corroborated by the protein-based search data detailed in figure 8.3 and table 8.2. Abbreviations: 3'-AMP – 3'-adenosine monophosphate; 2'-C-3'-dA – 2'-carbonyl-3'-deoxyadenosine; 3'-dA – 3'-deoxyadenosine.

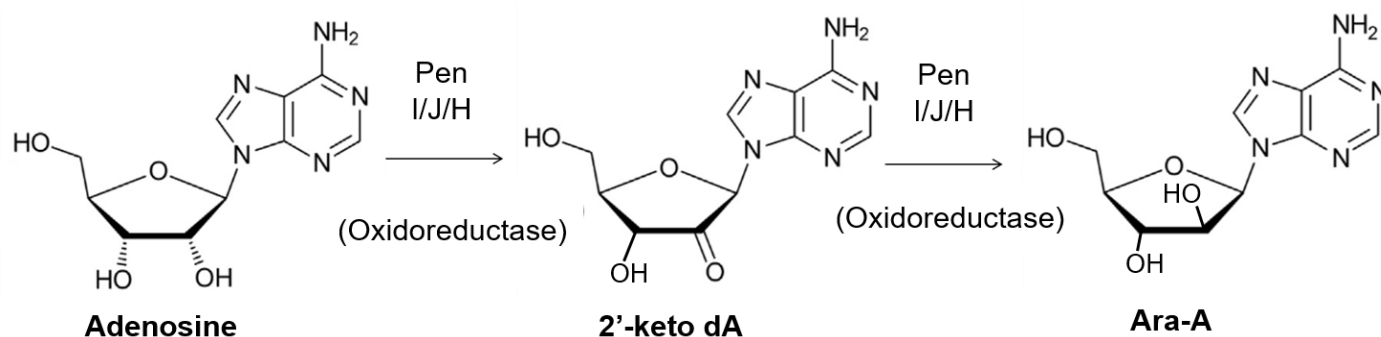


Figure 8.3: Pathway for arabinofuranosyl adenine (vidarabine) synthesis described by Wu *et al.* (2017). Like the cordycepin synthesis pathway, this relies on an oxidoreductase in order to manipulate the position of hydroxyl group(s) on the furanose ring.

8.1.3 Searching Fungal Genomes for *Cns1-3* Homologues Using tBLASTn

A deeper search for *Cns1-3* gene homologues in the fungal kingdom was conducted using the tBLASTn search tool on the NCBI website. This used inputs of amino acid sequences from each of the genes, and searched the whole genome shotgun (wgs) database for translated matches with a protein query. For the match translations, all six reading frames were considered, to maximise the sensitivity of the search and account for variations in sense/antisense orientations of genes. This is the basis of the enhanced sensitivity of tBLASTn compared to BLASTn. The wgs database houses complete genome sequences, often unannotated, for a large range of fungal species. As of July 2020, at the time of the search, 1688 ascomycete and 465 basidiomycete species had their genomes sequenced and were available on the database. Some major clades of the ascomycetes were better represented than others [figure 8.4]. Sordariomycetes was a particularly well-represented class (505 species), with the order Hypocreales also well represented (242). 11 species of the *Cordyceps sensu lato* were represented, including *Cordyceps cicadae*, *Ophiocordyceps sinensis*, and *Beauveria bassiana*. Every single fungal species represented in the wgs database was included in each of the tBLASTn searches for *Cns1-3* homologues.

Results of the searches were filtered to only include matches with e values of less than 0.01, query coverages of over 70% and identity matches of over 50%.

The matches included those from species noted in the BLASTp searches, as well as multiple others. Many of the new matches have been found in unannotated genome sequences, and hence the corresponding proteins are not included in the nr protein database. Being a more sensitive search, tBLASTn is a better tool for finding previously-undiscovered homologues of genes and gene clusters.

Species which showed matches for all three genes, or combinations of two of the *Cns* genes are detailed in table 8.3. These fungi have a diversity of ecological properties – ranging from pathogens of plants and endophytes to moulds and pathogens of animals. As well as the

previously-discovered *Acremonium chrysogenum* and *Aspergillus nidulans*, five new species were found to have *Cns1*, 2, and 3 homologues in their genomes. Upon closer inspection of the sequenced genomes, these species – *Aspergillus quadrilineatus*, *Sarocladium oryzae*, *Sarocladium brachiariae*, *Paramyrothecium roridum*, and *Verticillium tricorpus* – appear to have the three genes arranged proximally to each other. The positions and orientations of the *Cns1-3* homologues in the genomes of these species are presented to scale in figure 8.6.

Gene phylogenies for matches from species featured in table 8.3 are presented in figure 8.5, for *Cns1*, 2, and 3 homologues, as well as concatenated sequences from the three genes. Phylogenies were constructed using the tool available on the website phylogeny.fr. A MUSCLE alignment was used, with Gblocks alignment curation, and a maximum likelihood construction method. The phylogenies for each of the genes as well as the concatenation show similar clustering, and broadly correlate with phylogenetic relationships between the different species.

NCBI Genome Database – Number of Species Sequenced in Various Taxa

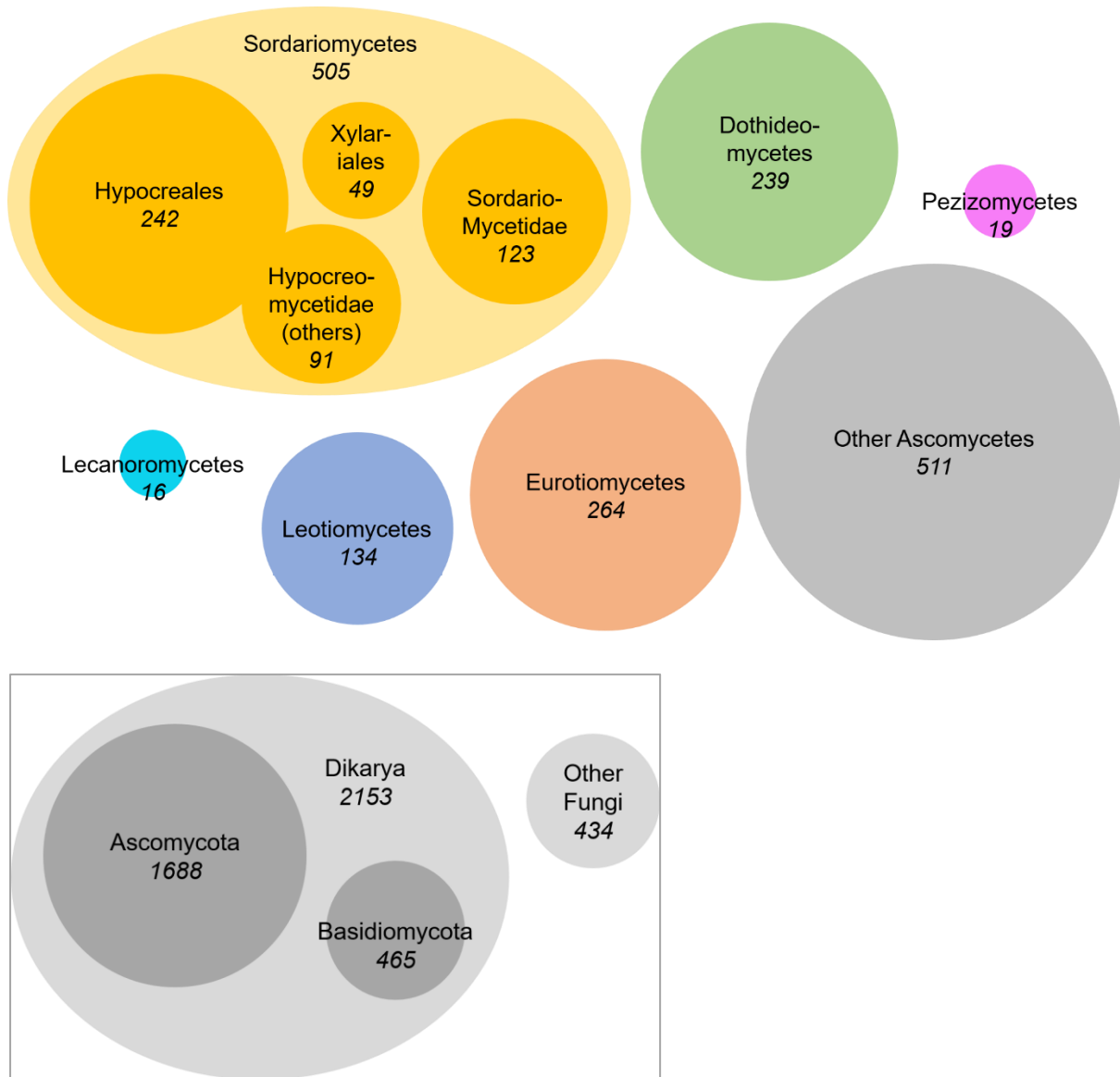


Figure 8.4: Sequenced genomes available in various fungal taxa on the NCBI genome database, by number of species. Taxa containing the *Cordyceps* (Sordariomycetes, Hypocreales) are fairly-well represented. As of 2020, 41 species of the Clavicipitaceae had their genome sequence available on the database, with 74 total entries.

Table 8.3: Species with Cns1 and 2 (and 3) Homologous Genes Present.

Species	Isolate	Genome accession number	Reference	Cns4?	Fungal ecology/ notes
Cns1, Cns2, & Cns3:					
<i>Cordyceps militaris</i>	CM01	MQTM01000004.1	Zhang 2016	Yes	Pathogen of caterpillars
<i>Cordyceps militaris</i>	CM01	AEVU01000219.1	Zheng <i>et al.</i> 2011	Yes	
<i>Acremonium chrysogenum</i>	ATCC 11550	JPKY01000075.1	Terfehr <i>et al.</i> 2014	Yes	Mould; produces antibiotic cephalosporin C
<i>Sarocladium oryzae</i>	JCM 12450	BCHE01000007.1	Manabe <i>et al.</i> 2015	No	Sheath rot disease in rice
<i>Sarocladium oryzae</i>	Saro-13 isolate	LOPT01005630.1	Hittalmani <i>et al.</i> 2016	No	
<i>Sarocladium brachiariae</i>	HND5	RQPE01000004.1	Yang & Huang 2018	No	Endophyte, found on <i>Brachiaria bizantha</i> (signalgrass) [Liu <i>et al.</i> 2017]
<i>Paramyothecium roridum</i>	NRRL 2183	PXOD01001108.1	Proctor <i>et al.</i> 2018	No	Generalist plant pathogen, leaf spots
<i>Verticillium tricorpus</i>	MUCL 9792	JPET01000003.1	Seidl <i>et al.</i> 2015	Yes	Generalist plant pathogen, wilts
<i>Verticillium tricorpus</i>	PD593	NMXK01000002.1	Shi-Kunne <i>et al.</i> 2017	Yes	
<i>Aspergillus quadrilineatus</i>	NRRL 201	JAAXYA010000110.1 and others	Steenwyk <i>et al.</i> 2020	Yes	Mould; can be a cause of aspergillosis in humans
<i>Aspergillus nidulans</i>	MO80069	JAAFYM010000027.1 and others	Bastos <i>et al.</i> 2020	Yes	Mould; model aspergilli species; has known teleomorph (<i>Emericella</i>)
<i>Aspergillus nidulans</i>	FGSC A4	AACD01000055.1	Galagan <i>et al.</i> 2005	Yes	
Cns1 and Cns2:					
<i>Penicillium paxilli</i>	ATCC 26601	AOTG01000149.1	Berry <i>et al.</i> 2015	No	Mould

Cns2 and Cns3:					
<i>Corynespora cassiicola</i>	CCAM1 isolate	POSB01000912.1 and others	Lopez <i>et al.</i> 2018	No	Generalist tropical plant pathogen [Dixon <i>et al.</i> 2009]
<i>Alternaria gansuensis</i>	LYZ1412	WBTE01001328.1 and others	Li & Nzabanita 2019	No	Plant pathogen
<i>Alternaria brassicae</i>	J3	SMOM01000005.1	Rajarammohan <i>et al.</i> 2019	No	Pathogen of brassicas, leaf spots
<i>Parastagonospora avenaria</i>	f. sp. tritici Jansen 4-55	QVWU01002218.1 and others	Syme <i>et al.</i> 2018	No	Plant pathogens
<i>Parastagonospora avenae</i>	f. sp. avenae S258	QVXB01000775.1 and others	Syme <i>et al.</i> 2018	No	
<i>Curvularia geniculata</i>	W3	PQMW01000012.1	Siqueira <i>et al.</i> 2018	No	Plant and animal pathogen, soil
<i>Curvularia lunata</i>	W3	PELC01000012.1	Siqueira <i>et al.</i> 2018	No	Animal pathogen, including humans
<i>Curvularia lunata</i>	CX-3	JFHG01001651.1	Gao <i>et al.</i> 2014	No	
<i>Curvularia papendorfii</i>	UM 226	JXCC01000071.1	Kuan <i>et al.</i> 2015	No	
<i>Exserohilum turcica</i>	Et28A	AIHT01000518.1	Ohm <i>et al.</i> 2012	No	Pathogen of maize, blight
<i>Penicillium camemberti</i>	FM013	CBVV010000108.1	Cheeseman <i>et al.</i> 2013	No	Mould used in camembert, brie and other cheeses
<i>Penicillium bifforme</i>	FM169	CBXO010000001.1	Ropars <i>et al.</i> 2013	No	
<i>Penicillium fuscoglaucum</i>	FM041	CBXP010000191.1	Ropars <i>et al.</i> 2013	No	Mould, food spoilage

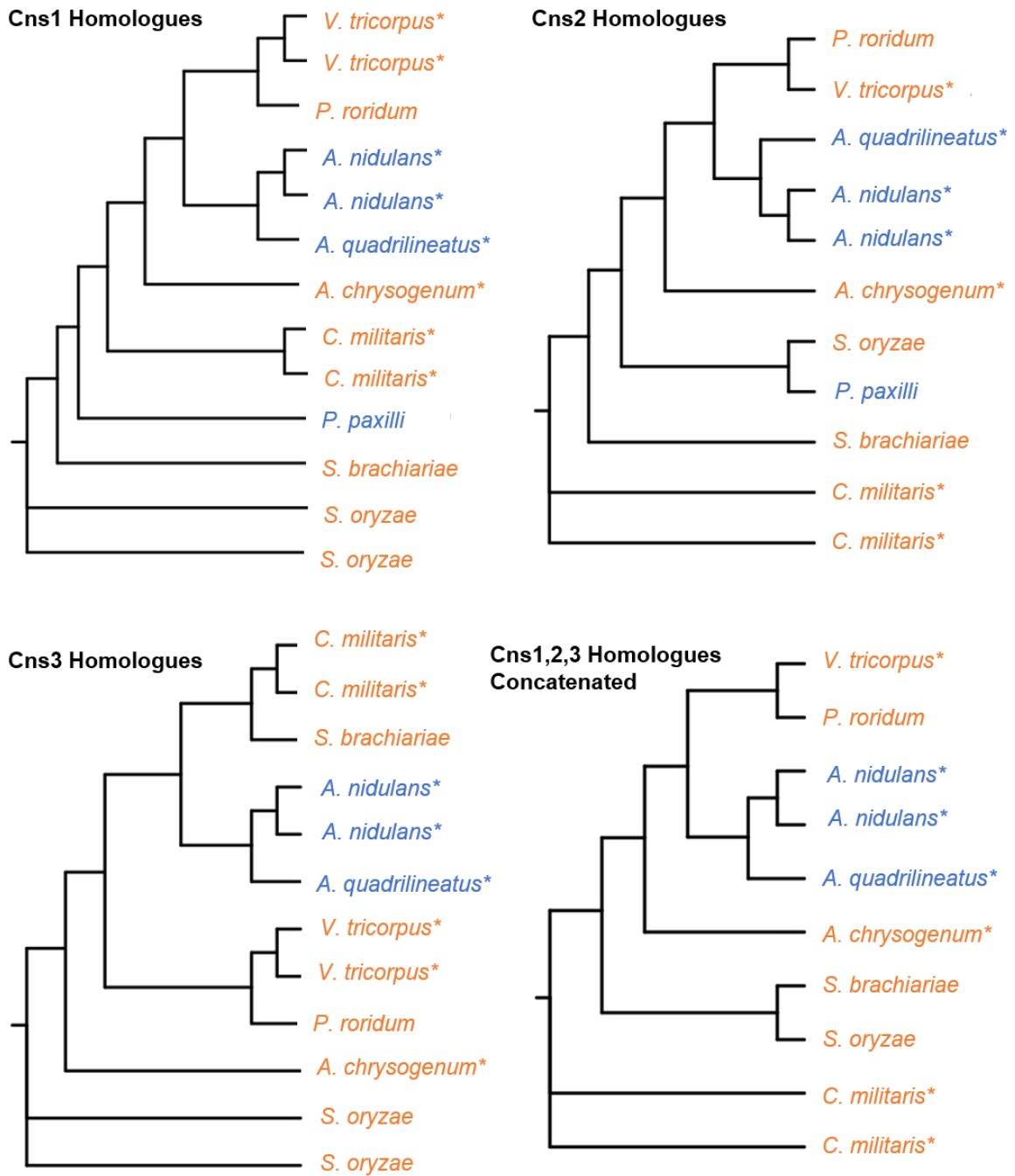


Figure 8.5: Phylogenies of *Cns1*, *2*, *3*, and concatenated *Cns* homologue sequences. The phylogeny.fr website was used to construct these. Alignment used was MUSCLE, with Gblocks curation; and a maximum likelihood construction method. Asterisks indicate the finding of a *Cns4* homologue in the same genome. Orange: Sordariomycetes; Blue: Eurotiomycetes.

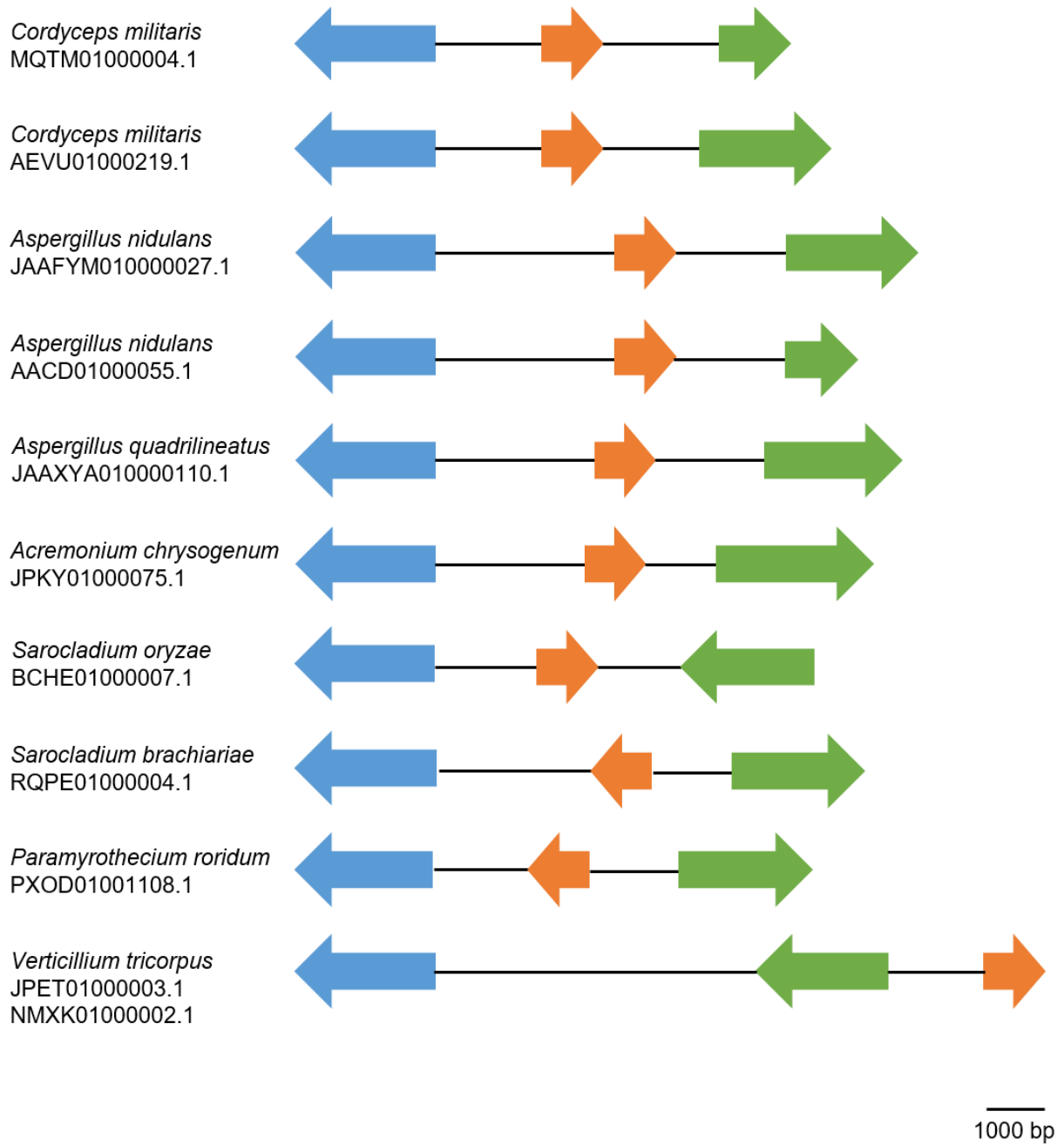


Figure 8.6: To-scale diagrams of the arrangement of *Cns1*, *2*, and *3* homologues in species possessing all three genes. Blue: *Cns1*, orange: *Cns2*, green: *Cns3* homologues.

8.2 CORDYCEPS MILITARIS IN PLANTS

Several of the fungal species found to possess gene clusters homologous to the cordycepin-pentostatin gene cluster in *C. militaris* reside in plants. Therefore preliminary experiments were performed to attempt the infection of crop plants with various strains of *Cordyceps militaris* – in order to establish whether this species can be endophytic. Soil was inoculated using spores from agar cultures of *C. militaris*. These efforts had limited success, with bands for *Cns1* (chosen for PCR detection locus) showing for some samples of rye, oat, buckwheat, and millet leaves from plants grown in *CM2*, *CM16*, *KCTC 6064*, and *CBS 128.25* isolate-inoculated soil [figure 8.7]. Care was taken to sterilise both soil and the surface of seeds prior to the experiments. Control (non-inoculated soil-grown) plants were also used. These techniques have mitigated against false positives resulting from contamination. Plants were kept apart from each other, and subjected to separately-performed treatments. These PCR matches indicate that *Cordyceps militaris* may be able to at least transiently infect a range of crop plant species, although this may be an artificially-opportunistic infection with high exposure from spores.

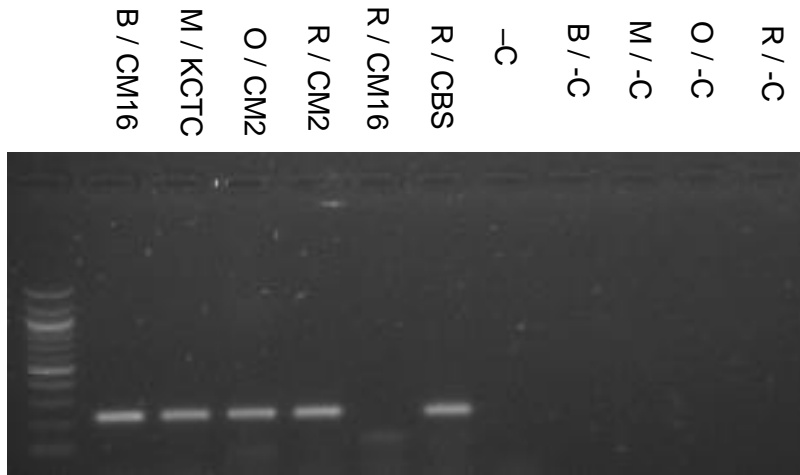


Figure 8.7: Agarose gel showing PCR screens for *Cordyceps militaris* in leaves following inoculation of soil with spores and subsequent seeding of plants. Primers for the *Cns1* gene were used. Conidia from four week old potato dextrose agar cultures of *C. militaris* isolates *CM2*, *CM16*, *KCTC 6064*, and *CBS 128.25*, suspended in sterile water were used for inoculation as indicated in labels above. B = buckwheat, M = millet, O = oat, R = rye. Control (-C) plants were not inoculated with spores; the -C lane is a no-template PCR control. Lane 1 has a 100bp ladder.

8.3 DISCUSSION

To consider the evolution of the cordycepin-pentostatin biosynthesis system it was pertinent to turn attention to the cordycepin-pentostatin gene cluster, the *Cns* genes. The findings from protein domain analysis and BLASTp searches support the functions of these genes described in the proposed synthesis pathway of cordycepin [Xia *et al.* 2017]. Protein *Cns1* is an oxidoreductase, whilst *Cns2* has a metal-dependent phosphohydrolase domain. The BLASTp searches suggest that the *Cns2* gene plays its role in the synthesis as a result of gene duplication and subfunctionalisation of the highly-conserved SAICAR synthase-encoding gene which plays an essential role early in purine synthesis. *Cns3* interestingly is a bifunctional

protein involved both in the synthesis of cordycepin and its protector molecule pentostatin – using the N-terminal nucleotide kinase domain and C-terminal HisG domain (present in ATP phosphoribosyltransferases) respectively. These descriptions not only support findings by Xia and colleagues but are also consistent with proposed synthesis pathway for vidarabine, another nucleoside analogue co-produced with pentostatin as the protector molecule [Xia *et al.* 2017; Wu *et al.* 2017]. The gene cluster for this system, present in the bacterium *Streptomyces antibioticus* also contains genes encoding (multiple) oxidoreductases, a phosphohydrolase, SAICAR synthase, and an ATP phosphoribosyl transferase [Wu *et al.* 2017]. Together these findings provide evidence that the production of nucleoside analogues can arise independently in different lineages. This convergent evolution has occurred via subfunctionalisation and/or gene duplication from elements of conserved purine metabolism.

Further to this, the results of the tBLASTn searches for homologues of *Cns1*, *Cns2* and *Cns3* in *C. militaris* found homologous cordycepin-pentostatin gene clusters in seven other fungal species – including two (*Aspergillus nidulans* and *Acremonium chrysogenum*) previously described [Xia *et al.* 2017] – and five others – *Aspergillus quadrilineatus*, *Sarocladium oryzae*, *Sarocladium brachiariae*, *Paramyrothecium roridum*, and *Verticillium tricorpus*). The three genes were proximally located in all of these. Given the large phylogenetic distances between some of these, as well as the total absence in many related species to these (most apparent in the *Aspergillus* genus) – these findings suggest the horizontal transfer of *Cns* genes between different species. Horizontal genetic transfers between eukaryotes are not particularly well known – but have been described before, for example between *Aspergillus* relative *Penicillium camemberti* and other species following contact in the food environment [Cheeseman *et al.* 2014].

If this were to be true, then perhaps the cordycepin-pentostatin gene cluster may have passed between different fungal species present in plants – given that *S. oryzae*, *P. roridum*, and *V. tricorpus* are known plant pathogens, and *S. brachiariae* an endophyte. There may be other fungal species containing the cluster not found here – and fungal species can have wide

geographical distributions. This raises the question of the evolutionary benefit of possessing this metabolic capability in the content of inhabiting a plant host – without which the trait would have surely been lost through deleterious mutations. This question is of further interest with regards to *Cordyceps militaris* considering the known endophytic life stages of related species (and fellow entomopathogens) such as *Beauveria bassiana* and *Metarhizium anisopliae* [Vega *et al.* 2008], which lack the ability to produce cordycepin. Cordycepin has been found to act as a transcription inhibitor in plants [Bai *et al.* 2018]. The results from the plant inoculation experiment with *C. militaris* indicate that this species may at least be able to develop opportunistic systemic infection of plants when roots are exposed to spores – although this work is preliminary.

Only seven species in addition to *C. militaris* were detected to have homologues of all genes *Cns1*, *Cns2*, and *Cns3* in the tBLASTn search results – thus possessing the complete set of genes involved in cordycepin and pentostatin synthesis known as yet. However, there were other species of interest which came up in the searches with matches to one of the *Cns* genes. *Paecilomyces hepiali* has been found to colonise *Ophiocordyceps sinensis*, and has been proposed to be responsible for its production of cordycepin and hence the cause of the long traditionally used (ethnopharmacological) effects of this fungus on inflammation and pain in the human body [Yu *et al.* 2016]. *P. hepiali* possesses a clear homologue to the *Cns3* gene, with an identity match of 80.8 per cent. It seems plausible that perhaps *P. hepiali* produces pentostatin (the synthesis for which *Cns3* is involved in), and that this compound, not cordycepin, causes the properties of *O. sinensis* remedies. *O. sinensis* extracts have previously been reported to contain no cordycepin, unlike *C. militaris* [Huang *et al.* 2003].

We may also speculate about another species of interest, which possesses a homologue to *Cns2*. This is *Aspergillus sydowii*, one of fifteen species in the genus to be identified here, which unlike relatives *A. nidulans* and *A. quadrilineatus* does not possess homologues to the other cordycepin synthesis genes *Cns1* and *Cns3*. *A. sydowii* has been found in sea fan corals (*Gorgonia spp.*), and reported to be a disease-causing pathogen of these animals in the

Caribbean [Alker *et al.* 2001], but since then has also been isolated from healthy hosts [Toledo-Hernandez *et al.* 2008]. This species has also been found in Mediterranean waters [Greco *et al.* 2017]; and may also not be as host specific as previously thought – having been found in a Caribbean sponge species *Spongia obscura* [Ein-Gil *et al.* 2009]. Interestingly, the nucleoside analogue vidarabine, produced in a similar protector-protégé system to cordycepin and also co-produced with pentostatin, has been found in a sea fan, *Gorgonia (Eunicella) cavolini* [Cimino *et al.* 1984]. A pair of similarly-modified nucleoside analogues, spongothymidine and spongouridine, are produced in the Caribbean sponge *Tectitethya crypta* [Mayer *et al.* 2010]. This suggests that the production of nucleoside analogues may be an effect conferred by the colonisation of fungi such as *Aspergillus sydowii* to their marine hosts – these animals. Studies on fungal assemblages in sponges have found over 80 taxa in one specimen [Paz *et al.* 2010; Wiese *et al.* 2011]. The terrestrial-marine boundary may not be a barrier to cosmopolitan ascomycete lineages and the secondary metabolites that they carry. This could be an important point, considering the potential pharmacological properties of nucleoside analogues – with cordycepin an anti-inflammatory, and vidarabine being an antiviral and leukaemia drug. Poriferan and coral hosts could represent a reservoir of nucleoside analogues and other future lead compounds.

CHAPTER 9: DISCUSSION AND CONCLUSIONS

When I started this PhD project, there was little published research investigating the role of cordycepin in the biology of the fungus best known to produce it – *Cordyceps militaris*. This was despite a wealth of research into the properties of cordycepin as a polyadenylation inhibitor and the resultant effects of its introduction into mammalian systems, particularly as an anti-inflammatory and in several signal transduction pathways [Radhi *et al.* 2021]. We had a two hypotheses on cordycepin production in *C. militaris* [Wellham *et al.* 2019]. Firstly we proposed that the ability to co-produce of cordycepin and pentostatin [Xia *et al.* 2017] had been passed between very few unrelated fungal species via horizontal transfer of the biosynthesis gene cluster. Secondly, we hypothesised that cordycepin aided the infection of *C. militaris*' insect host by suppressing the host immune system, and that pentostatin stabilised cordycepin in host cells. Evidence supporting both the hypotheses were obtained during this project.

9.1 Understanding Degeneration in *Cordyceps militaris*

In chapter 3, reduced expression of sexual development-related genes and reduced production of multiple metabolites were demonstrated to have occurred with reduced cordycepin production in a degenerated strain of the *Cordyceps militaris* isolate CM2. Degeneration has been described previously as a decline in cordycepin production by *C. militaris* cultures are repeated subcultivation over an extended period of time [Yi *et al.* 2017]. The results in chapter 3 suggest this process to have more complex effects than just a decline in the production of cordycepin and its protector molecule pentostatin. Among those downregulated were several velvet genes. Velvet proteins have roles as regulators of secondary metabolism and sexual development [Bayram & Braus 2012]. Therefore the

downregulation of master regulator methyl transferase-encoding gene *LaeA* and velvet genes in particular indicates that wider metabolic consequences, possibly mediated by epigenetic changes, are associated with degeneration. Other sexual development-related genes downstream of these regulators were also downregulated. These changes suggest that degeneration represents a shift in favour of the vegetative state and away from the teleomorph.

When the degenerated and parental control strains of the *CM2* isolate were compared in *Galleria mellonella* infection assays, described in chapter 5, it was evident that the degenerated strain produced a far lesser pathogenic response. This was marked particularly in reduced fungal emergence rates and levels of caterpillars injected with conidia, indicating a reduced growth rate and colonisation success in the host. It is evident that the degenerated strain has simultaneously reduced cordycepin and pentostatin production, reduced sexual development-related gene expression, and is poorer at successfully infecting a model insect host. This suggests a link between cordycepin production, sexual development, and pathogenicity. The latter two factors make sense considering the fact that infection of the host by *C. militaris* directly leads to formation of sexual fruiting bodies on fertile stromata. Further to this, experiments described in chapter 6, in which *C. militaris* cultures were extracted and cultured from caterpillar haemolymph one day after injection with spores, showed substantial upregulation of sexual development-related and cordycepin synthesis genes. This suggests that these genes are important in the early stages of infection.

9.2 Roles of Cordycepin and Pentostatin in *Cordyceps militaris*

The above findings play into the hypothesis that cordycepin plays a role in aiding the host infection process [Wellham *et al.* 2019; Woolley *et al.* 2020]. Insights into the biological role of this cordycepin were gained from experiments detailed particularly in chapter 5, using host models. Supporting previous findings, pure cordycepin was demonstrated to cause suppression of the upregulation of immune response genes in *Galleria mellonella* and *Drosophila melanogaster* cell models following stimulation with curdlan [Woolley *et al.* 2020].

The genes effected were *Lysozyme* and *Attacin A* respectively, measured in extracted haemolymph cells of injected *G. mellonella* and treated S2 cells of *D. melanogaster*.

No stringent evidence for the activity of pentostatin alone was obtained in the insect models. However, pentostatin enhanced the effects of cordycepin on immune gene expression in both the *D. melanogaster* (at a cordycepin low dose) and *G. mellonella* models. This supports the previous characterisation of pentostatin as a protector of cordycepin in the context of the host cell [Xia *et al.* 2017]. In caterpillars injected with washed conidia, additionally supplemented cordycepin with pentostatin enhanced the fungal emergence of the degenerated strain. These findings suggest that cordycepin aids the infection of the host by *C. militaris*, at least in part by suppression of the insect immune system; and that pentostatin, by stabilising cordycepin in the host cell, enhances these effects. It seems likely that the reduced capacity of the degenerated strain to infect the host is at least partly due to reduced cordycepin production by the fungus.

9.3 The *Cordyceps-Galleria* Model System

After a period of method development, described in chapter 4, a suitable model system was used for assessing *Cordyceps militaris* infection in an insect host. This system, consisting of the injection of conidia, cordycepin and pentostatin into *Galleria mellonella* larvae proved useful in gaining the insights from the results described above. Injection-based methods with these caterpillars, also used in other recent studies [Woolley *et al.* 2020; Kato *et al.* 2021] provide a new model for entomopathogenic fungal infection to complement research performed with related species *Beauveria bassiana* and *Metarhizium anisopliae*. Given the use of these two species in biological control, and the transferable effects of cordycepin demonstrated to aid their infection of insects [Woolley *et al.* 2020; Kato *et al.* 2021] – using this model could have implications for control of insect pests. The use of a degenerated strain and its parental control in this model system provides further insight into the problems faced when fungal species are cultured for long periods of time in laboratory conditions. We propose

that this is similar to the effects described as strain attenuation in the species used in bioinsecticides [Safavi 2012; Ansari & Butt 2011].

It is worth noting that the use of the *CM2* isolate, from which the parental control and degenerated (PCS and DS) strains were derived, provided an effectively clonal system. This was due to the fact that a single mating type was present and mating was not possible here for this heterothallic fungus. While this was ideal for control purposes, it should also be considered that gene expression differences, as well as phenotypic traits such as pathogenicity could be subject to higher variation should a mixture of two mating types have been used, i.e. a dikaryotic strain. Expression of sexual development-related genes in particular would likely be affected by the presence of both mating types. Finally, given a possible link between sexual development, cordycepin production, and pathogenicity, conditions favouring mating behaviour on a dikaryotic strain may also produce positive effects on cordycepin production or pathogenicity, or vice versa.

9.4 Evolution of Cordycepin and Pentostatin Biosynthesis

In chapter 8, BLAST searches using sequences from the genes *Cns1*, 2, and 3 in the cordycepin-synthesis biosynthesis gene cluster uncovered evidence for the production of these secondary metabolites in seven other fungal species, including two previously described [Xia *et al.* 2017]. In all of these matches, the homologous genes were arranged proximally, indicating co-production of cordycepin and pentostatin as in *C. militaris*. The large phylogenetic distances between some of these species, and the fact that only seven matches were uncovered after searches of genomes of over two and a half thousand fungal species indicate that this is a very rare trait. Furthermore, not one of the other 74 species within the Clavicipitaceae family with *C. militaris* was found to possess the gene cluster. These findings suggest that the biosynthesis of cordycepin with pentostatin has been passed between different species, by horizontal transfer of the gene cluster. The only species to be a known insect pathogen was *C. militaris* itself, with three of the others being known plant pathogens. It is evident that cordycepin and pentostatin co-production is not widely-used tool among

entomopathogens, and additionally that there are varying biological functions of these metabolites together in the ecology of different fungal species.

9.5 Further Work and Concluding Remarks

As well as the insights gained from successful experiments described above in the various chapters in this thesis, there were also challenges and experiments yielding negative results. Attempts were made to reverse the process of degeneration in the degenerated strain – restoring cordycepin production. These efforts involved exposure of the fungus to the host in several ways, using host-based cultivation media as well as the direct re-isolation from spore-injected caterpillars. A significantly-increased cordycepin production in the fungus was not achieved, with only a slight promising sign of increased expression of cordycepin and sexual-development related genes in the fungus that was isolated from caterpillar haemolymph one day post injection with spores. Perhaps only several repeats of this process would work, with the reversal of degeneration (like degeneration) being a gradual process. This could be the case if epigenetic control of gene expression is responsible for degeneration – and thus reversing these epigenetic changes is a similarly gradual process as the fungus adjusts to the new context of habitual exposure to hosts.

The *Cordyceps-Galleria* model system involving injections yielded interesting results. However, it had disadvantages – namely the inability to assess the point of death in caterpillars. Additionally, injections caused injury in the caterpillars, contributing to the melanisation, which can be a response to both infection and bodily damage. This was mitigated by the observation of only full melanisation; and by monitoring controls – which were far below the spore treated groups anyhow. However, less invasive methods for introducing fungal material and metabolites to the caterpillars were explored, with limited success. Generally these were unable to provide sufficient levels of infection. *Galleria mellonella* is a useful model species, being easily manipulated and having a sequenced genome – but it is not a known host of the fungus. In future work, a revised model system could be developed involving the use of a genuine host of *C. militaris*, and with more realistic field conditions –

perhaps in a location where the fungus grows commonly. In known host species of *C. militaris*, evolutionary adaptations to cordycepin production by the pathogen could be discovered. Effects of cordycepin on non-host insects in the wider ecology should be investigated if the application of the metabolite or the fungus were to be adopted for biological control use.

Artificial manipulation of the fungus could provide further verification of the role of cordycepin in host infection. This could include genetic modification of a high cordycepin-producing isolate, generating a knock-out mutant for cordycepin synthesis genes (*Cns* cluster); or conversely, over-expression via the transgenic introduction of a promoter and *Cns* gene cassette in a low cordycepin-producing isolate. The infection assay methods described in this thesis could be used to compare these mutants against appropriate controls.

In conclusion, this project has provided insights into the biological role of the modified nucleoside cordycepin, with its protector molecule pentostatin, in the ecology of *Cordyceps militaris*. This metabolite aids infection of the insect host via suppression of the insect immune system. Culture degeneration, marked by reduced cordycepin production, is accompanied by reduced sexual development-related gene expression, other metabolite changes and reduced pathogenic response. The co-production of cordycepin and pentostatin is attributed to a rare biosynthesis cluster only present in a handful of mostly distantly related fungi. There is evidence that it is a trait that has been subject to horizontal gene transfer and has a variety of purposes depending on ecological context of the species. These findings have potential implications of biological control of insect pests – further extension of an alternative method to using harmful pesticides by use of *C. militaris* as the control agent. Tailored selection of strains, or co-administration of fungal biological control agents with secondary metabolites could be pursued in this regard.

REFERENCES

- Adnan, M. et al. (2017):** Effect of pH, temperature and incubation time on cordycepin production from *Cordyceps militaris* using solid-state fermentation on various substrates. *CyTA Journal of Food*. 15: 617-621
- Alker, A. P. et al. (2001):** Characterisation of *Aspergillus sydowii* (Thom et Church), a fungal pathogen of Caribbean sea fan corals. *Hydrobiologia* 460: 105-111
- Altincicek, B. & Vilcinskis, A. (2006):** Metamorphosis and collagen-IV-fragments stimulate innate immune response in the greater wax moth, *Galleria mellonella*. *Developmental & Comparative Immunology* 30: 1108-1118
- Altincicek, B. et al. (2007):** Microbial metalloproteinases mediate sensing of invading pathogens and activate innate immune responses in the lepidopteran model host *Galleria mellonella*. *Infection and Immunity* 75: 175-183
- Aravind, L. & Koonin, E. V. (1998):** The HD domain defines a new superfamily of metal-dependent phosphohydrolases. *Trends in Biochemical Sciences*. 23: 469-472
- Aravind, L. et al. (2004):** A novel family of P-loop NTPases with an unusual phyletic distribution and transmembrane segments inserted within the NTPase domain. *Genome Biology*. 5: R30
- Ashraf, S. et al. (2019):** The polyadenylation inhibitor cordycepin reduces pain, inflammation and joint pathology in rodent models of osteoarthritis. *Scientific Reports*. 9: 4969
- Ashton, G. D. & Dyer, P. S. (2016):** Sexual development in fungi and its uses in gene expression systems. In: *Gene Expression Systems in Fungi: Advancements and Applications* (Eds: Schmoll, M. & Dattenbock, C.) (New York: Springer)
- Bai, B et al. (2018):** Combined transcriptome and translome analyses reveal a role for tryptophan-dependent auxin biosynthesis in the control of *DOG1*-dependent seed dormancy. *New Phytologist* 217: 1077-1085
- Baik, J. S. et al. (2012):** Cordycepin induces apoptosis in human neuroblastoma SK-N-BE(2)-C and melanoma SK-MEL-2 Cells. *Indian Journal of Biochemistry and Biophysics* 49: 86-91

- Basith, M. & Madelin, M. F. (1968):** Studies on the production of perithecial stromata by *Cordyceps militaris* in artificial culture. *Canadian Journal Botany* 46: 473-480
- Bastos, R. W. et al. (2020):** Functional characterisation of clinical isolates of the opportunistic fungal pathogen *Aspergillus nidulans*. *Molecular Biology & Physiology*. 5: e00153-20
- Bayram, O. S. & Braus, G. H. (2012):** Coordination of secondary metabolism and development in fungi: the velvet family of regulatory proteins. *FEMS Microbiology Reviews* 36: 1-24
- Bayram, O. S. et al. (2010):** LaeA control of velvet family regulatory proteins for light-dependent development and fungal cell-type specificity. *PLoS Genetics*
<https://doi.org/10.1371/journal.pgen.1001226>
- Bergerat, A. et al. (1997):** An atypical topoisomerase II from archaea with implications for meiotic recombination. *Nature* 386: 414-417
- Berry, D. et al. (2015):** Draft genome sequence of the filamentous fungus *Penicillium paxilli* (ATCC 26601). *Genome Announcements* 3: 2
- Bi, Y. et al. (2018):** Cordycepin augments the chemosensitivity of human glioma cells to temozolomide by activating AMPK and inhibiting the AKT signaling pathway. *Molecular Pharmaceutics*. 15: 4912-4925.
- Browne, N. et al. (2013):** An analysis of the structural and functional similarities of insect hemocytes and mammalian phagocytes. *Virulence* 4: 597-603
- Cannon, P. F. & Kirk, P. M. (2007):** *Fungal Families of the World*. (Wallingford: CABI Publishing)
- Cereneus, L. et al. (2008):** The proPO-system: pros and cons for its role in invertebrate immunity. *Trends in Immunology* 29: 263-271
- Chambers, M. C. et al. (2012):** How the fly balances its ability to combat different pathogens. *PLoS Pathogens* 8: e1002970.
- Chamcheu, J. C. (2019):** Role and therapeutic targeting of the PI3K/Akt/mTOR signaling pathway in skin cancer: a review of current status and future trends on natural and synthetic agents therapy. *Cells* 8: 803
- Champion, O. L. et al. (2018):** Standardization of *G. mellonella* larvae to provide reliable and reproducible results in the study of fungal pathogens. *Journal of Fungi* 4: 108

- Chandler, D. (2016):** Basic and applied research on entomopathogenic fungi. In: *Microbial Agents of Insect and Mite Pests: From Theory to Practice*. (Ed.: Lacey, L.) (New York: Academic Press)
- Chang, C. Y. et al. (2005):** Determination of adenosine, cordycepin and ergosterol contents in cultivate *Antrodia camphorate* by HPLC method. *Journal of Food and Drug Analysis* 13: 338-342
- Che, Z. M. et al. (2004):** Study on the breeding of a new variety of *Cordyceps militaris* by mutation with ultraviolet radiation. *Food and Fermentation Industries* 30: 35-38
- Cheeseman, K. et al. (2014):** Multiple recent horizontal transfers of a large genomic region in cheese making fungi. *Nature Communications* 5: 2876
- Chen, A. et al. (2017):** A Novel technique for rejuvenation of degenerated caterpillar medicinal mushroom, *Cordyceps militaris* (ascomycetes), a valued traditional Chinese medicine. *International Journal of Medicinal Mushrooms* 19: 87-91
- Chen, B. X. et al. (2020):** Transcriptome analysis reveals the flexibility of cordycepin network in *Cordyceps militaris* activated by L-alanine addition. *Frontiers of Microbiology* DOI: 10.3389/fmicb.2020.00577
- Chen, L. et al. (2018):** Metabolomic comparison between wild *Ophiocordyceps sinensis* and artificial cultured *Cordyceps militaris*. *Biomedical Chromatography* 32: e4279
- Chen, L. I. et al. (2012):** Fast determination of adenosine and cordycepin in *Cordyceps* and its deserted solid medium. *Chinese Journal of Chromatography* 30: 711-715
- Chen, Y. et al. (2019):** Study of the whole genome, methylome and transcriptome of *Cordyceps militaris*. *Scientific Reports* 9: 898
- Chiang, S. S. et al. (2017):** Effect of light-emitting diodes on the production of cordycepin, mannitol and adenosine in solid-state fermented rice by *Cordyceps militaris*. *Journal of Food Composition and Analysis* 60: 51-56
- Cho, H. J. et al. (2006):** Cordycepin (3'-deoxyadenosine) inhibits human platelet aggregation induced by U46619, a TXA2 analogue. *Journal of Pharmacy and Pharmacology* 58: 1677-1685
- Cho, H. J. et al. (2007):** Inhibitory effects of cordycepin (3'-deoxyadenosine), a component of *Cordyceps militaris*, on human platelet aggregation induced by thapsigargin. *Journal of Microbiology and Biotechnology* 17: 1134-1138

- Cho, Y. et al. (2008):** Discovery of novel nitrobenzothiazole inhibitors for *Mycobacterium tuberculosis* ATP phosphoribosyl transferase (HisG) through virtual screening. *Journal of Medicinal Chemistry* 51: 5984-5992
- Choi, S. et al. (2011):** Cordycepin-induced apoptosis and autophagy in breast cancer cells are independent of estrogen receptor. *Toxicology and Applied Pharmacology* 257: 165-168
- Choi, Y. H. et al. (2014):** Anti-inflammatory effects of cordycepin in lipopolysaccharide-stimulated RAW 264.7 macrophages through Toll-like receptor 4-mediated suppression of mitogen-activated protein kinases and NF- κ B signaling pathways. *Drug Design, Development and Therapy* 8: 1941
- Choi, Y. H. et al. (2014):** Anti-inflammatory effects of cordycepin in lipopolysaccharide-stimulated RAW 264.7 macrophages through toll-like receptor 4-mediated suppression of mitogen-activated protein kinases and NF-kappa B signaling Pathways. *Drug Design, Development and Therapy* 8: 1941-1953
- Chung, T. W. et al. (2004):** Novel and therapeutic effect of caffeic acid and caffeic acid phenyl ester on hepatocarcinoma cell: complete regression of hepatoma growth and metastasis by dual mechanism. *FASEB Journal* 18: 1670-1681
- Cimino, G. et al. (1984):** Antiviral agents from a gorgonian, *Eunicella cavolini*. *Experientia* 40: 339-340
- Creek, D. J. et al. (2012):** IDEOM: an excel interface for analysis of LC-MS-based metabolomics data. *Bioinformatics* 28: 1048-9
- Cui, Z. Y. et al. (2018):** Cordycepin induces apoptosis of human ovarian cancer cells by inhibiting CCL5-mediated Akt/NF- κ B signaling pathway. *Cell Death Discovery* 4: 1-11
- Cunningham, K. G. et al. (1950):** Cordycepin, a metabolic product isolated from cultures of *Cordyceps militaris* (Linn.) Link. *Nature* 166: 949
- Currie, C. R. et al. (2003):** Experimental evidence of a tripartite mutualism: bacteria protect ant fungus gardens from specialized parasites. *Oikos* 101: 91-102
- Das, S. K. et al. (2008):** A new approach for improving cordycepin productivity in surface liquid culture of *Cordyceps militaris* using high-energy ion beam irradiation. *Letters in Applied Microbiology* 47: 534-538
- Das, S. K. et al. (2010):** Optimization of culture medium for cordycepin production using *Cordyceps militaris* mutant obtained by ion beam irradiation. *Process Biochemistry* 45: 129-132

- Das, S. K. et al. (2010b):** Medicinal uses of the mushroom *Cordyceps militaris*: current state and prospects. *Fitoterapia* 81: 961-968
- Debuchy, R. et al. (2010):** Mating systems and sexual morphogenesis in ascomycetes. In: *Cellular and Molecular Biology of Filamentous Fungi*. (Eds: Borkovitch, K. & Ebbole, D.) (Washington DC: ASM Press)
- Desrosiers, R. C. et al. (1976):** The sensitivity of RNA polymerases I and II from Novikoff hepatoma (N1S1) cells to 3'-deoxyadenosine-5'-triphosphate. *Nucleic Acids Research* 3: 325-342
- Deville-Bonne, D. et al. (2010):** Human and viral nucleoside/nucleotide kinases involved in antiviral drug activation: structural and catalytic properties. *Antiviral Research* 86: 101-120
- Dixon, L. J. et al. (2009):** Host specialization and phylogenetic diversity of *Corynespora cassiicola*. *Phytopathology* 99: 1015-1027
- Doetsch, P. W. et al. (1981a):** Synthesis and characterization of (2'-5')ppp3'dA(p3'A)_n, an analogue of (2'-5')pppA(pA)_n. *Nature*. 291: 355-358
- Doetsch, P. W. et al. (1981b):** Core (2'-5') oligoadenylate and the cordycepin analog: inhibitors of epstein-barr virus induced transformation of human lymphocytes in the absence of interferon. *Proceedings of the National Academy of Sciences* 78: 6699-6703
- Dubovskiy, I. M. et al. (2013):** More than a colour change: insect melanism, disease resistance and fecundity. *Proceedings of the Royal Society B* 280: 20130584
- Duncan, R. F. (1995):** Cordycepin blocks recovery of non-heat-shock mRNA translation following heat shock in *Drosophila*. *European Journal of Biochemistry* 233: 784-792
- Dyer, P. S. et al. (2003):** Genomics reveals sexual secrets of *Aspergillus*. *Microbiology* 149: 2301-2303
- Eads, B. D. & Hand, S. C. (1999):** Regulatory features of transcription in isolated mitochondria from *Artemia franciscana* embryos. *American Journal of Physiology* R1588-R1597
- Egeblad, M. & Werb, Z. (2002):** New function for the matrix metalloproteinases in cancer progression. *Nature Reviews Cancer* 2: 161-74
- Ein-Gil, N. et al. (2009):** Presence of *Aspergillus sydowii*, a pathogen of gorgonian sea fans in the marine sponge *Spongia obscura*. *The ISME Journal* 3: 752-755

- El-Gebali, S. et al. (2019):** The Pfam protein families database in 2019. *Nucleic Acids Research* 47: D427-D437.
- Enthroth, S. et al. (2019):** High throughput proteomics identifies a high-accuracy 11 plasma protein biomarker signature for ovarian cancer. *Communications Biology* 2: 221
- Fan, D. D. et al. (2012):** Enhancement of cordycepin production in submerged cultures of *Cordyceps militaris* by addition of ferrous sulfate. *Biochemical Engineering Journal* 60: 30-35
- Fan, H. et al. (2006):** Qualitative and quantitative determination of nucleosides, bases and their analogues in natural and cultured *Cordyceps* by pressurized liquid extraction and high performance liquid chromatography–electrospray ionization tandem mass spectrometry (HPLC–ESI–MS/MS). *Analytical Chimica Acta* 567: 218-228
- Farmer, P. B. & Suhadolnik, R. J. (1972):** Nucleoside antibiotics. Biosynthesis of arabinofuranosyladenine by *Streptomyces antibioticus*. *Biochemistry* 11: 911-916
- Galagan, J. E. et al. (2005):** Sequencing of *Aspergillus nidulans* and comparative analysis with *A. fumigatus* and *A. oryzae*. *Nature* 438(7071): 1105-1115
- Gallagher, B. M. & Hartig, W. J. (1976):** Utilization of uridine for RNA synthesis in the insect cell line CP-1268 derived from the codling moth, *Laspeyresia pomonella*. *In Vitro* 12: 165-172
- Gao, S. et al. (2014):** Genome sequence and virulence variation-related transcriptome profiles of *Curvularia lunata*, an important maize pathogenic fungus. *BMC Genomics* 15: 627
- Gauthier, C. et al. (2003):** Functional similarities and differences between *Candida albicans* Cdr1p and Cdr2p transporters. *Antimicrobial Agents and Chemotherapy* 47: 1543-1554
- Gobert, V. et al. (2003):** Dual activation of *Drosophila* toll pathway by two pattern recognition receptors. *Science* 302(5653): 2126-2130
- Gong, J. et al. (2018):** Lentiviral vector-mediated SHC3 silencing exacerbates oxidative stress injury in nigral dopamine neurons by regulating the PI3K-AKT-FoxO signaling pathway in rats with Parkinson's disease. *Cellular Physiology and Biochemistry* 49: 971-984
- Gopalan, H. N. B. (1973):** Cordycepin inhibits induction of puffs by ions in *Chironomus* salivary gland chromosomes. *Experientia* 29: 724-726
- Grayson, S. & Berry, S. J. (1973):** Estimation of the half-life of a secretory protein message. *Science* 180(4090): 1071-1072

- Greco, G. et al. (2017):** Another possible risk for the Mediterranean Sea? *Aspergillus sydowii* discovered in the Port of Genoa (Ligurian Sea, Italy). *Marine Pollution Bulletin*. 122: 470-474
- Guijas, C. et al. (2018):** Metabolomics activity screening for identifying metabolites that modulate phenotype. *Nature Biotechnology* 36: 316-320
- Guo, F. Q. et al. (2006):** Identification and determination of nucleosides in *Cordyceps sinensis* and its substitutes by high performance liquid chromatography with mass spectrometric detection. *Journal of Pharmaceutical and Biomedical Analysis* 40: 623-630
- Haering, C. H. et al. (2003):** Building and breaking bridges between sister chromatids. *Bioessays* 25: 1178-1191
- Hanvey, J. C. et al. (1984):** Evidence for the conversion of adenosine to 2'-deoxycoformycin by *Streptomyces antibioticus*. *Biochemistry* 23: 904-907
- Hanvey, J. C. et al. (1988):** 8-Ketodeoxycoformycin and 8-ketocoformycin as intermediates in the biosynthesis of 2'-deoxycoformycin and coformycin. *Biochemistry* 27: 5790-5795
- Hawksworth, D. I. (2001):** The magnitude of fungal diversity: the 1.5 million species estimate revisited. *Mycological Research* 105: 1422-1432
- Hawley, S. A. (2020):** Mechanism of activation of AMPK by cordycepin. *Cell Chemical Biology* 27: 214-222
- He, L. et al. (2009):** Effect of mineral elements on colony types of *Cordyceps militaris* in subculturing. *Journal of Shenyang Agricultural University* 40: 672-677
- He, W. et al. (2010):** Cordycepin induces apoptosis by enhancing jnk and p38 kinase activity and increasing the protein expression of bcl-2 pro-apoptotic molecules. *Journal of Shenyang Agricultural University* 11: 654-656
- He, Y. et al. (2019):** Metabolomic variation in wild and cultured *Cordyceps* and mycelia of *Isaria cicadae*. *Biomedical Chromatography* 33: e4478
- Heppner, F. L. & Becher, B. (2015):** *Immune attack: the role of inflammation in Alzheimer disease*. 16: 358r372.
- Hibbett, D. S. et al. (2007):** A higher-level phylogenetic classification of the fungi. *Mycological Research* 111: 509-547

- Hittalmani, S. et al. (2016):** De novo genome assembly and annotation of rice sheath rot fungus *Sarocladium oryzae* reveals genes involved in helvolic acid and cerulenin biosynthesis pathways. *BMC Genomics* 1791: 271
- Ho, D. W. H. et al. (2019):** Single-cell transcriptomics reveals the landscape of intra-tumoral heterogeneity and stemness-related subpopulations in liver cancer. *Cancer Letters* 459: 176-185
- Hodge, K. T. (2003):** Clavicipitaceous anamorphs. In: *Clavicipitalean Fungi*. (Eds: White, J. F. et al.) (New York: Marcel Dekker)
- Holbein, S. et al. (2009):** Cordycepin interferes with 3' end formation in yeast independently of its potential to terminate RNA chain elongation. *RNA* 15: 837-849
- Holliday, J. et al. (2004):** Analysis of quality and techniques for hybridization of medicinal fungus *Cordyceps sinensis*. *International Journal of Medicinal Mushrooms* 6: 147-160
- Hong, I. P. et al. (2010):** Fruit body formation on silkworm by *Cordyceps militaris*. *Mycobiology* 38: 128-132
- Hong, S. et al. (2005):** Ascochlorin inhibits matrix metalloproteinase-9 expression by suppressing activator protein-1-mediated gene expression through the ERK1/2 signaling pathway: inhibitory effects of ascochlorin on the invasion of renal carcinoma cells. *Journal of Biological Chemistry* 280: 25202-25207
- Hongsanan, S. et al. (2017):** An updated phylogeny of sordariomycetes based of phylogenetic and molecular clock evidence. *Fungal Diversity* 84: 25-41
- Huang, L. et al. (2009):** Determination and analysis of cordycepin and adenosine in the products of *Cordyceps* spp. *African Journal of Microbiology Research* 3: 957-961
- Huang, L. F. et al. (2003):** Simultaneous separation and determination of active components in *Cordyceps sinensis* and *Cordyceps militaris* by LC/ESI-MS. *Journal of Pharmaceutical and Biomedical Analysis* 33: 1155-1162
- Huang, L. F. et al. (2004):** Simultaneous determination of adenine, uridine, and adenosine in *Cordyceps sinensis* and its substitutes by LC/ESI-MS. *Journal of the Central South University of Technology* 11: 295-299
- Humber, R. A. (2000):** Fungal pathogens and parasites of insects. In: *Applied Microbial Systematics* (Eds: Priest F. & Goodfellow, M.) (Kluwer Academic)
- Hung, L. T. et al. (2009):** Effect of temperature on cordycepin production in *Cordyceps militaris*. *Thai Journal of Agricultural Science* 42: 219-225

- Hung, L. W. et al. (1998):** Crystal structure of the ATP-binding subunit of an ABC transporter. *Nature* 396: 703-707
- Hung, Y. P. (2015):** Effect of the salts of deep ocean water on the production of cordycepin and adenosine of *Cordyceps militaris*-Fermented Product. *AMB Express* 5: 53
- Hunter, K. W. et al. (2008):** Mechanisms of metastasis. *Breast Cancer Research* 10: S2
- Huxham, I. M. et al. (1989):** Inhibitory effects of cyclodepsipeptides, destruxins, from the fungus *Metarhizium anisopliae*, on cellular immunity in insects. *Journal of Insect Physiology* 35: 97-105
- Hywel-Jones, N. L. (2002):** Multiples of eight in *Cordyceps* ascospores. *Mycological Research* 106: 2-3
- Jacyna, J. et al. (2019):** Urinary metabolomic signature of muscle-invasive bladder cancer: a multiplatform approach. *Talanta* 202: 572-579
- James, T. Y. et al. (2006):** Reconstructing the early evolution of the fungi using a six gene phylogeny. *Nature* 443: 818-822
- Jeong, J. W. et al. (2011):** Induction of apoptosis by cordycepin via reactive oxygen species generation in human leukemia cells. *Toxicology In Vitro* 25: 817-824
- Ji, R. R. et al. (2016):** Pain regulation by non-neuronal cells and inflammation. *Science* 354: 572-577
- Jiang, Y. & Yao, Y. J. (2002):** Names related to *Cordyceps sinensis* anamorph. *Mycotaxon* 84: 245-254
- Jiansheng, M. (2008):** Research progress on the extraction and purification of cordycepin from *Cordyceps militaris*. *Journal of Anhui Agricultural Sciences* 36: 1929
- Jin, L. H. et al. (2008a):** Identification and functional analysis of antifungal immune response genes in *Drosophila*. *PLoS Pathogens* 4: e1000168
- Jin, L. H. et al. (2008b):** Microarray analysis of the gene expression profiles of SL2 cells stimulated by LPS/PNG and curdlan. *Molecules & Cells* 25: 553-558.
- Jorjao, A. L. et al. (2018):** From moths to caterpillars: ideal conditions for *Galleria mellonella* rearing for *in vivo* microbiological studies. *Virulence* 9: 383-389
- Kang, N. et al. (2017):** Development of high cordycepin-producing *Cordyceps militaris* strains. *Mycobiology* 45: 31-38

- Karaffa, L. & Kubicek, C. P. (2003):** *Aspergillus niger* citric acid accumulation: do we understand this well working black box? *Applied Microbiology and Biotechnology* 61: 189-196
- Karlson, P. (1984):** *Kurzes Lehrbuch der Biochemie 12* (New York: Auflage Thieme)
- Kato, T. et al. (2021):** Effects of cordycepin in *Cordyceps militaris* during its injection to silkworm larvae. *Microorganisms*. 9: 681.
- Keeney, S. et al. (1997):** Meiosis-specific DNA double-strand breaks are catalysed by Spo11, a member of a widely conserved protein family. *Cell* 88: 375-384
- Kibbe, W. A. (2007):** OligoCalc: an online oligonucleotide properties calculator. *Nucleic Acids Research* 35: W43-W46
- Kim, D. H. et al. (2015):** LC-MS-based absolute metabolite quantification: application to metabolic flux measurement in trypanosomes. *Metabolomics* 11: 1721-1732
- Kim, H. G. et al. (2006):** Cordycepin inhibits lipopolysaccharide-induced inflammation by the suppression of NF-Kapp β through Akt and p38 inhibition in RAW 264.7 macrophage cells. *European Journal of Pharmacology* 18: 192-197
- Kim, H. S. et al. (2002):** The *VeA* gene activates sexual development in *Aspergillus nidulans*. *Fungal Genetics and Biology* 37: 72-80
- Kim, J. R. et al. (2002):** Larvicidal Activity against *Plutella xylostella* of cordycepin from the fruiting body of *Cordyceps militaris*. *Pest Management Science* 58: 713-717
- Kingston, R. L. et al. (1996):** The structure of glucose-fructose oxidoreductase from *Zymomonas mobilis*: an osmoprotective periplasmic enzyme containing non-dissociable NADP. *Structure* 4: 1413-1428
- Kirk, P. M. (2020):** Index Fungorum & Species Fungorum websites. indexfungorum.org speciesfungorum.org (Accessed 2020)
- Kirk, P. M. et al. (Eds.) (2008):** *Dictionary of the Fungi*, 10th Edition. (Wallingford: CABI Publishing)
- Klenow, H. (1963):** Formation of the mono-, di- and triphosphate of cordycepin in ehrlich ascites-tumour cells *in Vitro*. *Biochimica et Biophysica Acta* 76: 347-353
- Kobayashi, Y. (1982):** Key to the taxa of the genera *Cordyceps* and *Torrubiella*. *Transactions of the Mycological Society of Japan* 23: 29-364

- Kodama, K. et al. (1979):** Isolation of 2'-deoxycoformycin and cordycepin from wheat bran culture of *Aspergillus nidulans* Y 176-2. *Agricultural and Biological Chemistry* 43: 2375-2377
- Kolas, N. K. et al. (2004):** Novel and diverse functions of the DNA mismatch repair family in mammalian meiosis and recombination. *Cytogenetic and Genome Research* 107: 216-231
- Kondrashov, A. et al. (2012):** Inhibition of polyadenylation reduces inflammatory gene induction. *RNA* 18: 2236-2250
- Kong, H. G. et al. (2019):** The *Galleria mellonella* hologenome supports microbiota-independent metabolism of long-chain hydrocarbon beeswax. *Cell Reports* 26: 2451-2464
- Kramer, G. J. & Nodwell, J. R. (2017):** Chromosome level assembly and secondary metabolite potential of the parasitic fungus *Cordyceps militaris*. *BMC Genomics* 18: DOI: 10.1186/s12864-017-4307-0
- Kredich, N. M. & Guarino, A. J. (1960):** An improved method of isolation and determination of cordycepin. *Biochimica et Biophysica Acta* 41: 361-363
- Kryukov et al. (2014):** Insecticidal and immunosuppressive effect of the ascomycete *Cordyceps miliatrix* on the larvae of the colorado potato beetle *Leptinotarsa decemlineata*. *Biology Bulletin* 4: 276-283.
- Kryukov, V. Y. et al. (2011):** Local epizootics caused by teleomorphic cordycipitoid fungi (Ascomycota: Hypocreales) in populations of forest lepidopterans and sawflies of the summer–autumn complex in siberia. *Microbiology* 80: 286-295.
- Kuan, C. S. et al. (2015):** Dissecting the fungal biology of *Bipolaris papendorfii*: from phylogenetic to comparative genomic analysis. *DNA Research* 22: 219-232
- Kwadha, C. A. et al. (2017):** The biology and control of the greater wax moth, *Galleria mellonella*. *Insects* 8: 61
- Lange, A. et al. (2018):** Genome sequence of *Galleria mellonella* (greater wax moth). *Genome Announcements* 6: e01220-17
- Lee, E. J. et al. (2009):** Cordycepin causes p21WAF1-mediated G2/M cell-cycle arrest by regulating c-jun N-terminal kinase activation in human bladder cancer cells. *Archives of Biochemistry and Biophysics* 490: 103-106
- Lee, E. J. et al. (2010):** Cordycepin suppresses TNF-alpha-induced invasion, migration, and matrix metalloproteinase-9 expression in human bladder cancer cells. *Phytotherapy Research* 24: 1755-1756

- Lee, H. H. et al. (2017):** Characterization of newly bred *Cordyceps militaris* strains for higher production of cordycepin through HPLC and URP-PCR analysis. *Journal of Microbiology and Biotechnology* 27: 1223-1232
- Lee, S. K. et al. (2019):** Improved cordycepin production by *Cordyceps militaris* KYL05 using casein hydrolysate in submerged conditions. *Biomolecules*. 9: 461
- Lennon, M. B. & Suhadolnik, R. J. (1976):** Biosynthesis of 3'-deoxyadenosine by *Cordyceps militaris*: mechanism of reduction. *Biochimica et Biophysica Acta* 425: 532-536
- Levdikov, V. M. et al. (1998):** The structure of SAICAR synthase: an enzyme in the *de novo* pathway of purine nucleotide biosynthesis. *Structure* 6: 363-376
- Li, L. et al. (2019):** Metabonomics study of the serum from ovarian cancer patients. *European Journal of Gynaecological Oncology* 40: 722-727
- Li, Y. & Nzabanita, C. (2019):** Study on swainsonine in *Alternaria gansuense* with genomics and liquid chromatography mass spectrometry. Unpublished
- Liu, X. B. et al. (2017):** *Sarocladium brachiariae* sp. nov., an endophytic fungus isolated from *Brachiaria brizantha*. *Mycosphere* 8: 827-834
- Liu, Y. Q. et al. (2012):** Ribavirin, a nucleoside with potential insecticidal activity. *Pest Management Science* 68: 1400-1404
- Liu, Z. et al. (2002):** Molecular evidence for teleomorph-anamorph connections in *Cordyceps* Based on ITS-5.8S rDNA sequences. *Mycological Research* 106: 1100-1108
- Lopez, D. et al. (2018):** Genome-wide analysis of *Corynespora cassiicola* leaf fall disease putative effectors. *Front Microbiol.* DOI: doi.org/10.3389/fmicb.2018.00276
- Lou, H. et al. (2019):** Advances in research on *Cordyceps militaris* degeneration. *Applied Microbiology and Biotechnology* 103: 7835-7841
- Lu, A. et al. (2014):** Insect prophenoloxidase: The view beyond immunity. *Frontiers of Physiology* 5: 252
- Maina, U. M. et al. (2018):** A review on the use of entomopathogenic fungi in the management of insect pests of field crops. *Journal of Entomology and Zoology Studies* 6: 27-32
- Manabe, R. et al. (2015):** Genome sequencing of eukaryotic microorganisms. Unpublished

- Mao, X. B. et al. (2004):** Hyperproduction of cordycepin by two-stage dissolved oxygen control in submerged cultivation of medicinal mushroom *Cordyceps militaris* in bioreactors. *Biotechnology Progress* 20: 1408-1413
- Mao, X. B. et al. (2005):** Optimization of carbon source and carbon/nitrogen ratio for cordycepin production by submerged cultivation of medicinal mushroom *Cordyceps militaris*. *Process Biochemistry* 40: 1667-1672
- Mao, X. B. et al. (2006):** Significant effect of NH₄⁺ on cordycepin production by submerged cultivation of medicinal mushroom *Cordyceps militaris*. *Enzyme Microbial Technology* 38: 343-350
- Mascarin, G. B. & Jaronski, S. T. (2016):** The production and uses of *Beauveria bassiana* as a microbial insecticide. *World Journal of Microbiology and Biotechnology* 32: 177
- Mascarin, G. M. & Jaronski, S. T. (2016):** The production and uses of *Beauveria bassiana* as a microbial insecticide. *World Journal of Microbiology and Biotechnology* 32: 177
- Masuda, M. et al. (2007):** Enhanced production of cordycepin by surface culture using the medicinal mushroom *Cordyceps militaris*. *Enzyme Microbial Technology* 40: 1199-1205
- Masuda, M. et al. (2011):** Production of cordycepin by a repeated batch culture of a *Cordyceps militaris* mutant obtained by proton beam irradiation. *Journal of Bioscience and Bioengineering* 111: 55-60
- Mateo, J. et al. (2020):** Genomics of lethal prostate cancer at diagnosis and castration resistance. *Journal of Clinical Investigation* 130: 1743-1751
- Mayer, A. M. S. et al. (2010):** The odyssey of marine pharmaceuticals: a current pipeline perspective. *Trends in Pharmacological Sciences* 31: 255-265
- Metzenberg, R. L. & Glass, N. L. (1990):** Mating type and mating strategies in *Neurospora*. *Bioessays* 12: 53-59
- Minson, A. C. & Creaser, E. H. (1969):** Purification of a trifunctional enzyme, catalysing three steps of the histidine pathway, from *Neurospora crassa*. *Biochemical Journal* 114: 49-56
- Mitchell, J. P. & Carmody, R. J. (2018):** *International Review of Cell and Molecular Biology* Vol. 335. (Elsevier).
- Moore, D. et al. (2011):** *21st Century Guidebook to Fungi*. (Cambridge University Press)

- Mushtaq, S. et al. (2018):** Natural products as reservoirs of novel therapeutic agents. *EXCLI Journal* 17: 420-451
- Nakamura, H. et al. (1974):** Structure of coformycin, an unusual nucleoside of microbial origin. *Journal of the American Chemical Society* 96: 4327-4328
- NCBI Database Websites:** BLAST (<https://blast.ncbi.nlm.nih.gov/>); conserved domains database (CDD) (<https://www.ncbi.nlm.nih.gov/cdd/>). Accessed in 2020.
- Ng, T. B. & Wang, H. X. (2005):** Pharmacological actions of *Cordyceps*, a prized folk medicine. *Journal of Pharmacy and Pharmacology* 57: 1509-1519.
- Ni, M. & Yu, J. H. (2007):** A novel regulator couples sporogenesis and trehalose biogenesis in *Aspergillus nidulans*. *PLoS One* 2: e970
- Ni, M. & Yu, J. H. (2007):** A novel regulator couples sporogenesis and trehalose biogenesis in *Aspergillus nidulans*. *PLoS One* 2: e970
- Nikoh, N. & Fukatsu, T. (2000):** Interkingdom host jumping underground: phylogenetic analysis of entomoparasitic fungi of genus *Cordyceps*. *Molecular Biology and Evolution* 17: 629-638
- Noh, E. M. et al. (2010):** Cordycepin inhibits TPA-induced matrix metalloproteinase-9 expression by suppressing the MAPK/AP-1 pathway in MCF-7 human breast cancer cells. *International Journal of Molecular Medicine* 25: 255-260
- Oh, J. et al. (2019):** Metabolomic profiling reveals enrichment of cordycepin in senescence process of *Cordyceps militaris* fruit bodies. *Journal of Microbiology* 57: 54-63
- Ohm, R. A. et al. (2012):** Diverse lifestyles and strategies of plant pathogenesis encoded in the genomes of eighteen Dothideomycetes fungi. *PLoS Pathogens* 8: e1003037
- Overgaard, K. H. (1964):** The inhibition of 5-phosphoribosyl-1-pyrophosphate formation by cordycepin triphosphate in extracts of Ehrlich ascites tumor cells. *Biochimica et Biophysica Acta* 80: 504-507
- Pan, B. S. et al. (2015):** Cordycepin induced MA-10 mouse Leydig tumor cell apoptosis by regulating p38 MAPKs and PI3K/AKT signaling pathways. *Scientific Reports*. 5: 13372
- Paoletti, M. et al. (2007):** Mating type and the genetic basis of self-fertility in the model fungus *Aspergillus nidulans*. *Current Biology* 17: 1384-1389
- Pareek, V. et al. (2020):** Metabolomics and mass spectrometry imaging reveal channelled de novo purine synthesis in cells. *Science* 368(6488): 283-290

- Paz, Z. et al. (2010):** Diversity and potential antifungal properties of fungi associated with a Mediterranean sponge. *Fungal Diversity* 42: 17-26
- Pegler, D. N. et al. (1994):** The Chinese “Caterpillar Fungus”. *Mycologist* 8: 3-5
- Peng, W. et al. (2019):** Integrated transcriptomics, proteomics, and glycomics reveals the association between up-regulation of sialylated n-glycans/integrin and breast cancer brain metastasis. *Scientific Reports* 9: 17361
- Pereira, T. C. et al. (2018):** Recent advances in the use of *Galleria mellonella* model to study immune responses against human pathogens. *Journal of Fungi* 4: 128
- Piotrowski, I. et al. (2020):** Interplay between inflammation and cancer. *Reports of Practical Oncology and Radiotherapy: Journal of Great Poland Cancer Center in Poznan and Polish Society of Radiation Oncology*. 25: 422
- Posada, F. and Vega, F. E. (2005):** Establishment of the fungal entomopathogen *Beauveria bassiana* (Ascomycota: Hypocreales) as an endophyte in cocoa seedlings (*Theobroma cacao*). *Mycologia* 97: 1195-1200
- Proctor, R. H. et al. (2018):** Evolution of structural diversity of trichothecenes, a family of toxins produced by plant pathogenic and entomopathogenic fungi. *PLoS Pathogens* 14: e1006946
- Rachmawati, R. et al. (2018):** Production of the insect toxin beauvericin from entomopathogenic fungi *Cordyceps militaris* by heterologous expression of global regulator. *Agrivita* 40: 177-184
- Radhi, M. et al. (2021):** A systematic review of the biological effects of cordycepin. Unpublished.
- Rajarammohan, S. (2019):** Near-complete genome assembly of *Alternaria brassicae* - a necrotrophic pathogen of Brassica crops. *Molecular Plant-Microbe Interactions* 32: 928-930
- Ramarao, N. et al. (2012):** The insect *Galleria mellonella* as a powerful infection model to investigate bacterial pathogenesis. *Journal of Visual Experiments* 70: e4392
- Rao, Y. K. et al. (2010):** Constituents isolated from *Cordyceps militaris* suppress enhanced inflammatory mediator’s production and human cancer cell proliferation. *Journal of Ethnopharmacology* 131: 363-364
- Reizer, J. et al. (1992):** A new subfamily of bacterial ABC-type transport systems catalyzing export of drugs and carbohydrates. *Protein Science* 1: 1326-1332

- Rinschen, M. M. et al. (2019):** Identification of bioactive metabolites using activity metabolomics. *Nature Reviews Molecular Cell Biology* 20: 353-367
- Ropars, J. et al. (2013):** *Penicillium* genomes assembly and annotation. Unpublished
- Rottman, F. & Guarino, A. J. (1964):** The inhibition of phosphoribosyl-pyrophosphate amidotransferase activity by cordycepin monophosphate. *Biochimica et Biophysica Acta* 89: 465-468
- Rowland, P. et al. (1994):** The three-dimensional structure of glucose 6-phosphate dehydrogenase from *Leuconostoc mesenteroides* refined at 2.0Å resolution. *Structure* 2: 1073-1087
- Saboury, A. A. et al. (2002):** A product inhibition study on adenosine deaminase by spectroscopy and calorimetry. *Journal of Biochemistry and Molecular Biology* 35: 302-303
- Samuels, R. I. et al. (1988):** The role of destruxins in the pathogenicity of 3 strains of *Metarhizium anisopliae* for the tobacco hornworm *Manduca sexta*. *Mycopathologia* 104: 51-58
- Sari, N. et al. (2016):** Improved cordycepin production in a liquid surface culture of *Cordyceps militaris* isolated from wild strain. *Biotechnology and Bioprocess Engineering* 21: 595-600
- Sato, H. & Shimadzu, M. (2002):** Stromata production for *Cordyceps militaris* (Clavicipitales: Clavicipitaceae) by injection of hyphal bodies to alternative host insects. *Applied Entomology and Zoology* 37: 85-92
- Schatschneider, S. et al. (2018):** Quantitative isotope-dilution high-resolution-mass-spectrometry analysis of multiple intracellular metabolites in *Clostridium autoethanogenum* with uniformly ¹³C-labeled standards derived from *Spirulina*. *Analytical Chemistry* 90: 4470-4477
- Scheltema, R. A. et al. (2011):** PeakML/mzMatch: a file format, Java library, R library, and tool-chain for mass spectrometry data analysis. *Analytical Chemistry* 83: 2786-93
- Schroder, H. C. et al. (1981):** A novel metabolic effect of the adenosine deaminase inhibitor coformycin, a potentiator of antiviral adenosine analogues. *Antiviral Research* 1: 383-391
- Schroeder, A. et al. (2006):** The RIN: an RNA integrity number for assigning integrity values to RNA measurements. *BMC Molecular Biology* 7:3
- Schurko, A. M. & Logsdon, J. M. (2008):** Using a meiosis detection toolkit to investigate ancient asexual “scandals” and the evolution of sex. *BioEssays* 30: 579-589

- Seidl, M. F. et al. (2015):** The genome of the saprophytic fungus *Verticillium tricorpus* reveals a complex effector repertoire resembling that of its pathogenic relatives. *Molecular Plant-Microbe Interactions* 28: 362-373
- Seo, J. A. et al. (2004):** The *gprA* and *gprB* genes encode putative G protein-coupled receptors required for self-fertilization in *Aspergillus nidulans*. *Molecular Microbiology* 53: 1611-1623
- Seo, J. W. et al. (2018):** Application of metabolomics in prediction of lymph node metastasis in papillary thyroid carcinoma. *PLoS One* 13: e0193883
- Serafini, M. S. et al. (2020):** Transcriptomics and epigenomics in head and neck cancer: available repositories and molecular signatures. *Cancer of the Head & Neck*. 5: 2
- Shih, I. L. et al. (2007):** Effects of culture conditions on the mycelial growth and bioactive metabolite production in submerged culture of *Cordyceps militaris*. *Biochemical Engineering Journal* 33: 193-201
- Shi-Kunne, X. et al. (2017):** Evolution within the fungal genus *Verticillium* is characterised by chromosomal rearrangement and gene loss. *Environ. Microbiology* 20: 1362-1373
- Showalter et al. (1992):** Improved production of pentostatin and identification of fermentation cometabolites. *Journal of Antibiotics* 45: 1914-1918
- Shrestha, B. et al. (2004):** Instability in *in Vitro* fruiting of *Cordyceps militaris*. *Journal of Mushroom Science and Production* 2: 140-144
- Shrestha, B. et al. (2005):** Distribution and *in vitro* fruiting of *Cordyceps militaris* in Korea. *Mycobiology* 33: 178-181
- Shrestha, B. et al. (2012):** The medicinal fungus *Cordyceps militaris*: research and development. *Mycological Progress* DOI 10.1007/s11557-012-0825-y
- Shrestha, B. et al. (2016):** Coleopteran and Lepidopteran hosts of the entomopathogenic genus *Cordyceps* sensu lato. *Journal of Mycology* 2016 Article 7648219
- Silva, R. et al. (2020):** Evaluating liquid biopsies for methylomics profiling of prostate cancer. *Epigenetics* DOI: 10.1080/15592294.2020.1712876
- Singulani, J. L. et al. (2018):** Applications of invertebrate animal models to dimorphic fungal infections. *Journal of Fungi* 4: 118
- Siqueira, K. A. (2018):** Genomes of the mercury-resistant fungi *Curvularia geniculata*-W3 and *Aspergillus terreus*-W25. Unpublished

- Siqueira, K. A. (2018):** Genomes of the mercury-resistant fungi *Curvularia lunata* and *Aspergillus terreus*. Unpublished
- Sowa-Jasiłek, A. et al. (2016):** *Galleria mellonella* lysozyme induces apoptotic changes in *Candida albicans* cells. *Microbiological Research* 193: 121-131
- Soklič, A. (2020):** Gobarsko Društvo Gorje website photo collection (<http://www.gorjanski-gobar.si/as/indexlat.htm>)
- Steenwyk, J. L. et al. (2020):** Pathogenic allodiploid hybrids of *Aspergillus* fungi. *Current Biology* 30(13): 2495-2506
- Suhadolnik, R. J. et al. (1964):** The biosynthesis of cordycepin. *Journal of the American Chemical Society* 86(5): 948-949
- Suhadolnik, R. J. (1989):** Stereospecific 2'-amination and 2'-chlorination of adenosine by *Actinomadura* in the biosynthesis of 2'-amino-2'-deoxyadenosine and 2'-chloro-2'-deoxycoformycin. *Archives of Biochemistry and Biophysics* 270: 374-382
- Sumner, L. W. et al. (2007):** Proposed minimum reporting standards for chemical analysis. *Metabolomics* 3: 211-221
- Sumner, L. W. et al. (2014):** Proposed quantitative and alphanumeric metabolite identification metrics. *Metabolomics* 10: 1047-1049
- Sun, C. et al. (2019):** Spatially resolved metabolomics to discover tumor-associated metabolic alterations. *Proceedings of the National Academy of Sciences* 116: 52-57
- Sun, H. et al. (2018):** Preservation affects the vegetative growth and fruiting body production of *Cordyceps militaris*. *World Journal of Microbiology and Biotechnology* 34: 166
- Sun, S.J. et al. (2017):** Molecular analysis and biochemical characteristics of degenerated strains of *Cordyceps militaris*. *Archives of Microbiology* DOI 10.1007/s00203-017-1359-0
- Syme, R. A. (2018):** Pan-*Parastagonospora* comparative genome analysis—effector prediction and genome evolution. *Genome Biology and Evolution* 10: 2443-2457
- Taberman, H. et al. (2016):** Structural and functional features of the NAD(P) dependent Gfo/Idh/Moca protein family oxidoreductases. *Protein Science* 25: 778-786
- Tang, J. et al. (2018):** Enhancing cordycepin production in liquid static cultivation of *Cordyceps militaris* by adding vegetable oils as the secondary carbon source. *Bioresearch Technology* 268: 60-67

- Tautenhahn, R. et al. (2008):** Highly sensitive feature detection for high resolution LC/MS. *BMC Bioinformatics* 9: 504
- Terfehr, D. et al. (2014):** Genome sequence and annotation of *Acremonium chrysogenum*, producer of the β -lactam antibiotic cephalosporin C. *Genome Announcements* 2: e00948-e00914
- Toledo-Hernandez, C. et al. (2008):** Fungi in healthy and diseased sea fans (*Gorgonia ventalina*): is *Aspergillus sydowii* always the pathogen? *Coral Reefs* 27: 707-714
- Tuli, H. S. et al. (2014):** Optimization of fermentation conditions for cordycepin production using *Cordyceps militaris* 3936. *Journal of Biological and Chemical Sciences* 1: 35-47
- Tuli, H. S. et al. (2017):** Cordycepin: A *Cordyceps* metabolite with promising therapeutic potential. From *Fungal Metabolites* (Springer) pp 761-782
- Vallim, M. A. et al. (2000):** *Aspergillus* SteA (sterile12-like) is a homeodomain-C₂/H₂-Zn⁺² finger transcription factor required for sexual reproduction. *Molecular Microbiology* 36: 290-301
- Vega, F. E. et al. (2008):** Entomopathogenic fungal endophytes. *Biological Control*. 46: 72-82
- Vega, F. E. et al. (2009):** Fungal entomopathogens: new insights on their ecology. *Fungal Ecology* 2: 149-159
- Vega, F. E. et al. (2018):** The use of fungal entomopathogens as endophytes in biological control: a review. *Mycologia* 110: 4-30
- Vidal, S. & Jaber, L. R. (2015):** Entomopathogenic fungi as endophytes: plant-endophyte-herbivore interactions and prospects for their use in biological control. *Current Science* 109: 46-54
- Vilcinskas, A. et al. (1997):** Effects of the entomopathogenic fungus *Metarhizium anisopliae* and its secondary metabolites on morphology and cytoskeleton of plasmatocytes isolated from the greater wax moth, *Galleria mellonella*. *Journal of Insect Physiology* 43: 1149-1159
- Vongsangnak, W. et al. (2017):** Genome-scale metabolic network of *Cordyceps militaris* useful for comparative analysis of entomopathogenic fungi. *Gene* 626: 132-139
- Wang, Y. et al. (2004):** Integrated extracting technology of cordycepin and polysaccharides in *Cordyceps militaris*. *Acta. Bot. Boreali-Occidentalia Sinica* 25: 1863-1867

- Wang, Y. et al. (2020):** Diverse function and regulation of CmSnf1 in entomopathogenic fungus *Cordyceps militaris*. *Fungal Genetics and Biology* 142: 103415
- Wang, Y. et al. (2020):** Diverse function and regulation of SmSnf1 in entomopathogenic fungus *Cordyceps militaris*. *Fungal Genetics and Biology* 142: 103415
- Wang, Y. et al. (2020):** Shotgun lipidomics-based characterization of the landscape of lipid metabolism in colorectal cancer. *Biochimica et Biophysica Acta* 1865: 3
- Wang, Y. X. et al. (2010):** Electrophoretic karyotype analysis of *Paecilomyces militaris*, the anamorph of *Cordyceps militaris*. *Journal of the Anhui Agricultural University* 37: 716-719
- Want, E. J. et al. (2010):** Global metabolic profiling procedures for urine using UPLC-MS. *Nature Protocols* 5: 1005-1018
- Webster, J. & Weber, R. W. S. (2007):** *Introduction to Fungi*. (Cambridge University Press).
- Wellham, P. A. D. et al. (2019):** Coupled biosynthesis of cordycepin and pentostatin in *Cordyceps militaris*: implications for fungal biology and medicinal natural products. *Annals of Translational Medicine* 7: S85.
- Wellham, P. A. D. et al. (2021):** Culture degeneration reduces sex-related gene expression, alters metabolite production and reduces insect pathogenic response in *Cordyceps militaris*. *Microorganisms*. 9: 1559.
- Wen, T. C. et al. (2014):** Optimization of solid-state fermentation for fruiting body growth and cordycepin production by *Cordyceps militaris*. *Chiang Mai Journal of Science* 41: 858-872
- Wen, T. C. et al. (2016):** Enhanced production of cordycepin by solid state fermentation of *Cordyceps militaris* using additives. *Chiang Mai Journal of Science* 43: 972-984
- Wen, T.C. et al. (2012):** A molecular genetic study on fruiting-body formation of *Cordyceps militaris*. *African Journal of Microbiology Research* 6: 5215-5221
- White, T. J. et al. (1990):** Amplification and direct sequencing of fungal ribosomal RNA genes for phylogenetics. In: *PCR Protocols: a Guide to Methods and Applications*. (Eds: Innis, M. A. et al.) (San Diego: Academic Press)
- Wiese, J. et al. (2011):** Phylogenetic identification of fungi isolated from the marine sponge *Tethya aurantium* and identification of their secondary metabolites. *Marine Drugs* 9: 561-585
- Winnebeck, E. C. et al. (2010):** Why does insect RNA look degraded? *Journal of Insect Science* 10: 159

- Winterstein, D. (2001):** *Cordyceps* (Kernkeulen), Gourmets in Pilzreich. *Der Tintling* 6: 24-30
- Wojda, I. & Jakubowicz, T. (2007):** Humoral immune response upon mild heat-shock conditions in *Galleria mellonella* larvae. *Journal of Insect Physiology* 53: 1134-1144
- Wojda, I. et al. (2009):** Humoral immune response of *Galleria mellonella* larvae after infection by *Beauveria bassiana* under optimal and heat-shock conditions. *Journal of Insect Physiology* 55: 525-531
- Wong, Y. Y. et al. (2010):** Cordycepin inhibits protein synthesis and cell adhesion through effects on signal transduction. *Journal of Biological Chemistry* 285: 2610-2621
- Woo, M. S. et al. (2005):** Curcumin suppresses phorbol ester-induced matrix metalloproteinase-9 expression by inhibiting the PKC to MAPK signaling pathways in human astrogloma cells. *Biochemical and Biophysical Research Communications* 335: 1017-1018
- Woolley, V. C. et al. (2020):** Cordycepin, a metabolite of *Cordyceps militaris* reduces immune-related gene expression in insects. *Journal of Invertebrate Pathology* 177: 107480
- Wu, P. et al. (2017):** An unusual protector-protégé strategy for the biosynthesis of purine nucleosidase antibiotics. *Cell Chemical Biology* 24: 171-181
- Wyss-Coray, T. (2016):** Ageing, neurodegeneration and brain rejuvenation. *Nature* 539: 180-186
- Xia, Y. et al. (2017):** Fungal cordycepin biosynthesis is coupled with the production of the safeguard molecule pentostatin. *Cell Chemical Biology* 24: 1479-1489
- Xie, J. W. et al. (2010):** Analysis of the main nucleosides in *Cordyceps sinensis* by LC/ESI-MS. *Molecules* 15: 305-309
- Xie, J. W. et al. (2010):** Analysis of the main nucleosides in *Cordyceps sinensis* by LC/ESI-MS. *Molecules* 15: 305-314
- Xiong, C. et al. (2013):** Increasing oxidative stress tolerance and subculturing stability of *Cordyceps militaris* by over-expression of a glutathione peroxidase gene. *Applied Microbiology and Biotechnology* 97: 2009-2015
- Yakunin, A. F. et al. (2004):** The HD domain of the *Escherichia coli* tRNA nucleotidyltransferase has 2',3'-cyclic phosphodiesterase, 2'-nucleotidase, and phosphatase activities. *Journal of Biological Chemistry* 279: 36819-36827

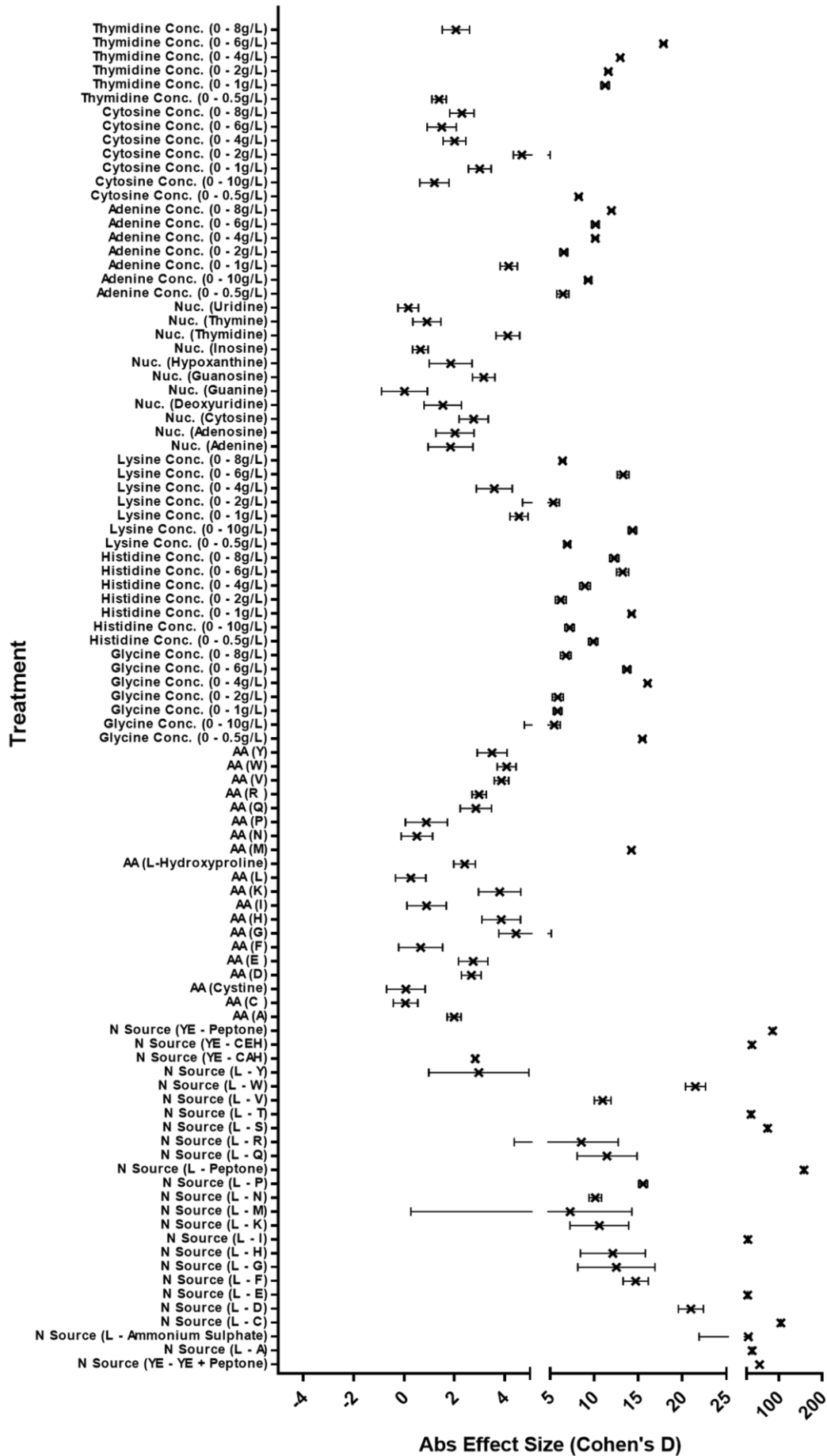
- Yan, H. et al. (2008):** A study on *Cordyceps militaris* polysaccharide purification, composition and activity analysis. *African Journal of Biotechnology* 7: 4004-4005
- Yang, F. Q. et al. (2009):** Determination of nucleosides and nucleobases in different species of *cordyceps* by capillary electrophoresis-mass spectrometry. *Journal of Pharmaceutical and Biomedical Analysis* 50: 307-314
- Yang, F. Q. et al. (2010):** Determination of nucleotides, nucleosides and their transformation products in *Cordyceps* by ion-pairing reversed-phase liquid chromatography-mass spectrometry. *Journal of Chromatography A* 1217: 5501-5510
- Yang, Y. & Huang, G. (2018):** Genomic characteristics and comparative genomics analysis of the endophytic fungi *Sarocladium brachiariae*. Unpublished
- Yin, J. et al. (2017):** Transcriptome-wide analysis reveals the progress of *Cordyceps militaris* subculture degeneration. *PLoS One* 12: E0182679
- Yin, Y. L. et al. (2012):** Genome-wide transcriptome and proteome analysis on different developmental stages of *Cordyceps militaris*. *PLoS One* 7: e51853
- Yokoyama et al. 2004:** Development of a PCR-based mating-type assay for Clavicipitaceae. *FEMS Microbiol. Lett.* 237: 205-212
- Yu, K. W. et al. (2001):** Chemical properties and physiological activities of stromata of *Cordyceps militaris*. *Journal of Microbiology and Biotechnology* 11: 266-274
- Yu, Y. et al. (2016):** Draft genome sequence of *Paecilomyces hepiali*, isolated from *Cordyceps sinensis*. *Genome Announcements* 4: e00606-e00616
- Zhang, G. & Liang, Y. (2013):** Improvement of fruiting body production in *Cordyceps militaris* by molecular assessment. *Archives of Microbiology* 195: 579-585
- Zhang, H. et al. (2012):** The optimization of extraction of cordycepin from fruiting body of *Cordyceps militaris* (L.) Link. *Advances Materials Research* 393: 1024-1028
- Zhang, J. et al. (2015):** A metabolomics approach for authentication of *Ophiocordyceps sinensis* by liquid chromatography coupled with quadrupole time-of-flight mass spectrometry. *Food Research International* 76: 489-497
- Zhang, J. G. et al. (2013):** Production of cordycepin by *Cordyceps militaris* using submerged liquid culture: optimization of the culture medium and repeated batch fermentation. *Journal of Food, Agriculture and Environment* 11: 534-538
- Zhang, Y. (2016):** *Cordyceps militaris* genome, accession number: MQTM01000004.1

- Zhang, Y. J. et al. (2010):** Influence of air permeability on growth of *Cordyceps militaris*. *Guangdong Agricultural Sciences* 4: 45-47
- Zhao, H. Q. et al. (2013):** Characterisation of nucleosides and nucleobases in natural *Cordyceps* by HILIC-ESI/TOF/MS and HILIC-ESI/MS. *Molecules* 18: 9755-9769
- Zhao, X. et al. (2019):** Cordycepin and pentostatin biosynthesis gene identified through transcriptome and proteomics analysis of *Cordyceps kyushensis* Kob. *Microbiology Research* 218: 12-21
- Zheng, P. et al. (2011):** Genome sequence of the insect pathogenic fungus *Cordyceps militaris*, a valued traditional Chinese medicine. *Genome Biology* 12: 10.1186/gb-2011-12-11-r116
- Zheng, P. et al. (2013):** Genetics of *Cordyceps* and related fungi. *Applied Microbiology and Biotechnology* 97: 2797-2804.
- Zheng, Z. et al. (2011):** *Agrobacterium tumefaciens*-mediated transformation as a tool for insertional mutagenesis in medicinal fungus *Cordyceps militaris*. *Fungal Biology* 115: 265-274
- Zheng, Z. et al. (2015):** Identification of the genes involved in the fruiting body production and cordycepin formation of *Cordyceps militaris* fungus. *Mycobiology* 43: 37-42
- Zhong, S. et al. (2009):** Advances in research of polysaccharides in *Cordyceps* species. *Food Technology and Biotechnology* 47: 304-308
- Zhong, S. Y. et al. (2015):** Fast simultaneous determination of 13 nucleosides and nucleobases in *Cordyceps sinensis* by UHPLC-ESI-MS/MS. *Molecules* 20: 21816-21825
- Zhu, L. N. et al. (2014):** Isolation and purification of a polysaccharide from the caterpillar medicinal mushroom *Cordyceps militaris* (Ascomycetes) fruit bodies and its immunomodulation of RAW 264.7 macrophages. *International Journal of Medicinal Mushrooms* 16: 247-257
- Zureik, M. et al. (2002):** Sensitisation to airborne moulds and severity of asthma: cross sectional study from European community respiratory health survey. *British Medical Journal* 325: 411-414

APPENDICES

SUPPLEMENTARY MATERIAL FROM CHAPTERS 1 AND 2

Forest Plot: Factors Affecting Cordycepin Production



Forest Plot: Factors Affecting Cordycepin Production (continued)

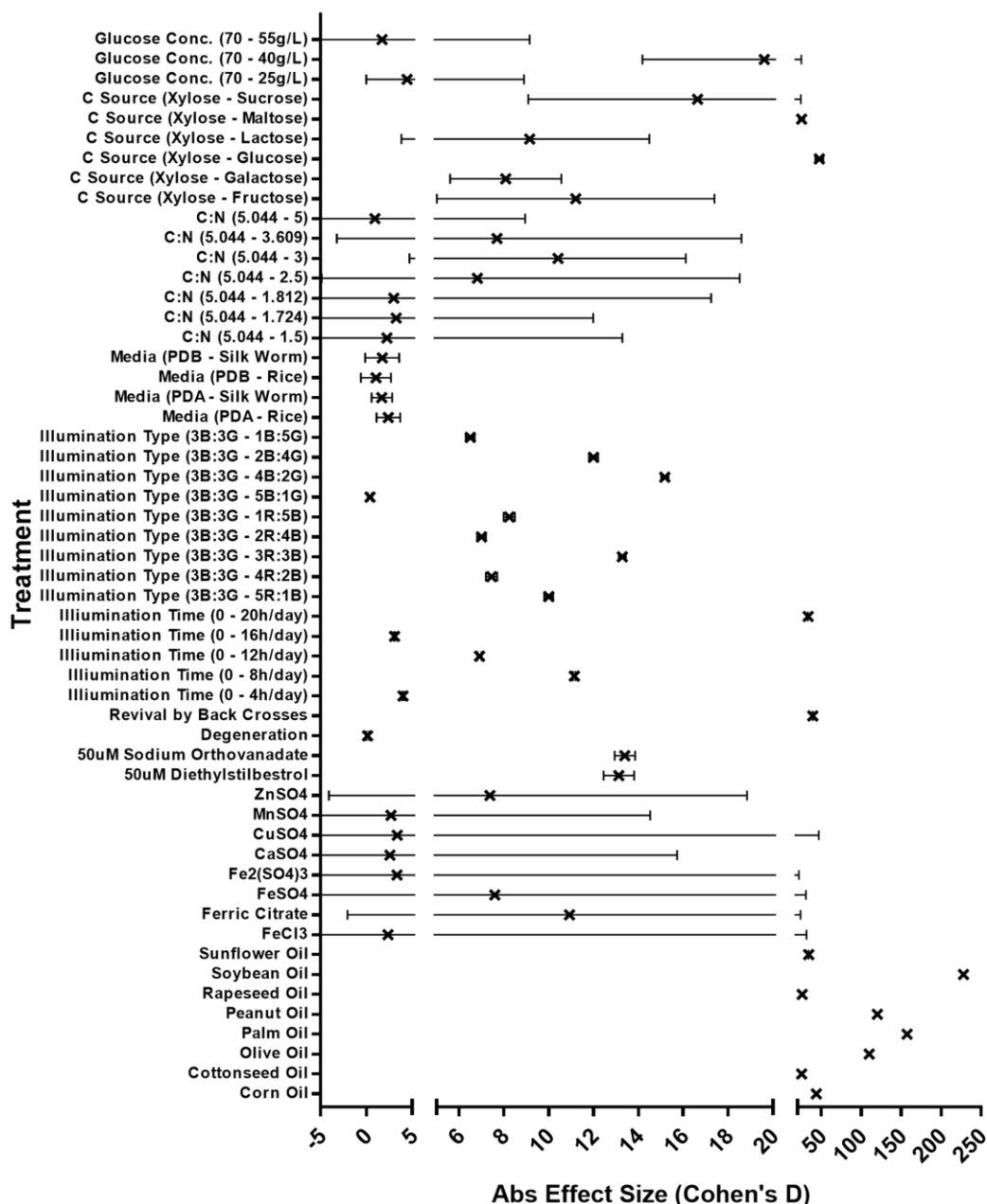


Figure S1: Forest plot showing published tested factors affecting cordycepin production in *C. militaris* cultures. Effect size, in the form of Cohen's D is used. [After Wen *et al.* 2016; Mao & Zhong 2006; Mao *et al.* 2005; Lee *et al.* 2007; Kang *et al.* 2017; Chiang *et al.* 2017; Chen *et al.* 2017; Fan *et al.* 2012; Tang *et al.* 2018]. Abbreviations: AA – amino acid, N – nitrogen, B – blue, G – green. Changes are shown as from the lowest cordycepin-producing treatment to the highest. More examples of similar studies are detailed in table 1.8.

Heatmap in R: Script Used

```
mydata<-read.csv(file.choose()) # load a data file – in csv form
head(mydata) # see first few rows
attach(mydata) # so that you can refer to columns by name
library(cluster) # load cluster package
library(factoextra) # if it doesn't work, load from the menu bars
library(pheatmap)
mydata.set<-scale(mydata[-1]) # standardise variables
k.means.fit<-kmeans(mydata.set,4)
attributes(k.means.fit)
k.means.fit$centers
k.means.fit$cluster
k.means.fit$size
wssplot <- function(data, nc=15, seed=1234){
  wss <- (nrow(data)-1)*sum(apply(data,2,var))
  for (i in 2:nc){
    set.seed(seed)
    wss[i] <- sum(kmeans(data, centers=i)$withinss)}
  plot(1:nc, wss, type="b", xlab="Number of Clusters",
       ylab="Within groups sum of squares")}
wssplot(mydata.set, nc=6) # To plot a graph to find the optimum number of clusters
#Optimum number seems to be 4 for example
clusplot(mydata.set, k.means.fit$cluster, main='2D representation of the Cluster solution',
         color=TRUE, shade=TRUE,
         labels=2, lines=0) # PCA plot
d<-dist(mydata.set,method="euclidean")
H.fit<-hclust(d,method="ward.D")
plot(H.fit,cex=0.3)
groups <- cutree(H.fit, k=4) # for four clusters
rect.hclust(H.fit, k=4, border="red") # Hierarchical cluster plot
library(pheatmap)
pheatmap(t(mydata.set), cutree_cols = 4)
```

SUPPLEMENTARY MATERIAL FROM RESULTS CHAPTERS (3-8)

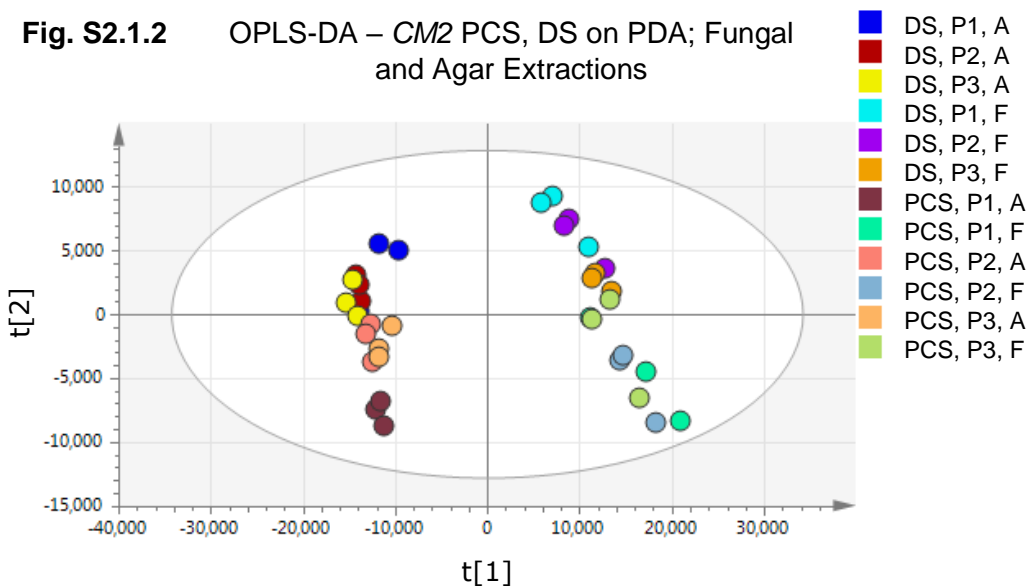
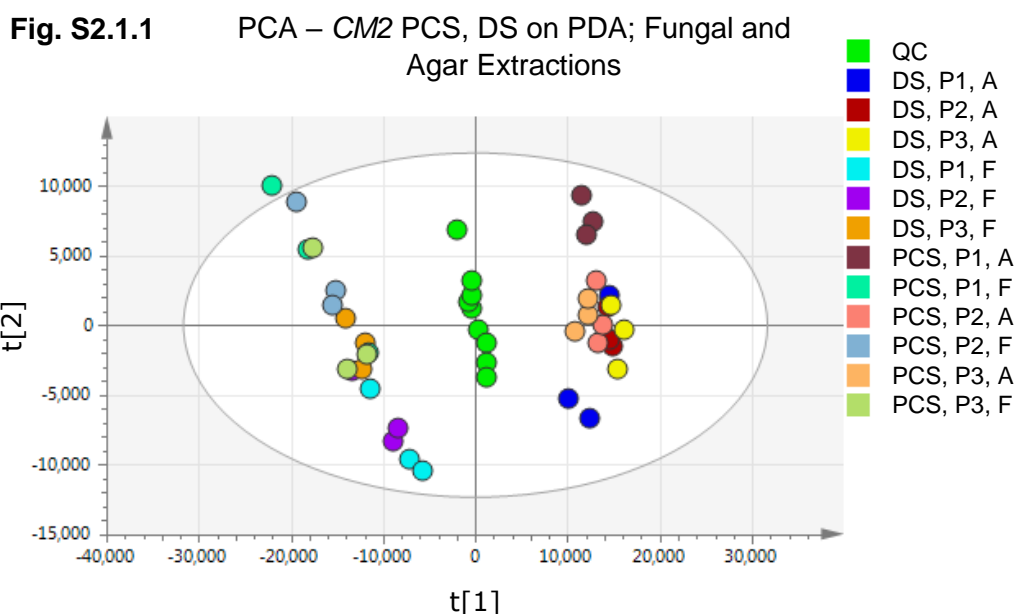


Figure S2.1: PCS vs. DS LC-MS multivariate analyses. Principle component analysis (PCA, fig. S2.1) and orthogonal partial least squares-discriminant analysis (OPLS-DA, fig. S2.2) plots for an untargeted LC-MS run of extracts from *CM2* parental control (PCS) and degenerated (DS) strains on potato dextrose agar (PDA); including also the repeated QC sample outputs (PCA only). Metabolites were extracted from both fungal (F) and agar (A) material. There were three replicates, taken from three different agar plates (indicated by P1,2,3) in each case – totalling 9 samples for each treatment. These multivariate analyses are based upon relative concentrations of all identified and putatively-identified metabolites following XCMS, MzMatch, and IDEOM processing of data. These figures were produced using SIMCA-P (v4) software.

Fig. S2.2.1 OPLS-DA – *CM2* PCS on PDA; Fungal and Agar Extractions

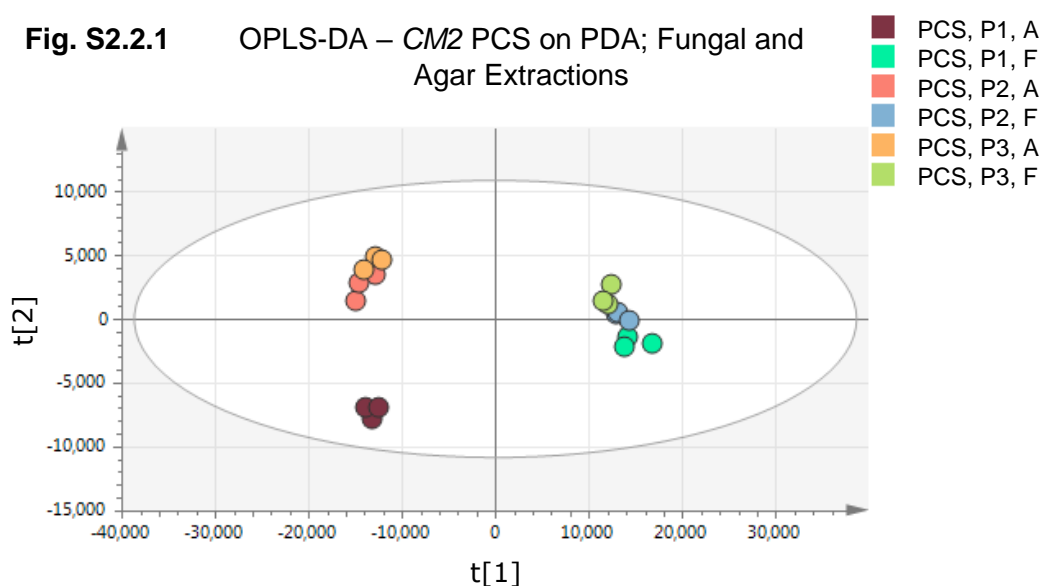


Fig. S2.2.2 OPLS-DA – *CM2* DS on PDA; Fungal and Agar Extractions

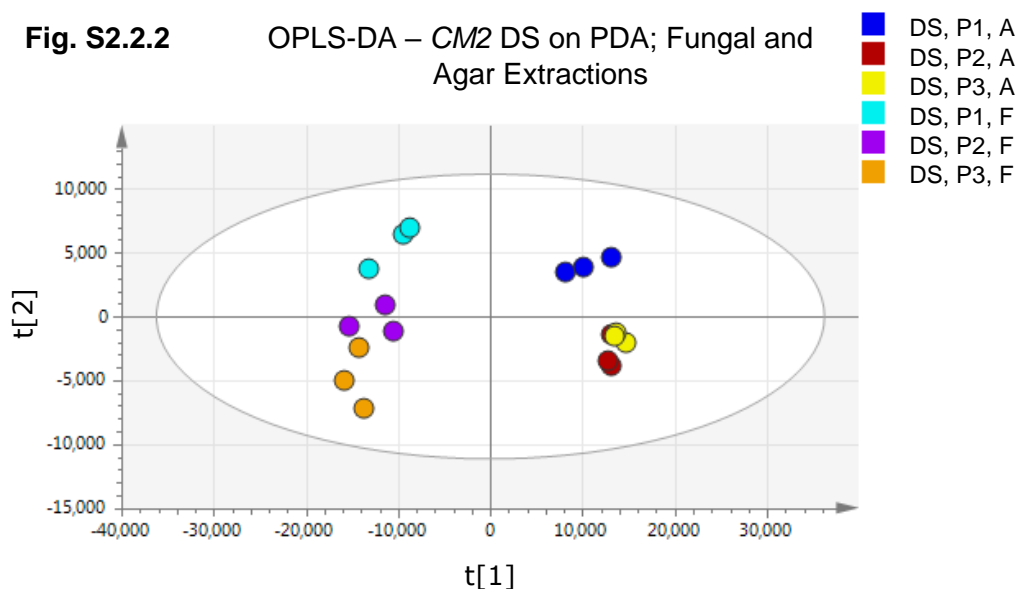


Figure S2.2: PCS vs. DS LC-MS multivariate analyses (2). Orthogonal partial least squares-discriminant analysis (OPLS-DA) plots for an untargeted LC-MS run of extracts from *CM2* parental control (PCS; fig. S2.2.1) and degenerated (DS; fig. S2.2.2) strains on potato dextrose agar (PDA). Metabolites were extracted from both fungal (F) and agar (A) material. There were three replicates, taken from three different agar plates (indicated by P1,2,3) in each case – totalling 9 samples for each treatment. These multivariate analyses are based upon relative concentrations of all identified and putatively-identified metabolites following XCMS, MzMatch, and IDEOM processing of data. These figures were produced using SIMCA-P (v4) software.

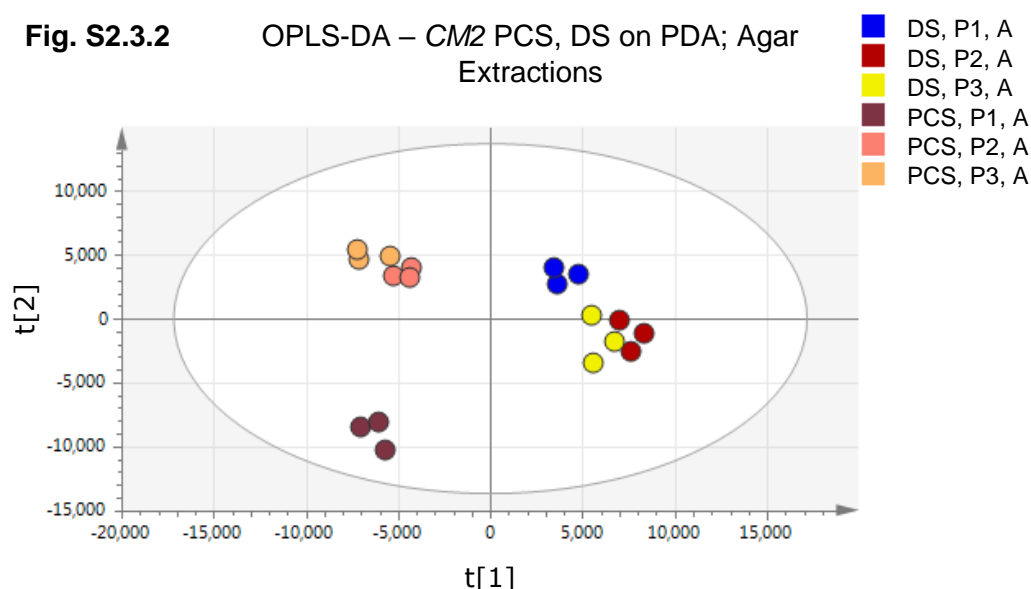
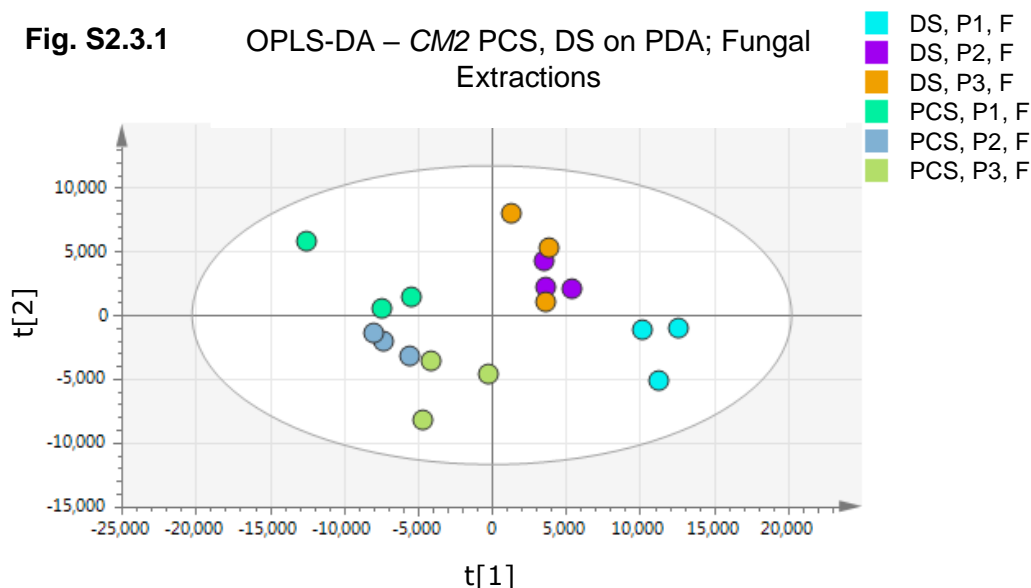


Figure S2.3: PCS vs. DS LC-MS multivariate analyses (3). Orthogonal partial least squares-discriminant analysis (OPLS-DA) plots for an untargeted LC-MS run of extracts from CM2 parental control (PCS) and degenerated (DS) strains on potato dextrose agar (PDA). Metabolites were extracted from both fungal (F; fig. 3.10.3 A) and agar (A; fig. 3.10.3 B) material. There were three replicates, taken from three different agar plates (indicated by P1,2,3) in each case – totalling 9 samples for each treatment. These multivariate analyses are based upon relative concentrations of all identified and putatively-identified metabolites following XCMS, MzMatch, and IDEOM processing of data. These figures were produced using SIMCA-P (v4) software.

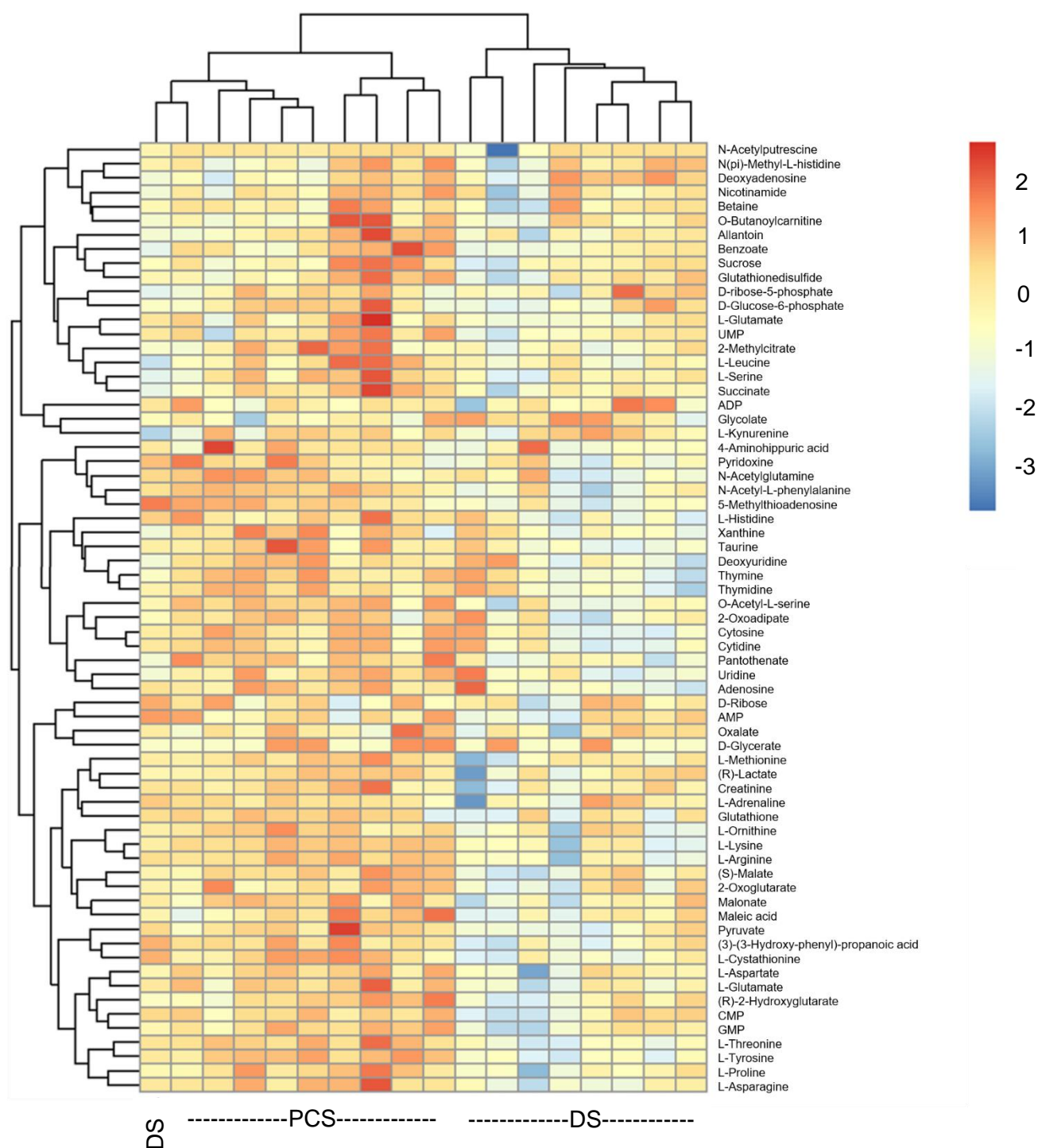


Figure S3: PCS vs DS (fungal and agar extractions combined) LC-MS heatmap with identified metabolites. Heatmap featuring identified metabolites in an untargeted LC-MS run of extracts from *CM2* parental control (PCS) and degenerated (DS) strains on potato dextrose agar (PDA). Metabolites were extracted from fungal and agar material, and combined relative concentrations are considered here – from both extraction types. There were three replicates, taken from three different agar plates in each case – totalling 9 samples for each treatment. This analysis is based upon relative concentrations of metabolites identified using accurate mass and retention times based on authentic standards, following XCMS, MzMatch, and IDEOM processing of data. Concentrations were transformed prior to heatmap construction using a logarithm with base 10. This figure was produced using R version 4.0.0 software, with the heatmap package (“pheatmap”).

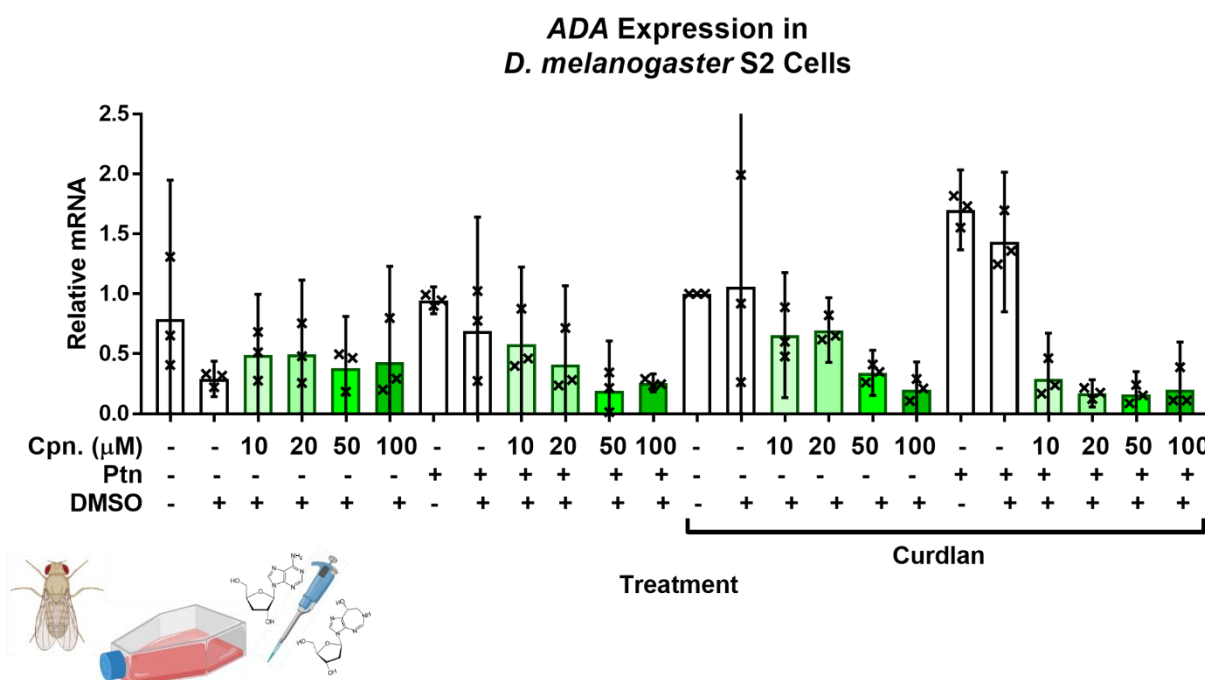


Figure S4: Relative expression of Adenosine Deaminase (ADA) in *Drosophila melanogaster* S2 cells following stimulation curdlan (cdl), with or without previously-added cordycepin (cpn) of various concentrations and 1.5nM pentostatin (ptn). DMSO = dimethyl sulfoxide, the solvent used for cordycepin and pentostatin. Cells were sampled four hours after treatment. Expression levels are relative to the control gene *Ribosomal Protein 49 (Rp49)*, and all values were normalised to the curdlan-only treatment. Error bars show 95% confidence intervals, and comparisons between means as calculated using t-test, with Bonferroni corrections, are shown in table 4.1. Three biological replicates, with each point representing an average from three technical replicates are shown.

Bacterial Colonies from Extracted Haemolymph of *Cordyceps militaris*-Injected *Galleria mellonella* Caterpillars

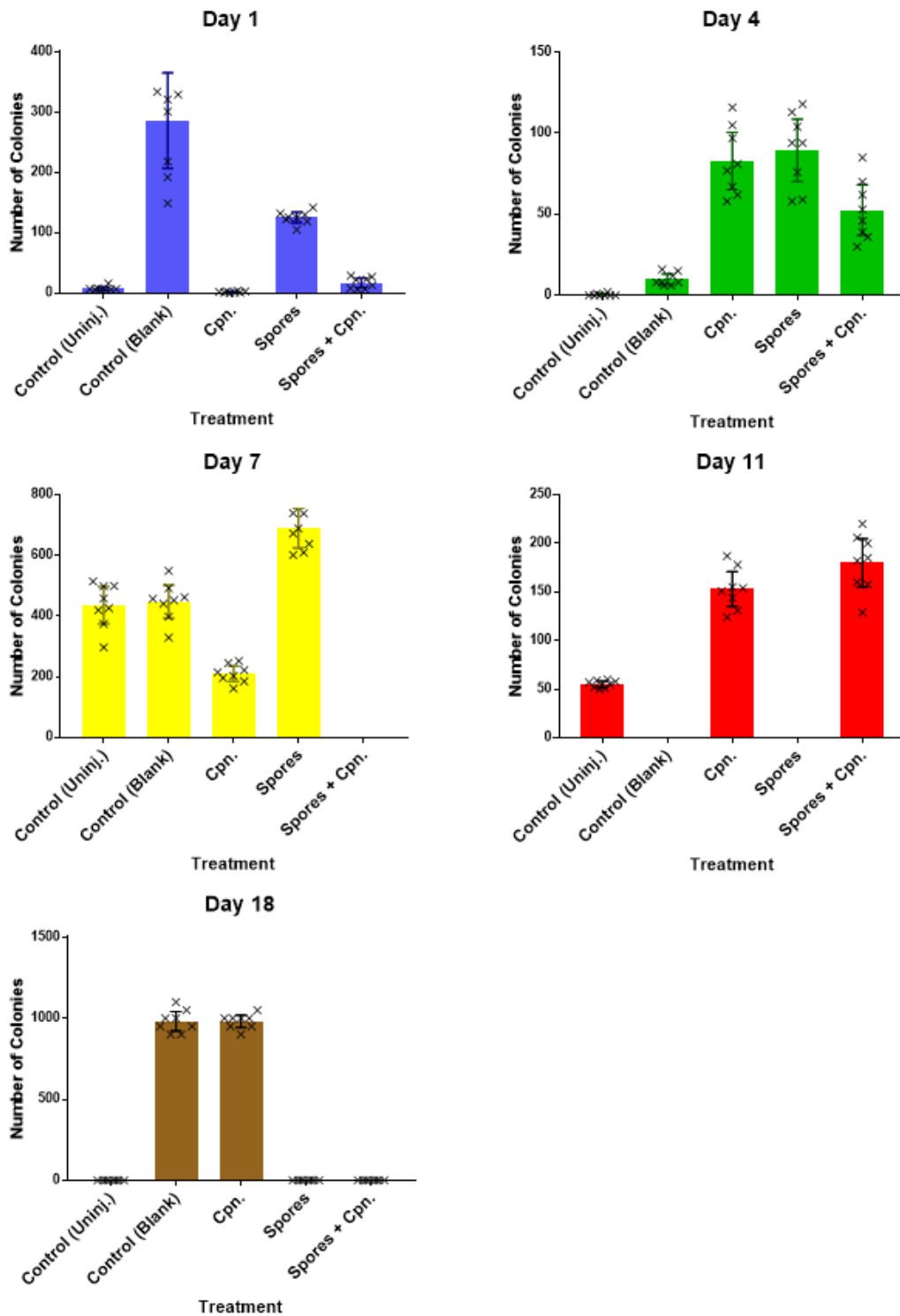


Figure S5: Numbers of bacterial colonies isolated from extracted haemolymph of *C. militaris* spore-injected *G. mellonella* caterpillars. Spores of the degenerated strains of the CM2 *C. militaris* isolate from four week-old potato dextrose broth (PDB) cultures were used for injection. Prior to injection, spores were washed in phosphate-buffered saline (PBS); they were injected in suspensions of sterile PBS. Controls of uninjected, blank (PBS only), and cordycepin only (Cpn.) were used, as well as cordycepin injected with spores in PBS (Spores + Cpn.). Haemolymph was extracted as time points of 1, 4, 7, 11, and 18 days post injection, as indicated in graph titles. For each replicate, 100 μ L of 40x diluted haemolymph from five caterpillars in PBS was spread onto plates. Errors bars show 95% confidence intervals; n = 8. Note that zero values in the 18 day graph in “spores” and “spores + cpn.” Treatments were due to full growth of *C. militaris*. Bacterial lawns were formed in all of the “spores + cpn.” at 7 days and “control (blank)” and “spores” at 11 days – where no bars are on the graphs.

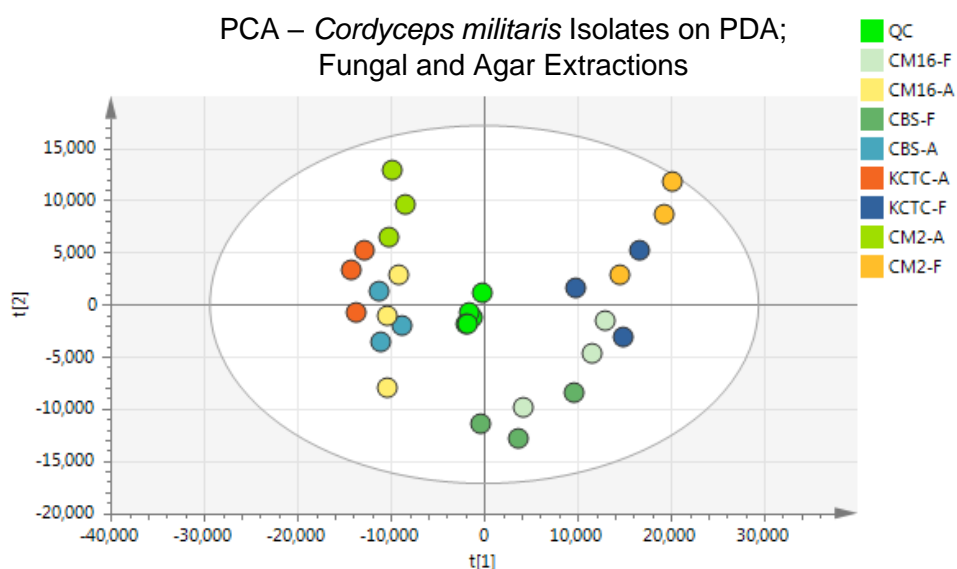


Figure S6.1: Principle component analysis plot for an untargeted LC-MS run of several *Cordyceps militaris* isolates on PDA; including also the repeated QC sample outputs. Metabolites were extracted from both fungal (F) and agar (A) material, hence also taking into account metabolite secreted into the media. There are three replicates, from separate agar plates for each treatment. These multivariate analyses are based upon relative concentrations of all identified and putatively-identified metabolites following XCMS, MzMatch, and IDEOM processing of data. These figures were produced using SIMCA-P (v4) software.

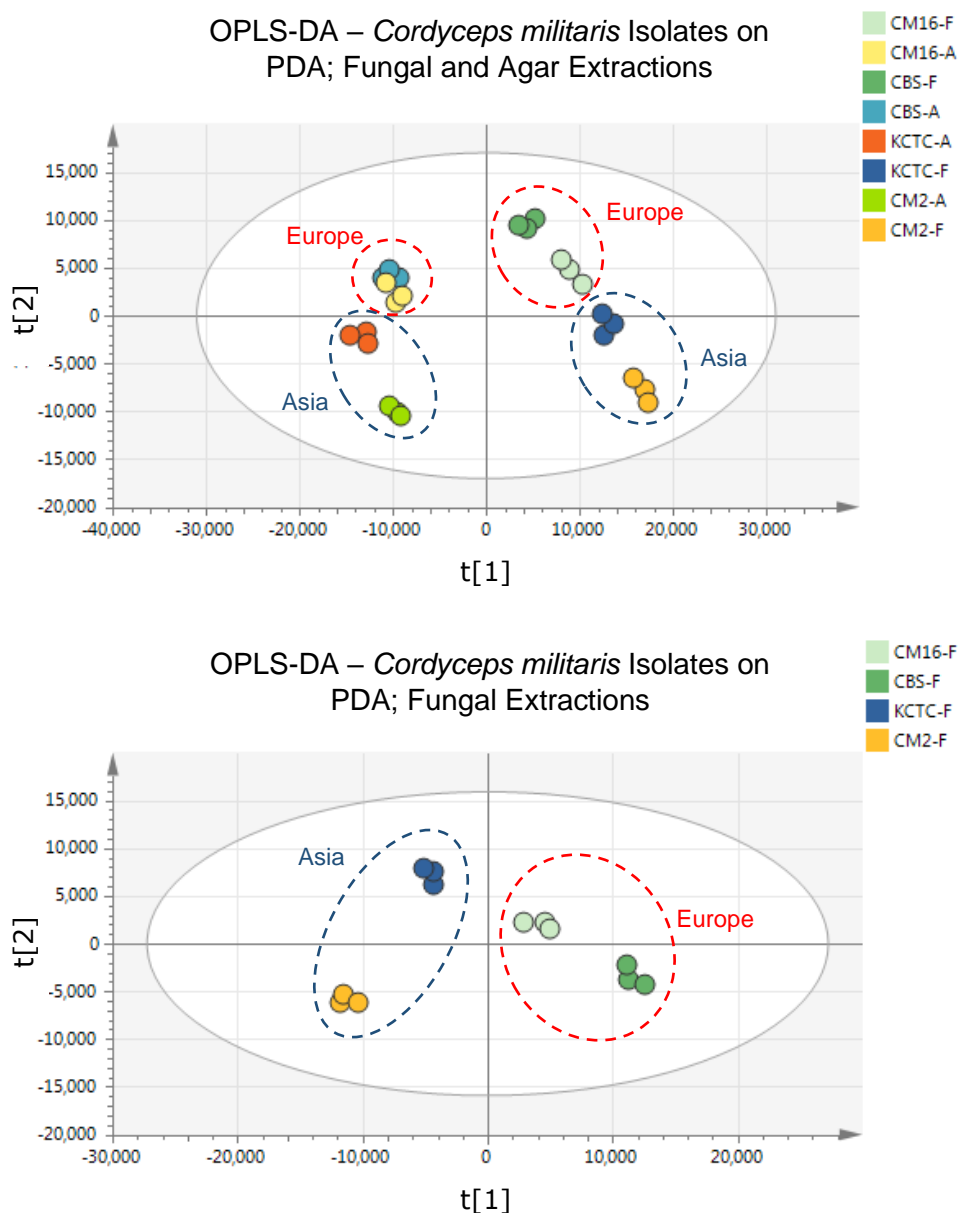


Figure S6.2: Orthogonal partial least squares-discriminant analysis (OPLS-DA) plots for an untargeted LC-MS run of several *Cordyceps militaris* isolates on PDA. Clustering of samples of isolates from Europe and Asia together on the plots are highlighted with dotted red and blue rings respectively. See the legend of figure S6.1 for further details.